MASSEY UNIVERSITY
ENGINEERING

MODULAR MECHATRONICS TECHNOLOGY FOR FIBRE-BASED MANUFACTURING AND BIOFABRICATION RESEARCH

Juan Schutte

2019

SUPERVISOR:
Prof Johan Potgieter

CO-SUPERVISOR:
Dr. Xiaowen Yuan

PREFACE:

This dissertation is presented in partial fulfilment of the requirements for the degree of:
Doctor of Philosophy
in
Engineering

Conducted at
Massey University, Albany, New Zealand

The author declares that this is his own work except where due acknowledgment has been given.

This work is dedicated to God through the gift of life, by which all things are made possible.

All thanks, praise, and honour to God through which I can do all things.

ABSTRACT

There exists an opportunity within manufacturing for the development of technology capable of creating complex fibre-based structures. Additive Manufacturing (AM) has become increasingly relevant due to its ability to generate parts of a higher complexity relative to other traditional techniques. 3D Printing (3DP) technology is a form of AM through which much of this type of complex manufacturing is conducted. Currently this technology allows for the processing of many materials through a range of mechanisms. Whilst 3DP development has predominantly focussed on synthetic polymer and metal production, there is opportunity for this technique within Tissue Engineering (TE). This field is motivated by the shortage of donor organ tissues such as the cornea. AM is a potential methodology for the controlled manipulation of biomaterial/biopolymer as a form of production within TE. It is however critically limited in its ability to process submicron and nanofiber to generate fibre-based constructs such as those found within the cornea (stroma). This limitation yields restrictions in not only bio-printing based applications but also within attempts to innovate in traditional fibre-reinforcement based industry. There is a manufacturing based opportunity for the research and development of a technology capable of overcoming these limitations. The current restrictions within this field were evaluated through an analysis of relative literature. This led to the identification of electrospinning as a viable technology for both synthetic and biopolymer submicron and nanofiber production. The limitations of this technology were evaluated, leading to the potential for overcoming these utilising traditional methods of 3DP. Further evaluating current literature led to a hypothesized manufacturing technique. Additionally this literature indicated the need for development of a novel technology capable of performing research and development related work within this field. This resulted in much experimentation related to the generation of technology/componentry/mechanisms related to both the testing of the hypothesis as well as capable of facilitating future research. Work related to an increase in electrospinning productivity via electric field related manipulation was conducted as an attempt to reduce system complexity. This work did not circumvent the requirement for environmental control; as such, a method for the implementation of this to aid in productivity was required. Development of mechanisms yielded a strong requirement for a modular system allowing these components to be varied in accordance with the processing requirements. This ability to manipulate the system was achieved through the creation of both a function based coding strategy as well as the derivation of a potential modular electronics (PCB-stacking) technique. The derived novel technology's success was demonstrated through a range of experimentation related to implemented forms of technology within the final machine. Regarding the forming of electrospun material, the direct method of electrospinning-based deposition of material upon molds did not achieve generation of the desired objects as such a method of fibre acquisition was implemented. Regarding collagen electrospinning, no dramatic variation on fibre distribution (alignment) could be derived in comparing the parallel or rotating mandrel-inspired approaches. Functionalisation strategies utilising ultrasonically generated vapour demonstrated promising capability in the bonding of synthetic polymers whilst acting to disrupt the more sensitive biopolymer. The use of corona discharge plasma for crosslinking yielded promising results for synthetic polymer ultimate tensile strength however, the proximity analysis/optimisation of this requires further research if this is to be applied to electrospinning-based AM. Finally, the ability to utilise the developed technology to generate both an automated manufacturing technique for fibre-based additive manufacturing and the creation of associated 3D forms was demonstrated as viable, thus validating this research project.

ACKNOWLEDGEMENTS

This thesis and the associated work would not have been possible without the continual support of many people.

Firstly, I would like to thank my parents, Wouter Stephanus Schutte and Gale Valarie Schutte. Without your incredible sacrifices, unyielding love and undeniable support, this achievement would not have been possible. Thank you for making the sacrifices to bring me to this country and allowing me to pursue my dreams, for all this and more I am eternally grateful.

I would like to thank my sister, Kelsey Schutte. You have helped to keep me sane, which has definitely been no small feat! Your kindness and intelligence have, and continue to, inspire me. Thank you for listening to all the crazy and always being there when I needed to destress.

I would like to thank my grandparents Jacobus Schutte, Jeanette Schutte, Valerie Buys, Christo Buys and John Will. Your examples of sacrifice, courage, determination, and resilience in the face of adversity, have motivated and inspired me to work hard and believe that with dedication my goals can be achieved.

I would like to thank my supervisor Professor Johan Potgieter. Your support not only in respect to this PhD but also the industry and life-orientated mentorship has been an invaluable part of this journey. I am incredibly grateful for all of the amazing opportunities you have provided to me, your enthusiasm and ‘can do’ attitude is truly inspirational.

I would like to thank Massey University you have facilitated my growth through your engineering department. I would like to thank my co-supervisor Xiaowen Yuan as well as the lecturers, teachers and mentors I have been privileged to experience. Your guidance, lessons, and knowledge, have helped me become the engineer I am today.

I would like to thank my post-graduate colleagues. You have joint me at various stages of this crazy adventure. Thank you for all your support through the sleep deprivation and temporary insanity. I wish you all the best in all of your current and future endeavours.

I would like to thank the New Zealand National Science Challenge for not only funding this work, but for being actively involved in my progression as both a student and a researcher within New Zealand. Thank you for allowing me the unique opportunity to develop and learn from the local international experts in fields of Science and Technology.

I would like to thank my industry collaborators GNS Science and RevolutionFibres for providing me with technology and materials critical for the completion of this work. Your readiness to collaborate and guidance through this work has been invaluable.

TABLE OF CONTENTS

LIST OF FIGURES

LIST OF TABLES

LIST OF EQUATIONS

LIST OF PUBLICATIONS

Papers

The following papers are included at the end of this thesis in the form of Appendix A: Papers Published.

Schutte, J., Yuan, X., Dirven, S., & Potgieter, J. (2017). The opportunity of electrospinning as a form of additive manufacturing in biotechnology. 24th International Conference on Mechatronics and Machine Vision in Practice (M2VIP), 6. [8]

Schutte, J., Potgieter, J., Dirven, S., & Yuan, X. (2017). The effects of electrospinning collection surface modification on nylon 6-6 placement. 24th International Conference on Mechatronics and Machine Vision in Practice (M2VIP), 6. [7]

Wjesundira, P., Schutte, J., & Potgieter, J. (2017). The effects of acetone vapour inter-layer processing on fused deposition modelling 3D printed acrylonitrile butadiene styrene. 24th International Conference on Mechatronics and Machine Vision in Practice (M2VIP), 6. [2]

Schutte, J., Wijisundira, P., Harris, M., & Potgieter, J. (2018). Evaluation of the effects of controlled ultrasonic acetone vaporisation on Fused Deposition Modelling 3D Printed Acrylonitrile Butadiene Styrene. 25th International Conference on Mechatronics and Machine Vision in Practice (M2VIP), 5. [1]

Schutte, J., Leveneur, J., Yuan, X., & Potgieter, J. (2018). Evaluation of the effects of corona discharge plasma exposure proximity to Fused Deposition Modelling 3D Printed Acrylonitrile Butadiene Styrene. 25th International Conference on Mechatronics and Machine Vision in Practice (M2VIP), 6. [10]

Posters

The following posters are included at the end of this thesis in the form of Appendix B: Posters Published.

New Zealand Product Accelerator: The Potential of Bioprinting Technologies in the production of Complex Collagen Tissues (2016)

New Zealand Product Accelerator: The Potential for Biofabrication of complex collagen tissues through Bioprinting methodologies (2016)

New Zealand Product Accelerator: Novel 3D printing technologies for the production of complex fibre structures (2017)

National Science Challenge: The pathway to composite nanofiber based 4D Bioprinting (2018)

National Science Challenge: The pathway to composite nanofiber based 4D Bioprinting (2019)

Chapter 1 INTRODUCTION

1.1 Additive Manufacturing

Manufacturing technology has predominantly specialised in the use of synthetic material for polymer based techniques. Additive Manufacturing is a form of manufacturing gaining much interest due to it's potential for a more sustainable practice (in that it generates far lower waste by-product in comparison to Subtractive manufacturing) [12]. This technique relies on the successive introduction of material in a specific order to develop/generate a final structure [12, 13]. One of the most prominent forms of this technology is 3D Printing; this is a rapidly growing prototyping and manufacturing technology that occurs in many different forms for various materials and functionalities (depicted in Figure 1). The fundamental feature of this technology is the layer-by-layer introduction and processing of material to generate three-dimensional objects. Due to differences in the properties of various materials (e.g. viscosity thermal reactivity etc.) three distinct processing methodologies have been developed namely: material deposition, processing of powders or processing of liquids [14].

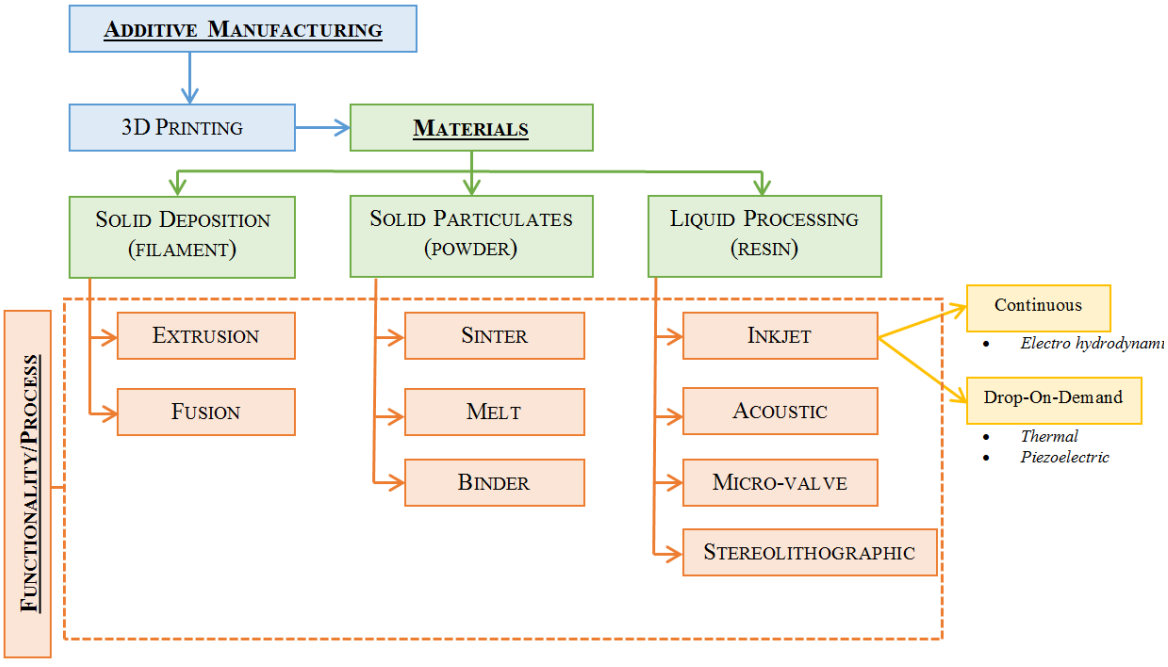

Figure 1: Flowchart depicting the materials and functionalities employed within 3D printing[8]

1.1.1 Mechanisms for material interaction

Many additive manufacturing methodologies rely on the application of pressure and heat to deposit or process the material into the desired form [12]. Deposition printing occurs through mechanical or pneumatic actuation often utilising heating elements to aid in the accurate deposition and post deposition fusing of material (an example of this process is illustrated in Figure 2). The processing of powders occurs through laser melting, laser sintering (Figure 3), electron beam melting, or binder jet application. The processing of liquids occurs through stereolithographic (photo-polymerisation) (Figure 5), inkjet (Figure 4), micro-valve, or acoustic techniques. The introduction of material differs between techniques of additive manufacturing generally, Deposition occurs as a continuous extrusion at predefined locations whereas in the processing of liquids through inkjet technology material introduction occurs as singular droplets onto a substrate. These techniques differ substantially to that of stereolithographic liquid processing and the techniques employed in most powder processing additive manufacturing. In these forms of printing material is introduced as a layer or 'bed' of material which then undergoes processing [15].

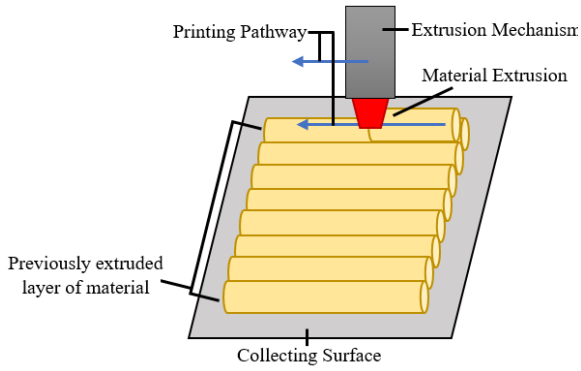

Figure 2: Elements associated with Extrusion based 3D Printing[2]

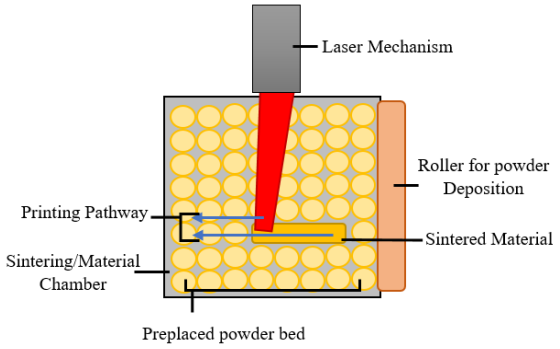

Figure 3: Elements associated with Laser-Sintering based 3D Printing

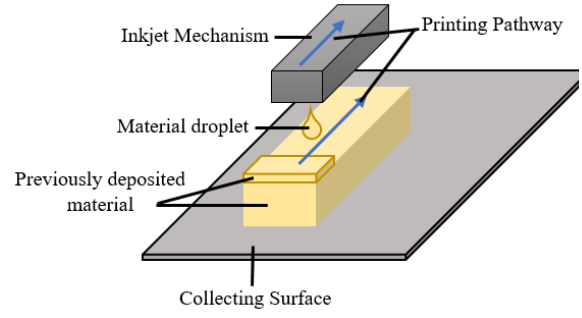

Figure 4: Elements associated with Inkjet based 3D Printing

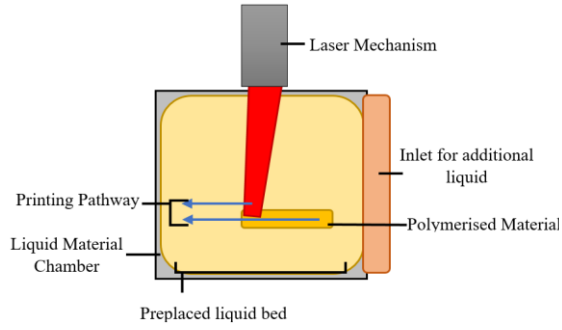

Figure 5: Elements associated with Stereolithographic based 3D Printing

1.1.2 Viscosity, support material and resolution

Material viscosities restrict the type of methodology utilised. Higher and lower viscosities are better processed by deposition and liquid processing methodologies respectively [13, 15]. Both deposition and droplet-based liquid processing methodologies often require support structures/material when complex objects containing overhangs are produced. This must be removed through some form of post processing to yield the desired object [15]. Stereolithographic and powder processing additive manufacturing involves the layer-by-layer introduction of a bed/layer of powder material through a powder spreading/roller mechanism allowing previous layers to act as support material, thus this requires less post processing (material removal). Material deposition additive manufacturing in the form of extrusion techniques have relatively limited resolutions when compared to other forms of additive manufacturing [13] as well as having a dependency on 'support material' depositions for complex parts (e.g. having overhanging extrusions). Due to this dependency post processing to improve the surface quality of material deposition AM is often required. Currently the highest printing resolution occurs in liquid processing additive manufacturing, specifically that of droplet based printing.

The above 3D printing technologies typically utilize common manufacturing materials (Synthetic polymers and Metals) however recently similar additive manufacturing methodologies have been utilized in tissue engineering.

1.2 Tissue Engineering and Organ Fabrication

Tissue engineering is an interdisciplinary approach to the construction of biological substitutes for the repair or replacement of impaired biological systems through the utilisation of technology [16, 17]. This work is highly motivated by the increasing requirement for organ transplantation and the relative reduction of available transplantable equivalents (donor organs). This international shortage has been labelled as a public health crisis for international health [18]. Figure 6 demonstrates the disproportionate relationship between donor organs and organ requirement for the USA[19].

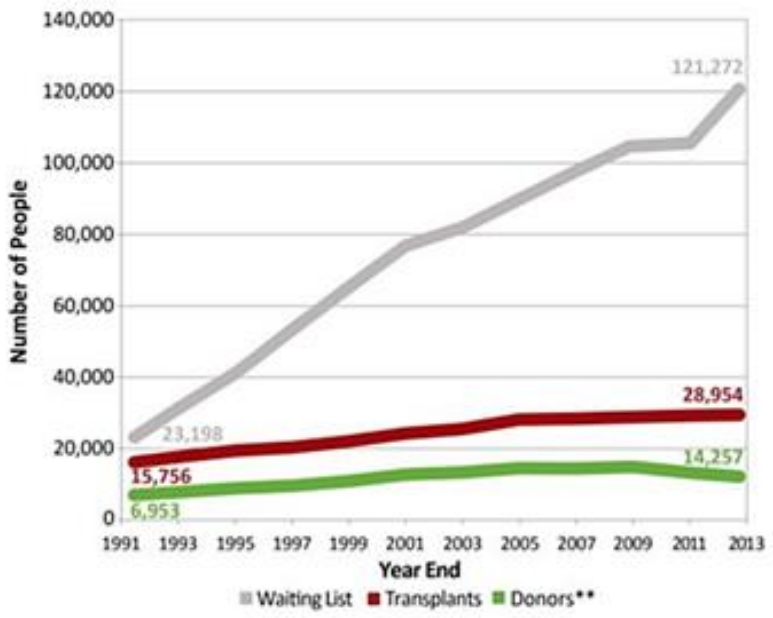

Figure 6: Graph showing Organ transplant, donation and waiting list statistics [15]

It is due to this donor organ deficiency that much research has been conducted regarding the generation of both synthetic and biological replacements in the form of prosthetics and engineered/manufactured tissue. Within this field Anthony Atala's work (1999) in generating a synthetic bladder through the usage of a patients cells seeded into a molded bladder scaffold was fundamental for the future developments of organ fabrication via additive manufacturing [20]. Following Atala's work, Boland utilised inkjet technology for bio-fabrication and was awarded the first bio-printing patent in 2003 [20]. Since then much research and development has occurred in the field of organ fabrication through bio-printing. This technology can be described as the arrangement of biological (cells and proteins) and biologically compatible matter (referred to as bio-ink) in a manner that results in a useful organic structure. This arrangement of material has allowed for the production/mimicking of tissues and in some cases organs, which in turn yields developmental benefits to current medical practices [21-24]. This capability of on-demand-production of desirable biological structures has the potential to decrease (or even eradicate) the complexities associated with organ transplant surgeries (availability of adequate/optimal donor organs) as well as increased capability for medical research. Whilst this is a rapidly developing technology, there are still many limitations that need to be overcome to allow for the bio-printing fabrication of all organs/tissues. In order to understand these limitations the constituents of common tissues and their in vivo relationship must be reviewed. Of these constituents, Collagen is the most abundant protein within invertebrates and can be found in various forms as part(s) of biological constructs, approximately 28 differing forms in the human body [25, 26]. The abundance of collagen has resulted in many studies acquiring the protein from many various sources such as rat tail, fish scales and calf skin [26] for research. Many tissues/organs are in some way comprised of collagen. Through the analysis and an understanding of the structure and functionality within these, the formation of requirements for replication of collagen-based objects can be established. The cornea is a good example of a collagen-based tissue for which there is a donor organ deficiency. Whilst this project does not intend to yield a fully functional bio-fabricated cornea, it is motivated by the lack of these and as such, an understanding of this dilemma is required.

1.3 The Cornea dilemma

The cornea is an avascular tissue situated directly above the pupil region of the eye. The average dimensions of which have been recorded as being 10.5-12.75mm in diameter, 512-569.5 µm in central thickness and having anterior curvature of 7.06-8.66mm [27]. The tissue makes up approximately 15% of the ocular coating [28] and is responsible for the protection of the eye from harmful UV wavelengths, dust, and germs [29]. It functions to refract/bend light onto the eye lens and is majorly responsible (70%) for the focussing of light onto the retina enabling sight [30, 31]. General requirements for this tissue include a high degree of transparency (for optimal light transferal), relatively high strength and flexibility (for retaining form), the ability to sustain tissue hydration and the capability for partial regeneration. The variation of these requirements can develop into serious ailments [29, 32] (injuries or dystrophies/degenerative disorders resulting in tissue malfunction) which if severe enough can require the removal and replacement of the tissue.

The Cornea Research Foundation of America states that 100 000 corneal transplants are conducted each year. This is a relatively small number when compared to the approximately 10 million people who suffer from corneal blindness. It is estimated that globally 180 million people suffer from severely impaired vision [33] .

Recently an increase in popularity of refractive surgeries such as LASIK, a procedure that alters the cornea, has resulted in a decrease in suitable donor tissue. Given these trends, the demand for replacement corneas is expected to increase in the coming years. Thus, developments regarding the fabrication of similar tissue analogues are of great medical interest. As previously stated this project intends to further develop the research in this developing field through the analysis of this tissue and does not intend to replicate/generate an equivalent.

1.4 Problem Space: The need for Fibre-based Fabrication

Whilst the development of a corneal analogue is of incredible interest and a definite motivating feature of this research, the creation of such a tissue is not within the scope of this project. This is largely due to the limitations in manufacturing capability to generate micron and submicron fibre-based objects. This ability is highly desirable in fields other than tissue engineering. This is motivated by the desire to be able to control the orientation of fibre layouts within objects allowing for a greater control of the isotropic or anisotropic reactions to force. Objects comprised of such structures are of great commercial significance in other industries such as aeronautics, sporting, defence force, and filtration. Currently there exists no 3D printing method in which such a complex sub-micron fibre-based object can be generated. In the context of this project, a complex fibre-based structure relates to structures in which fibre characteristics such as diameter, orientation, and alignment occur in a controlled manner and directly affect structural properties. Popular implementations of such structural requirements include the utilisation of carbon fibre re-enforcement or fibreglass molding where large part strength to weight ratio is required.

1.5 Problem Statement

Current 3D printing processes are unsuitable for the generation of structured complex micron and sub-micron fibre-based structures required in the emulation of native tissues (e.g. the stroma) and generation of solely fibre-based reinforced objects. This is due to the inability for nanofiber fabrication, and a reliance on extensive heat and pressure for high-resolution printing within additive manufacturing. Thus, a novel 3D printing process is required to facilitate production of these objects.

1.6 Research Aim and Thesis Statement

This research aims to generate a novel 3D printing technique capable of generating functionalized objects comprised of alternating layers of aligned and bonded submicron and nano-fibre. This project does not intend to yield a fully functional bio-fabricated cornea, rather this research is focused on the furthering of developments within the fibre based manufacturing and bio-printing portion of tissue engineering in the hopes of contributing to the resolving of issues similar to those described in the introduction.

1.7 Research Methodology

The methodology employed in the development of research is justified by the understandings developed in the Literature Review. The following highlights the progression of the project initiatives, including how and where these will be completed.

Research is conducted through an analytical and practical approach utilizing the collaboration associated global leaders in engineering to achieve a desirable result. Following the analytical review, novel initiatives were conceptualized (hypothesis). From these, developments were undertaken yield a system capable of resolving the projects problem statement (sub-micron and nano-scaled fibre-based fabrication).

The practical developments within the project are:

- The generation a cost effective research and development method for investigations related to bio-fabrication through electrospinning
- The implementation of an advanced parallel electrode and rotating mandrel based electrospinning apparatus/mechanisms
- Generation of a modular system for project related and future research oriented developments
- The implementation of automated functionalization strategies utilising vapour, lithography and plasma technology
- The application of curvature deformation to generated a corneal analogous structure.

The processes by which these are realised are:

Engineering (practical development) – relating to the development of a means to fabricate research objects

- Initial testing equipment is designed using SolidWorks.
- Testing equipment in the form of modular electrospinning and vapour/functionalization application systems are constructed utilizing the Massey University Albany workshop equipment.
- Testing equipment is optimized and sample parts are generated for initial analysis.
- A final machine is designed using SolidWorks.
- A final machine combining all successful parameters from previous systems is constructed utilizing the Massey University Albany workshop equipment.
- The final machine is optimized yielding a documented machine procedure.
- A procedure for the generation of objects is developed and alterations to which documented

These practical developments of the project incorporate machine design and construction, where the majority of the component construction for the development of the desired technology is completed alongside/with the aid of the following established Masters project:

1.7.1 Masters Aid: Implementing a control system for vapour based cross-linking/bonding of object.

The purpose of this Masters will be the construction and implementation of a machine capable of transferring electro-spun material to an area in which it can undergo exposure to vaporized cross linking agents and other cross-linking post processing. An example of which will be the exposure of collagen to vaporized Riboflavin and then (if required) exposure to the photo-activator UV light.

The completion of the practical portion of the project allows for the generation of sample objects for analysis. These samples are generated utilising the parameters displayed in *Table 1: Parameters for sample generation*.

Table 1: Parameters for sample generation

Synthetic polymer Studies	Polymer	Solvent	Voltages	Air Gap Distances	Delivery Rates	Functionalisation material	Functionalisation strategies
	Nylon 6,6	Formic Acid	45kV	250mm	1ml/h	3D Systems photo curable resin (expired)	Vapour UV (309nm)
Biopolymer Studies	Polymer	Solvent	Voltages	Air Gap Distances	Delivery Rates	Functionalisation material	Functionalisation strategies
	Collagen Type I (hoki scales)	Acetic	30kV	125mm	1ml/h	Riboflavin	Vapour & UV

Sample preparation – relating to the processing of the resultant object for analysis

- The samples are gold-coated, utilizing Massey University's Nanostructured coatings DSR1 device, one hour prior to microscopy.
- Variation of machine procedure parameters yields six different groups, which will contain five samples each. This is to minimize the potential anomaly-based variation in resultant object.
- Samples are generated from the modifications of the electrospinning time, rate of extrusion, magnetic field manipulation, electrical field manipulation, functionalization exposure rate, and functionalization exposure layer variation.

Engineering analysis – relating to the structural and mechanical properties of the resultant object, utilised to determine the functionality of developed research

- The topographical and surface structural analysis of initial and final parts is conducted through Massey University's Hitachi TM3030Plus scanning electron microscope (SEM).
- Information regarding the mechanical capabilities/properties of the samples is derived from Massey University's INSTRON 5967.

Statistical analysis – relating to the comparative analysis of resultant objects

- All data is collated and managed within a comprehensive data management system (database), in which all variation is recorded and graphical assessment generated.
- T-tests are conducted utilizing analysis data to generate trends where a p-value less than 0.05 are considered statistically significant.

1.7.2 Project conclusion

The capabilities for the developed technology are derived from the experimental results allowing for an indication of the potential of the derived fibre-based manufacturing technologies. The ability for the generated work to produce both synthetic and biopolymer orientated fibre-based 3D forms will be discussed and a conclusion to the project provided. The required future developments related to the utilized technology as well as the field of research will be outlined as recommendations.

1.8 Delimitations

This research project will not investigate the biocompatibility of the resultant structures or alternative materials/materials science for the production of tissue. This project does not intend to generate a .stl-processing capable 3D printer. The project does not intend to generate a medical grade corneal equivalent.

1.9 Overview of Thesis

Chapter 1: Introduction – Here relevant fields are introduced to establish the context of the problem space (research scope) of the project, namely additive manufacturing, tissue engineering, the cornea dilemma, and the need for a form of fibre-based manufacturing.

Chapter 2: Literature Review – Here an analysis of the current understandings within the fields of interest are discussed with an emphasis on research related to resolving the research problem. Within this project, the Literature Review discusses current capabilities within fibre-based additive manufacturing and evaluates these relative to tissue engineering, highlighting a potential benchmark biomaterial (collagen) and structure (stroma). The current capabilities within bio-printing are evaluated and the need to look at alternative forms of manufacturing established. Electrospinning is highlighted as a means to produce layers of submicron and nanofiber. The requirements for this process and its associated limitations are discussed. Methodologies to overcome the restrictions of this technique are evaluated with respect to additive manufacturing.

Chapter 3: Post Literature Review Hypothesis – Here a literature-derived methodology for overcoming the limitations within the problem space is declared. A sequential method of electrospinning aligned submicron and nanofiber and the ability to manipulate this alignment for the successive layering is described along with the ability to functionalise (bond) these fibres therefore creating a multi-layered structure of fibre occurring art varying alignments. Here the requirement to develop novel technology to accomplish this type of research and methodology validation is also declared.

Chapter 4: Experimental Component Development – This portion of the thesis describes the experimentation led development of mechanisms and technology required to generate the novel machine required for fibre-based additive manufacturing research and development. Here much discussion is related to the integration of automated technology with regards to electrospinning, vapour, plasma and lithography techniques. Portions within the chapter also discuss methodologies to overcome productivity-based limitations within the electrospinning process via electric field manipulation.

Chapter 5: Final Development of a novel Fibre based manufacturing research and development machine – The final amalgamation of technology as well as the implemented code to control this is discussed. Here the spatial limitations of the resultant machine are described to allow for the future development of modules.

Chapter 6: Discussion of evaluations related to the Hypothesis – Experimentation associated with the project that is responsible for the progression and development of mechanisms and machine functionality are described within this chapter. These include work related to mold/casting based approaches, the use of collectors for biomaterial-based electrospinning, the evaluation of functionalisation techniques, the evaluation of the machines capabilities, and the evaluation of the ability to validate the post-literature review hypothesis through this projects developments.

Chapter 7: Future Work and Recommendations –This section highlights the future optimization relative to developments and technology derived within the project. These relate to vapour, plasma, environmental control, code, electronics and component isolation relative to implemented high voltage.

Chapter 8: Project Conclusion – The project is surmised with reference to various stages of development and a statement made regarding the project's success.

Chapter 9: References – This section lists the established/published work from which this thesis and the work therein has been developed.

Chapter 2 LITERATURE REVIEW

This chapter discusses the literature that was utilised to derive the required direction for project progression. From this, the nature of the technology developed within the project was established. The review develops an understanding of the potential of current technology for the production of micron and nanofiber-based three-dimensional objects. The review analyses attempts made within traditional synthetic polymer 3D printing and then further explores the potential application of such 3D printing technology within biopolymer research (Tissue Engineering related work). With regards to the bio-based motivating element a further investigation regarding the requirements for such work is conducted relative to a chosen polymer (collagen) and potential structure (corneal stroma). From the limitations of current technology, a need to identify technology better suited for sub-micron fibre production (electrospinning) is justified. This techniques ability to process synthetic and the chosen biological material is then evaluated, from which additional techniques and technology are identified which allow for the generation of a framework for the project hypothesis.

2.1 Fibre-orientated composite 3D printing

The utilisation of fibre within 3D printing is of increasing research interest [34, 35]. This form of manufacturing aims to allow the generation of parts having not only greater mechanical abilities but also the ability to vary these capabilities relative to the characteristics of implemented fibre. Major requirements for the use of fibre to reinforce/strengthen polymer-based objects include the nature of fibre-polymer integration/bonding and the ability to control the orientation of fibre within the object.

Traditionally the generation of fibre-reinforced objects has occurred in a sequential manner whereby fibres are arranged in the desired form in the desired orientations. This arrangement is followed by the controlled implementation of polymer (typically in solution) to act to bind the fibres into the desired form. To achieve the required object, complex machinery (e.g. mold-based and weaving-based systems) and environmental control (typically this is related to the uniform application of pressure to ensure optimal polymer distribution/impregnation). Much research has been conducted regarding the use of 3D printing (3DP) technologies as a means to generate similar structures. This intends for the 3DP techniques related to the controlled introduction of material to be leveraged to control both the fibre-polymer integration as well as the resultant fibre characteristics (placement and orientation). From this ability, multi-material objects having engineered properties related to both the nature of implementation as well as the type of fibre utilised are intended to be generated.

Within research two styles of fibre-based printing have been discussed, namely continuous-fibre and short-fibre 3DP. Short-fibre-based methods involve the mixing of fibre segment within a polymer melt that can then be formed into a filament for extrusion-based printing. Alternatively, these pieces of fibre can also occur within resins in an attempt to leverage off lithography based printing [36]. The technique of printing using segmented fibre embedded in polymer has been described as having limited success relative to traditional methods of manufacturing. This limitation can be associated with the general lack in direct control of the fibre orientation

within the production. This project intends to focus on the generation of fibre-based objects in which the characteristics of this fibre is to be controlled; as such, short-fibre technology will not be further investigated. Alternatively, continuous-fibre-based methods attempt to utilise a length of fibre that is continually fed either in parallel to the extrusion or as part of a pre-made filament [34, 35]. This research has led to developments of commercial machines/products such as the MarkOne by Markforged, which is an FDM inspired approach to generate fibre-reinforced 3D printed parts. It is worth noting that due to the inherent lack of control associated with the material in its glass transition phase during the FDM process, the orientation of distributed fibre material will vary.

A major limitation of the current work within fibre-orientated 3DP relates to its dependency on established methods of 3DP. This results in the associated limitations of these techniques with respect to resolutions and processing effects upon the utilised material. Given the future interest in technology developed within this project to be capable of biopolymer-based manufacturing, there is a requirement to further evaluate the viability of such 3D printing techniques with respect to Tissue engineering.

2.2 Fundamentals of Tissue Engineering

Tissue engineering has been described as the result of a combination of biomimicry, autonomous self-assembly and grouping of mini-tissue building blocks [23]. In this instance, biomimicry refers to the desire for replication of biological constructs. Successful biomimicry is dependent on the understanding and replication of the fundamental aspects/constituents of biological constructs. Early cellular components are capable of self-induced/generated organisational development, which allows for the formation of required micro-architecture and biological function, and is referred to as autonomous self-assembly. This capability is due to the inherent capabilities of early cellular components to generate extracellular matrix (ECM) components, appropriate cell signalling, autonomous organisation, and patterning. Additionally tissues can often be segmented into small functional parts or mini-tissues, which can be appropriately placed and through the aid of tissue/cellular properties such as self-assembly the larger functional tissue/organ can be mimicked/produced [23].

Thus, for accurate tissue engineering an adept understanding within the fields of engineering, imaging, biomaterials, cell biology, biophysics, and medicine with respect to the desired biological construct are required. These aspects of tissue engineering occur in many of the studies surrounding the fabrication of tissues and organs through utilisation of bio-printing technologies [37-39].

2.2.1 Bio-printing technologies

3D Bio-printing technologies have been described as beneficial disruptive technologies for the advancement of Tissue Engineering and Regenerative Medicine[40]. This additive manufacturing based practice of utilising organic material to generate organic objects and tissues is known as bio-printing [16, 23]. The most prominent forms of bio-printing technology are extrusion-based, droplet-based and laser assisted printing. These techniques are classified as either direct or indirect, where direct refers to the layer-by-layer introduction of material to generate the final structure and indirect refers to the generation of sacrificial molds/scaffolds into which material is distributed and allowed to mature ,after which these can require post-processing to remove [16]. The mechanisms, within these techniques vary [21], and can allow for the manipulation of organic matter

at a macro (cell aggregate), micro (single cell) and nano(cells and proteins) level to generate various biological constructs highly sought after in the medical field [41]. Bio-printing at a macro level attempts to construct tissues through the precise placement of a collection of cells. The most prominent form of macro level this is that of extrusion printing. At a micro level the technology acts to construct tissues through the replication of precise cell placements. The most prominent form of this being inkjet or laser jet printing [21]. Some biological constructs are comprised of components with dimensions in the nanometre scaling (cells and proteins), as such methodologies for the replication of these constructs through fabrication at a nanometre level is of interest. This technology has been utilised to generate a variety of medicine related products such as drug testing models, controlled drug delivery systems, permanent implants, custom implants and biomimetic scaffolds[42].

The following summaries the commonplace differences in established bio-printing technology and references reviews such as those by Mandrycky *et al* (2016)[43], Gomes *et al* (2017)[40] and Zhang *et al* (2018)[42]. Of specific engineering interest are the differences between process able bio-inks, acceptable viscosities, cell viability, vertical print quality, and resultant cell density. These differences are described below:

Currently extrusion-based bio-printing is the most popular technique albeit still limited by the printability of available hydrogels[40]. Laser assisted bio-printing was described as capable of processing bio-inks in a moderate range of 1-300mPa/s whereas inkjet techniques were associated with lower viscosity ranges (3.5-12mPa/s [23, 43]). This differs with extrusion techniques which require bio-material to have relatively high viscosity (ranging from 30mPa/s-over 6x10^7mPa/s [43]) to restrict the unwanted leaking of material from the extrusion mechanism [41]. Both inkjet and laser assisted techniques were associated with poor and fair vertical structure quality whilst having high print resolution (with some inkjet techniques such as electrohydrodynamic printing capable of resolutions <10µm) whereas extrusion techniques had good vertical structure quality with moderate resolution (generally unable to accurately produce biological objects smaller than 100µm [44]). Typically resolutions in the range of 10-1000µm are utilised. Inkjet, Laser assisted and extrusion techniques had low (<10^6 cells/mL), medium (<10^8 cells/mL) and High (in the case of cell spheroids) resultant cell densities. The resultant cell viability of extrusion techniques are lower than that of droplet-based bio-printing, where cell survival rates are dependent on extrusion pressure and nozzle size [23]. There are many forms of Inkjet bio-printing (Figure 8) as such it has been recorded as capable of producing droplet sizes ranging from <1pL to >300pL with deposition rates from 1 -10000 droplets per second, these capabilities have allowed for the production of 50µm wide lines (produced via patterned drops) of one or two cells [23]. Inkjet technology is limited in that it requires the bio-ink to be in liquid form, thus to attain a functional (solid) tissue/result post inkjet processing of the result is generally required (post print cross-linking via chemical, pH or ultraviolet mechanisms). Both the inkjet and extrusion bio-printing processes are also limited by the depositing mechanism namely issues associated with nozzle size, nozzle clogging (through material sedimentation and aggregation), spatial accuracy, exertion of shear stress on material [23, 24, 42, 45]. Current bio-printing practices predominantly focus on the accurate placement of a cell or group of cells. Most of these practices are limited by the predominant reliance on the utilisation of heat and pressure for higher resolutions which can yield complications and damages(known as denaturing) to the biological material (illustrated in Figure 7), an exception being that of electrohydrodynamic printing [46, 47].

From the above literature [40, 42] the following limitations in bio-printing developments have been derived, namely:

- limitations in nano and nanocomposite object generation
- a lack of productivity (the process takes too long),
- a lack of multi-cell implantation
- limited organ nutritional supply strategies
- high distribution density
- precise spatial positioning
- limited success in generating vascularity
- oriented blood vessel growth

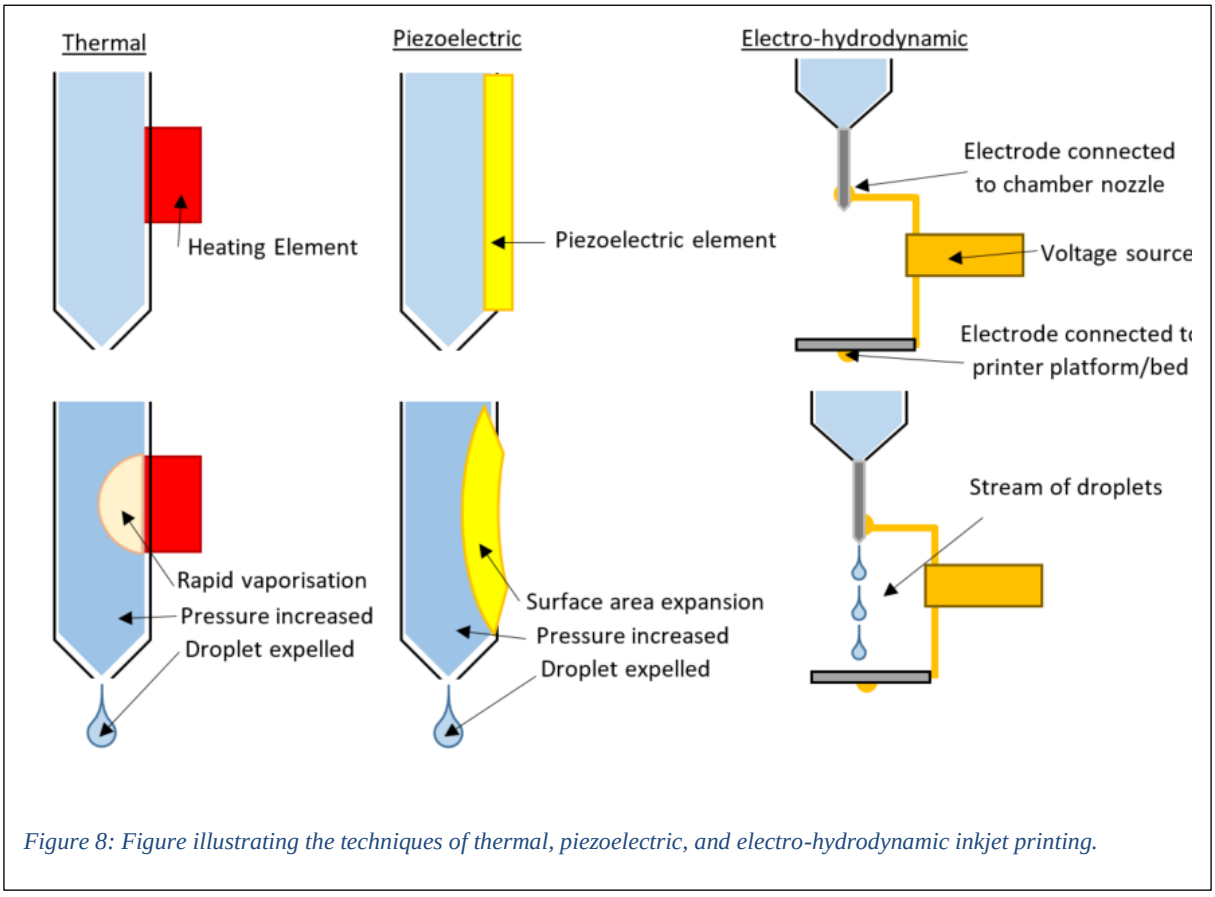

Figure 8: Figure illustrating the techniques of thermal, piezoelectric, and electro-hydrodynamic inkjet printing.

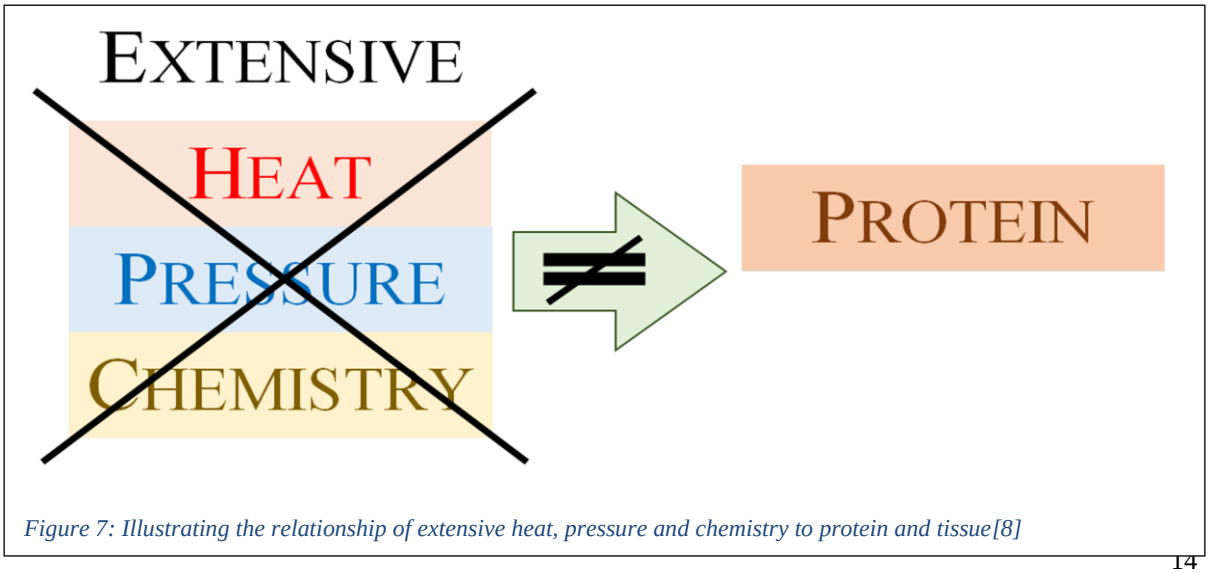

Figure 7: Illustrating the relationship of extensive heat, pressure and chemistry to protein and tissue[8]

In general, there is a lack of additive and bio-printing methodologies for the production of fibre for the generation of fibre based constructs that can be seen in biological structures such as tendon, cornea, muscle etc. These limitations reveal a requirement to further investigate the development of a biopolymer friendly form of nanofiber production based additive manufacturing technology. Thus, an understanding of the current technology for the generation of biological constructs is not sufficient for the reproduction of tissues. To further understand the requirements for the production of tissues found in the human body an understanding of the building blocks of these tissues needs to be developed. One such prominent building block within tissues is the protein collagen.

2.3 Collagen

All collagen is comprised of a repeating amino acid sequence within which there is a right hand twisted triple helix commonly referred to as tropocollagen. Tropocollagens are made from two identical α-chains (referred to as the α1-chains) and a third α2-chain. These α-chains are arranged in a left-handed polyproline II-type (PPII) helical conformation coil with a one-residue stagger relative to other α-chains. [48, 49] The tight packing of these PPII Helixes requires every third residue to be glycine, which in turn results in a X-Y-Gly sequence where X and Y can be any amino acid. The most common sequence of collagen is ProHypGly (where Pro (Proline):28% and Hyp (Hydroxyproline):30%)[25] [26, 48-50] [Figure 9].

Whilst collagen appears in various forms, the most prominent form of fibril collagen is type I collagen. [25, 51] Type I collagen is known as a FACIT (Fibril Associated Collagens with Interrupted Triple helices) collagen and appears in many biological constructs as a fundamental element yielding structure and strength. For the purpose of this research project a focus will be made on Type I collagen.

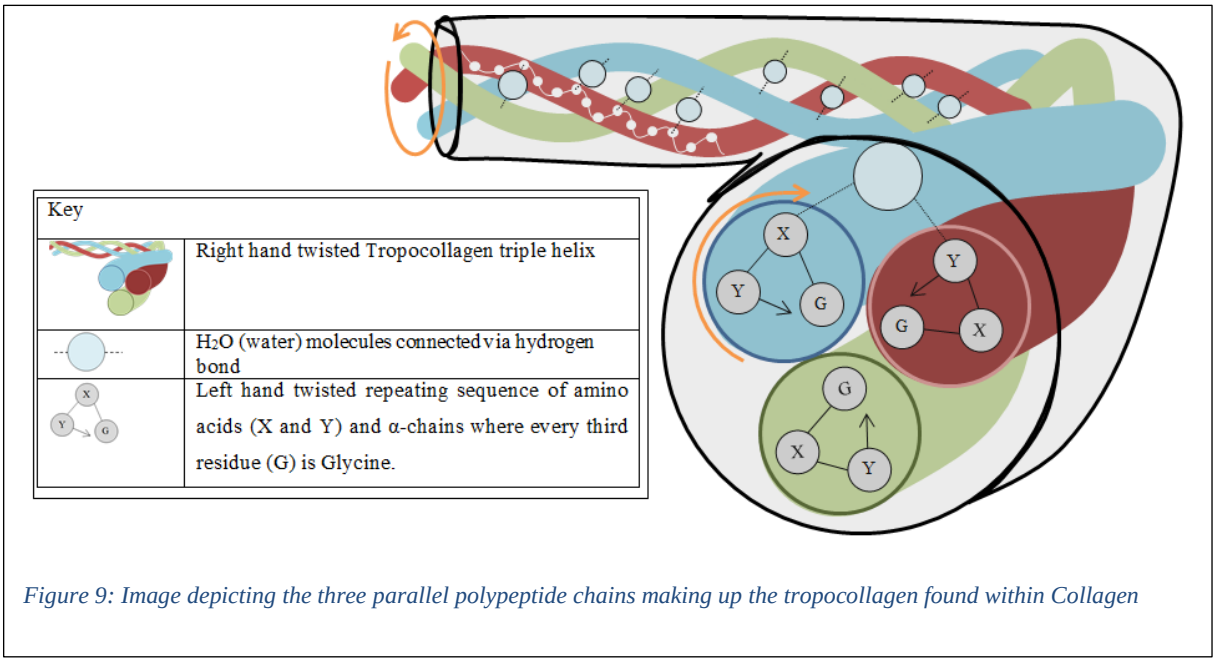

Figure 9: Image depicting the three parallel polypeptide chains making up the tropocollagen found within Collagen

2.3.1 Natural collagen fibre formation

Through the hierarchal arrangement of tropocollagen in groups of 5 staggered collagen, macroscopic collagen fibres like those seen in type I collagen are formed. The staggering results in gaps and overlaps between tropocollagen which generate fibre deformation known as D-banding (this can be seen through microscopy of collagen fibres) [Figure 10]. Within the human body these collagen fibres have diameters ranging from approximately 50-80nm [26, 50, 52].

2.3.1.1 Collagen based Structures

The strength of collagen-based structures is derived from the alignment and anisotropy of the collagen fibres [37]. To retain this alignment and anisotropy, adequate cross linking of the fibres (and fibre tropocollagen) is required. Thus these collagen based structures can be disrupted/modified by factors such as the exposure to high temperatures, solvents and changes in acidity which could alter these cross-links and deform the alignment or anisotropy within the tissue.

Given the prevalence of this protein, the ability to precisely control it will be fundamental to the generation of functional tissue and organ equivalents. To better understand the control required in collagen manipulation for Bio-printing and tissue generation an analysis of an existing predominantly collagen construct is required.

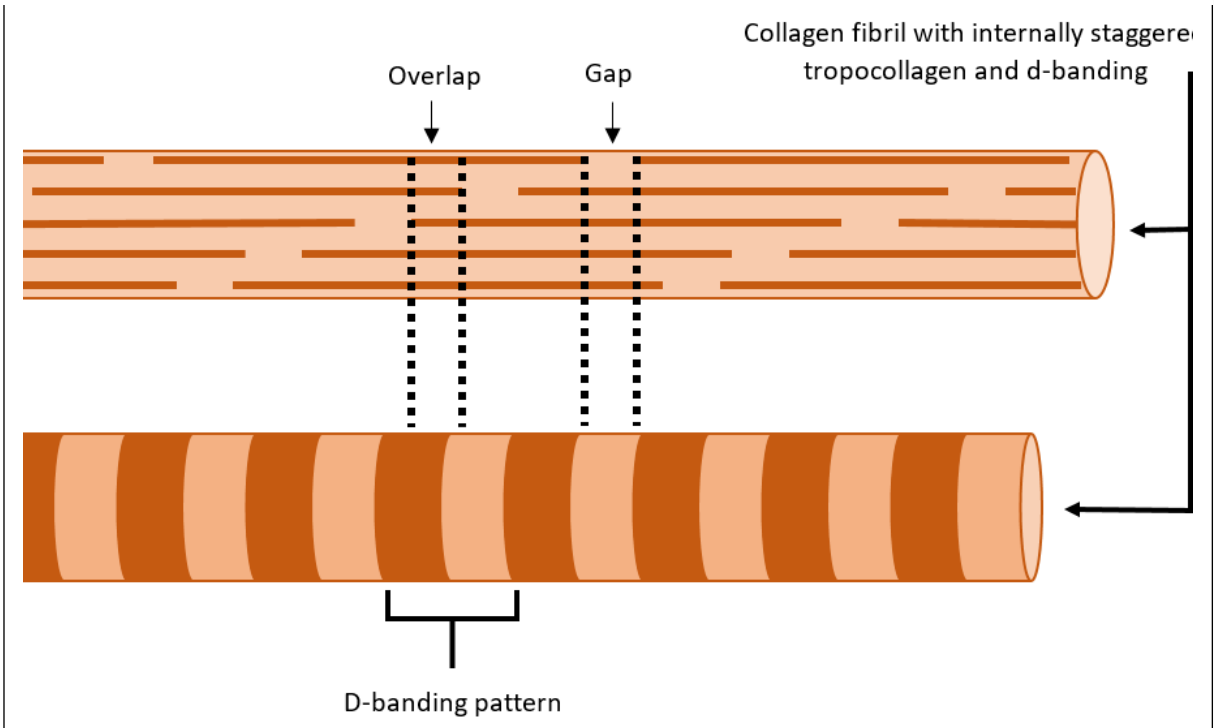

Figure 10: Figure illustrating a collagen fibre's internal staggered tropocollagen and source of d-banding

2.4 The Cornea

The Cornea is a good example of a primarily collagen based tissue. Corneal functionality is dependent on a very specific structural layout comprising of very specific cellular properties. The precise composition gives the cornea its strength, shape, and transparency [53-56]. Corneal tensile strength has been recorded as approximately 3-5MPa and the elongation at break approximately 0.19MPa [57]. It is also due to this precise nature of the corneas composition that difficulties have been experienced in attempting to replicate/manufacture the tissue[53].

Six different layers make up the cornea, each having various properties; these layers are the Epithelium, Bowman's Layer, Stroma, Dua's Layer, Decement's Membrane and the Endothelium [29, 58]. Additional information regarding these layers can be found in *Table 2: Information regarding the layers of the cornea* [58-60].

Table 2: Information regarding the layers of the cornea

Layer Name	Layer size	Layer Composition	Layer Responsibility
Epithelium	50µm (+/-10% of cornea)	5-7 stacked layers of cells	Prevents foreign objects from entering the eye and aids in hydration and transferal of nutrients and oxygen to the eye.
Bowman's Layer	10 µm	Acellular layer of densely packed collagen fibrils (Type I,III,V,VII)	Hypothesised to maintain stroma structural integrity, be a barrier against viral infection and trauma, and facilitate rapid stromal recovery.
Stroma	500µm (+/-90% of cornea)	Precisely aligned collagen nanofibers arranged in intersecting lamellae.	Provides both shape and mechanical properties (strength form and elasticity) to the cornea.
Dua's Layer	6.6-13.810µm	5-8 lamellae (predominantly type I collagen) situated in transverse, oblique and longitudinal directions.	
Decemet's Membrane	10-12 µm	Acellular layer of fibronectin, laminin, and Type IV collagen.	A tough and highly elastic layer providing much of the tissue's fluid regulation and preventing infection and injury.
Endothelium	20 microns wide and 4-6 microns thick	400 000 hexagonal cells	Removes excess fluid from the stroma ensuring stromal transparency.

Whilst the cornea is made up of seven differing layers, the majority of the tissue is comprised of the Stroma Layer; as such, a focus is made on understanding the features and requirements of this layer.

2.4.1 The stroma

The stroma is the largest layer within the Cornea and provides much of this tissues structural integrity and properties. The stroma is primarily constructed from highly ordered type I collagen nanofibers which are orientated parallel to the corneal surface. These occur as laminated lamellae which are embedded in a matrix comprised of water, type VI and non-FACIT collagens, glycoproteins (large insoluble molecules), proteoglycans, other soluble proteins such as fibronectin and laminin, glycosaminoglycans, keratin sulfate, dermatin sulfate, inorganic salts and keratocytes(which lie between stromal lamellae) [59, 61, 62].

2.4.1.1 Stromal lamellae

The collagen nanofibers within this layer typically have diameters 20-35nm, length 940um, and are spaced at approximately 30nm intervals within lamellae (sheets of parallel nanofibers) [Figure 12 and Figure 11]. Approximately 200-250 lamellae occur within the stroma [53], and it is hypothesised that the specific order of fibrils within these is regulated by stromal specific proteoglycans which occur as ring like structures surrounding fibrils [39]. The lamellae being approximately 2µm thick and 0.2mm wide are anchored in Bowman's layer and yield much of the corneas rigidity and structural stability [59, 61, 62].

The replication of aspects of this tissue will be fundamental in the progression towards the future capability to replicate not only this tissue but also similar biological constructs. Thus given that the collagen within tissues such as the stroma occurs as precisely aligned nanofiber lamellae, methodologies for the recreation of this alignment must be investigated.

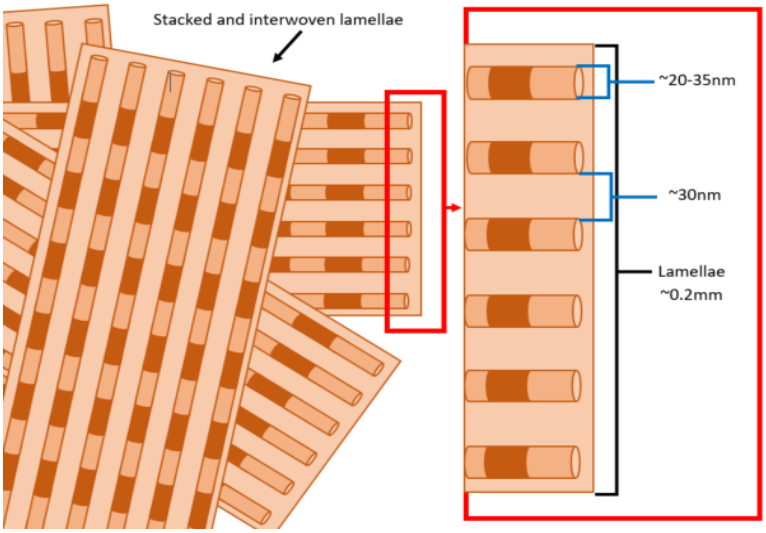

Figure 12: Figure demonstrating the aligned nature of collagen fibres within stacked and interwoven lamellae

Figure 11: SEM imaging of interwoven lamellae, from Collagen, Structure and Mechanics[5] .

2.5 Tissue engineering and bio-printing of collagen

Due to the fundamental nature of collagen within biological constructs, it has been studied and utilized in many tissue engineering and bio-printing applications. The use of collagen has been predominantly as a supporting scaffold to mimic the ECM and allow for cellular development/growth and proliferation of imbedded cell types [16, 63]. This research project is interested in the development of tissue engineering technology for the formation of predominantly collagen-based tissues with a focus on the layout and organisation of collagen in these tissues.

Given that the cornea is a good analogue for this focus, tissue engineering surrounding the development of corneal or stromal tissues is of interest. *Ghezzi et al* [53] reviewed these developments in 2015 and stated two predominant areas of tissue engineering with respect to the cornea, namely that tissue engineering was either of an allogenic or synthetic focus. Allogenic tissue engineering refers to the utilisation of donor tissue and as such is the preferred form of tissue engineering however due to a severe lack in donor graft material synthetic polymers have been studied as alternatives [38]. Tissue engineering of the stroma layer has had relatively limited success due to challenges involving stromal structural complexity, mechanical strength and transparency. Predominantly the attempts to tissue engineer these forms of tissues have been lab-based harvesting and culturing of cells utilising methods promoting stromal-like growth [37, 38, 53, 64-66]. One such lab-based approach to generate a stroma-like structure was conducted at the Department of Ophthalmology within Auckland University. Here a process of repeated and extensive centrifugal exposure to generate a scaffold of aligned collagen from a solution with high collagen concentration was utilised [67]. This process included 30 hours of continual centrifugal exposure at 4ºC and 2500rpm, samples were collected and then subjected to another 10hours after which samples were combined and exposed to a further hour of spinning. The final sample was then put into a humid chamber at 37ºC for 4 hours and dehydrated for 12 hours after which they rehydrated using MilliQ water for 4 hours. Thus, process required approximately 60 hours to yield the stromal analogue. The study was however limited in its ability to produce relevant fibres in layers of varying orientations [Figure 13 taken from [67]]. Additional limitations of this process related to the low productivity and the inability to easily scale this process for mass production. Thus, there is a continual interest to further investigate alternative means of production compatible with the requirements of tissue engineering and bio-printing.

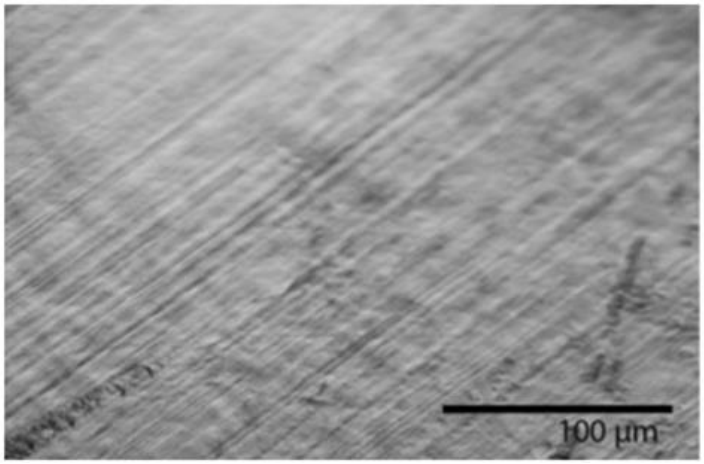

Figure 13: Microscopy of Lab based tissue demonstrating fibre alignment

Whilst current bio-printing methodologies are successful at replicating certain features found in-vitro, the technology is currently unable to generate all tissue requirements utilising a singular form of bio-printing technology. Thus, an inclusion of multiple forms of additive manufacturing based technology could potentially yield better results/tissues. Whilst this research project could be structured to follow a biomimicry-based approach, the desired outcome intends to yield a manufacturing research capability of both synthetic and bio-based fabrication relevance. Thus prior to further investigating a means for production of stroma-like structures, the engineering evaluation of this must occur.

2.6 Engineering Perspective on stroma-like Fibre implementation

The structural and functional properties of tissues have developed through years of evolution to overcome problems relating to the ability to survive. This does not necessarily mean that these developments and the nature of their results are optimal. An example of this lack in optimality would be the evolution of bipedal motion which is dependent on the functionality of muscle arrangements which can be classified as class III levers (having mechanical advantage of less than 0.1 and thus are highly inefficient) [68]. From an engineering perspective legs are a far less optimal design for simplistic mobility if compared to wheels, which is why we have cars with wheels instead of cars with legs. From this reasoning it becomes apparent that the analysis of the role of the cornea should be evaluated from an engineering perspective before embarking on a purely mimicry based approach.

The human eye can be described as a pressurised chamber [Figure 14] [69]; by removing the cornea, an opening in this pressurised chamber is created. This opening requires a seal in the form of a donor cornea or equivalent prosthesis. This replacement would not only have to be bio-compatible but would also require relatively isotropic properties as an imbalance could incur pressure concentrations which in turn could result in a rupture/breaking of the seal.

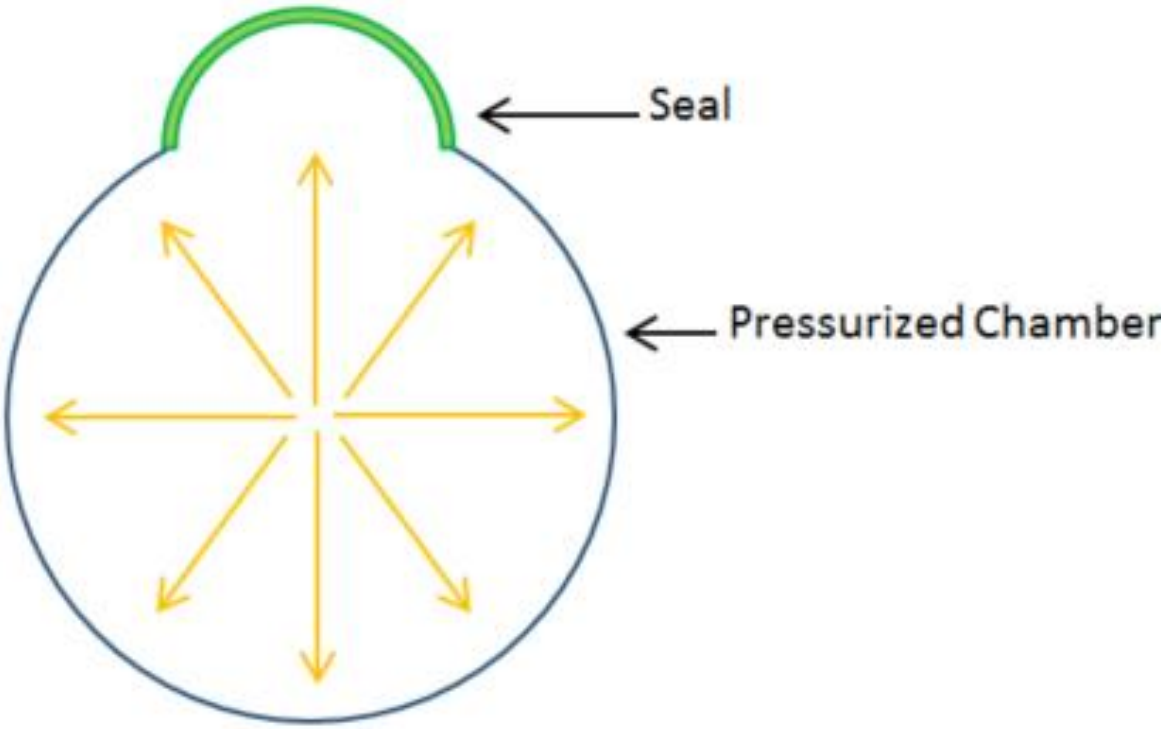

Figure 14: Interpretation of eye as pressurised chamber

The utilisation of interwoven fibre at varying orientations can be traced back to tribal traditions such as Raranga, the art of weaving, found within New Zealand's Māori culture [70]. Whilst this cultural practice predominantly makes use of harakeke, a form of flax found in New Zealand, engineers have developed this technique and applied it to many materials such as glass and carbon fibre. Carbon fibre is a popular choice for reinforcing or constructing objects of relatively high strength to weight ratio [35]. Typically, this occurs as the use of aligned fibres, which are woven into mats (to generate a higher degree of isotropy). These mats are also usually impregnated with a resin to retain fibre placement/mat shape as well as form a bond between fibres. This type of reinforcement can be seen in many industry such as the professional sailing (Americas cup), cycling (Tour De France) and motor sport (Formul1).

Coincidentally this engineering based approach at fibre alignment for strength is analogous to that of the evolutionarily developed stroma. As such, this project acknowledges the natural design of the stroma as similar to the fibre-based structures this project aims to create through 3D printing. As such, this structure alongside the aforementioned synthetic fibre-reinforced objects can be utilised as structural benchmarks for this project. It is worth noting that through the development of capability to enable such fabrication, there is a potential to create a new system through which much future research and development within fields of manufacturing and material science can be conducted. This desire to develop a manufacturing research and development system required an evaluation of alternative technology capable of submicron and nanofiber production that had the potential to be utilised in additive manufacturing.

2.7 Deriving Nano-fibres

Forcespinning, Melt blowing, flashspinning, biocomponentspinning, phase separation, drawing, and electrospinning are all methodologies that can be utilised to fabricate nano-fibres. The generated material often occurring as a mat comprised of randomly arranged nano-fibre. Electrospinning is a relatively repeatable and scalable process which has achieved popularity due to its ability to control the dimensions of generated fibres [71]. This technique (with the exception of melt electrospinning) does not expose material to the high temperatures associated with processes such as Meltblowing and Forcespinning allowing for fabrication utilising temperature sensitive polymers or proteins. When compared to Template synthesis or Self-assembly, the electrospinning process is relatively simple, potentially yielding less room for error. Other techniques such as Phase-separation (limited to certain polymers) or drawing (a discontinuous process) are relatively simplistic, however these lack the scalability and control associated with electrospinning [11]. In general, for nano-fibre production electrospinning, whilst not perfect and limited by timeous/productivity and solvency recovery issues, it appears as an optimal methodology for the future progression of this project.

2.8 Electrospinning

Electrospinning (electrostatic spinning) is a relatively rapid, efficient, and inexpensive process in which an electric field is utilised in the generation of nanofibers [72-74]. Nano- and micro-scale fibres have been electro-spun from over 200 polymers (both natural and synthetic polymers) [57]. This process can occur through the utilisation of a controlled or uncontrolled extrusion/feed system [11]. Given that controlled systems allow for greater control of fibre properties (quality and diameter) as well as having a higher success rate in electrospinning, these will be of predominant interest in this research project. The electrospinning process can be described as having three distinctive parts namely the Solution, the Charged Extruder and the Collecting Surface [49, 73] [75] [71] [Figure 15]. Currently the process is limited to the fabrication of mats (two-dimensional objects).

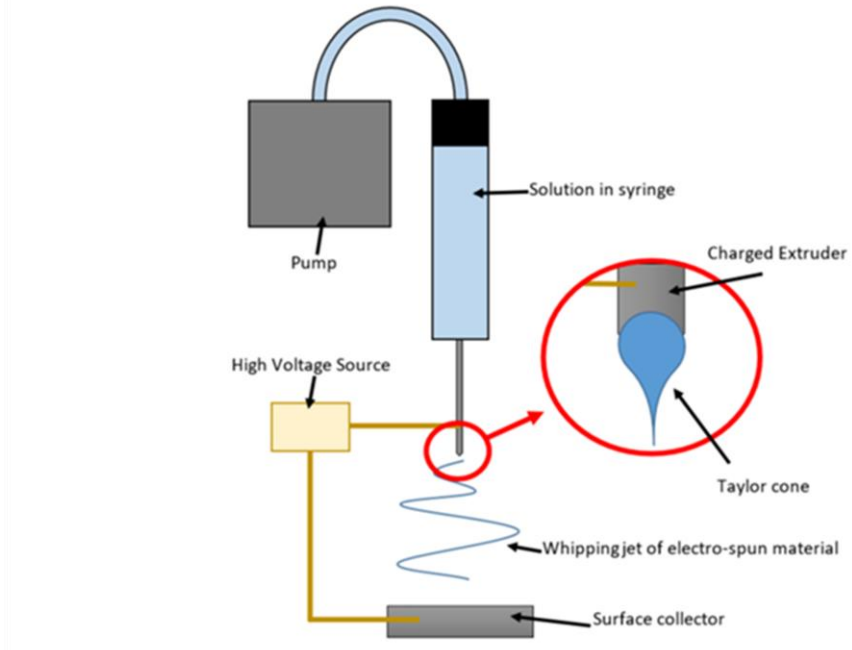

Figure 15: Figure illustrating the components and features of electrospinning

2.8.1 The fundamentals of an electrospinning process

2.8.1.1 Fundamental process:

In a typical process the 'Solution' is introduced into the system via the 'Charged Extruder' which forms a liquid droplet of the solution and implements a sufficiently high voltage (generally above 20 kV) [76] to charge the solution. This voltage results in the stretching of the droplet due to the mutual electrostatic repulsion between surface charges and Coulombic force from the external electric field[77]. The elongated and conical droplet is known as a Taylor cone. When the electrostatic forces overcome the surface tension forces of the solution an electrified stream of liquid jets out from the Taylor cone and approaches the oppositely charged 'Collecting surface'. This electrified stream continues to experience stretching as well as whipping processes whilst the solvent evaporates resulting in a fibre of the desired material. The 'Collecting surface' may be actuated which will result in variation within the collected fibre alignment.[73] [75] When required the 'Charged Extruder' will cease operation and all actuation of the 'Collecting surface' will stop resulting in fibres of the desired material in desired alignments situated upon the 'Collecting surface'.

2.8.1.2 Fundamental forces:

Electrospinning is an electrostatics-based process with the technology leveraging off established principles within this science. The movement of charge is of particular interest within this technology and is distinctively different to that of arcing techniques (such as those seen in welding) as it utilises relatively low current and as such does not generate or allow for the formation of an electrical arc through electrical breakdown. Coulombs Law (Equation 1) is often referred to when describing forces within the process, namely the understanding that repulsion occurs between similar/like charges and attraction occurs between opposite charges (Figure 17). It is worth noting the inversely proportional relationship between distance and coulombic force namely a greater force will be achieved at a smaller distance between charges. This principle is a major factor required to understand the actuation of electrospun material. Similarly, it is beneficial to understand the derivation of electrostatic force effects upon a charged element within an electric field (Equation 2 and Figure 16). From the relationships established in Equation 1 and Equation 2 we can derive a further Equation 3, which highlights a similar relationship between the magnitude of an electric field for a set distance, this will be greater for smaller distances.

$$F = \frac{kq_1Q_2}{d^2}$$

Equation 1: Coulombs law which describes the force between two charges q_1 and Q_2 in relation to the distance between these d^2, where k is the electrostatic constant (k=9x109Nm2/C).

$$E = \frac{F}{q} \longleftrightarrow F = Eq$$

Equation 2: The algebraic relationship of Electric Field magnitude(E) to Coulombic Force (F) for a given charge q.

$$E = \frac{\frac{kq_1Q_2}{d^2}}{q} \longleftrightarrow E = \frac{kQ_2}{d^2}$$

Equation 3: The use of Coulomb's Force equation in the ratio of electric field magnitude to identify relationships of magnitude (E) to distance (d)

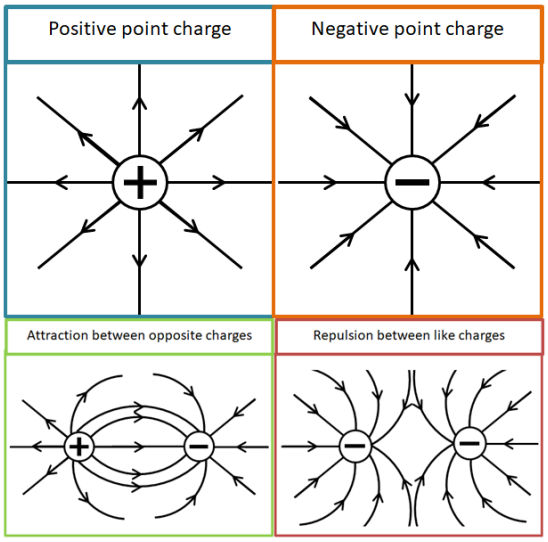

Figure 17: Image depicting the standard electric field line vector diagrams for point charges and the relation of attraction and repulsion between these

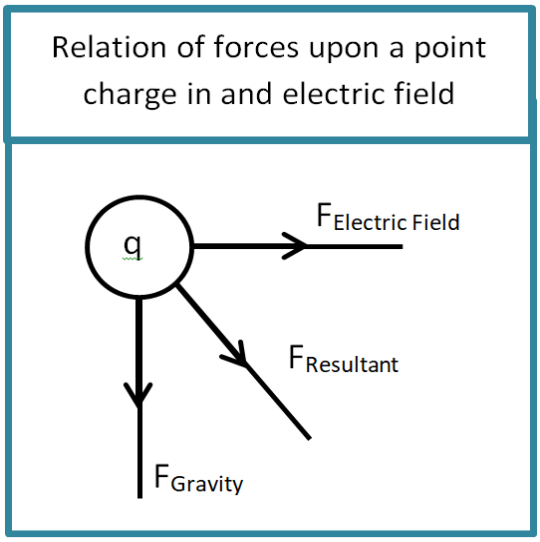

Figure 16: Image depicting the standard force vector diagram of a charge subjected to multiple forces including that of an Electric Field

It is also important to recognise the part of the additional fundamental forces acting upon the material, specifically the forces of surface tension. The convex meniscus generally generated within electrospinning (prior to the addition of charge and subsequent Taylor cone formation) is a good indication of how the internal cohesive forces between the molecules of the solution hold it together. It is important to note that a meniscus will only form when the surface forces are equal to forces exerted by gravity (equilibrium is reached) and that the surface tension forces are weaker than those occurring uniformly on internal molecules. Equation 4 aided by Figure 18 describes the surface tension forces and their relation to one another as well as highlights potential means for derivation of certain values.

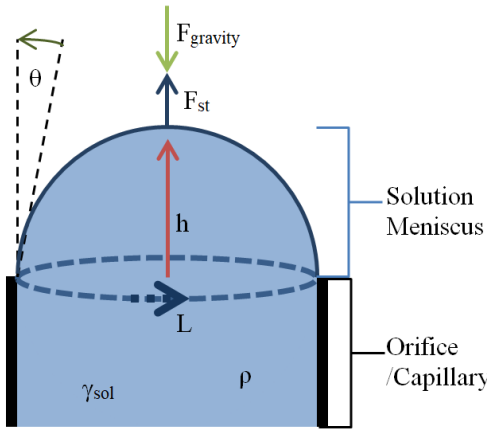

Figure 18: Image depicting the fundamental factors influencing the surface tension of a formed meniscus.

$$\gamma_{sol} = \frac{F_{st}}{Lcos\theta} \longleftrightarrow F_{st} = \gamma_{sol}\, Lcos\theta$$

$$note \rightarrow F_{st} = F_{gravity} = mg = \rho V g$$

$$thus \rightarrow \rho V g = \gamma_{sol}\, Lcos\theta$$

$$\gamma_{sol} = \frac{Lcos\theta}{\rho V g}$$

$$\gamma_{sol} = \frac{(2\pi r)cos\theta}{\rho((\pi r^2)h)g}$$

Equation 4: The nature of the surface tension force (F_{st}) in relation to the length at which it acts (in the case of a meniscus this is typically a circumference, L) and the contact angle between surface and solution θ are described. The relation of this to gravity in the case of a meniscus helps in determining integral values such as γ_{sol} the coefficient of surface tension for a derived solution.

To yield material actuation within electrospinning electrostatic forces must overcome the cohesive surface tension forces that occur at the material surface. These fundamental forces and principles of electrostatics help to illustrate the origin of the Taylor cone upon a material surface, namely the repulsion of charges within a material forming distortions directed/attracted to an oppositely charged area (within electrospinning this is the ground) and subsequent jetting of material (illustrated in Figure 20 and Figure 19). Whilst the above discussed electrostatic and surface tension equations are helpful in illustrating the fundamental physics of electrospinning, this research will not endeavour to generate a novel mathematical model to simulate the process. Much of the discussed principles are the basis for the processes within this technology, however these do not take into account factors such as resistances, rheology, additional external forces, and changes in forces all of which affect the jet and as such represent only an overview of the science. For further material on further in depth derivations taking into account these factors, the author suggests examples such as Ismail *et al's* 2016 work in [9] and Stepanyan *et al's* 2016 work in [78].

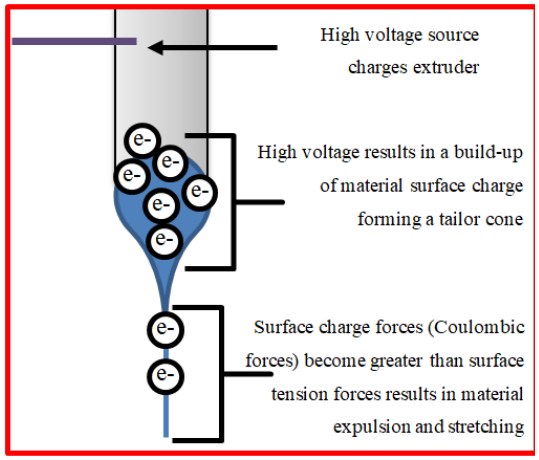

Figure 20: Image illustrating the build-up of charge and the subsequent electrostatic force within the Solution resulting in surface distortion (Taylor cone formation) and jetting of material.

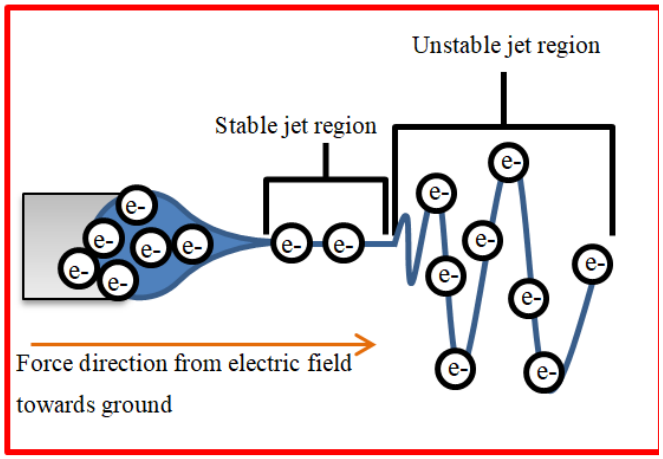

Figure 19: Image depicting the two regions of material jetting in electrospinning derived from[9].

Additional forces of interest within electrospinning include the nature of Van Der Walls forces occurring on the generated sub-micron and nanofiber. These frictional forces are best demonstrated by the ability of the fibres to be generated vertically upwards against the force of gravity and 'stick' to the collecting surface.

2.8.1.3 Fundamental properties:

The three major elements of the process namely, the 'Solution', 'Charged Extruder' and 'Collecting Surface' each contain a set of variables that have a direct effect on the nature of resultant electrospun fibre morphology. It should be noted that these variables have no standardised values and will vary according to the polymer processed. These and the nature of their relationship is described below and illustrated in *Table 3: Table describing the fundamental properties of electrospinning and the effects of the variation to these [51, 54]*.

2.8.1.3.1 Solution:

Typical electrospinning requires an aqueous solution of polymer (the desired material) dissolved in an acidic solvent. The main variables of interest for this include its conductivity, polymer concentration, and solvent boiling point. The critical conductivity for a solution will yield a Taylor cone and region of instability capable of

stretching fibres decreasing their resultant diameters, this capability can be modified by either the addition of salt or solvent utilised [73, 75, 76, 79]. At a critical concentration, uniform fibres are generated from increased entangled polymer chains which overcome forces from the surface tension and the electric field (this capability is modified through the w/v% utilised) [73, 75, 76, 79]. To ensure that wet electrospinning (the electrospinning of fibre that retains solvent at deposition) does not occur a solvent with a critical boiling point that will allow for ease of evaporation during jetting should be utilised [71, 79, 80].

2.8.1.3.2 Charged Extruder:

A charge is induced using a voltage source connected to the extruding mechanism through which the material is introduced to the system. The characteristics of the electrospinning process as well as the resultant fibre are influenced by this applied voltage, distance from collecting surface and rate of extrusion/flow of solution. The applied voltage is often in the range of several kilovolts and varying this will have an effect on factors such as spinning current, beaded morphology, fibre morphology and fibre structure. Increasing the voltage results in longer and smaller (diameter) fibres, however beaded morphology is likely to occur reducing the surface area [72, 76, 79]. The distance between the extruder and the collecting surface influences the fibre evaporation rate, deposition time and inconsistency interval. These factors affect the properties of the resultant fibre e.g. decreasing of this distance results in a wet fibre containing a beaded structure [72, 79]. Increasing the extrusion/flow rate of the solution results in larger fibre diameters as well as beaded morphology as such for smaller diameters a low rate of extrusion/flow should be implemented [72, 73, 75, 76, 79].

2.8.1.3.3 Collecting surface:

This surface will collect the material which is undergoing the electrospinning process. The resultant fibre will be affected by the type of collecting surface used as well as actuation of the surface (namely the speed of actuation). Factors such as the crystal orientation of fibres and evaporation of solvent are influenced by the speed of collecting surface rotation/actuation[72].

A note must be made that due to the accumulation of charge from the charged electrospun fibres on the collecting surface, electrospinning material is restricted to a thickness of approximately 3-4mm [81]. This limitation is acceptable for this research project (given the scale of the benchmark/example tissue); however this may not be true for projects aimed at mimicking larger scaled tissue. For such cases, a plausible solution could be the combining/laminating of sheets.

Humidity and Temperature have an effect on the evaporation of solvents utilised. An increase in temperature will increase the rate of evaporation yielding smaller fibre diameters. Some studies have utilised techniques of heating the Collecting Surfaces to enforce the evaporation of residual solvent upon fibres leading to increased fibre porosity [82].

Table 3: Table describing the fundamental properties of electrospinning and the effects of the variation to these [51, 54]

Property	**Too Low**	**Critical Value**	**Too High**	**Modified through**
Solution solvent boiling point: • Indicates volatility • Affects evaporation	• Dry formation of polymer at Extruder • blockages	• Easy solvent evaporation • dry nanofiber formation	• 'Wet electrospinning', • solvent coated fibres forming beads.	• solvent characteristics
Solution concentration: • Reaction of polymer chains to electric field and surface tension • Affects viscosity	• Broken Entangled polymer chains • fragmentation • beaded fibres	• Increased chain entanglement • uniform bead-less fibres • Concentration directly proportional to diameter	• Restricts flow • dry formation at the extruder • blockages	• w/v% of solution
Solution conductivity: • Affects taylor cone formation • Affects fibre diameter	• Unable to form Taylor cone/electrospin	• Increased surface charge • taylor cone formation • increase whipping/jet instabilities stretching fibres thinner(smaller diameter)	• Decrease in tangential electric field • reduction in electrostatic forces on surface	• polymer characteristics • solvent characteristics addition of salt
Applied Flowrate to Charged Extruder: • Affects introduction of material	• Timeous restrictions on production	• Slower flowrates are preferred as these aid in generating stable jets	• Reduction in surface charge density • incomplete drying, • beaded fibres • larger diameters. • Can result in droplets or streams of material (break in meniscus).	• Extrusion actuation modifications
Applied Voltage to Charged Extruder: • Affects strength of electric field	• Unable to form Taylor cone/electrospin	• Taylor cone formation and electrospinning of smooth fibre	• Decrease in taylor cone size • reduction in fibre stretching • beaded fibres	• Vary power supply/ supply output.
Distance of Charged Extruder to Collecting Surface: • Affects deposition time, evaporation rate and instability interval	• Wet electrospinning solvent • beaded fibre.	• Larger distances preferable as increased evaporation and instability interval result in smaller fibre diameter. • Fibre diameter and distance inversely proportional.	Generated electric field not strong enough to accurately transfer fibre	Manual or automated placement of Collecting Surface.

2.8.2 A nature based analogue

To better understand the fundamental process of electrospinning it is helpful to compare this to a simplistic analogue commonly found in nature, namely the technique employed by spiders to generate large web formations. Due to the potential difference between geographical areas of high and low pressure, wind is generated. This potential difference is symbolic of the potential difference generated between the high voltage and grounded sections of an electrospinning apparatus which in turn generate an electric field. The spider releases fibre which is then carried in the wind until it collides with a surface much in the same way that the fibres generated at the electrospinning nozzle are moved through the electric field and deposited onto the collecting surface [Figure 21].

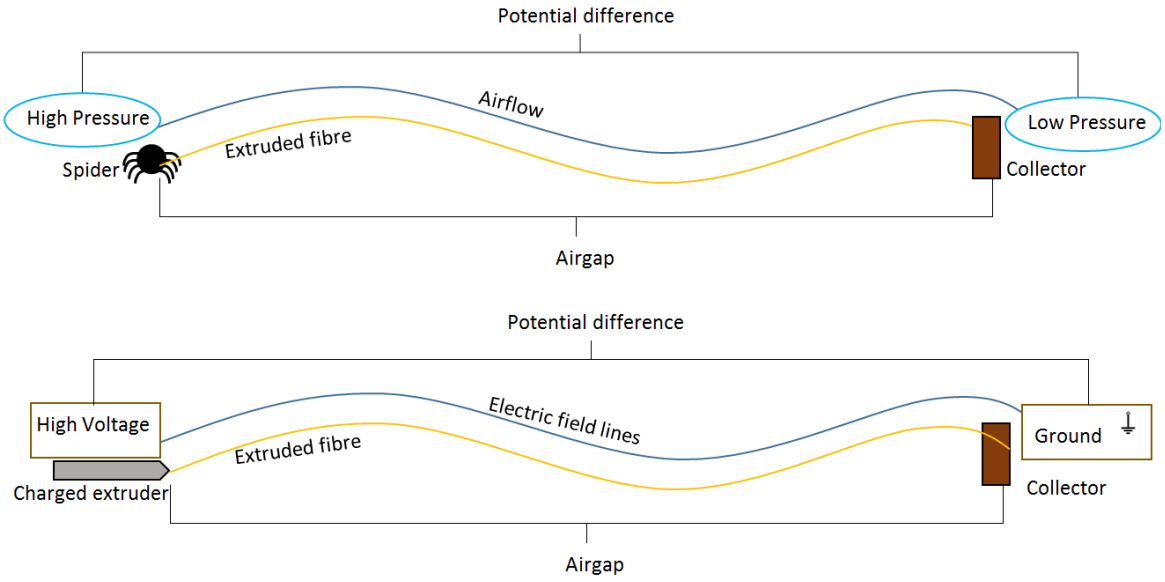

Figure 21: A comparison between the fibre formations of a spider and electrospinning

2.8.3 Electrospinning solvent limitations and alternatives

Through electrospinning both synthetic and organic polymers can be processed. Solvents utilized within this process are typically of an acidic nature which could result in toxicity yielding complications in biocompatibility[73]. Melt electrospinning is an alternative form of electrospinning which utilises heat to melt polymers allowing for electrospinning with less concern for toxicity from solvents. This is however a relatively underdeveloped process (limited to approximately 100 published articles) and currently is recorded as only capable of producing fibres much larger than those seen in traditional electrospinning [74]. Additionally this technique utilises high temperatures that we are attempting to avoid. Coaxial electrospinning refers to electrospinning which utilises a 'needle within a needle' system. This technique allows for the introduction of an additional material into the electrospinning process and yields sheath-core fibres where the inner and outer material of the fibres differ [Figure 22]. The outer/sheath material assists or carries the inner material in the electrospinning process. This is a particularly useful characteristic for materials which would otherwise not be able to undergo the electrospinning process, or require hazardous solvents for electrospinning. Emulsion electrospinning can yield similar results, however instead of requiring complex needle components this form of electrospinning utilises a chemical means of separation between the materials within a single solution [83]. Coaxial and emulsion electro-spun fibres tend to be larger than those generated by traditional electrospinning [83, 84]. As such traditional electrospinning is potentially better for the replication of stromal-like collagen nanofibers.

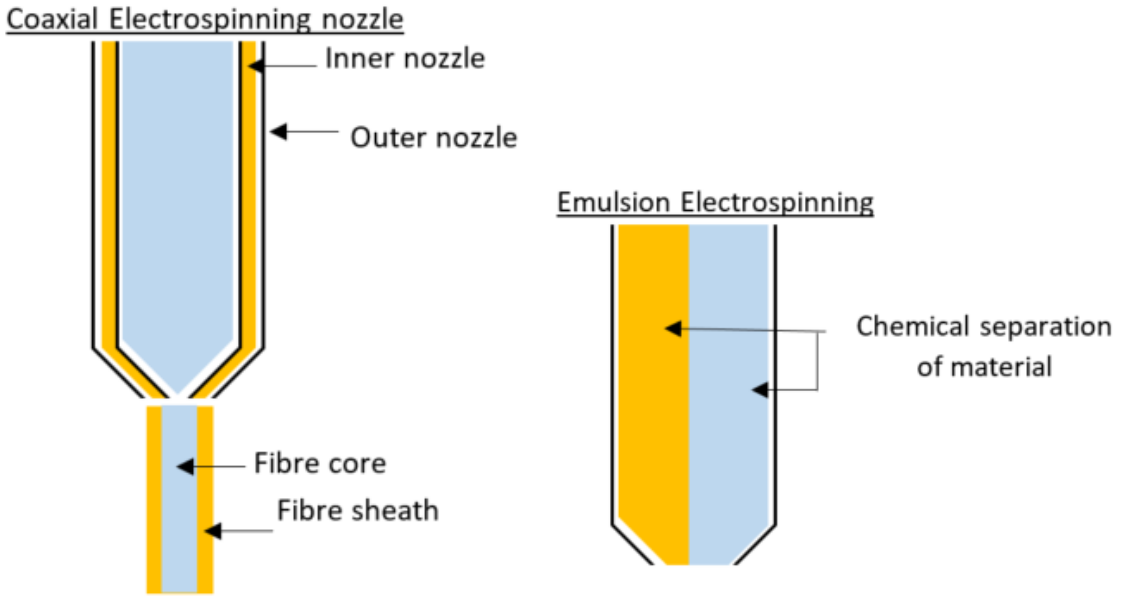

Figure 22: Figure demonstrating the differences in coaxial and emulsion electrospinning nozzle

2.8.4 Electrospinning efficiency

Standard electrospinning occurs through the utilisation of a single nozzle charged extruder which produces a single jet/stream of material. *Nayak et al* sited this as a cause for relatively low production of fibre over a given time period and stated an average production of 300mg/h [11]. This review described three mechanisms in which the throughput of electrospinning could be increased, namely; single needle yielding multiple jets, multiple needles, and needless. Although the mechanism for yielding multiple jets from a single charged extruder has yet to be fully understood/analysed, it is known that either the disruption of the electric field distribution or the partial blocking of the extruder can result in the formation of multiple jets. The use of multiple extruder needles yield complications, as the proximity of the needles (and their subsequent electric field) can alter the field properties of neighbouring needles. Thus for accuracy this mechanism requires adequate spacing between needles (increasing machine spatial requirements). It should be noted that these requirements differ between types of needle gauge and material. In general this mechanism is limited by issues derived from a lack in uniformity in the electric fields which yield uneven fibre deposition, clogging of needles, material dripping (a lack/failure of electrospinning) [11]. To overcome these issues needless systems have been utilised. These mechanisms have gained popularity for large scale electrospinning based nano-fibre manufacturing (e.g. Revolution fibres' – AGL electrospinning device [Figure 23][11]. This research project is currently not concerned with the throughput associated with standardised electrospinning; however, future development through the utilisation of a needless mechanism may be incorporated for higher production of research materials.

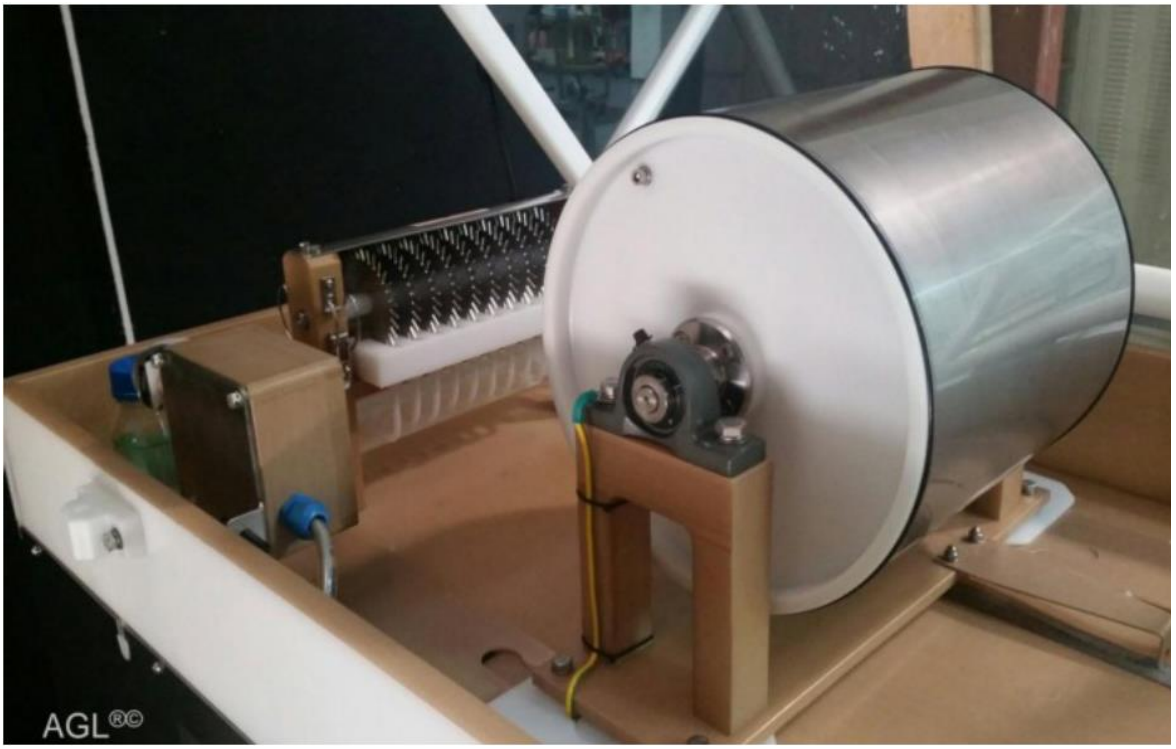

Figure 23: Revolution Fibres' AGL electrospinning device taken from [11]

2.8.5 Electrospinning aligned fibre

Many methodologies involved in the polymerisation (generation) of type I collagen gel, including that of standardised electrospinning onto a flat collecting plate, yield networks of randomised fibrils [63, 77]. The alignment of which can be altered through the application of strain, thermodynamics or magnetism during polymerisation [63]. Within electrospinning techniques the modification and actuation of the collecting surface can help generate alignment in produced fibres. The collecting surface has been split to generate a parallel electrode configuration with an airgap (sometimes filled with non-conductive collecting plate), and has been actuated to form rotating drum, disk, and conveyor collectors [73, 75, 77]. The use of rotational actuation generates alignment of fibre in the direction of rotation; this alignment and relatively even distribution is due to the mutual electrostatic repulsion between deposited fibres [77]. It must also be noted that by varying rotation speed, resultant fibre alignment can also be manipulated [72]. A major advantage of this mechanism is that it retains functionality when scaled for larger manufacturing requirements. This project is however interested in the generation of layers of differing orientations of aligned fibre. This type of control over direction of alignment is achievable via the use of parallel electrodes [6].This methodology exploits the electrostatic attraction of the formed nanofiber to oppositely charged areas, resulting in the stretching of the fibre between electrodes[72]. This mechanism has been recorded as relatively limited by scale (relative alignment lost at gaps greater than 30mm [85-87]. A recent study by Orr *et al* demonstrated that through the combination of alignment mechanisms these spatial limitations could be relatively overcome. In this study, a combination of ceramic magnets, parallel copper electrodes and distilled water was utilised to allow for alignment over a 100mm distance [85]. Another relatively underdeveloped method that allows for even greater control of distributed fibre is that of direct writing electrospinning. This control is derived from the automation of either collector or extruder at short collection distances. These shorter distances allow for the reduction in randomised jet instabilities this will however result in less evaporation yielding wet electrospinning.

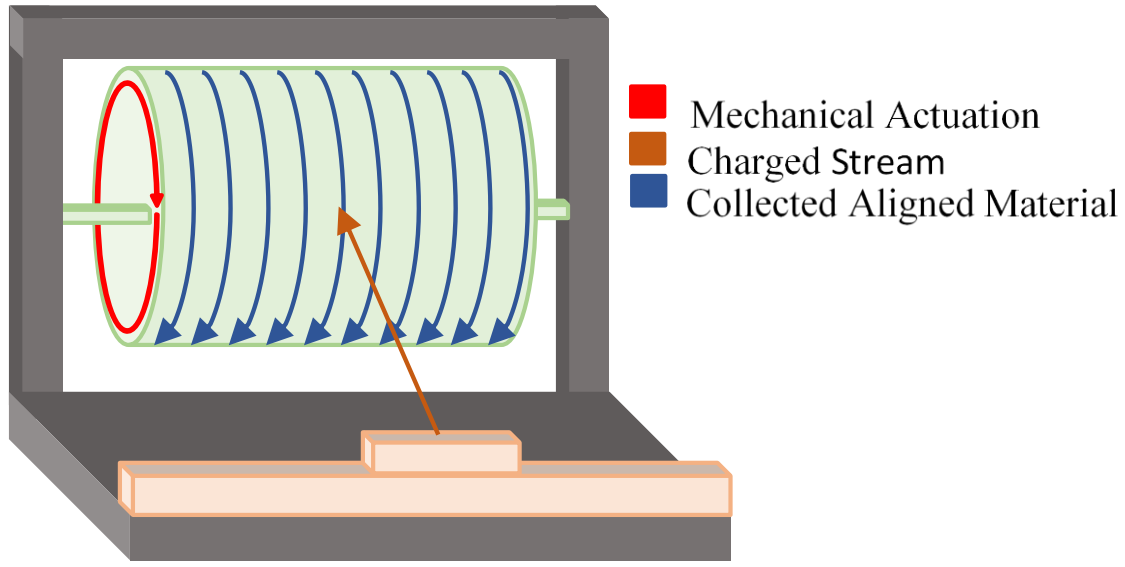

Figure 24: Figure demonstrating the basic operations for rotating mandrel electrospinning

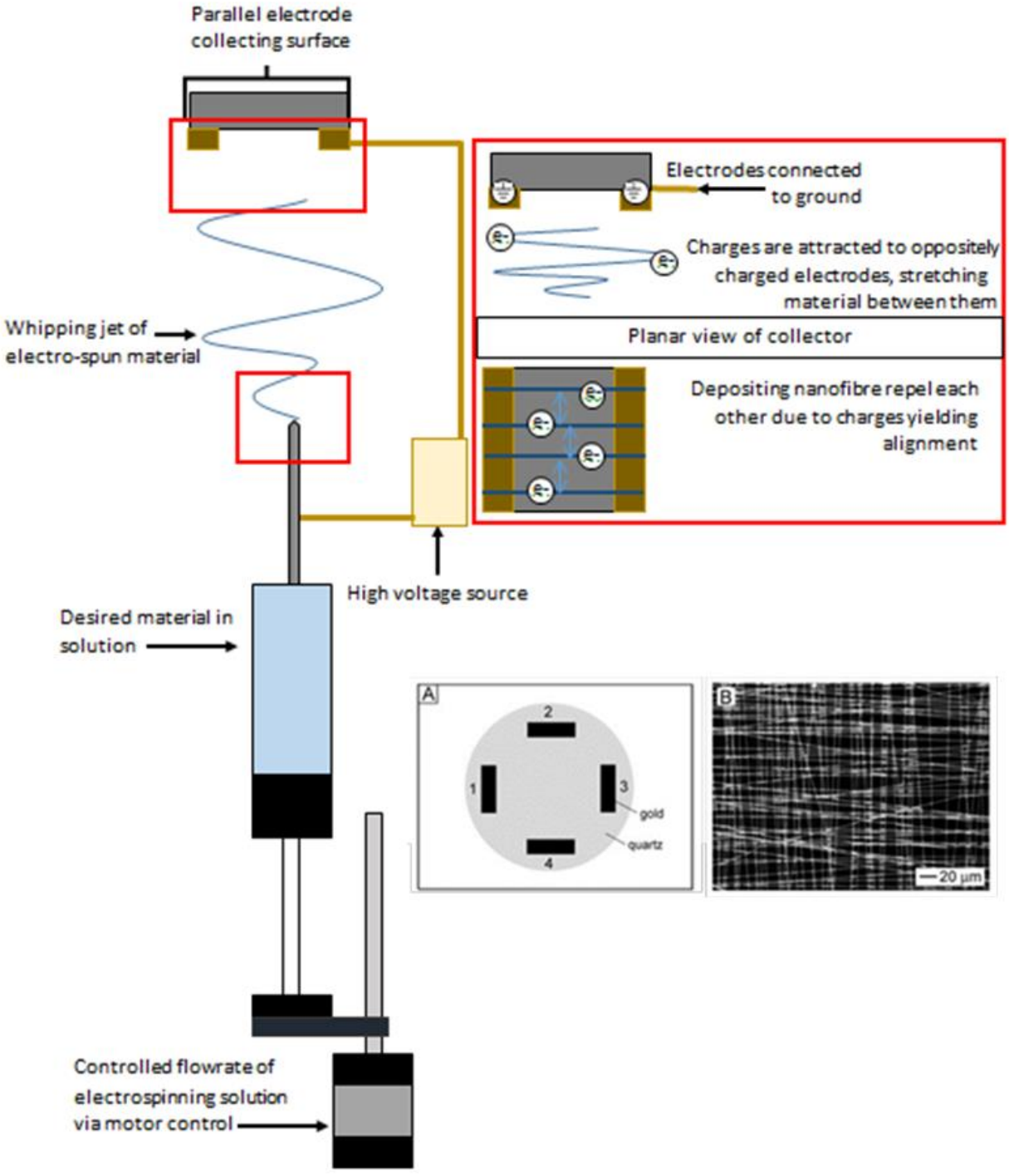

Figure 25: Image depicting the use of split electrodes to generate specific alignment patterns with examples A and B taken From [6]

There has been much interest regarding the use of electrospinning as a technology for the development of tissues or tissue scaffolds. The ability to produce a suitable biodegradable polymer scaffold from electro-spun collagen is of increasing interest[71, 88]. Collagen is the most abundant fibrous protein it can be sourced through various processes from various biological structures such as rat-tails and fish scales [25, 89]. As collagen type I is of predominant interest within this research project methodologies for the formation of aligned fibres of this collagen type will be investigated.

2.8.6 A review of Collagen Electrospinning for Tissue Engineering

Due to its prominence in tissue, Type I collagen can be acquired from a variety of sources such as rat tail, fish scales and calf skin [26] for electrospinning. Electrospinning yields results which are analogous to tissues containing aligned nanofibers (e.g. the stroma), however for this technology to be feasible for tissue engineering applications the resultant fibres must have similar degradation rates to natural equivalents, have similar functional properties (mechanical and optical), and be biocompatible. In order to achieve this studies have been conducted regarding the electrospinning of either single-polymer or multiple-polymer spinning of collagen [57]. As this research project is focused on the yielding of solely collagen based structures, only single-polymer collagen electrospinning is of interest.

Type I collagen has been successfully electro-spun into nanofibers in a range of studies [71, 88, 90-93]. "*Table 4: Showing the various electrospinning parameters utilized in previous studies*" demonstrates the utilisation and progression of collagen in electrospinning from 2006-2018. These studies were analysed to further develop an understanding of the norms and trends associated with these studies, from which future work can be justified. Voltages, delivery rates, and collector displacements within these studies were in the range of approximately 15-47kV, 1-7ml/h, and 100-250mm respectively. The following highlights the key understandings derived from these previous works:

In 2006 Zhong et al [88] noted that through the use of a rotating mandrel collector at a rotation speed of 10-20m/s high collagen fibre alignment could be attained. This study also revealed that an increase in alignment increased scaffold density and reduced the porosity. It also discussed the utilisation of cross-linking as a post process to decrease surface roughness. In 2009 Dong et al [94] expressed concerns for the toxic nature of solvents such as HFP (1, 1, 1,3,3,3 hexafluoro-2-propanol) which are prominent in electrospinning and the effects these have on collagen (reduction in hydrophobicity) and its fundamental chemical structural composition. HFP is the most commonly utilized solvent for the electrospinning of collagen (this is due to its relatively low boiling point of 61 °C which helps promote dry formation of fibrils [71, 88]. The highly volatile and cytotoxic nature of this substance is well known and some state that the use of it denatures collagen to a gelatin [90, 93] and thus is not desirable with respect to biocompatibility as well as studies dependant on a collagen result [95]. The denaturation of the protein has been described as due to with the fluorinated nature of HFP [93]. Dong et al used this understanding of the limitations in traditional solvents as the basis for their investigation into benign solvents. The study investigated the use of a combination of water, alcohol, and salt as a potential solvent. Their process achieved fibre formation and a note was made regarding the decrease in diameter with increase in salt concentration. Interestingly this limitation did not affect future utilisation of HFP , Jha et al (2011) [96], in collagen electrospinning for tissue engineering based applications. This study did however included extensive post processing, namely dissolving into ice cold 18MΩ-cm(resistivity to the flow of ions) water, 1-12hours of glutaraldehyde cross-linking, blocking in 0.1 M glycine, rincing in phosphate buffered saline (PBS), and finally disinfecting in 70% alcohol. This study actively utilised the generated tissue in wound healing and analysed the rate of recovery. Interestingly it noted a presence of banding in smaller diameter fibres, however argued that this was potentially irrelevant due to the general support of cell infiltration even stating that it is "not necessary to fully recapitulate the structure of native fibril to generate a biologically relevant tissue." Rather three key variables were stated for accurate tissue engineering, namely quality of initial material, the

conditions of electrospinning and the post processing methodologies utilised. In 2012 Meng et al [97] utilised an interesting technique of *in situ* cross-linking through the utilisation of a rather complex solution formation process. Understanding that the lack of inter and intramolecular cross-linking left electrospun material relatively vulnerable and having the desire to not utilise toxic solvents or cross-linking agents, Meng et al decided to incorporate a combination of ethanol, 1-ethyl-3-(3-dimethyl-aminopropyl)-1-carbodiimide hydrochloride (EDC), N-hydroxysuccinimide (NHS), and 20x PBS to generate a solvent to which collagen was added. Whilst yielding similar tensile strength to native tissue this process is potentially limited by its generation of relatively large fibre diameters, 0.42+/-0.11µm, due to higher viscosities. More recently in 2016 studies utilising both HFP and benign solvents such as Acetic acid can be seen in studies such as those by Dhand *et al* [98] and Castilla-Casadiego *et al* [93] respectively. A 2018 study by Le Corre-Bordes *et al* [99] compared the electrospinning of collagen (therein referred to as denatured whole chain collagen derived from New Zealand based hoki fish scales) utilising of acetic or citric acid as the benign solvent. This investigation noted that a lower concentration of collagen from cold-water fish was required in comparison to mammalian derived collagen (in this study bovine gelatin) and yielded lower diameters for studies utilising acetic acid (150-350nm).

Table 4: Showing the various electrospinning parameters utilized in previous studies

Name	Collagen source	Solvent	Concentration	Input Voltages	Air Gap Distances	Delivery Rates	Collecting Surface	Resultant Fibre Diameter
Zhong *et al:* (2006)[88]	Type I (calf skin)	HFP (1,1,1,3,3,3 hexafluoro-2-propanol)	0.08g/ml	15kV	150mm	1ml/h	15 m/s Approx. 19098rpm	
Dong et al: (2008)[90]	Type I 5% type III	Phosphate-buffered saline and ethanol. With a ratio of ethanol to buffer = 1:1	0.16g/ml	20kV	100mm	1ml/h	Rotating drum at 1m/s	210nm (at 20x salt concentration)
Jha et al: (2011) [96]	Type I	HFP (1,1,1,3,3,3 hexafluoro-2-propanol)	Varied	22kV	250mm	3-7ml/hr	*NS, **Ass: Stationary plate	Nominally 1µm
Meng et al: (2012) [97]	Type I	Ethanol, EDC, NHS, 20x PBS	0.16g/ml	20kV	120mm	0.5ml/h	Rotating drum at 5m/s	0.42+/-0.11µm
Dhand et al: (2016)[92]	Type I (Bovine)	Hexafluoro propanol	0.08g/ml	13kV	170mm	1ml/h	Stationary plate	~100nm
Castilla-Casadiego et al (2016)[93]	Type I	Acetic Acid	2,5,7 and10% w/v	20kV-47kV	100mm	1ml/h-5ml/h	Rotating mandrel 1554	~175-400nm
Le Corre-Bordes et al (2018) [99]	Type I (Hoki)	Acetic Acid	5-40wt%	30kV	100mm	Gravity fed	Stationary SEM pins	150-350nm
		Citric Acid	5-30wt%					300+/-25nm

*Not stated, **Assumed

2.8.7 Additional noteworthy developments for corneal and three dimensional electrospinning fabrication

Recent design and process-orientated developments relating to corneal tissue engineering have yielded techniques such as:

- The laser perforation of electrospun scaffolds to increase the porosity and integration of biomaterial [100]
- An introduction of a novel method of collecting aligned electrospun fibre [101]
- The application of heat to collectors in the attempt to evaporate residual solvents and thereby increase fibre porosity [82]
- The use of a hemispherical collector designed to achieve fibres aligned radially from a semi-sphere summit [102]

A note should be made regarding the studies which have utilised multiple polymers/additional polymers together with collagen studies [57, 100, 103]. These combinations overcome difficulties associated with the hydrophobicity/functionality of electrospun collagens. Whilst such studies have been employed in investigations focused on corneal reproduction/tissue engineering this research will instead focus on the alternative functionalisation techniques employed in solely collagen-based electrospinning. In many electrospinning studies electro-spun fibres lack the functionality derived from fibre-to-fibre cross-linking seen in natural tissue and other manufacturing processes. From an engineering perspective there is a lack of structural bonding holding the fibres together (an example would be a lack in resin in a carbon fibre matrix).

2.9 Functionalisation of Electro-spun Fibres

The post processing of electrospun fibres such as collagen is often in the form of crosslinking, the bonding of adjacent fibrils together to formulate a functional group/scaffold[104]. It is through this bonding that the mechanical strength, elasticity and wear resistance of the natural collagen fibre-based constructs is derived [91].

2.9.1 Functionalisation through chemistry

From a chemical/chemistry perspective there are two predominant methodologies for functionalisation, namely covalent chemical and amino-acid side chain intermolecular cross-linking [105].

Covalent chemical cross-linking makes use of agents such as glutaraldehyde, epoxy compounds, and isocyanates neighbouring collagen fibrils can be covalently coupled. Glutaraldehyde is a popular choice found in many studies due to its availability, low cost, solubility in aqueous solution and rapid reactivity [88, 105, 106]. This process is however limited in that agent properties become embedded in the fibre yielding issues in biocompatibility. In particular, glutaraldehyde is highly toxic and as such is not an ideal candidate as an agent for cases requiring implantation or heightened exposure. The process known as amino acid side chain intermolecular cross-linking does not embed agent contaminants, rather agents such as carbodiimide or azyl azide act as catalysts promoting the bonding of already present and reactive amino acid side chains. These agents are advantageous in that they can easily be removed after the crosslinking has occurred [105]. A recent study comparing the application of the agents glutaraldehyde, genipin, EDC and ADC-NHS yielded that collagen crosslinked with either N-(3-dimethylaminopropyl)-N0-ethyl-carbodiimide hydrochloride (EDC) or EDC with N-hydroxy-sulfosuccinimide (EDC–NHS) was optimal at retaining fibre morphology, resisting degradation and ensuring stability in physiological fluid over time[91].

2.9.2 Functionalisation through engineering

From an engineering perspective there are two predominant methodologies for functionalisation, namely polymerizing compound and physiochemical cross-linking [105].

Collagen fibre structures can be reinforced through the exposure to polymerising compounds which act to hold the fibres in place retaining form and optimal structural functionality. This process is comparable to the common engineering practise of adding a resin-component to fibre matrixes, an example being the addition of resin to carbon fibres allowing for carbon fibre reinforcement. It must be noted that the resin-components are chemically separate from the fibre matrix and act purely as support and not a form of inter-fibre bonding. When utilising this method of functionalisation the requirements for biocompatibility of the polymer used must be equal to those of the resulting application [105]. For situations in which the application of chemical or polymerising agents is not viable, technology can be utilised to generate physiochemical cross-links. These processes make use of photooxidation, dehydrothermal treatment, dehydration and microwave irradiation to activate reactive amino acid side chains for bonding. One such physiochemical method known as UV irradiation includes the exposure of the collagen to 254 or 514 nm wavelength light. This method does not introduce any potentially toxic elements, however overexposure to treatments such as UV irradiation can degrade the collagen [105].

As this project deals with the generation of biocompatible structures, interest include the currently accepted medical practices which involve in vivo functionalisation of collagen fibre found in this projects introduction/motivation (i.e. treatments involving the cornea).

2.9.3 In vivo cross-linking

The cross linking of collagen *in vivo* to treat the corneal ailment known as keratoconus is of particular interest as these cases require a highly biocompatible crosslinking process. This crosslinking occurs through a physiochemical process where the collagen is exposed to liquid riboflavin/vitamin B2, which acts as a photosensitizer for the collagen, and ultraviolet A light (UVA), which acts as a photo-activator for the cross-linking process [107, 108]. Whilst the exact location of this crosslinking is unknown, it is hypothesised to occur at a molecular level, between individual fibrils or between fibrils and the surrounding matrix. This methodology has resulted in the stabilisation of the biomechanical properties of the collagen within the cornea for more than 10 years [109]. In general, this corneal collagen crosslinking procedure occurs as the introduction of riboflavin over a duration of time after which there is a pause which is assumed to allow for the riboflavin to interact with as much collagen as possible, this is followed by UVA exposure [108-110]. This process, specifically the speed and duration at which the cornea is exposed to riboflavin and UVA is limited by the in vivo nature of the treatment. Of interest is the potential to introduce this riboflavin-based crosslinking methodology to an additive manufacturing based approach whereby the riboflavin crosslinking occurs thoroughly within the resultant collagen tissue. Due to the uncertain nature of the location of the crosslinking through this treatment, there is a potential requirement to ensure that other cornea constituents such as proteoglycans and additional collagen types are included in this process. A note should be made regarding the already present cross-links in this in-vivo based procedure.

2.10 Application of Functionalisation

Predominantly the application of functionalisation agents has occurred as a post process separate to the electrospinning [104]. Of interest would be the inclusion of controlled/automated agent delivery. There is also interest in the inclusion of Additive manufacturing techniques as well as other coating mechanisms to achieve this goal.

2.10.1 Depositional Additive Manufacturing

Within Additive manufacturing, the two predominant forms of material deposition are extrusion and droplet based printing. Both of these techniques have been employed alongside electrospinning, generally in the form of a layer from one process being followed by a layer from the other process [81, 111, 112] (Figure 26). It is useful then to understand the processes involved in these 3D printing techniques, as these can be applied to future applications of functionalisation.

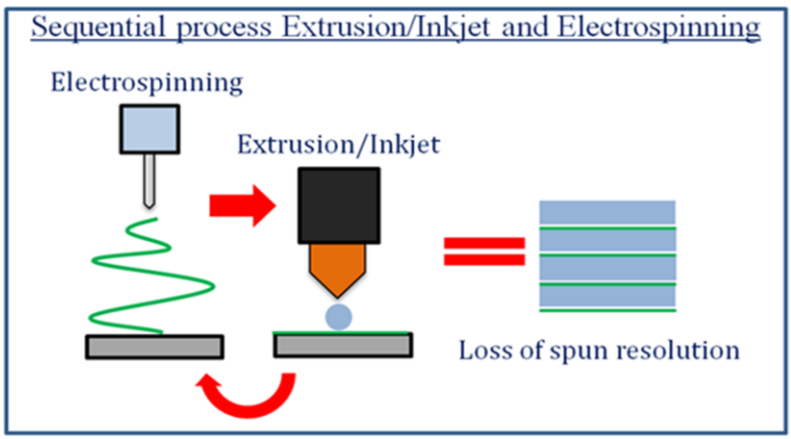

Figure 26: Image depicting the loss of electrospinning z-resolution via the introduction of extrusion/Inkjet methodologies.

Extrusion based printing is perhaps the simplest form of 3D printing, this utilises force from either pneumatic or mechanical mechanisms to generate a stream of material at precise locations. Unlike this, droplet based printing occurs in many forms, namely inkjet, acoustic and microvalve printing. Within these forms inkjet is the most popular this is in part due to acoustic printing being susceptible to failure from exposure to external disturbances commonly found within automation and 3D printing [113] and micro-valve printing yielding relatively poor resolution [113, 114]. Inkjet occurs as either continuous or drop-on-demand, the latter being preferential as it allows for greater depositional control [24, 45]. Additionally this occurs through two predominant mechanisms, namely thermal (rapid induction of extensive heat, 200-300ºC in bio-printing, resulting in rapid vaporisation forming a bubble and pressure wave which expels a droplet), and piezoelectric (induction of high pressure which expels a droplet). A note should be made regarding inkjet's electro-hydrodynamic jet printing a continuous printing form which employs similar mechanisms to electrospinning and relatively small droplets (resolution dependent on the same parameters found within electrospinning) are generated instead of fibres [24, 41, 46, 47, 73, 113-116]. Note that as with other forms of continuous inkjet printing there is relatively little control associated with electro-hydrodynamic printing.

One of the major drawbacks of implementing current additive manufacturing techniques as post processes is the loss of the z-based nano-scale resolution. Thus, there is interest in the ability for agent application at a nano-scale (as discussed in The Problem Space) and the potential of coating mechanisms to accomplish this. Due to the biological nature of the project, coating mechanisms that generate excessive heat such as plasma or arc spray coating mechanisms will not be of interest. A coating mechanism common to both additive manufacturing post processing as well as electrospinning crosslinking is the exposure of fabricated objects to vapour from a vapour bath mechanism [117-119]. This technique allows for an increased surface area exposure to functionalisation/processing agent however typically requires an extensive period of exposure to ensure maximum results. Typically, this process makes use of an actuator to encourage the vaporisation of a collection/bath of solution above which the part is hung [Figure 27]. Ultrasonic atomization (UA) is a good example of such an actuator. [120-122]. The component acts to generate a series of high frequency pulses within a solution, these pulses generate agitation upon the surface of the media which results in the dispelling of particulates in the form of vapour. This technique is capable of generating particulates below 100nm through the modification of transducer wave amplitude and frequency [120]. A key benefit for the utilisation of vapour for functionalisation is that the resolution of the object could potentially remain relatively unchanged, as interaction will occur at the resolution of the resulting vapours particulate (typically nano-scale). The major drawback for vapour techniques is the lack in ability to control the deposition of vapour particulates.

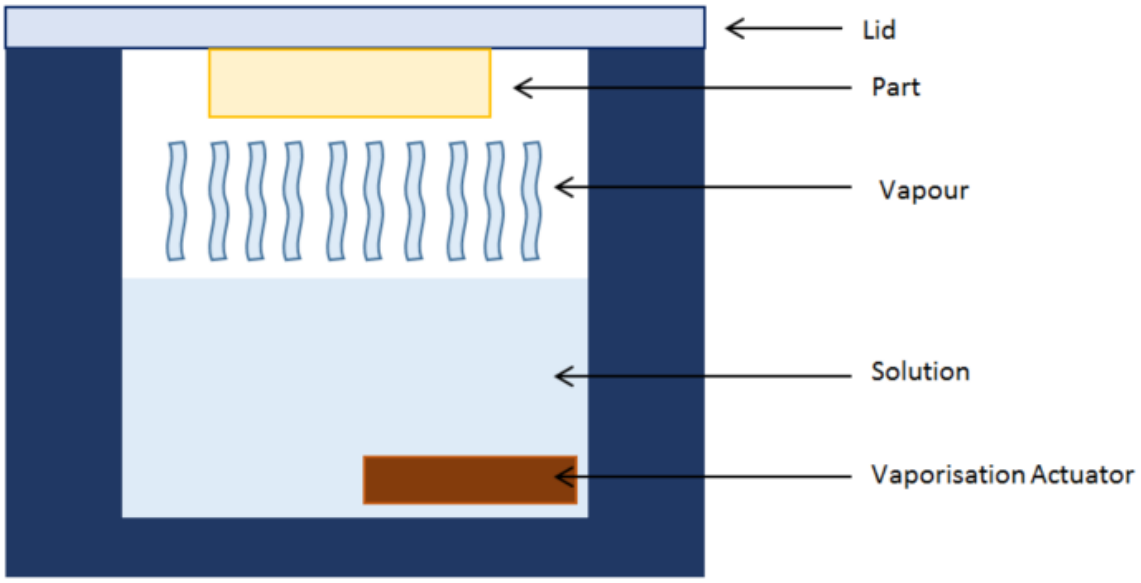

Figure 27: An example depiction of vapour exposure for post processing

2.11 Literature Review Summary

From the above review, the following understandings have been derived. Additive manufacturing research relating to the use of 3D printing in the generation of fibre-reinforced structures is highly relevant for the production of objects having greater mechanical capabilities. Additionally fields such as Tissue Engineering utilise 3D printing in the form of bio-printing to generate significant structures from biopolymers. Bio-printing mechanisms have the current capability to accurately distribute cells at a nanoscale (inkjet and electro-hydrodynamic bio-printing). These technologies however lack the capabilities to generate structures comprising of precisely placed and functionalised nanofibers in layers of alternating orientations such as those found in structures such as the stroma. The stroma is similar in structure to established fibre-reinforcement within typical engineering. Currently no Additive manufacturing technique whereby control related to the characteristics of produced fibre can simulate such structures exists. Electrospinning is a technology capable of this nanofiber production and controlled fibre placement however yields issues with fibre functionality and biocompatibility. Methodologies have been employed to resolve these limitations through the application of functionalisation agents; however, these have resulted in the loss of the desirable high-resolution. Vapour-based techniques could potentially resolve this limitation but these currently lack sufficient control for complex tissue fabrication.

The literature review has provided an understanding of the current potential for submicron and nanofiber-based fabrication through additive manufacturing. From this, a project hypothesis is formulated and future work justified.

Chapter 3 POST LITERATURE REVIEW HYPOTHESIS

The project hypothesis is focussed on resolving certain limitations within additive manufacturing namely control of fibre formation and alignment, the manipulation of constituents at nano-resolutions and the implementation of precision without extensive heat and pressure [15]. The understanding derived from the current Literature Review has yielded a hypothesized technique capable of implementing an additive manufacturing based approach to yield structures having submicron and nanofiber based characteristics, similar to those seen in the traditional fibre reinforced objects and biological tissues such as the stroma [Figure 29]. Utilizing established electrospinning technology aligned nanofibers will be produced in a single orientation. These will be collected upon a surface that will then be exposed to a coating of vaporized functionalization agent. This surface will then be actuated allowing for the electrospinning of a new layer of aligned fibre in a different orientation to the previous layer. Through the repetition of this action, the process will implement additive manufacturing's fundamental layer-by-layer approach to yield a structure. These will contain aligned fibre at varying orientations and be similar to tissues like the stroma [5, 65, 67]. Through variation in the areas of applied functionalization, complex three-dimensional objects can be generated (a technique similar to binderjet 3D printing). Currently there exists no means to accomplish the validation of this hypothesis as a manufacturing technology. As such work will be conducted to generate a novel research and development orientated device capable of both validating the intended hypothesis as well as allow for further research variations and development within this field [Figure 28].

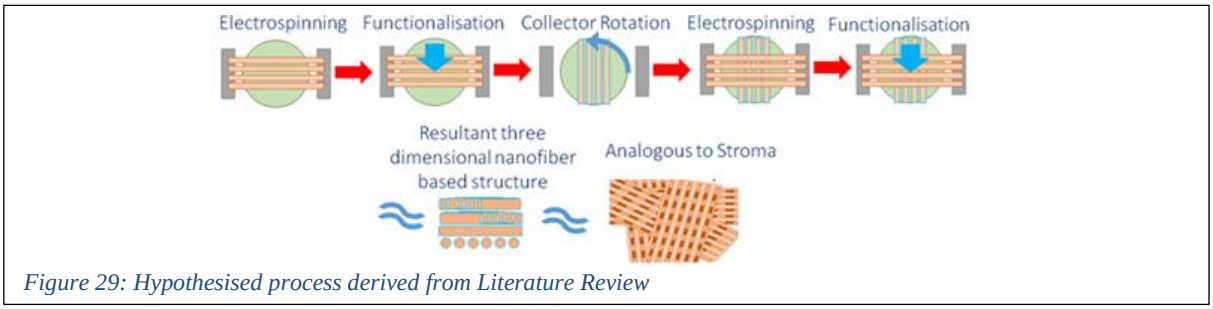

Figure 29: Hypothesised process derived from Literature Review

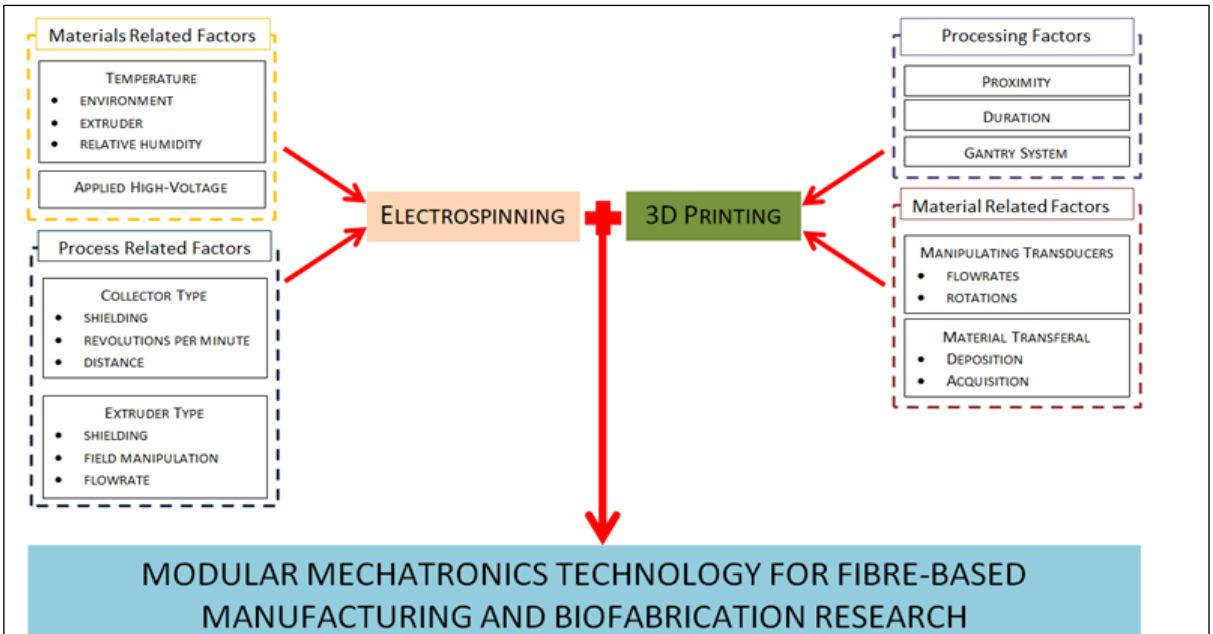

Figure 28: Flowchart demonstrating the technological requirements for the hypothesised research and development machine

Chapter 4 EXPERIMENTAL COMPONENT DEVELOPMENT

In order to evaluate the accuracy of the projects hypothesis within the project, various mechanisms/technologies were required. This chapter will discuss how this research and development was facilitated within the scope of the resources available for the project. The ideation, development, and evaluation of mechanisms and their resultant functionalities will be analysed within this chapter.

4.1 Project Research and Development Scope limitations

As with all engineering projects (specifically those dealing with mechanism/device development), this project was limited by time, available technology and finance. Namely funding for the PhD would last 3 years, Massey University's School of Engineering did not have any active electrospinning and polymer chemistry equipment relative to this type of research and the project finances were limited to approximately NZ$30, 000.00 for capital expenditure (equipment/materials purchasing).

Typical electrospinning devices are quite costly and with respect to this project can have limited control/automation capabilities. One such device is Electrospinz Esa1 device, which utilizes a relatively uncontrolled flowrate and collector positioning system which costs approximately NZ$15, 000.00 [Figure 30]. Another device having much greater capabilities of automation is the 4SPIN (CONTIPRO), unfortunately this device was not financially feasible costing approximately NZ$139, 110.46 [Figure 31].

Figure 30: The simplistic Esa1 electrospinning device by Electrospinz [3]

Figure 31: The 4SPIN modular electrospinning research device by CONTIPRO [4]

These were evaluated according to the mechatronics systems implemented and ease of reproduction of mechanism functionality relative to project requirements. If for example a requirement to reproduce a mechanism related to stepper motor control and this was already required/implemented elsewhere within the project, then the relative complexity in reproduction was reduced. Given that stepper motor control was a fundamental part of this project, the purchasing of mechanisms or devices which functioned solely on this form of control was not deemed financially viable (e.g. syringe pump devices). Table 5, Table 6 and Table 7 illustrate the evaluation techniques employed to derive the time relative to financial liability evaluations for the desired machinery, examples provided are for 'an electrospinning machine', 'High Voltage Power Supply', and 'Syringe Pump device'.

Table 5: Evaluation of time versus financial liability for the ESa1 Device

Device complexity	Cost	Future Integrative compatibility	Time for local production
Manual Gravitation based flowrate control and collector manoeuvrability. Use of High Voltage Power Supply.	Relatively high (~ NZ$15, 000.00)	Easily integrated via the implementation of relay and control mechanisms	Easily reproduced if High Voltage Power Supply is purchased

Table 6: Evaluation of time versus financial liability for the High Voltage Power Supply

Device complexity	Cost	Future Integrative compatibility	Time for local production
Highly precise electronic control and safety mechanisms	Relatively low (<NZ$1, 000.00)	Easily integrated via the implementation of relay and control mechanisms	Extensive time for testing and health and safety approval

Table 7: Evaluation of time versus financial liability for the Syringe Pump

Device complexity	Cost	Future Integrative compatibility	Time for local production
Precise stepper motor controlled lead screw actuation.	Relatively high (> NZ$2, 000.00)	Decentralizes machine functionality as control of extrusion is implemented elsewhere.	Relatively low due to similar requirements elsewhere within project

Whilst the department at which the project was conducted did not own equipment typically associated with this research, it did allow for the use of an extensive engineering workshop and technician capabilities to construct much of the desired mechanisms/technologies at a relative lower cost. Of particular relevance to this project was the ability to utilize the rapid prototyping technology within this facility to generate many of the required devices/parts of the project. One such technology was the Laser cutter (Universal Laser Systems PLS6.75, Figure 32) which allowed the prototyping of project parts through the processing of relatively cost effective Acrylic (PMMA) (approximately NZ$200.00 per 4.5mm by 2440mm by 1220mm sheets). This acrylic was utilized to generate much of the structural forms within the project and acted as a relative insulator between certain regions of electrostatic potential. Acrylic was also utilized as the preferred material within the project due to its ease of local manipulation and sourcing, however it should be noted that other materials with greater insulator properties could have been utilized e.g. glass. Additionally the local lathe and CNC (Computer Numerical Control) machining capabilities (Figure 33) allowed for the relative ease in manufacture of more complex aluminium parts (some of which being required to conduct charge). In general, the workshop facilities allowed for an ease in the fabrication of any engineered solution through its available technologies, these included both polymer and metal processing 3D printers, a large waterjet cutting machine, lathes, manual mill, and general tool selection (Figure 34).

Figure 32: Universal Laser Systems PLS6.75

Figure 33: SMTCL BRIO MILLER 8 CNC Machine

Figure 34: List of advanced capabilities within the Massey University Engineering workshop

4.2 Design and Development Philosophy

It is worth noting that much of the design and development work within this project was conducted for and in relation to the patent application (partially provided in Appendix C: Related Patent Application (partially disclosed)). A significant portion of this project involved the generation of devices capable of evaluating the various hypotheses discussed in future chapters. This development centred around a standard design philosophy involving ideation (the formulation of concepts/ideas), initial prototyping, design evaluation, optimisation. Certain mechanisms/devices within the project required repetition of this process until a functional result could be achieved. Typically, Ideation involved a rough sketch of concepts, the most developed of which were translated into Microsoft Word graphics. These were transformed into SolidWorks CAD if/when required and constructed through appropriate or available technologies and materials. Figure 35 further illustrates the cycle of the design philosophy utilised in the project and will provide a framework for discussions in component development discussions. To further illustrate the application of this ideology, the project can be described as involving three main areas requiring design and development, namely electrospinning, additive manufacturing/3D printing, and combined systems development. The electrospinning developments will relate to components such as the syringe pump, extruder, charge control mechanism and collector/collecting surfaces. With regards to additive manufacturing mechanisms relating to ultrasonic vaporisation, lithography and plasma material modification will be created. Finally, the developed work will undergo a systems integration process within which methodologies for productivity optimisation will be evaluated. These stages and their related components are illustrated in Figure 36.

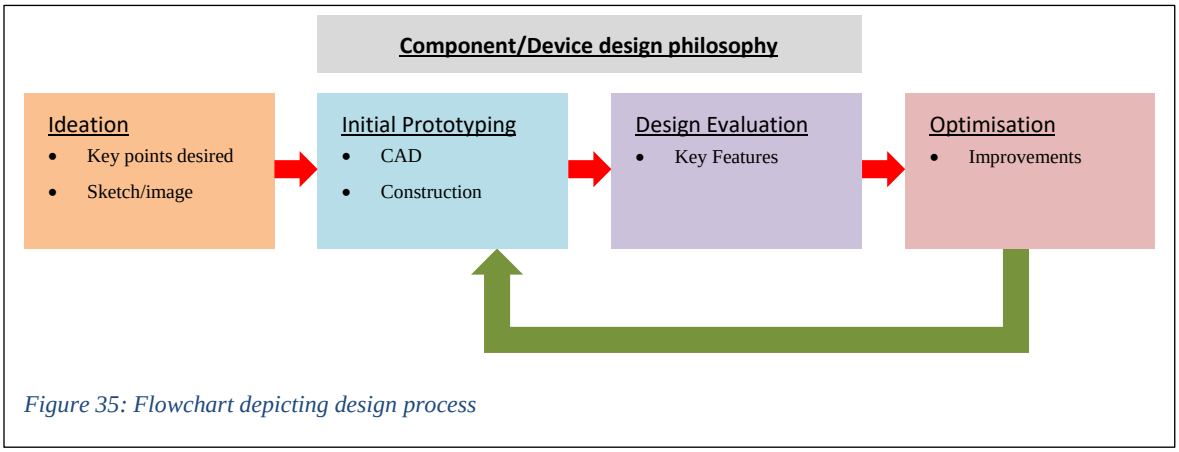

Figure 35: Flowchart depicting design process

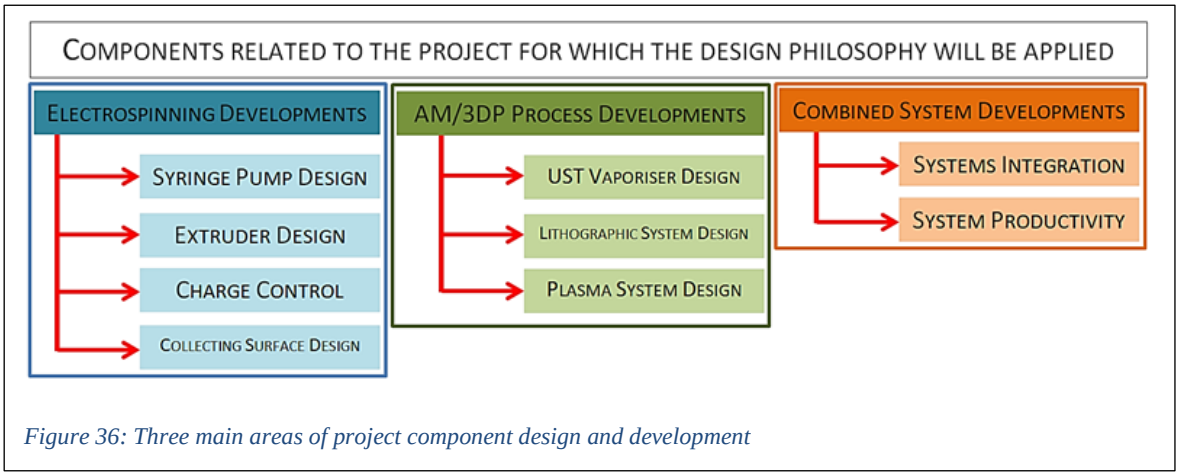

Figure 36: Three main areas of project component design and development

4.3 Material Actuation Development

Electrospinning processes require the introduction of material into or upon a charged surface, as such this section will detail the development of material actuation to the region of electrostatic actuation. The desirable flow rate within this project is modelled after studies found within literature relative to collagen namely 1mL/h [88, 90, 92, 93]. A highly prominent methodology to accomplish this is through the use of syringe pumps [72-74]. Ironically the syringe pump, which was identified as a relatively costly (approximately NZ$1, 000.00 to NZ$2, 000.00) yet simplistic device, required a relatively high degree of design modification and development.

4.3.1 Developmental progression

The development of this device can be described according to the device placement, the capabilities of available motors (flow rate) and charge proximity to conductive elements and the effects (electrical arcing). The construction of the device made use of a Nema 14 and various laser cut acrylic components, the progression including notable variations/developments for this device can be seen in Table 8: Material actuation development.

Table 8: Material actuation development

Component/Device design philosophy progression			
Ideation	**Initial Prototyping**	**Design Evaluation**	**Optimisation**
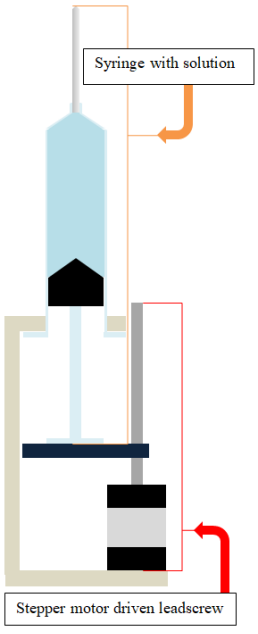	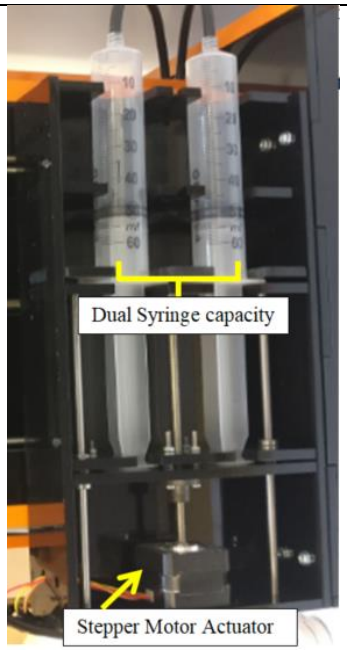		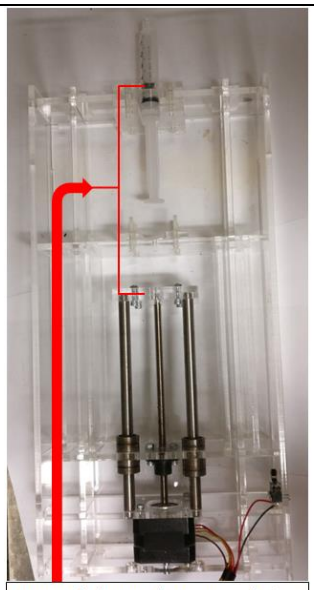
• Syringe attachment fixture • Stepper motor driven leadscrew actuated piston	• Large device • 2 x 60mL syringe capacity • Microstepping torque restrictions (skipping steps) • mL/h versus mL/mm restrictions	• Smaller device • Arcing of HV to conductive surfaces • Stepper motor disruption • Electronic components damaged (arcing)	• Dramatic removal of conductive elements • Grounding of motor housing

4.3.1.1 Device placement

Initial designs made direct use of a syringe pump within the process/printing working area (Figure 37), this required a larger area to accommodate the syringe pump with concerns of the motor electronics having impact on the electric field fundamental to electrospinning. To overcome these concerns a pipe and valve based system were incorporated (Figure 38). The small quantities utilised in a 10mL syringe resulted in a requirement to prime the tubing with material prior to actuation (i.e. there was not enough material in the syringe to be transferred to the point of extrusion. One potential method to overcome this requirement was through the use of a peristaltic pump. Unfortunately, due to the fundamental nature of these employing staggered/non-continuous actuation as well as the undesirable compressive force on the polymer solution, they were discredited.

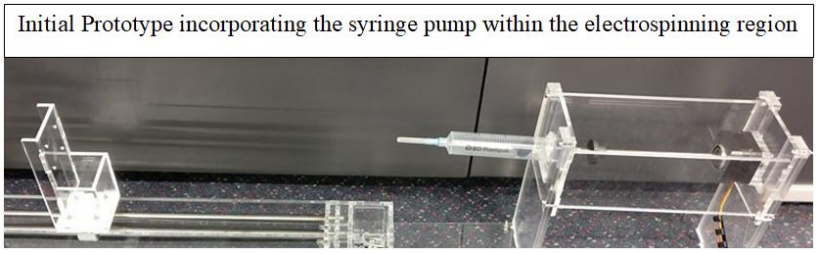

Figure 37: Prototype having syringe pump included in electrospinning region

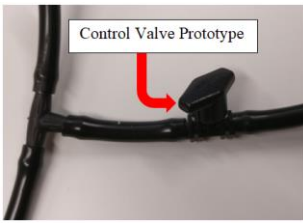

Figure 38: Control valve mechanism prototype

4.3.1.2 Flowrate

Initially a large syringe pump device was generated and made to be capable of actuating two 60mL syringes with the intent of allowing for future coaxial electrospinning experiments. This prototype did not account for the capabilities of the utilised lead screw as well as the stepper motor actuation required to yield relatively low flowrates (1ml/h). The Nema 14 motor utilised had a step angle of 1.8^{o}, which resulted in the requirement of 200 steps to generate one revolution of the motor shaft. The leadscrew lead was capable of providing 1mm in linear actuation per rotation. Thus, 200 steps of the motor would result in 1mm of linear actuation. The utilised standard 60ml syringes (diameter x and length y) would produce 1ml of extruded material for every 1mm of linear actuation. Thus to achieve a flowrate of 1ml per hour the motor will be expected to rotate once per hour, equating to 200 steps per hour which equates to 200/60 = 3.33$^{'}$ steps per minute and 0.05$^{'}$ steps per second. This speed is far too low for the motors to actuate smoothly, namely it would result in an inconsistent flowrate. A popular method to reduce these irregularities in stepper motor control is through microstepping, a technique which enables an increase in the number of steps possible for the motor per revolution via PWM of voltage. Namely, the 1/16th microstepping of the utilised motor will equate to 200 x 16 = 3200 steps per revolution. For the example flowrate of 1ml/h using the 60ml syringe this would allow for an increase in steps allotted per second to be approximately 0.9steps. This would still result in a relatively inconsistent flow rate, additionally one of the major limitations of utilising microstepping relates to this techniques reduction in the output motor torque. As such, the motor was unable to provide enough torque to the leadscrew to overcome the frictional forces of the syringe and its solution. The system was evaluated with the limitations of the utilised lead screw and syringe size being the components identified as resulting in mechanism failure. Modifications to the

leadscrew, namely a smaller lead, could potentially achieve the results required this would however be relatively expensive. Given that electrospinning does not require a large amount of material to be processed to generate fibre for flow rates of 1ml/h, a much smaller syringe capacity could be utilised. Thus instead a 1ml syringe (diameter 6.75mm and length 66.5mm) having output equivalent to 0.01ml per mm allowed for the actuation of 8.88' steps per second which in turn allowed for a much more regular flow rate. It is worth noting that this also allowed for a reduction in torque required by the motor to overcome frictional forces, this allows the system to fabricate with solutions of varied viscosities.

4.3.1.3 Electrical Arcing

A major problem faced within this mechanisms development was the tendency of the electric potential within the solution to arc towards the devices conductive rods and mechanical components. This resulted in the accumulation of charge in undesired regions as well as a disruption of the stepper motor or damage to electronic components such as motor controllers. Thus a further syringe pump device was generated which acted to dramatically separate the syringe from the conductive elements of the device. Additionally to aid in the unwanted disruption of rogue charge upon the motors, the housings were connected to ground.

4.3.1.4 Final Syringe Pump Design

The final syringe pump developed within the project was much more compact than previous renditions. This design acted to shield the conductive elements from one another via the use of acrylic coverings, additionally the mechanism was now equipped directly with two pushbuttons which allowed for the interaction of the user with the actuated platform during the loading of material. This interactivity is intended to allow for the controlled generation of the desired meniscus prior to the initiation of electrospinning. This design and its features are highlighted in Figure 39.

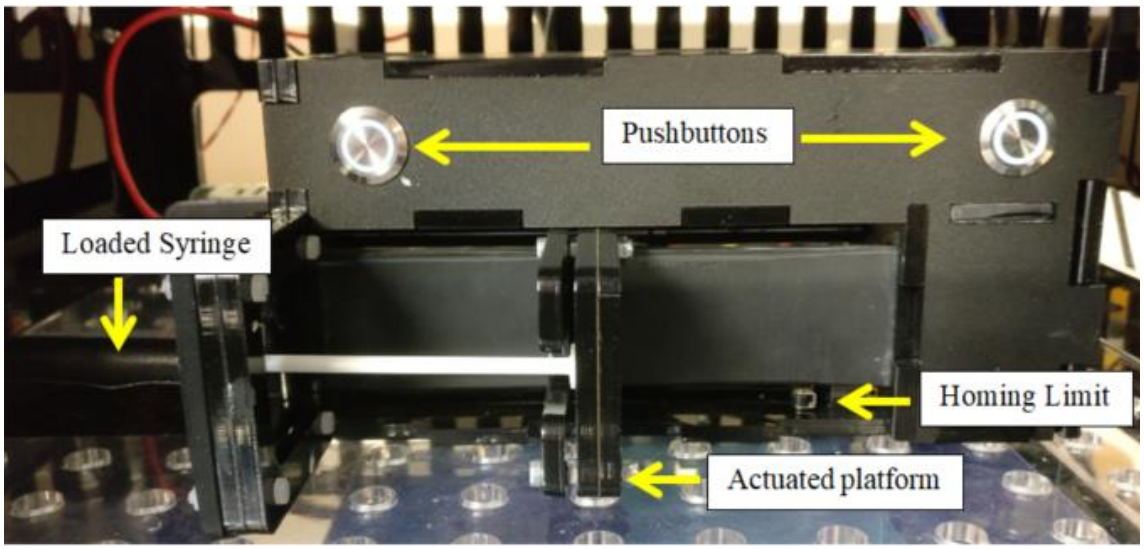

Figure 39: Final syringe pump design with covered conductive elements

4.4 Electrospinning Point of Extrusion (POE) Development

Some experimentation was done with respect to the nature of the point of extrusion (POE) within electrospinning, namely the regions at which the solutions would be exposed to the high voltage. Following literature [11], developments of these tended to favour a more 'nozzle-less' system in an attempt to yield a higher productivity of fibre.

4.4.1 Developmental progression

The POE components were manufactured through the computer numerical control (CNC) machining or waterjet cutting of aluminium. The main areas of interest within this area of development related to the nature of electrospinning Taylor cone formation relative to surface tension forces and the effects of component serviceability. The progression including notable variations/developments for this device can be seen in Table 9: POE developmental process.

Table 9: POE developmental process

Component/Device design philosophy progression			
Ideation	**Initial Prototyping**	**Design Evaluation**	**Optimisation**
		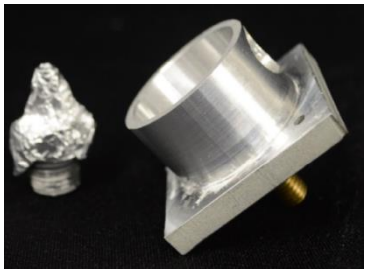	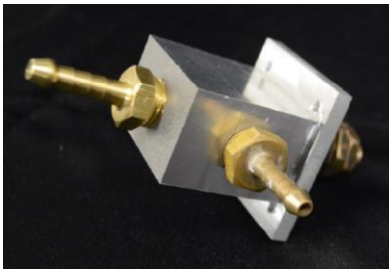
• nozzle/needless system • Bath of charged solution	• Machined aluminium with fitting	• Bath of material was largely unreactive resulting in tests with smaller nozzles and flat plate extruders	• Brass and aluminium nozzle system with smaller diameter and less surface tension to overcome

4.4.2 Taylor cone formation

Of interest with regards to the generation of electrospinning was the potential to increase the productivity of fibre fabrication through the implementation of a solution-bath like approach. This development was an attempt which was intended to further identify the potential for nozzle-less/actuator less charged solution-based techniques discussed in literature [11]. Initial tests involved the utilisation of a flat bar of aluminium upon which collagen-solution was distributed and charged to 45kV (with a grounded rod positioned 125mm from this) with the intended electrospinning region being kept at approximately 30^{o}C. This experiment generated no identifiable Taylor cone formation, it was hypothesised that this was potentially due to the difficulties in controlling the distributed area of solution. As such, a simple investigation in which the effects of distributed solution/bath surface area to the formation of a Taylor cone was conducted. This occurred through the use of a piece of aluminium in which three cavities having diameters 12mm, 6mm and 3mm were generated. These were filled with solution, allowing for a greater control of the surface area of the 'bath'. The experimental conditions utilised were the same as the initial test, with each test only filling the desired cavity. Unfortunately, no formation of a taylor cone could be identified from this evaluation which demonstrates a thorough requirement for the presence of a meniscus or stretching of the surface region to allow for a weakening of the surface tension forces and generation of a Taylor cone. This confirmed the literature derived explanation of the physics related to this electrospinning feature. Figure 40 demonstrates the four implemented surfaces utilised.

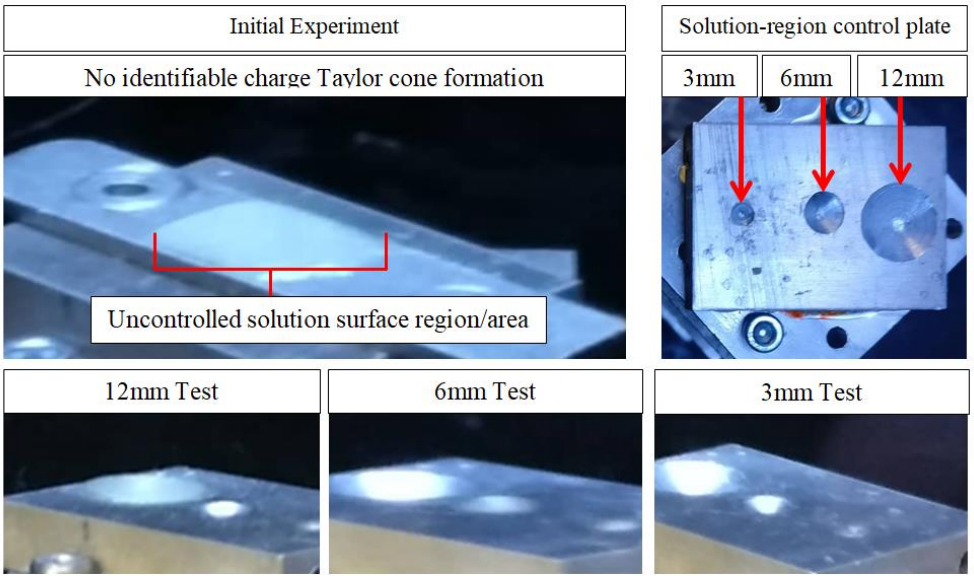

Figure 40: Attempt at identifying potential solution-bath extruder type

Following the nozzle-less experiment, nozzle-based equivalents were trialled. Initially an available 3mm polymer nozzle was covered in aluminium foil and to determine whether the meniscus from these would allow for adequate Taylor cone formation. These trials were successful and an extruder having a brass inlet and outlet was made, this was a largely successful extruder, the only limitations relating to serviceability and modularity. The last POE developed mimicked the rotating disk system employed in Revolution Fibres AGL electrospinning machine (depicted in Table 10 in the Ideation section). This device utilises an extrusion-less system in which a charged rotating disk moves through a vat/bath of 'Solution'. A disk having regions upon which solution having sufficient viscosity could be suspended was generated. This disk had slight recesses which when rotated through a viscous solution would act to collect and hold this material via surface tension. Electrospinning occurred by the application of high voltage to this rotating disk, as such one of the complications of this technique related to the insulation of the motor driving the rotation from the high voltage. This extruder operates at a constant rotational rate carrying the solution via surface tension adhesive forces with Taylor cone formation occurring when the rotated material reaches a critical magnitude within the electric field. Whilst designs along with prototypes relating to this technique were generated, due to concerns related to the additional complexity of an additional actuator and the effects of this on electric fields within the electrospinning chamber as well as the non-critical requirement of this within the project scope, this idea did not undergo further development. As such for the remainder of the project the nozzle-based approach was utilised. It is recommended that this technique be further evaluated within future research and development.

Table 10: Development of mimicked rotating disk extruder

Component/Device design philosophy progression	
Ideation	**Initial Prototyping**
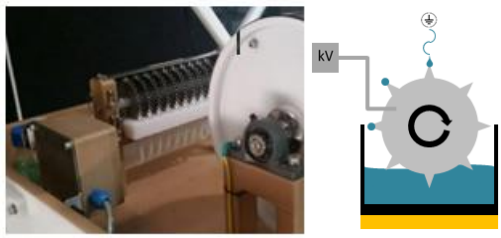	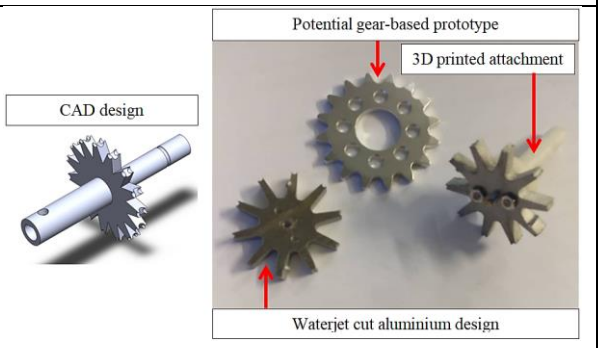
• rotating extruder utilised in the AGL design with hypothesised functionalities	• designed and prototyped singular disk extruder • non-conductive motor attachment

4.4.3 Component Serviceability

One of the largest limitations within the testing process related to post-testing cleaning/purging of the extruder system, namely the solidification of undesirable residue material within the extruder chamber. Additionally extruders could not easily be removed to account/manage these limitations. These restrictions in functionality promoted the need for a redesign allowing for an ease of cleaning and removal/replacement of extruder systems. These issues and the resultant development are described in Table 11: Redevelopment of extruder system for increased accuracy and serviceability. Modifications to the POE design included the removal of the 90^{o} angle within the extruder chamber and incorporated a modular approach whereby the utilised extruder type was attached to a charged plate via a sliding mechanism. This improved the serviceability and accuracy of these components, with the new design manufactured through the assembly of waterjet cut 6mm aluminium.

Table 11: Redevelopment of extruder system for increased accuracy and serviceability

Component/Device design philosophy progression	
Further Evaluation	**Further Optimisation**
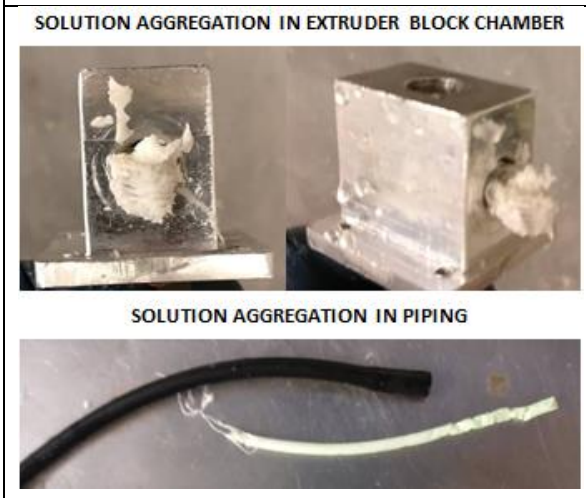	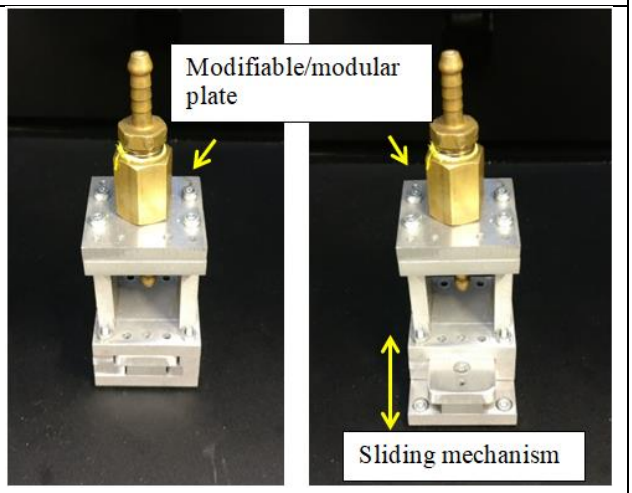
• Blockage in piping and extruder • Difficulties in cleaning/replacing items	• Waterjet cut aluminium (6mm) • Modular design for extruder variations • T-groove connection • Servo-motor controlled High Voltage connection

4.4.4 Charge control

In order to allow for an automated approach to electrospinning, some mechanism to control the moment at which the charge would be applied to the solution was required. This would allow for no unwanted electrospinning to occur in the setting of voltages (yielding a time disparity in processes and desired outcomes) and allow for a higher degree of Health and Safety (as emergency disconnection of the power to the extruder could be coded). In order to achieve this a high torque servo motor was attached to the charged electrode wire from the high voltage power supply via a laser cut acrylic mount (Figure 41).

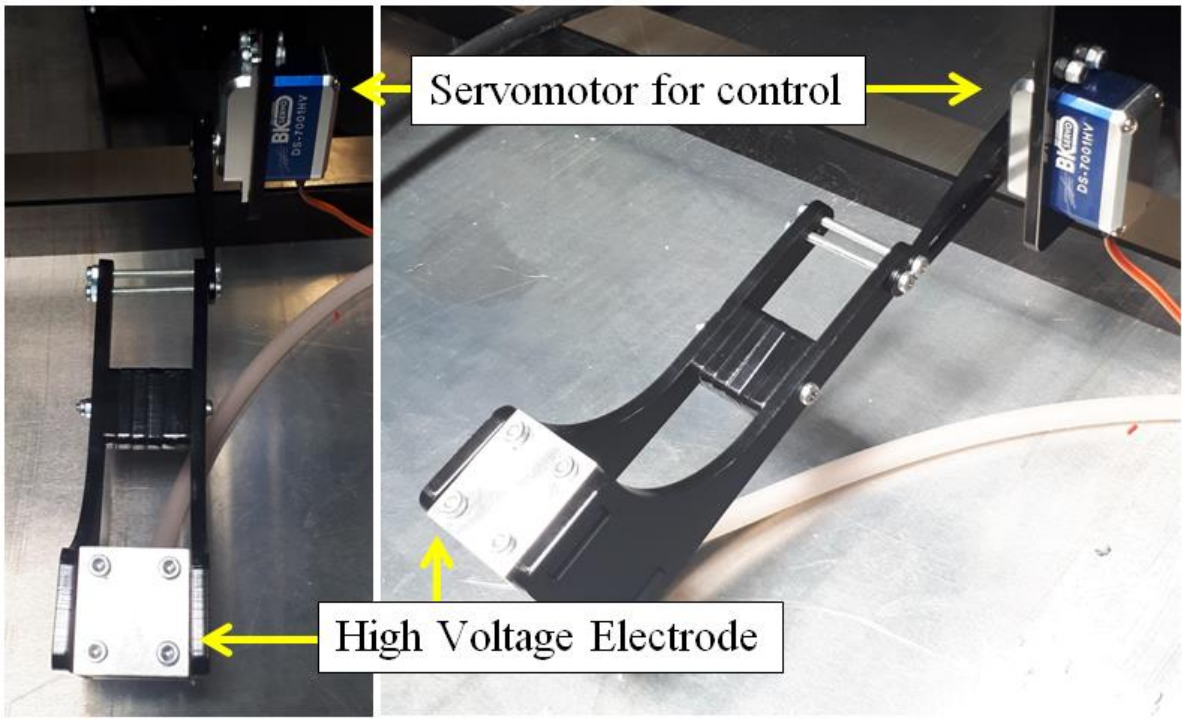

Figure 41: High Voltage plate connected to servomotor via acrylic mounting plates

4.5 Fibre Collection Development

The nature of fibre collection was of interest within this project due to the desire to fabricate three-dimensional objects from these. Given the difficulties in removing or manipulating fibre deposited against/onto substrates [81, 82], methodologies which would allow for direct interaction with these were investigated.

4.5.1 Developmental progression

In Chapter 2: Literature Review the parallel electrode technique was highlighted as a viable option for this project however, alternative methods were identified with potential to yield a higher productivity. The major developments with respect to this part related to a collector that would maximize productivity whilst retaining alignment and a method for the transferring and manipulating fibre into a three-dimensional form. To accomplish this development a range of technologies including a FDM 3D printer, Metal Lathe, CNC, waterjet cutter and laser cutter were utilised.

4.5.2 Fibre collection surfaces

Generated fibre was to be evaluated via SEM imaging, thus a means to transfer the surfaces from the electrospinning apparatus to evaluating technologies was required. In typical electrospinning studies, the transferal of generated material is achieved via removable material that is located within the proximity of collected fibre. Within this research, many removable surfaces have been generated to evaluate the nature of generated fibre. These forms did not develop as iterations or improvements of one another but rather as means for evaluating different outcomes within experimentation. This related to assessments of technique productivity, modified collector topography, fibre molding upon 3D forms and the processing of solely generated fibre based objects. In order to provide a benchmark for all experiments, flat/planar collectors were generated either from 3D printing of ABS or laser cut pieces of Acrylic. It is important to note the experimentation with 3D printed guide rods and acrylic structures upon which collectors were places to minimize error in manual collection. Additionally all collection surfaces with varied topography/dimensionality were 3D printed from ABS. The generated surfaces including their chief instigative purposes are depicted in Table 12.

Table 12: Generated surfaces including their chief instigative purposes

Collection surfaces utilised			
Productivity	**Collector topography**	**Fibre molding**	**Fibre based objects**
	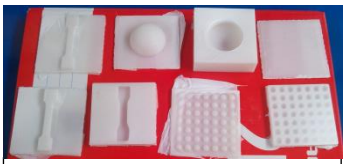 Various collector surfaces	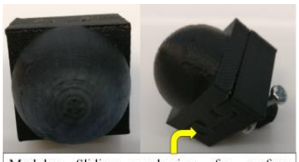 Modular Sliding mechanism for surface variation and easy removal	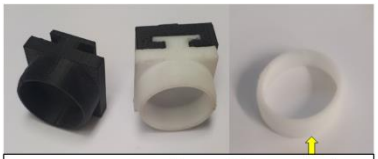 Version without sliding mechanism

4.5.3 Collection surface evaluation and development

The ‘fibre based object’ surface was quickly identified as being a capable form for the collection of fibre without a high risk of distorting and generated alignment characteristics (unlike the dome surface, which could have allowed for movement of fibre from uneven stress distribution. The usage of this surface and the related collected fibre is displayed in Figure 42.

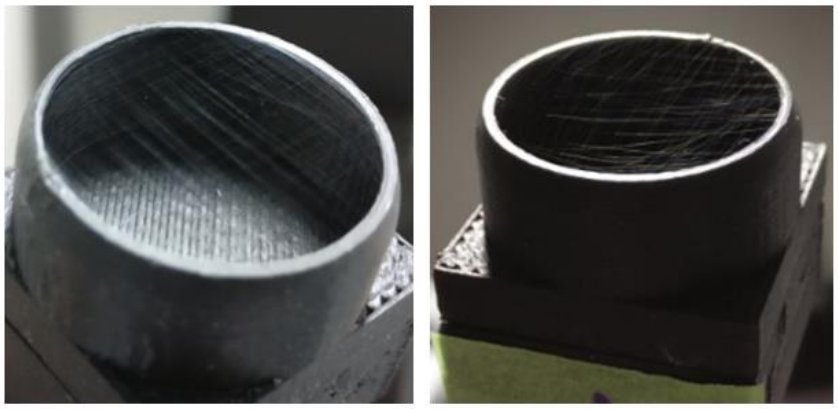

Figure 42: Displayed collections of fibre upon the 'fibre based object' collector demonstrating a clear variation of collection at 90^{o} angles

Following studies related to the nature of vapour distribution (discussed later within this chapter) the use of the ‘Fibre molding’ surface resulted in the identification of issues regarding the retention of fibre upon a spherical surface. This resulted in the either the premature breakage of deposited fibre away from the initial location or alternatively the reluctance of material to separate onto the collector. This uncontrolled material was able to either wrap upon the surface of the collector thus distorting prior and subsequently collected fibre alignments or dislodge from the surface of the collector (due to gravity) and disrupt the established fibre matrix. The analysis of the distribution of vapour particulate (discussed later within this chapter) resulted in the requirement for the surface to allow for the distribution of particulate through any acquired fibre. This resulted in a mesh like dome surface for this collector. This had the potential to further allow the fibre to bend around the now smaller collision region of the collector with the intent being that the fibre could stretch and fit upon the mesh. Unfortunately, this still did not allow for a smooth/controlled collection of fibre as can be seen in [Figure 43].

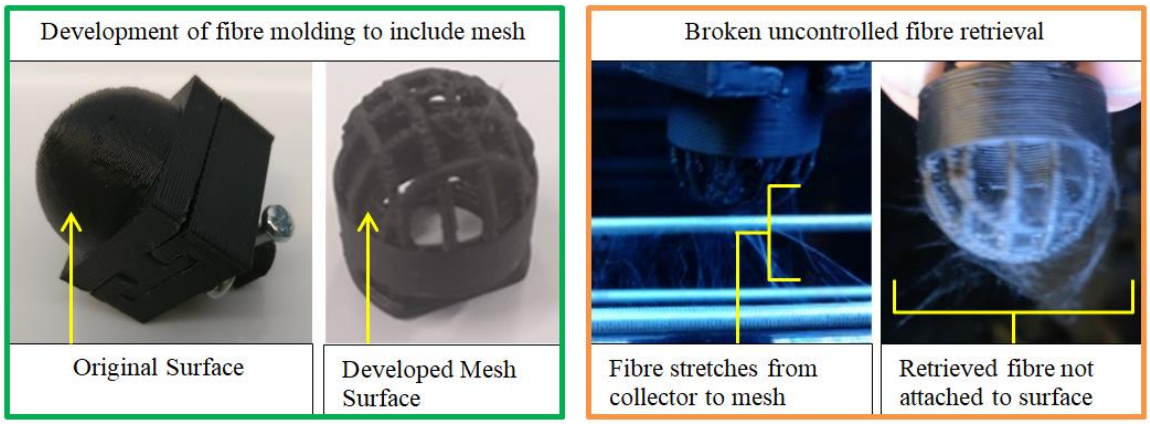

Figure 43: Development of fibre molding collector and limitations of these.

Given that these issues of fibre retention in transferal were not identified when using the 'fibre based object' styled collecting surfaces, it was hypothesised that there is a critical fibre length/distance at which the pressure/stress concentration of the collector will result in severing the fibre from its initial surfaces e.g. the electrodes. Additionally it is worth noting that the nature of the placement of this severed material will be relative to the surfaces between which the greatest surface tension occurs. These thoughts are illustrated in Figure 44 and demonstrated as a side profile of the collector being applied to the fibres.

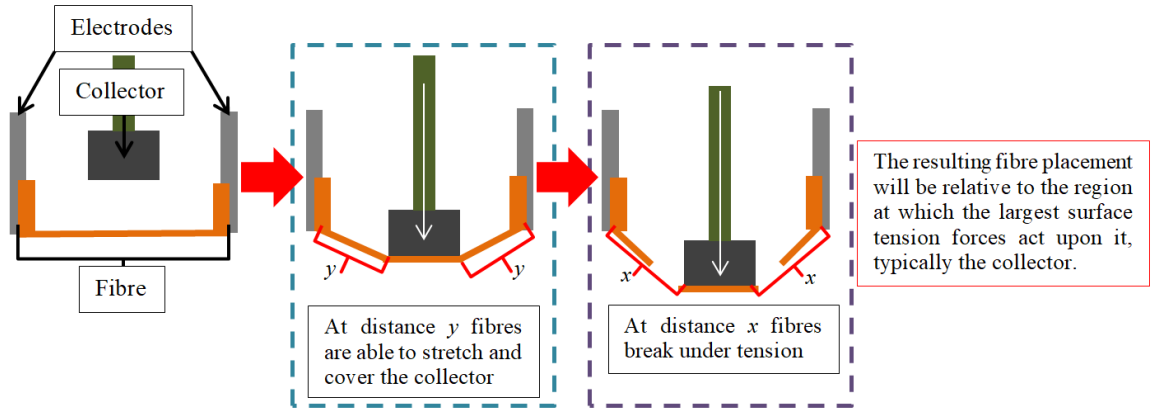

Figure 44: Hypothesised relationship between fibre severing and collector distance to electrodes

Given the nature of the Fibre molding collecting surface being a semi-sphere there existed limited means to ensure the fibres would wrap onto the entirety of this surface without changes made to the radius (height) of the extrusion. Additionally the failure for fibre to separate when desired was of concern, as the ability to actuate the collecting surface to the desired distance (x) would potentially result in collisions within the desired machines constraints. This understanding led to the investigation for the use of features (additional extrusions) surrounding the semi-sphere form to further enforce the separation [Figure 45].

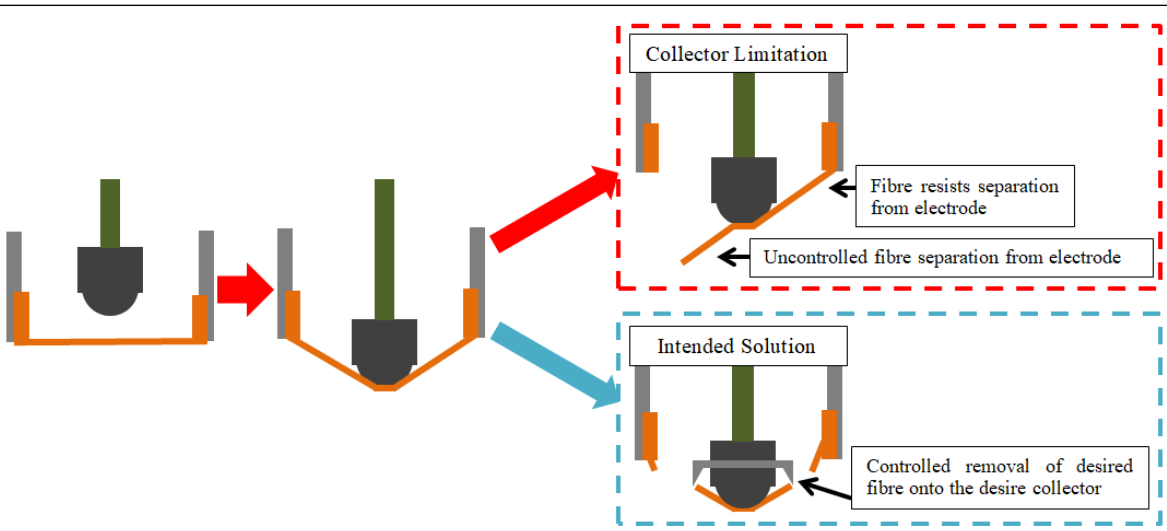

Figure 45: Intended solution for the enforcement of desired fibre separation.

Following this ideation an initial attempt was to 3D print a boundary wall to act similarly to that of the boundary wall of the 'fibre based objects' collector. Whilst this did somewhat achieve a controlled separation of fibre, as can be seen in the bridges formed between semi-sphere and boundary wall this surface continued to experience uncontrolled separation. Thus, a further attempt was made to instead utilise a thin serrated edge that would have a greater capability of severing the fibre. These attempts as well as the resulting final collector design are depicted along with notable features in Figure 46.

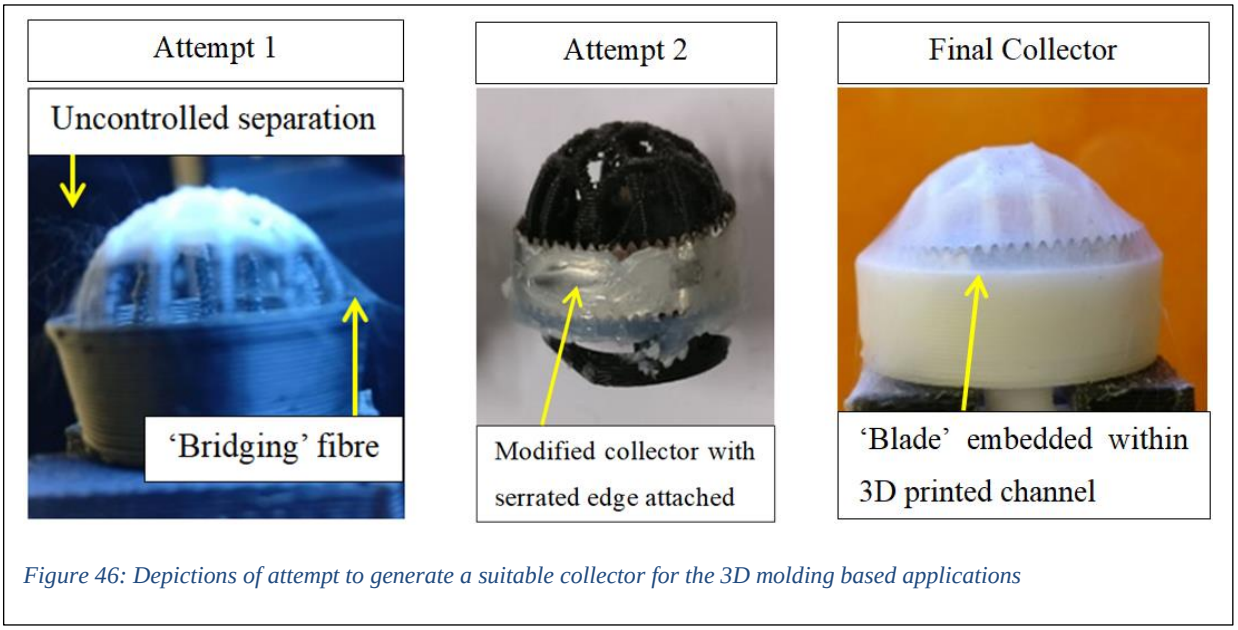

Figure 46: Depictions of attempt to generate a suitable collector for the 3D molding based applications

4.5.4 Fibre collection unit development

The initial parallel electrode studies made use of aluminium brackets, which were connected to ground (Figure 48). Whilst this system was capable of generating aligned fibre, this was restricted to a fibre length of 30mm (the maximum distance possible for this technique [87, 123]). Additionally restrictions related to the ease in scalability and productivity of the technique. A high quantity of fibres could be generated via a parallel electrode approach, however upon closer inspection (SEM image, Figure 47Figure 47) these fibres did not retain a strong degree of parallel alignment. This lead to the hypothesis that given a dense enough collection of electrospun fibres, resulted in material bridges between the grounded electrodes forming a new grounded plane upon which newly collected fibres can become randomly orientated. It is worth noting that this experimentation strongly indicates a critical time relative to alignment for this technique.

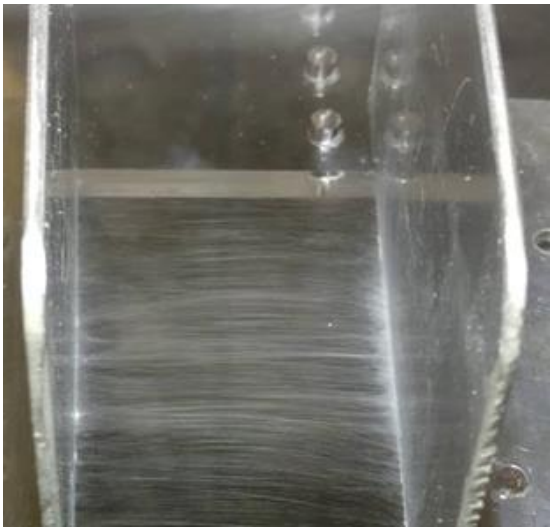

Figure 48: Example of fibres deposited between parallel electrodes

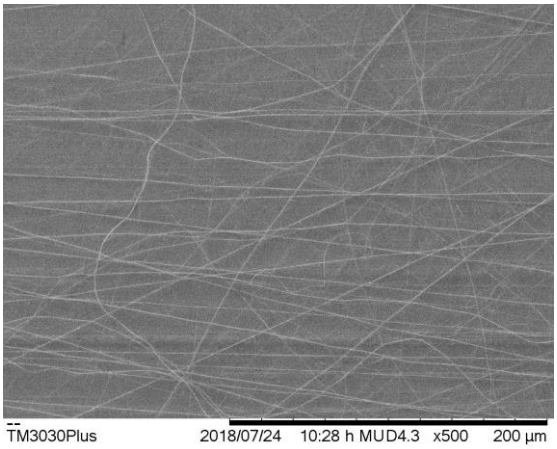

Figure 47 SEM image depicting fibres which have not adhered to the aligned nature expected in parallele electrode electrospining

Experimentation utilising biomaterial-based solution (collagen) demonstrated a much lower generation of fibre upon later developed complex collectors. To evaluate this limited output a new parallel electrode configuration/mechanism was constructed from two parallel bars of aluminium extrusion (12mm) which could be placed next to each other have a distance of 34, 24 , 10mm between one another. Initial evaluations of experiments using this identified a lack of consistent fibre formation across the gap. Fibres did however coat the aluminium bar. This further identified a relationship of solution reactivity (and thus resultant jet instability and subsequent whipping) to collector surface area. It was hypothesised that in order to achieve a desired formation of fibre between the airgap, a reduction of possible fibre routes (through the minimisation of attracting conductive surface area) was required. It is worth noting that this minimisation was restricted to the 30mm diameter and area limitations of the collecting surfaces, as these were required to be able to collect the distributed fibre. A simple, quick, and effective way to evaluate this was to attach a sponge to insulate the unwanted conductive regions. This allowed for the identification of fibres accumulating and ‘bridging’ from the sponge insulators towards the collector electrodes and was indicative of the potential for these to now stretch and form across the gap [Figure 51]. This technique was further developed to substitute the sponge with card

wrapped in insulation tape that could slide on the collector, masking unwanted regions. From this, a well-defined region of formed fibre was established across the airgap [Figure 50] which could be transferred onto a collecting surface for further evaluation. A final version of this form of collection unit was generated having a mechanism to modify the desired collection area [Figure 49].

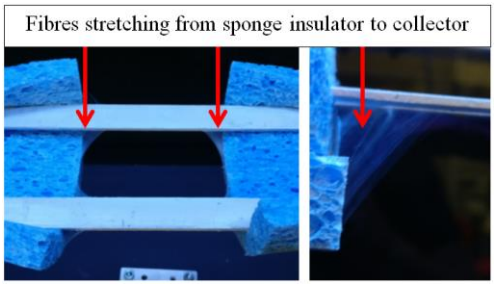

Figure 51: Utilisation of sponge as a temporary insulator and the results thereof

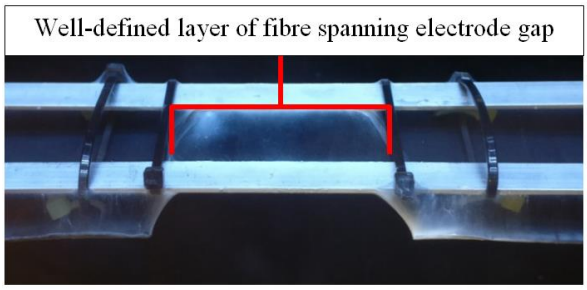

Figure 50: The formation of a desirable layer of fibre across the air-gap

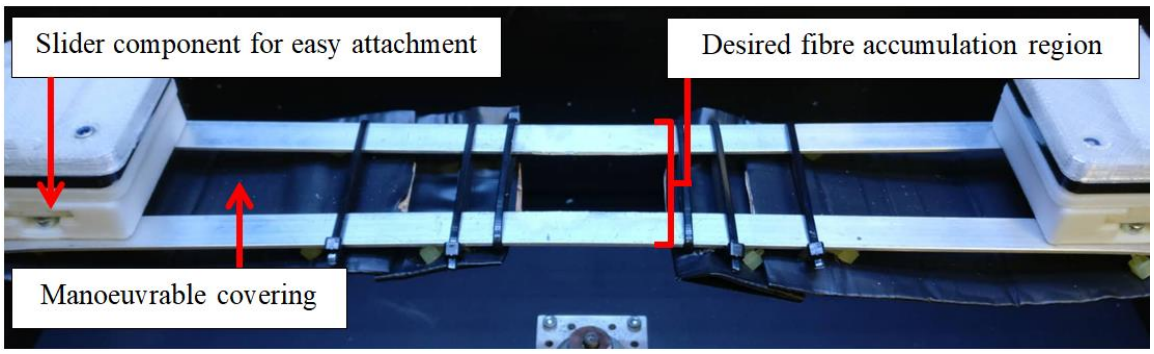

Figure 49: Parallel electrode configuration equipped with slider for easy attachment as well as manoeuvrable coverings to direct generated fibre.

4.5.5 Rotating Collector Development

One of the major limitations of the parallel electrode approach lies in its inability to efficiently collect large quantities of aligned ES fibre. These spatial restrictions are discussed in Chapter 2**:** Literature Review. Many large-scale electrospinning technologies prefer the use of a rotating mandrel/conveyor approach. Figure 52 depicts the NS 8S1600U device by Elmarco which applies a conveyor approach to spool large quantities of fibre generated by electrospinning [124].

Figure 52: Elmarco NS 8S1600U large scale electrospinning device

Whilst this technique has a higher capability in productivity for its scalability when compared to the parallel electrode configuration, the accessibility to generated fibre is limited. This limitation refers to the ease of removal of solely electrospun fibre from the collector. Typically, this mechanism is equipped with a removable covering upon which the fibres are collected. It is important to note the un-bonded nature of the fibres, namely that each generated strand of fibre is separate from the prior and subsequently strands. This makes it difficult to process or remove the aligned fibre material. Additionally for the purposes of further automation, the rotating mandrel approach was not identified as ideal. A similar alternative utilised in generating fibre for collection is the approach whereby the mandrel surface is replaced with rods between which there is an airgap. The collector acts similarly to the rotating mandrel approach however, in this design the spacing between rods allows for the aligned fibres to be collected. The construction of this mechanism is detailed in Table 13: Development of electrode mandrel hybrid collector.

Table 13: Development of electrode mandrel hybrid collector

Component/Device design philosophy progression			
Ideation	**Initial Prototyping**	**Design Evaluation**	**Optimisation**
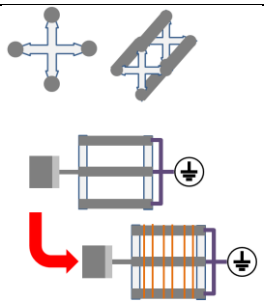	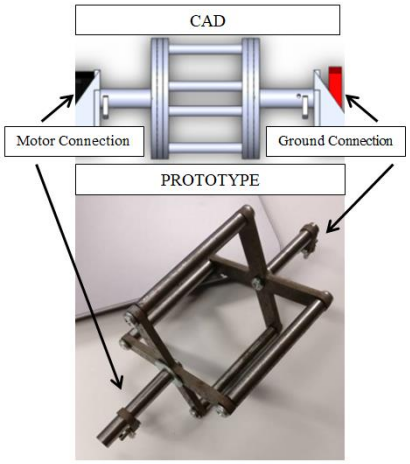	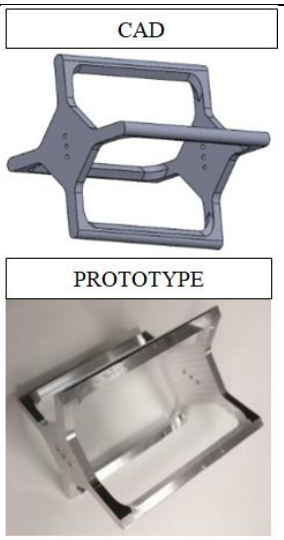	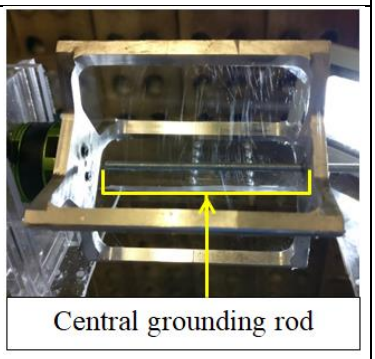
• Rotational collector • Similar to parallel electrode technique • Fibre collects between rods • Rods are grounded.	• Initial prototype • Modular construction • Heavy • Multiple points of failure	• Singular part for uniformity in rotation	• Ground electrode is positioned through the middle of the rotating collector and aids in rotational stabilization.

Note that the initial prototyping made use of steel rod segments which were modified (turned on a lathe) to fit into a waterjet cut mounting plate. A motor mounting rod was connected to one side of the collector and a stabilising rod, which was to be grounded on the other side. One of the main issues with this component was the resultant weight and potential irregularities that could result in instabilities of the part when actuated at high speed. Additionally there was a potential for the grounding mechanism (in this design a free spinning steel sleeve) to result in a friction weld thereby damaging other components. Thus in an attempt to remove these risks and potential harm to the user or machine componentry a second prototype was constructed from CNC machined aluminium. This design was modelled on similar collectors from the CONTIPRO 4SPIN device with this rendition allowing for a grounding rod to be placed within the middle of the collector both to enable electrospinning and ensure rotational stability. This design proved to be able to collect aligned fibre without the need for the entire component to be connected to ground. It is worth noting that the utilised rpm in generating aligned fibres was approximately 100 rpm and that according to literature the modulation of this would result in fibres of a smaller diameter and higher degree of alignment.

Studies documenting rotating mandrel electrospinning of nanofibers often have these collectors actuated at high speeds. Positional control of the collector was desirable for further automation, namely an automated approach to retrieving depositions between the rods. The speeds required could easily be achieved via brushless DC motors, however the control of these at high rpm becomes quite specialised. An alternative which could be readily implemented using the established stepper motor technology within the project comprised of a gearbox mechanism. This took the form of a stepper motor driven gear driving a much smaller gear (Figure 53). This was prototyped with waterjet cut steel gears and was reasonably functional at delivering a 5:1 gear ratio (which resulted in an output rotation of five times the input). The mechanism did suffer from the typical issues associated with tolerances in non-precision manufactured gearbox systems. It is worth noting that prior work demonstrated a capability to generate reasonably small fibres at lower rpms as such this portion of the research and development was not seen as critical. As such this project recommends the future development of this actuation element (either through the purchasing of a gearbox system or controlled high speed motor configurations).

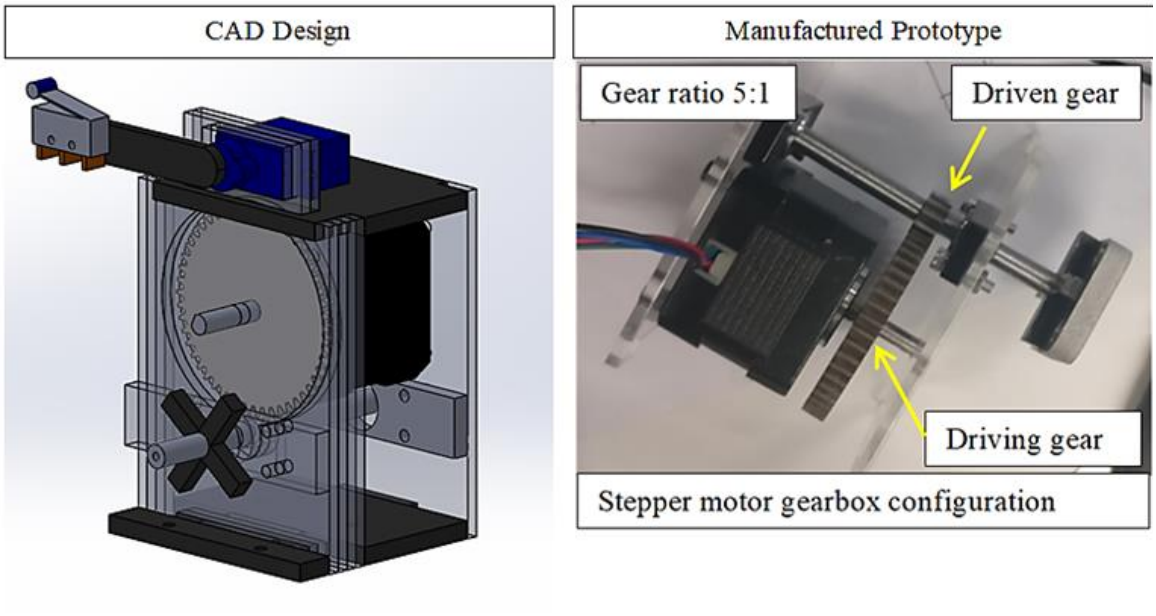

Figure 53: Simple gear based mechanism to increase motor output rpm

A limitation of the optimised aluminium collector related to the requirement for CNC machining and therefore high cost and complications in scalability. Thus, an alternative collector comprised of laser cut acrylic and threaded rod was generated. This new collector was designed to incorporate the modular elements implemented in other portions of the project. The laser cut components were to act to maintain the desired structure (namely aid in the rigidity of the cylindrical form) with rod to act as the collection points. These components were however susceptible to flexing under non-uniform load and due to the draft on these parts (caused by the cutting operation), this was prevalent in the design. A simple method to overcome this was the use of threaded rod, in this method the distance between the rotators acrylic disks was measured, and fastened/locked into place via the use of nylon coated (nylock) fasteners [Figure 54].

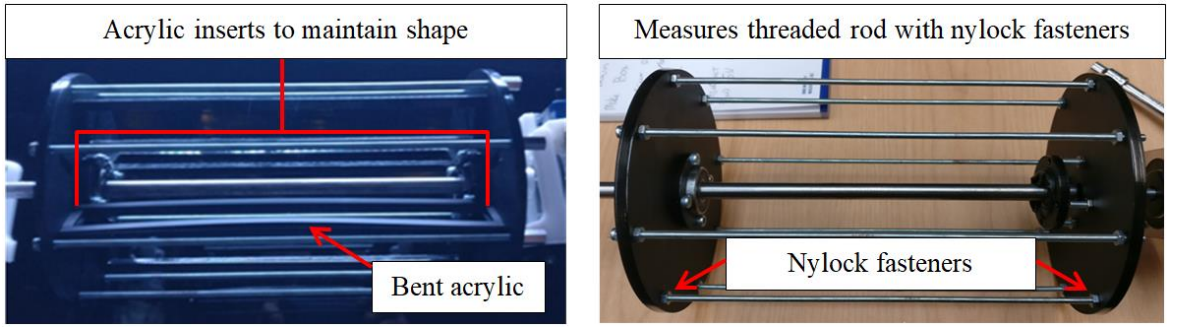

Figure 54: Versions of the rotating collector with both acrylic and threaded rod techniques

4.5.6 Rotating mandrel ground element development

The initial concept related to the grounding of the rotating mandrel intended for each rod rotating around the collector to be connected to a rotatable ground source. Thus acting like a series of parallel electrodes arranged in a circular fashion. This led to concerns relating to the connection of these rods that would be rotating at over 100rpm. As such rather than incorporate a parallel electrode approach an established understanding of how rotating mandrels currently work was incorporated, namely a centralised grounding rod around which a catchment region is rotated. This understanding is demonstrated within Figure 55 and can be seen to operate effectively when electrospinning Nylon 6,6-formic acid solution Figure 56.

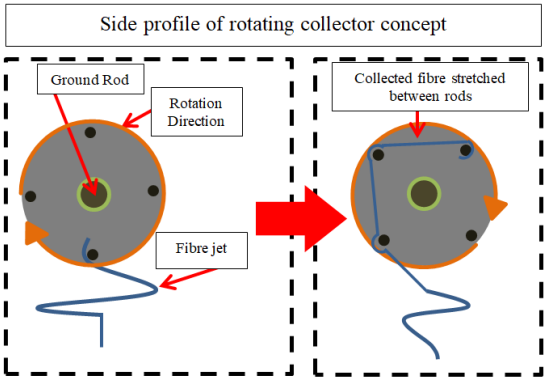

Figure 55: Illustration of concept relating to rod based rotating collector

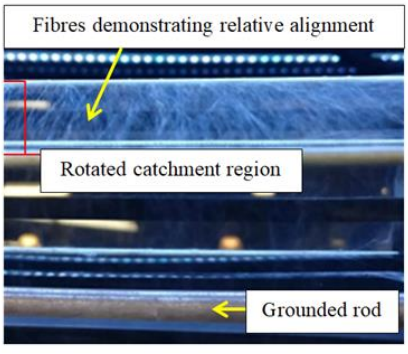

Figure 56: Nylon 6,6-Formic Acid experiment demonstrating effectiveness of rod based collector

4.5.7 Final rotating mandrel-based collector

The final developed form of the rotating mandrel based collector is depicted in Figure 57. This rendition includes an acrylic frame that was intended to both aid in the stabilisation and levelled nature of this components actuation as well as include holes upon which desired mechanisms could be attached. It is worth noting that this mechanism was attached to the actuating platform utilising 3D printed sliding components. This allowed for the interchangeability between this mechanism and the developed parallel electrode configuration.

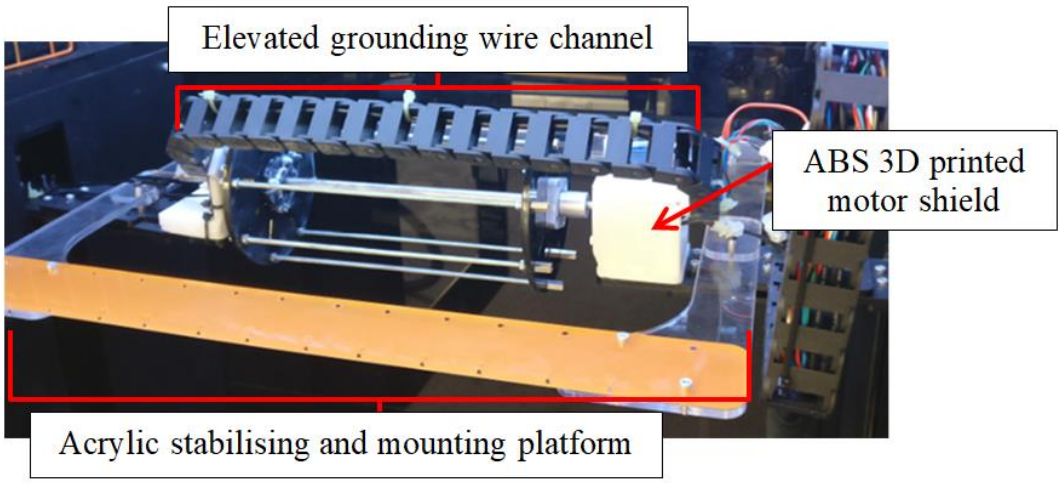

Figure 57: Final rotating mandrel based mechanism with grounding wire, motor and additional mechanism mounting attachments

4.5.8 Fibre transferral unit development

The retrieval and transferal of deposited fibres was required to allow for the processing of these to yield functional three-dimensional fibre based forms. This development and the features discussed therein are further illustrated in Table 14: Development of a fibre retrieval mechanism.

Table 14: Development of a fibre retrieval mechanism

Component/Device design philosophy progression			
Ideation	**Initial Prototyping**	**Design Evaluation**	**Optimisation**
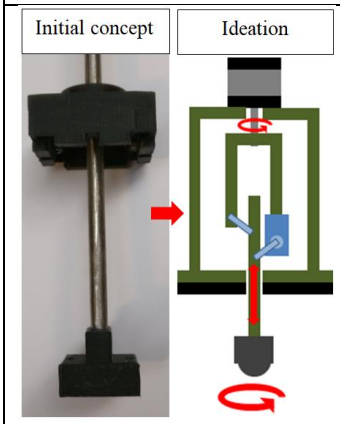	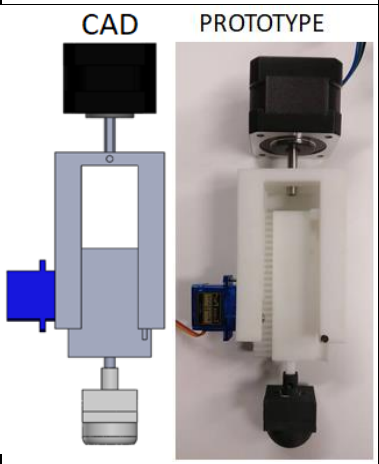		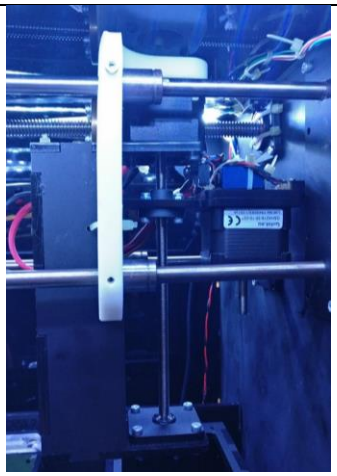
• Stepper motor controlled collection angle • Servomotor controlled piston • Desired collector attached to piston	• 3D printed prototype • Alternative rack and pinion mechanism utilised. • Modular capability for attached collection surface. • Rotation of large component	• Leadscrew linear actuation (similar to other mechanisms). • Rotation directly attached to collector	• 3D printed stabilising component to ensure uniform traversal.

For initial experiments in which the nature of deposited fibres was of interest, this retrieval was achieved manually. Later experiments utilising three-dimensional collecting surfaces utilised a 3D printed guide to ensure some degree of control when moving these collectors through the fibre. With respect to the automation of this component, an initial design intended to make use of a servomotor connected to a piston-like mechanism for linear actuation. This was modified to utilise a rack and pinion unit as this could allow for further positional control. Both of these ideas utilised a stepper motor from which the unit could be hung and rotated to allow for fibre retrieval at varied angles. Whilst the mechanism did demonstrate reasonable functionality, the linear actuation was replaced with an available stepper motor driven lead screw. This helped to dramatically increase accuracy (as no 3D printed actuator parts were required) as well as reduce development time (as additional coding was no longer required for positional control). A further improvement was made to instead mount the rotational motor onto the linear actuator. This reduced the load/torque required for rotating the collecting surface (this was now only required to overcome the load of the directly mounted collecting surface. The final prototype was equipped with a mounting platform allowing the addition of a servomotor which when combined with a cantilever/limit switch would allow for the further homing and positional control of the surface's rotation.

4.6 Functionalisation Device Development

The utilisation of vapour as a functionalisation strategy for fibre generated in electrospinning was discussed near the end of Chapter 2**:** Literature Review. This section highlighted ultrasonic vaporisation as a viable means for the automated generation of vapour having control of particulate size through frequency modulation. Current systems incorporating techniques using this media and technology are often separate and relatively of an indirectly controlled/exposure nature. This portion of research and development was interested in evaluating the potential to implement a controlled application of the desired functionalisation to acquired electrospun material within the scope of an automated system. Additionally this section of development also implemented designs for a lithography-based mechanism utilising 395nm wavelength LEDs that are commonly associated with stereolithographic 3DP, as well as a mechanisms to implement corona discharge plasma as a technique for polymer-fibre surface modification.

4.6.1 Developmental progression

The initial ideation of this part generated a nozzle-based system in which generated vapour would be accumulated, charged, and actuated in a controlled manner. Thus the resulting development centred on the methods for vapour generation, the actuation to direct the resultant occurrence of functionalisation. The design prototyping progression including notable variations/developments for this device can be seen in Table 15: Development of vapour based functionalisation unit.

Table 15: Development of vapour based functionalisation unit

Component/Device design philosophy progression			
Ideation	**Initial Prototyping**	**Design Evaluation**	**Optimisation**
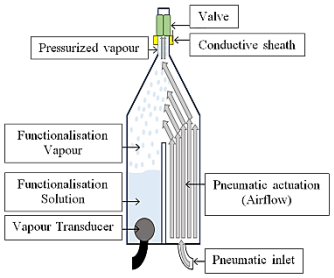	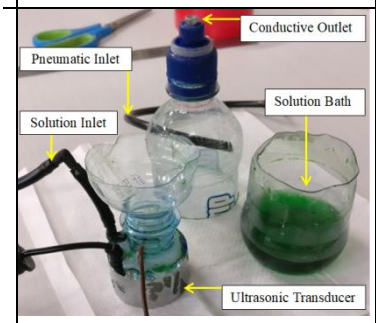	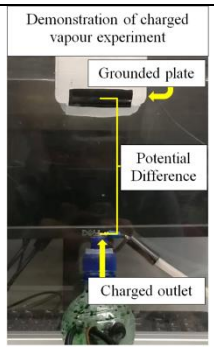	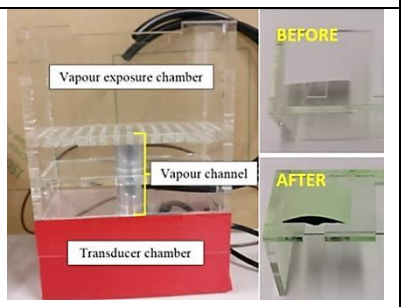
• Conductive outlet • Submerged transducer • Pneumatic actuation • Controllable outlet valve	• Constructed from water bottle • Aluminium nozzle as conductive outlet • Consumer-grade ultrasonic vaporiser • Funnel to return vapour condensation to transducer • Experimentation with water coffee, dye and expired resin	• Valve redundant . • Difficulties in quantifying resultant relationships of generated vapour and substrates. • Transducer overheating when not submerged	• Redesigned as a chamber for experimentation • Platform with paper experiments • Fibre experiments

The initial concept related to this device involved the use of a large nozzle like structure. This was intended to consist of two compartments namely one for vaporisation and the other to aid in the actuation of generated vapour via pneumatic actuation. The idealised concept would incorporate a valve to control the output of the vapour as well as a conductive sheath to exert an electrostatic charge upon particles and thus allow for the control of these to specified grounded targets. The prototyping of this consisted of a modified plastic bottle. Through this prototype, many modifications to the initial concept were highlighted. The first major change related to the placement of the ultrasonic transducer. The transducer utilised within this mechanisms was a simple commercial ultrasonic device. Typically these transducers are completely submerged within solutions and do not actively monitor the amount of vapour generated. They will however turn off if the solution within which they are submerged drops below a 'sensor'. This refers to an 'open connection' within the transducer circuit that ensures the device will not function if it is not connected to a ground. One of the difficulties associated with this device was the ability to control the quantity of vapour being generated from the solution. Additionally the requirement to submerge the transducer in a solution bath resulted in an increase in quantity of desired agent as well as complexity if this agent were to be modified/replaced. The modified funnel based solution inlet is depicted in Figure 58.

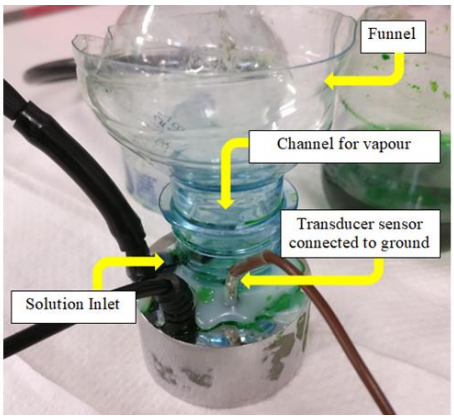

Figure 58: Modified transducer

The control of the quantity of vapour generated occurred via the controlled application of desired solution via a peristaltic pump upon the transducer. The now unsubmerged transducer device was no longer able to dissipate any thermal energy generated in operation. This was detrimental to the longevity of the component and as such, this component was partially submerged in water for initial experimentation. It is also worth noting that during the automation phase of the project, this component was set to activate only when required. Within the final rendition of the mechanism, a cooling fan was utilised in an attempt to prevent the component overheating [Figure 59]. This however resulted in the undesirable cooling of the surrounding air that is hypothesised to have resulted in an increase in air-moisture density at the region of vapour production. This resulted in a reduction of the generated vapour (as this was able to condense more readily into heavier solution droplets that could not be transported to the desired outlet. As such this cooling fan was not utilised in the final operation of the device, instead the device was partially submerged in water in an attempt to account for/dissipate heat generated [Figure 60].

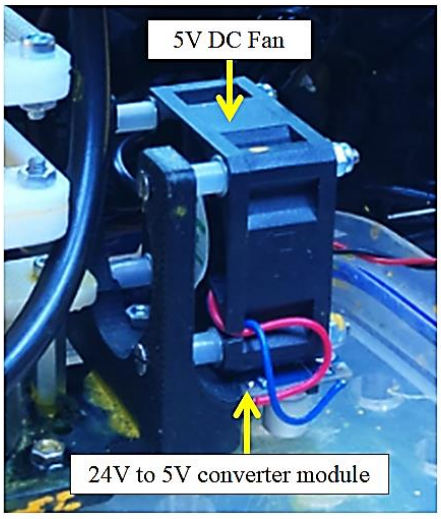

Figure 59: Utilised 5V DC transducer cooling fan

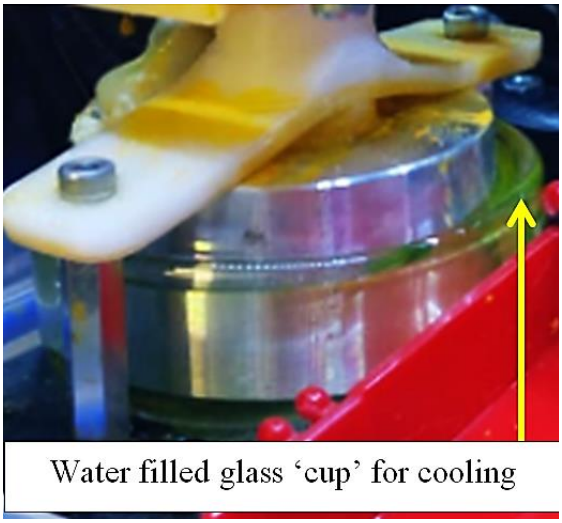

Figure 60: Glass 'cup' filled with water to cool the transducer/aid in thermal dissipation

This mechanism was tested with water, black coffee, food colouring, UV curable resin and riboflavin solutions at varying stages of its development. It is worth noting that through experimentation with the ultrasonic devices, a negative interaction between the type of solution and the housing of the device could occur. This was in the form of the deterioration of plastic housings and subsequent breaking of the units if exposed to reactive agents within the photo curable resin [Figure 61]. Due to this, versions of the transducers having aluminium housings were utilised.

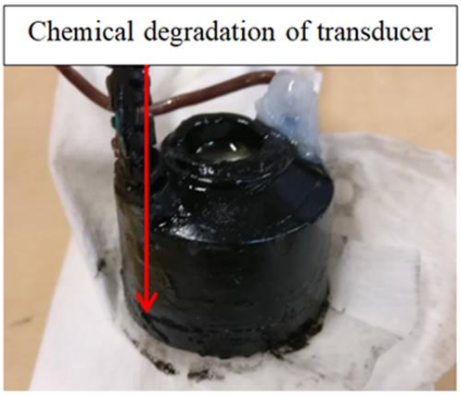

Figure 61: Degradation of transducer by solution

The second major modification related to the requirement for a control valve. Vapour particulate has a higher density in comparison to air and thus it naturally sinks/falls downward. The intended target for this generated vapour was developed to be suspended vertically above this mechanism. Thus, the occurrence of vapour upon this outlet could be restricted to the duration at which it was actuated out of the nozzle-like chamber as such no nozzle component was required to control the flow. It is also worth noting that this actuation occurred via an air pump having a modifiable and relatively low-pressure output to reduce the potential disruption of accumulated fibre.

The final modification related to the use of a conductive sheath to exert charge upon vapour particulate. This part was intended to aid in the ability to control and target the distribution of the vapour upon desired regions [as hypothesised in Figure 62].

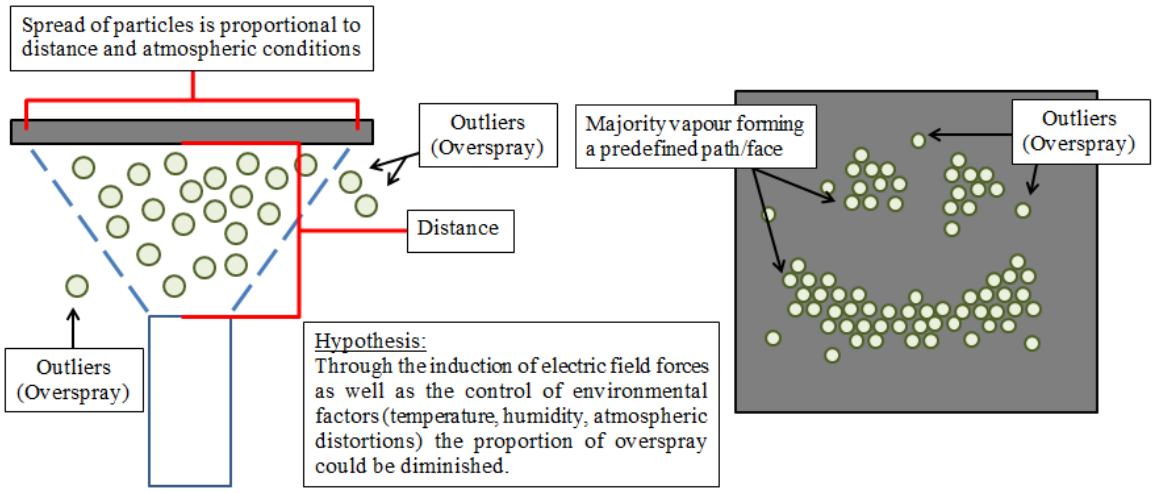

Figure 62: Illustration of the hypothesised principles and controlled application of vapour.

Whilst it is plausible to suggest that this control could be achieved through a x-y gantry system similar to those implemented in 3D printing. This development aimed to implement the vapour control at a nanometre scale. Not only would this require precise and expensive components for actuation, the nature of the vapour outlet and prevention of vapour condensation would require complex control over vapour particle size, nozzle temperature, and actuation. As such, the potential to direct the vapour particles in a similar fashion to the electrospinning actuation of nanofiber was evaluated. This aimed to identify whether or not the vapour particles could be charged and then directed to desired regions having been set to ground. This idea was similar to electrostatic techniques such as electrospraying have been utilised in the surface modification/coating industries. This was trialled however, no prominent effects on the distribution of the vapour could be identified. Additionally due to the occurrence of arcing within the experimental setup and concerns regarding the unwanted formation of plasma this concept and the development thereof is instead recommended for future research.

Through the testing and validation of the ultrasonic vaporisation mechanisms a limitation relating to the expulsion of large droplets of solution was identified. This was initially attributed solely to the propulsion of droplets by the transducer and as such, attempts were made to minimize the outlet orifice. These attempts highlighted a further restriction, namely that droplets could become suspended upon the surfaces near the outlet and result in blockages. The vapour and air pressure would then build up behind these and eventually burst through them, further projecting the unwanted large droplets upon desired surfaces. Additional attempts to minimise this risk included types of potential masks to act as catchment areas for the droplets, however these components were similarly blocked. Examples of this undesirable ejection of droplets, use of the masking technique masks and the effects of undesirable material on sensitive fibre structures are demonstrated in Figure 63.

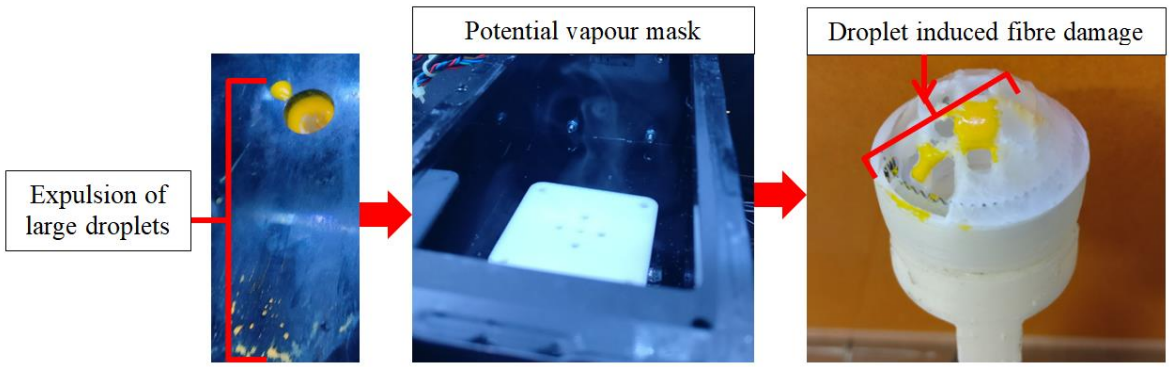

Figure 63: Image identifying the undesirable ejection of droplets, use of the masking technique and the effects of undesirable material on sensitive fibre structures

The final attempts at negating this sample damaging droplet expulsion took the form of a curved pipe that was installed prior to the mechanisms outlet. This included a horizontal section equipped with a secondary outlet orientated vertically downwards. This was intended to allow for the removal of non-vaporised material as these droplets now under the forces of gravity were intended to take the path of least resistance downwards. The first rendition of this concept did not however function as expected as whilst drainage of the unwanted material could be identified, this was not able to negate the expulsion of droplets at the surface Figure 65. This was hypothesised to be a result of the air pressure having the ability to push the blockages past the drainage point. Thus a second version of this concept was generated having a larger chamber within the horizontal section in which the solution droplets could fall into. This would reduce the surface area around the droplets thereby reducing the surface tension forces keeping these suspended. The new droplet chamber was equipped with a drain outlet much like the previous version. This achieved much more success and a final version of the ultrasonic transducer based vapour mechanism is depicted in Figure 64.

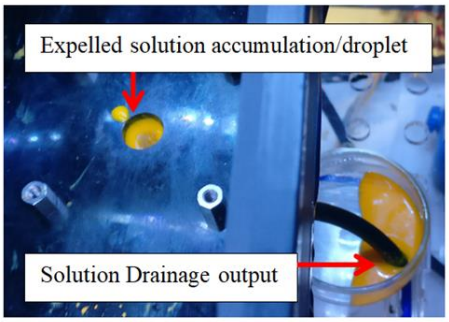

Figure 65: Initial drainage system unable to negate expulsion of solution droplets

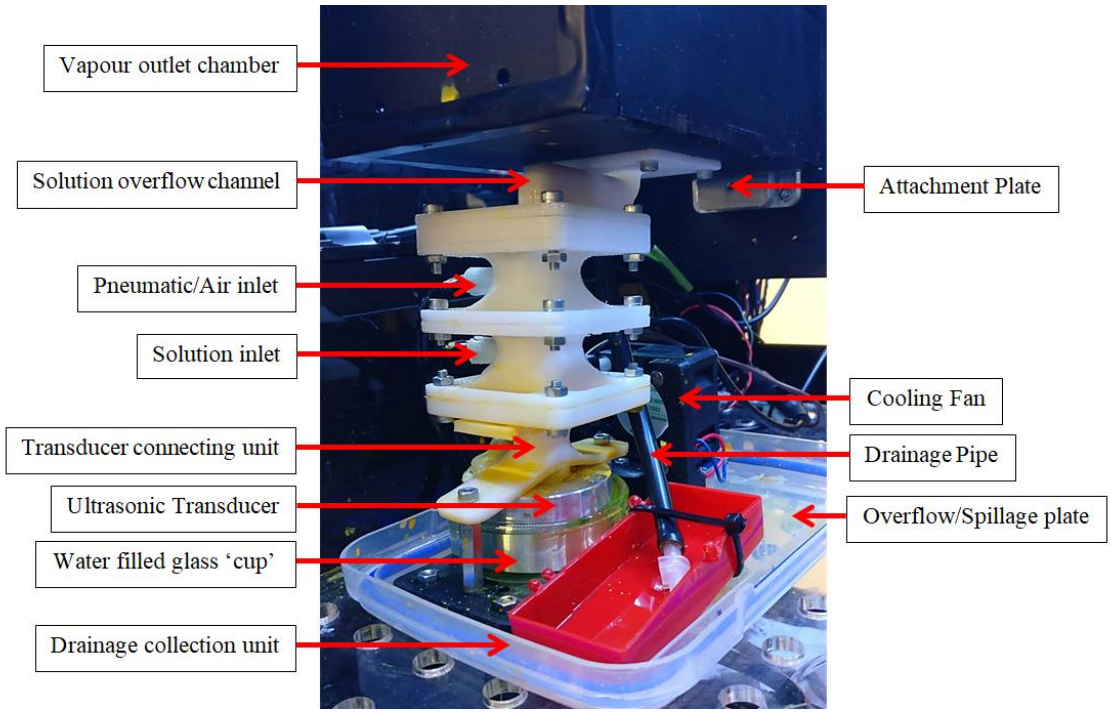

Figure 64: Final rendition of the vaporisation mechanism

4.6.1.1 Lithography Development

An established alternative methodology to control the nature of vapour-based functionalisation related to that of the utilisation of targeted lithographic exposure similar to that of traditional stereolithographic 3D printing. This could be incorporated through the use of a photo-sensitive/photo-curable functionalisation agent whereby through the application of either masking techniques or high precision lasers the accumulated vapour particulate can be selectively cured. In order to evaluate the feasibility of this concept a simple mechanism containing an array of powerful UV LEDs was created. This component was equipped with eight LEDs, components to help direct the light to desirable regions of exposure and a servomotor-based masking unit which when equipped would restrict the output light to desirable forms. This component alongside an experiment related to the curing of distributed vapour particles is demonstrated in Figure 66.

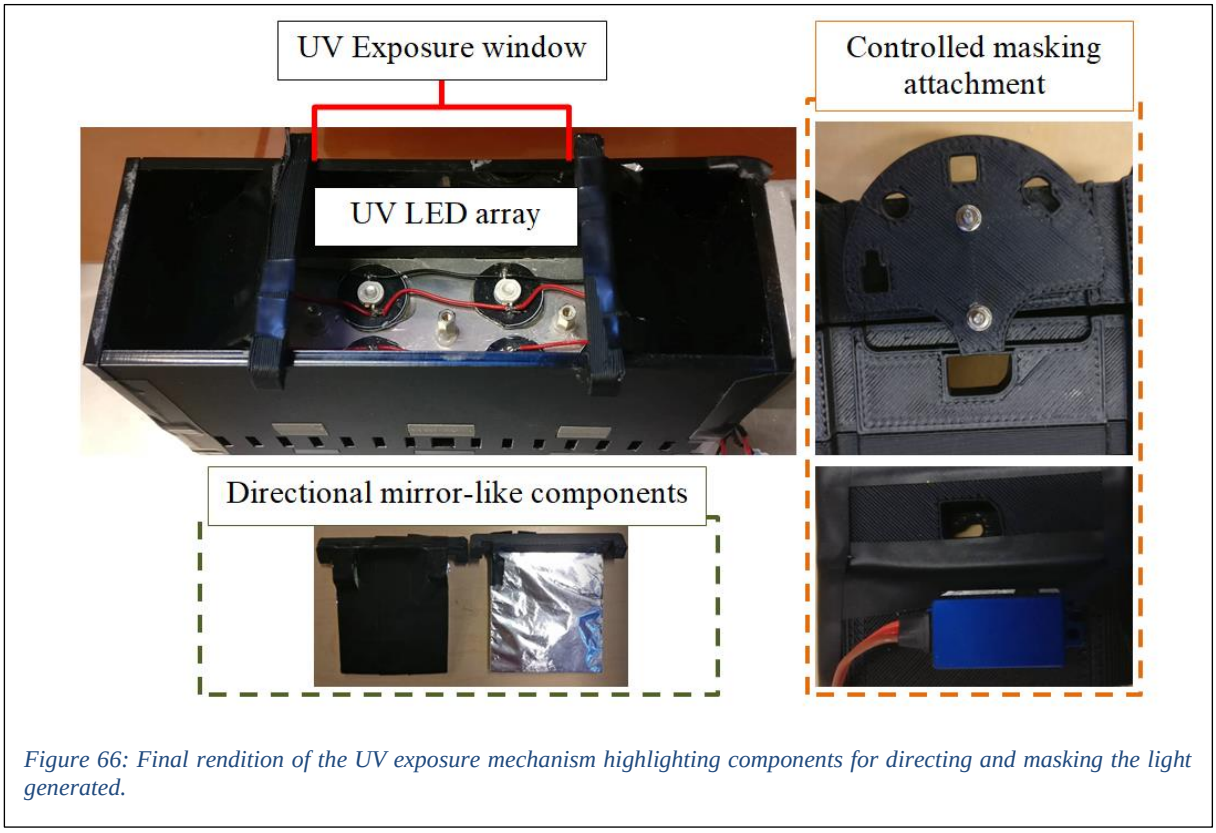

Figure 66: Final rendition of the UV exposure mechanism highlighting components for directing and masking the light generated.

4.6.1.2 Corona Discharge Plasma

Another technique to control the functionalisation of deposited material of interest within the project was that of plasma surface modification. This form of polymer processing is well established in many traditional polymer post-processing procedures [125-127]. The plasma acts to impart energy to the polymer chains resulting in the formation of additional cross-linking of these chains with one another thus re-enforcing the material. Given the vulnerability of un-functionalised fibres, many plasma-processing mechanisms which include high temperatures and pressure were not deemed viable options within this project. It is worth noting that techniques requiring vacuum chambers were not investigated due to the impracticality of implementing these within the greater project development. The Plasmatec-X (Figure 68), an adjustable and manoeuvrable benchtop plasma device was identified as a potential means to implement functionalisation. Unfortunately, to the aforementioned fibres weak structural integrity, the airflow from this device resulted in a disruption and breakage of the generated material. These limitations lead to the identification of corona discharge plasma as a viable technique [125, 126, 128, 129]. Within this process low voltages are applied at high frequencies to sharp electrodes/end effectors which causes the ionisation of surrounding gas [126]. The technology has been described as relatively inexpensive [128]. Through the assistance of the Institute for Geological and Nuclear Science (GNS Science) in New Zealand a device capable of this technique was constructed (Figure 67). The author would like to once again thank Dr. Jerome Levenier, Dr. John Futter and Dr. Bruce Crothers for their assistance in this work.

Figure 68: The Plasmatec-X by Tantec

Figure 67: Corona Discharge device developed at GNS

Whilst it was plausible to manoeuvre the point of plasma production utilising an x-y-gantry system similar to those in typical 3D printing, an evaluation of the nature of end effectors and the potential for a stationary alternative was investigated. This was largely motivated by the projects financial restrictions on purchasing actuators typical in nanofabrication as well as the relative volatility of the plasma stream to potentially arc to electronic circuitry. As such, the nature of plasma proximity both to sensitive materials as well as the proximity threshold of end-effectors was evaluated. Given the desired stationary nature of the point of plasma production, the ability to increase the region of plasma production and exposure was desirable.

Figure 69 demonstrates three forms of circle-based end-effector groupings namely having five, ten, and twenty points of intended plasma production. The first type having only five exposed wires arranged in a circular pattern yielded strong jets of plasma occurring at the tip of each wire. It is worth noting that the nature of this formation was somewhat erratic with the length of the projected plasma varying. The number of end points was then doubled and plasma could once again be seen, however the projection of this occurred at a somewhat smaller length. Finally, an end effector having twenty points of exposed wire was trialled, this demonstrated only a partial formation of plasma. One potential cause for this is the increase in capacitive loading from the increased amount of wire utilised. Further research is required to identify the optimal array of wiring versus plasma production. For future work within this project, the end effector having ten points of plasma production was utilised. The final developed mechanism equipped with sliding mechanisms is depicted in Figure 70.

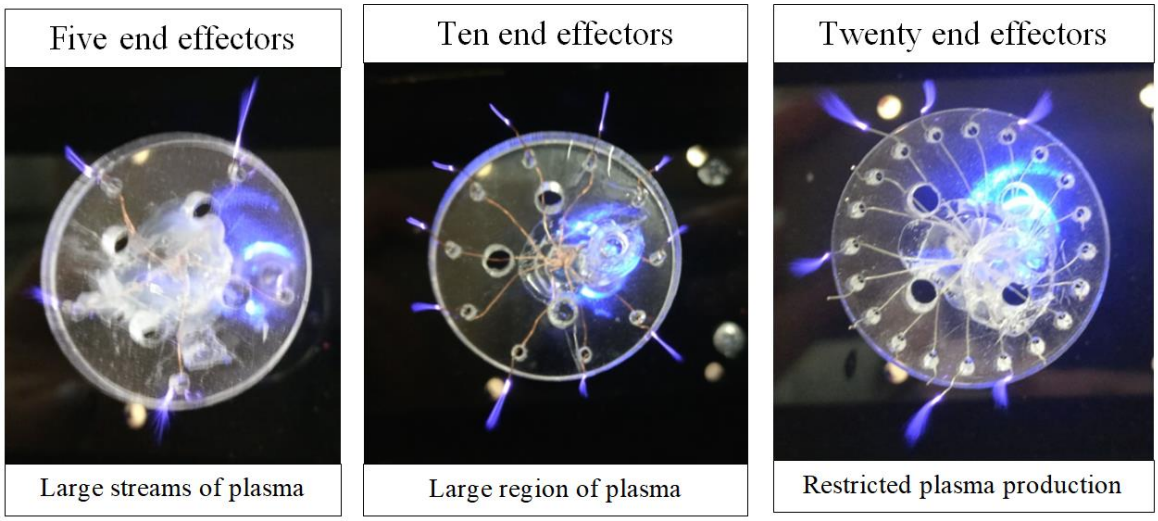

Figure 69: The effects of an increase in the potential number of points of plasma production for a utilised circular pattern/array

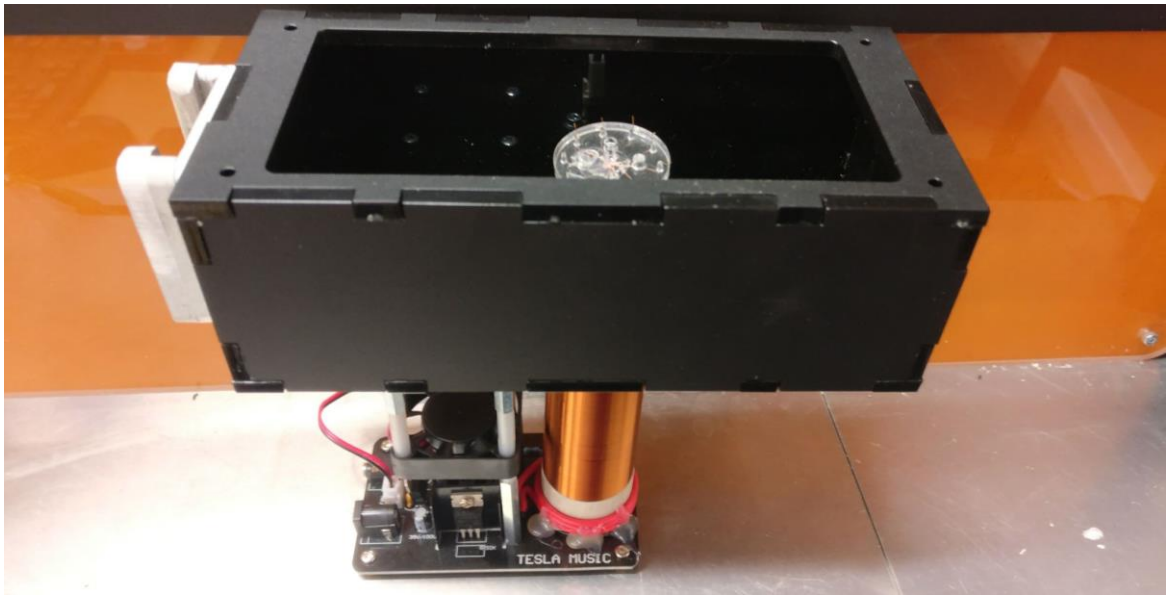

Figure 70: Final Corona Discharge Plasma-based mechanism

4.7 External Electric Field manipulation developments

The region of the electric field within an electrospinning process is defined by the spatial relationship between conductive elements as well as the dimensional properties of these. Example depictions of idealised fields for parallel electrode and rotating mandrel approaches to electrospinning are illustrated in Figure 71.

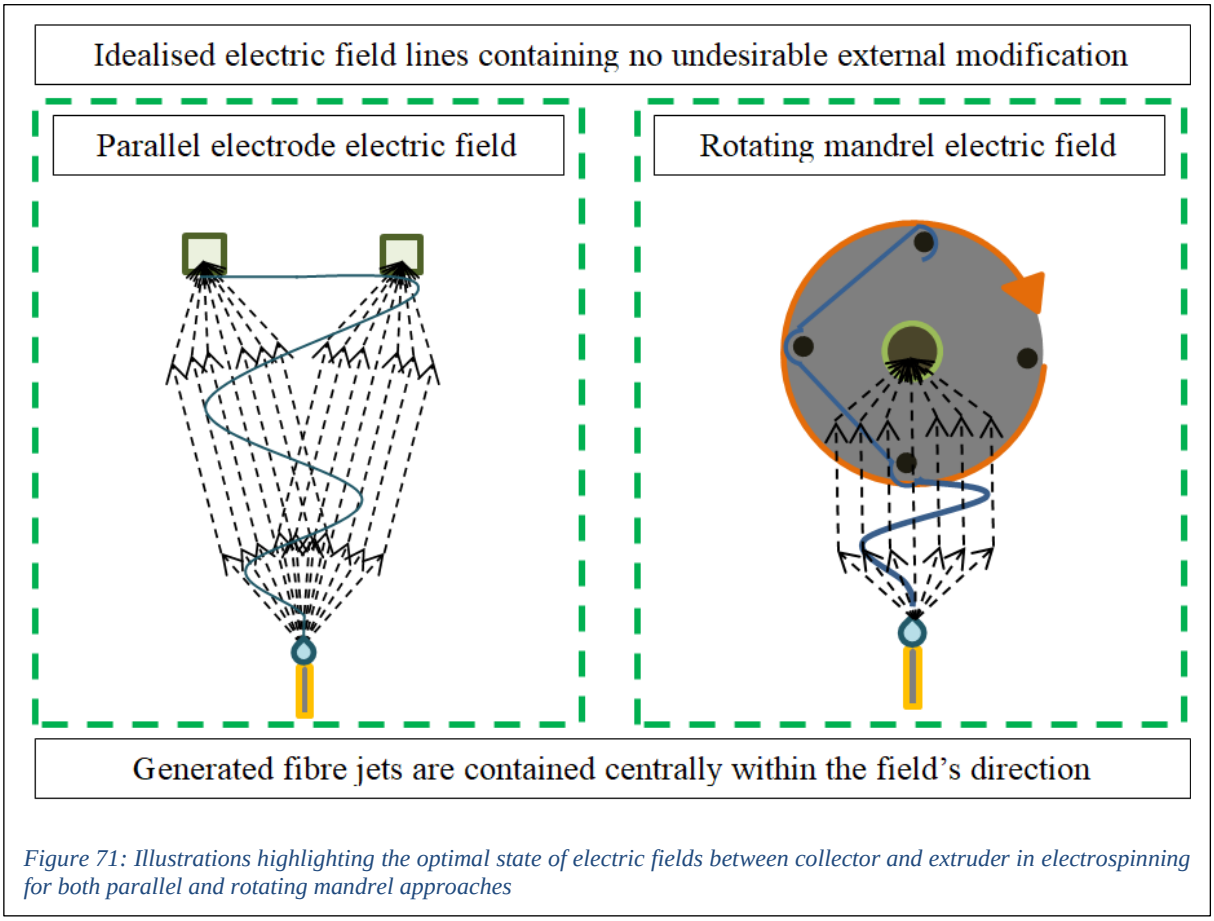

Figure 71: Illustrations highlighting the optimal state of electric fields between collector and extruder in electrospinning for both parallel and rotating mandrel approaches

Machinery reliant on precision in automation (e.g. 3D printers, laser cutters, CNCs, and lathes) is typically dependant on conductive components (e.g. motors, screws (leadscrews) and guiderails). Given that this project seeks to develop an automated form of additive manufacturing utilising electrospinning, some form of electric field manipulation/conditioning was required. Experiments aimed at the shaping or insulating of relative conductivity took the form of three types of development. These related to attempts made to mask/hide conductive elements, modifications to the extruder mechanism and modifications made to the desired collectors ground.

4.7.1 Conductive component shielding

The electrospinning jet is typically charged in the range of Kilovolts at which many materials particularly those of a conductive nature can be considered at relative ground. Thus, the metallic surfaces of the actuation elements must be adequately covered (shielded) to ensure that the pull towards the grounded collector is the relative direction of least resistance for the generated charged fibres/material. Figure 72 illustrates examples within the development of the project at which the generated fibres were attracted to these undesirable regions as well as the measures taken to reduce this. It is worth noting that efforts were also made to further the distance between conductive actuation elements from the nozzle. This was achieved through the extension of acrylic mounting plates from the actuators to the desired region of actuation.

Figure 72: Examples of the electrospun material having been attracted toward undesirable regions due to conductive elements and the resultant shielding utilising acrylic.

Another complication faced with regards to all collectors tested was the tendency of collected fibre to attach to and be distorted by nearby structures which could act as obstructions to the generated jet of material. This is illustrated in Figure 73 where fibres have attached to nearby acrylic (highlighted in yellow). Experiments with the electrode-mandrel hybrid mechanism noted the occurrence of fibres stretching from nearby acrylic towards the collector. This demonstrated that the proximity of the acrylic yielded interference for whipping jet of fibre.

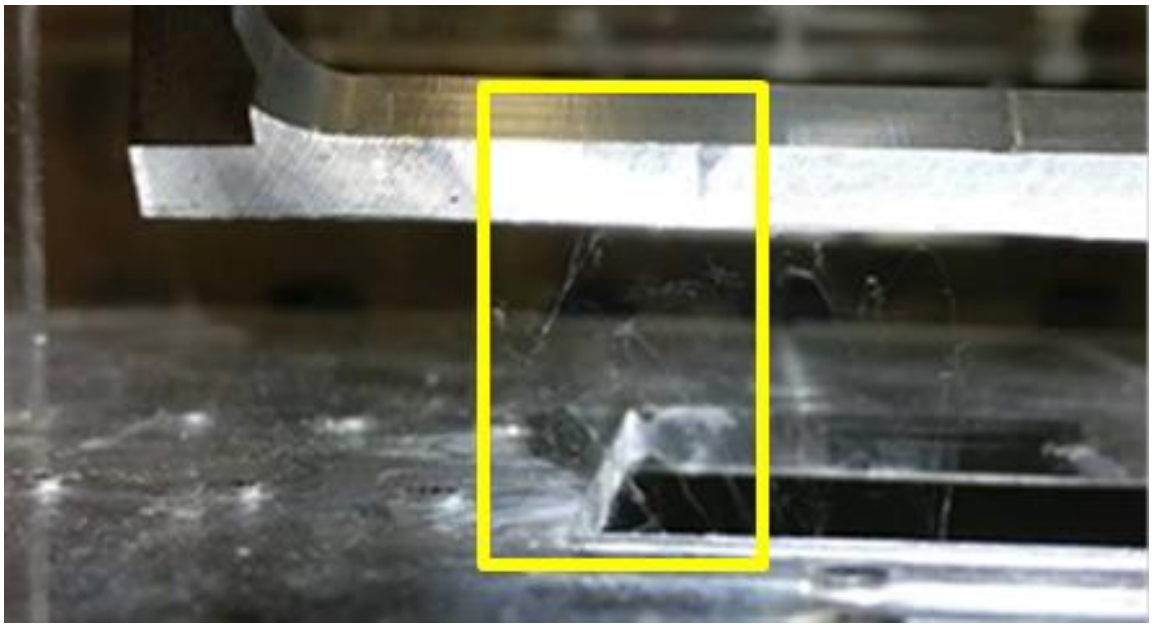

Figure 73: Interception of deposited fibres by acrylic (highlighted in yellow)

Regarding experiments utilising the rotating mandrel-based collector, a large accumulation of unwanted fibre could be identified upon the actuator. Much like the occurrence of the fibre upon conductive actuation based components this build-up of fibre was associated with the relative grounding of the motor coils during machine operation. In order to account for this, a 3D printed ABS housing was used in an attempt to insulate this component [Figure 74].

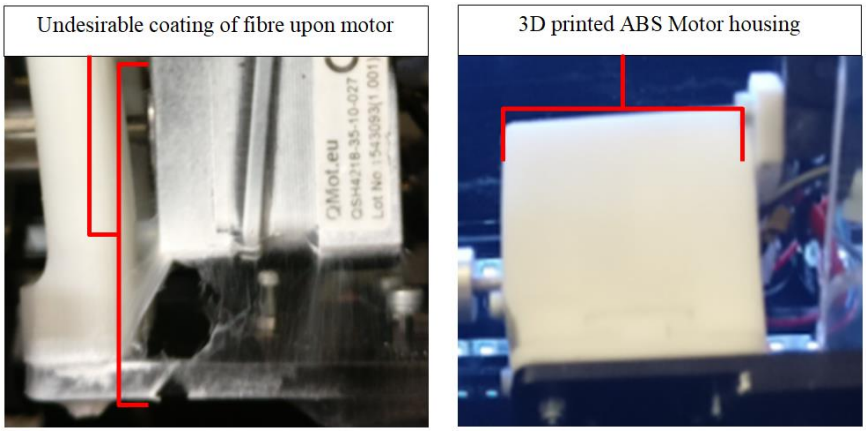

Figure 74: The occurrence of undesirable fibre upon the motor and the implemented deterrent

4.7.2 Taylor cone direction rectification/modification

With respect to the point of extrusion, much of the development of the component related to attempts related to modifying the nature of the electric field surrounding the nozzle. This took inspiration from established Electrohydrodynamic 3D printing. In this technique, an electrostatically charged droplet can be controlled by the implementation of conductive material in the form of a ring that is intended to act to guide the droplet to the desired region. The following development relates to the attempted application of similar techniques to account for and rectify the somewhat erratic formation of the Taylor cone at varied positions upon the extruded meniscus [Figure 75].

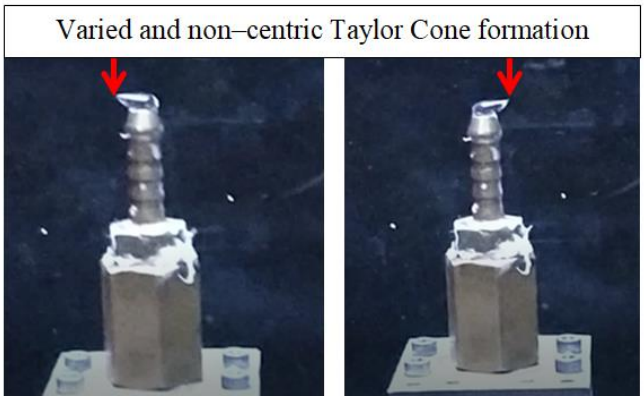

Figure 75: Images taken during an electrospinning test with emphasis on an uncontrolled varied occurance of the Taylor Cone

This work related to the placement of additional charged aluminium around/near the point of extrusion. The idealized electric field generated from a physics based understanding is illustrated in Figure 76. This concept intends to have the fibre jet developed in electrospinning is solely affected by an electric field having the desired trajectory, namely surround the potential point of extrusion with a region large enough to lock the material in the desired direction. The attempts made to further promote the development of such an environment are detailed in Table 16.

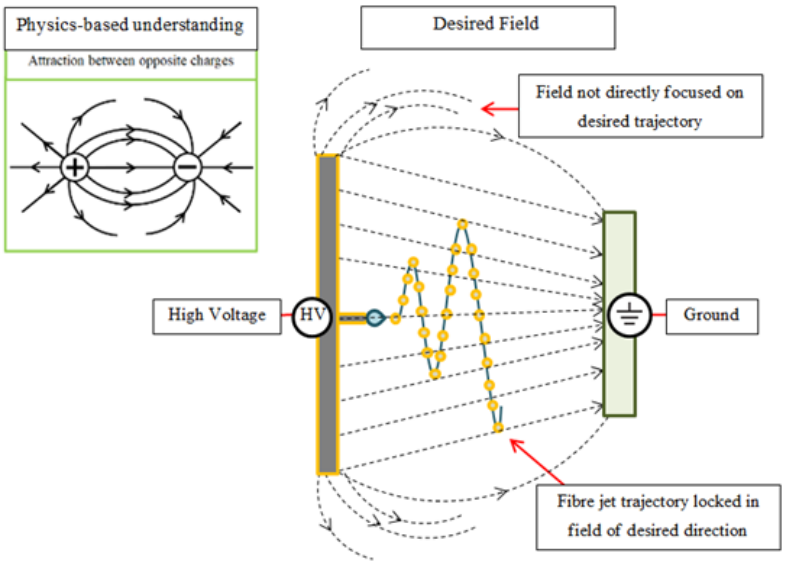

Figure 76: Desired electric field derived from additional conductive elements near the extruder

Table 16: Development of electric field modulating componentry

Initial Attempt	Refined Attempt	Final Attempt
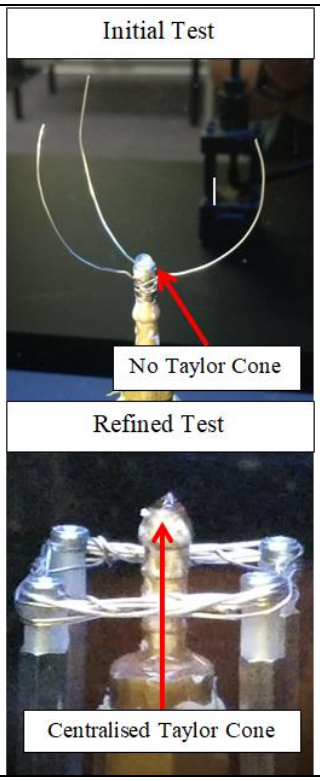	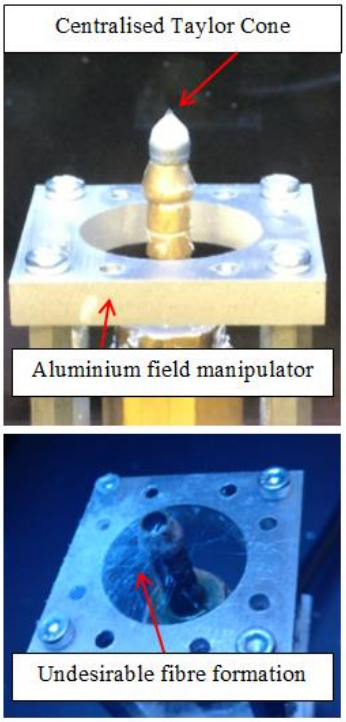	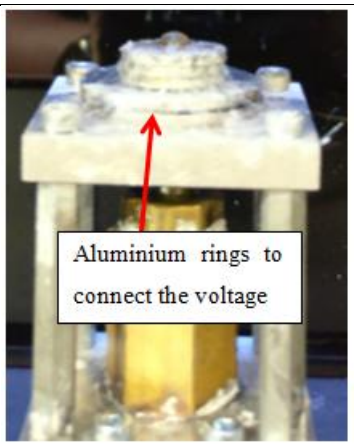
• Wire experiments to modulate the electric field. • Charge concentration at wire tip • Zero Taylor cone formation	• Taylor cone formation central at nozzle • Occurrence of fibres stretched towards platform	• Connecting plates to ensure equal potential between field modulating plate and nozzle

Initial attempts included the use of wire material extending away from the nozzle tip towards the collector however, this resulted in the concentration of charge occurring at the wire tip nearest the extruder and as such there was no longer a sufficiently high concentration within the solution to result in electrospinning. Following this realisation additional aluminium attachments were positioned below the nozzle tip. These included a plate having a circular cut out in the middle of which the extruder was placed. It is worth noting the occurrence of fibres stretching from the tip of the nozzle to this platform which seemed to indicate a variation in the charged nature of the aluminium (affecting the field) as such to circumvent this additional aluminium rings were placed to both surround and connect to the nozzle. Through these methods, a more centralised Taylor cone formation could be identified and as such, this form of controlling the electric field was deemed a viable option for further work regarding electrospinning production. As the nature of electrospinning productivity was not the focus of this study, this technique was not developed further.

4.7.2.1 Multiple nozzle extruder

The interchangeable nature of the sliding-mechanism based extruder design allowed for an ease in the development of additional methods of extrusion. Another attempt to increase the productivity of the electrospinning process, a mechanism for the modular addition of multiple nozzles was constructed [Figure 77].

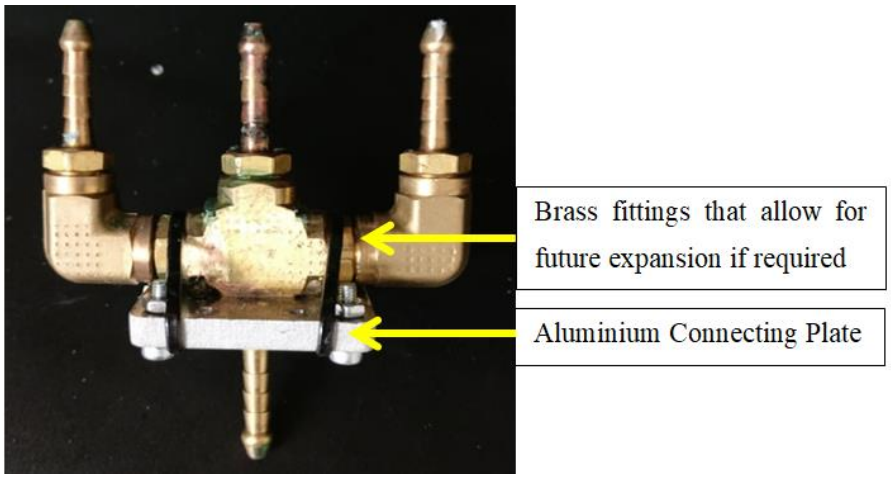

Figure 77: Brass extruder having the ability to increase the number of nozzle extruders

This consisted of four 3mm brass nozzles connected by brass fittings to allow for the electrospinning of material from three points of extrusion. Preliminary results from this mechanism indicated likelihood for the interference of each nozzles electric field with the nearby neighbour point of extrusion fields. This was identified by the collision and entanglement of fibres within the process distorting the idealised trajectory as well as the non-uniform distribution of fibre upon the collector [Figure 78].

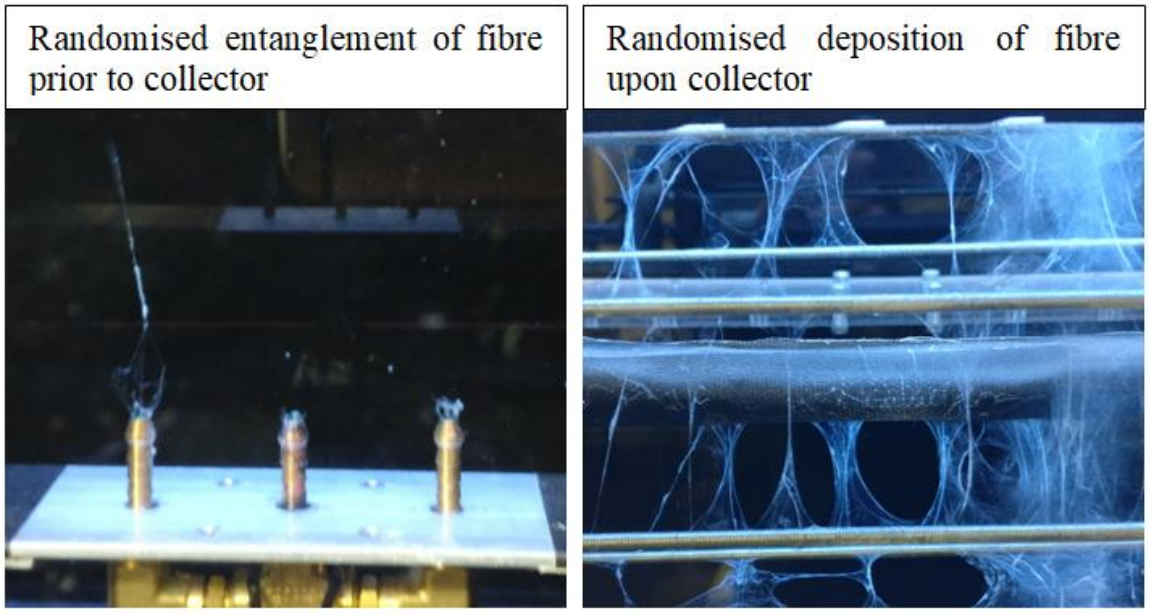

Figure 78: Images depicting the randomised entanglement or disruption of fibres both prior to and upon the collectors hypothesised to be caused by adjacent nozzle proximity

An attempt was made to negate this limitation by manipulating the fields surrounding the points of extrusion through the inclusion of additional aluminium based materials [Figure 79], however this did not yield substantial changes to the results and will require future research and development.

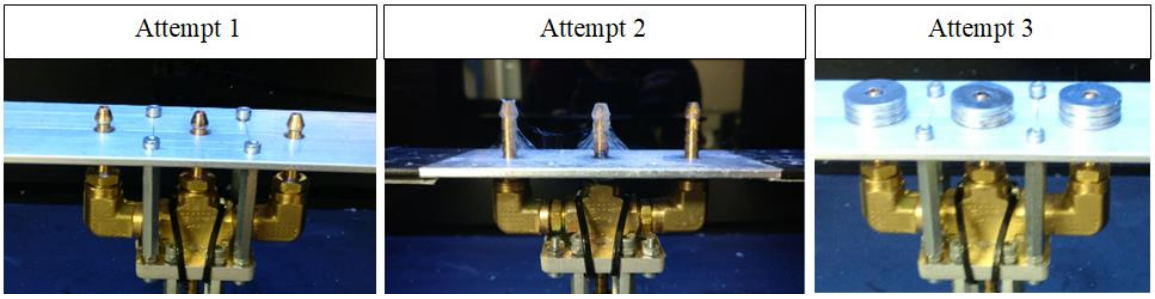

Figure 79: Application of additional conductive material in an attempt to modify the electric field and prevent fibre trajectory disruption occurring from adjacent nozzles

4.7.3 Field manipulation through ground rod modification

Given the understanding that the nature of the electric field formed is related to the nature of both the charged regions and grounded regions, an investigation into the modification of these forms was conducted. This research was majorly motivated by a sudden inability to generate fibres when switching from synthetic (Nylon 6, 6) to biomaterial (collagen) solutions. Figure 80 demonstrates the difference in output collagen fibres when compared to nylon fibres both generated utilizing a similar technique. As discussed in earlier sections related to parallel electrode mechanism development this variation in outcome is potentially related to the reactivity of the collagen solution and thus reduction in instabilities resulting in a varied collection.

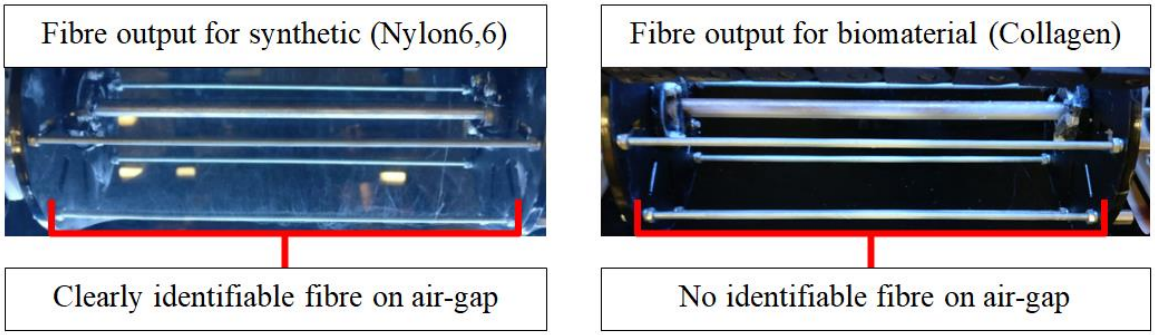

Figure 80: Comparison images depicting the variation in output fibre upon the collector for nylon 6, 6 and collagen respectively

It is worth noting that in the evaluation of the collagen experiments, the grounded rod situated in the middle of the rotating mandrel became coated with the desired fibre. As such electrospinning was occurring, the placement of resultant fibres was however not desirable. A simple quick and effective method to identify whether the modification of the grounded region could benefit the placement of this fibre formation was through the use of insulating tape upon regions of the grounded rod. Three variations on ground manipulation where evaluated, these are referred to as Rendition 1, Rendition 2 and Rendition 3 and are depicted with brief characteristics described in Table 17.

Table 17: The effects of ground rod modification for collagen based electrospinning utilising the developed rotating collector

Rendition 1	Rendition 2	Rendition 3
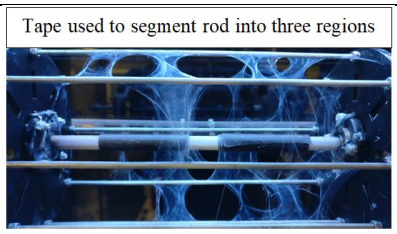	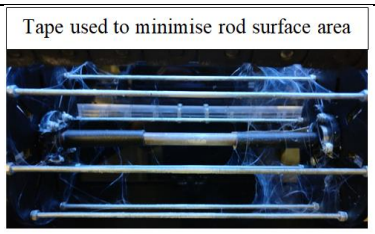	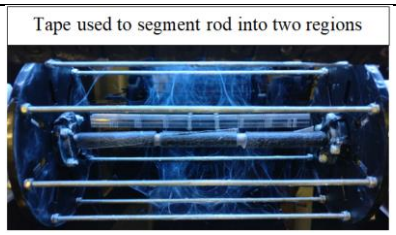
• Developed fibre occurred in inconsistent regions • Predominantly above taped area	• Similar to attempts to minimise parallel electrode surface area • Occurred mostly on one side	• Centralised fibre generation • Semi-consistent • Generation of parallel electrode

The development of fibre between the airgaps for Rendition 1 was a dramatic improvement in comparison to the inconsistent and somewhat non-existent occurrence in the unmodified experiments. Here the insulating tape was placed in such a manner as to create 3 different segments of exposed grounded rod. This was intended to promote the generation of fibre on the desired airgaps above these regions. This was not the case, and fibre can be seen to occur relatively inconsistently was however relatively inconsistently with a bias to form above covered/insulated portions of the rod. This seemed to represent an interruption of the multiple grounded regions with one another. Following experiments conducted in which the grounded area was minimised (see the earlier discussions relating to the modification of the parallel electrode collector), the second experiment (Rendition 2) occurred as purely the minimisation of the initial rod surface area. This experiment showed a clear lack of fibre developed above the conductive ground. This instead occurred inconsistently above the insulated/taped portions with a bias towards the right side. The final version (Rendition 3) yielded a much more acceptable outcome for the generated fibre. This now occurred much more consistently and centrally than other attempts. Ironically, in this experiment much of the guide rod was insulated/covered leaving only two small regions of this element exposed. This led to a hypothesis regarding the nature of the fibre trajectory, namely that the lower reactivity of the collagen meant that fibre trajectory is greatly limited to the nearest ground source. This meant that fibre generated perpendicular to the ground region would accumulate on this and not experience enough whipping to result in a formation upon alternative nearby structures (this ideology is illustrated in Figure 81). This understanding would explain the nature of fibre occurring centrally for Rendition 3.

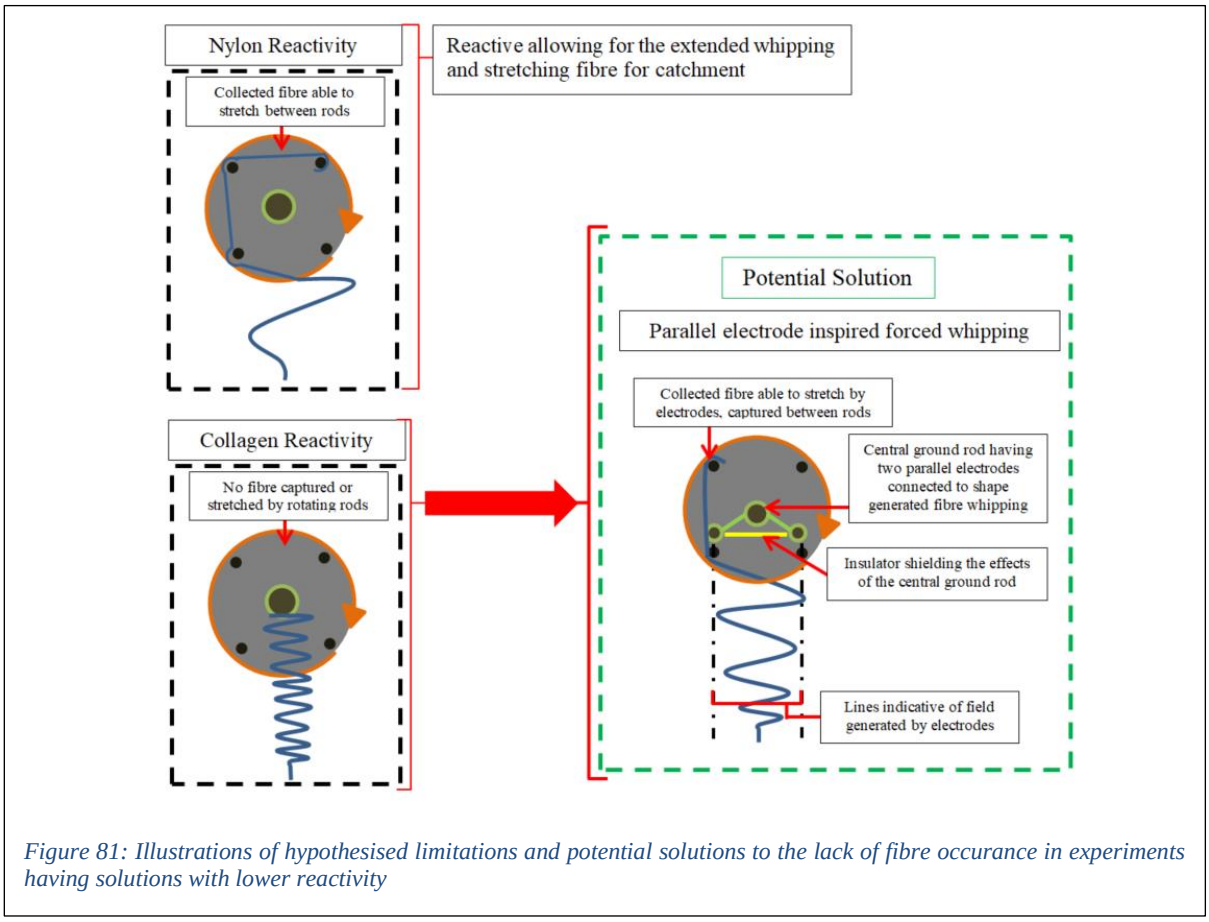

Figure 81: Illustrations of hypothesised limitations and potential solutions to the lack of fibre occurance in experiments having solutions with lower reactivity

Whilst the use of tape to control the resultant grounded rod surface area was effective in demonstrating the effects of ground modification of collected fibre distribution, this was not deemed a sufficiently controllable method/mechanism. Thus to allow for this type of modification a 3DP PLA (Polylactic Acid) part was generated which would both act to wrap around the ground rod as well as provide opportunity to further parts for the modification of the ground rod (Figure 82).

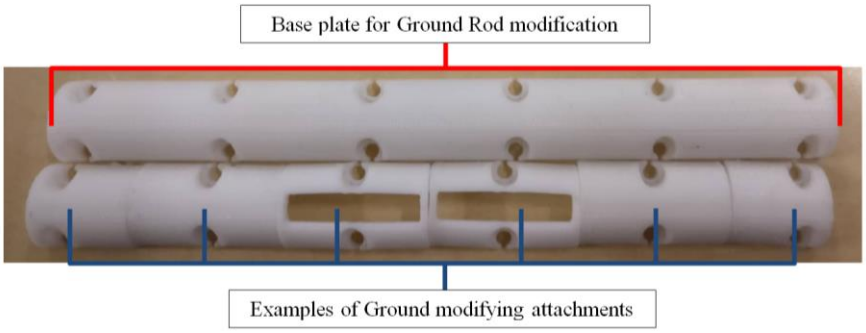

Figure 82: PLA 3D Printed Ground Rod modification components/coverings

Initial experiments with this 3D printed mechanism did not yield consistent outcomes. This led to a further realisation relating to the nature of the rotating rods of the mandrel collector. These were of a conductive nature and as such had the potential to result in a modification to the output fibre placement. In order to evaluate the effects of these rods on collected fibre placement, the entirety of the ground rod was insulated via 3D printed components and insulating tape. This resulted in a sporadic occurrence of fibre with a right bias (similar to the previous test: Rendition 2) which seemed to indicate that these rods were acting as independent ground rods. To further evaluate this coverings made from tape were wrapped around on either side of the collector. This demonstrated the reduction in regions of the occurring fibre and promoted the more central distribution/placement of these. This was similar to prior experiments relating to conductive region minimisation. As such to reduce the potentially undesirable effects of this conductivity these rods were wrapped in polyurethane tubing. This modified collector was then tested similarly to the initial test. The results of this demonstrated a dramatic reduction in the generated fibre that would seem to coincide with the lack of attracting ground based material. This limitation and the modified collector are depicted in Figure 83.

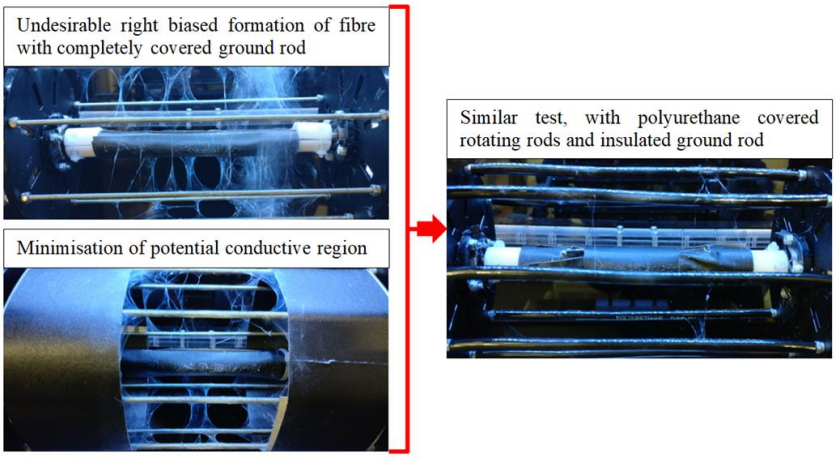

Figure 83: Experiments relating to the identification of the influence yielded by the conductive rotating rods and resultant fibre placement/production

One particular modification of interest involved the addition of two conductive plates that had the ability to be attached and connected to the ground rod within the confines of the rotating collector. This was intended to yield a combination of the benefits of parallel electrode and rotating mandrel electrospinning. The fibre formation for the initial tests utilising this new collector could only be identified upon the electrode portions. This once again was associated with the hypothesised lowed fibre whipping and large surface area of the electrode. Additionally there were concerns relating to the proximity of these electrodes to the rotating rods, with the potential for fibre to instead bridge between rod and electrode instead of across the desired air gap. To account for these limitations, the exposed grounded portions were modified/reduced by using tape. This demonstrated a familiar result having a right-biased accumulation of sporadic fibre placements (see Rendition 2). In an attempt to centralise the produced fibre placement, the electrode surface area was further reduced as well as the collector's surface area. Whilst this did aid in a more central production of fibre this was much in much lower quantities to what had previously been generated. This evaluation and progression is depicted in Figure 84.

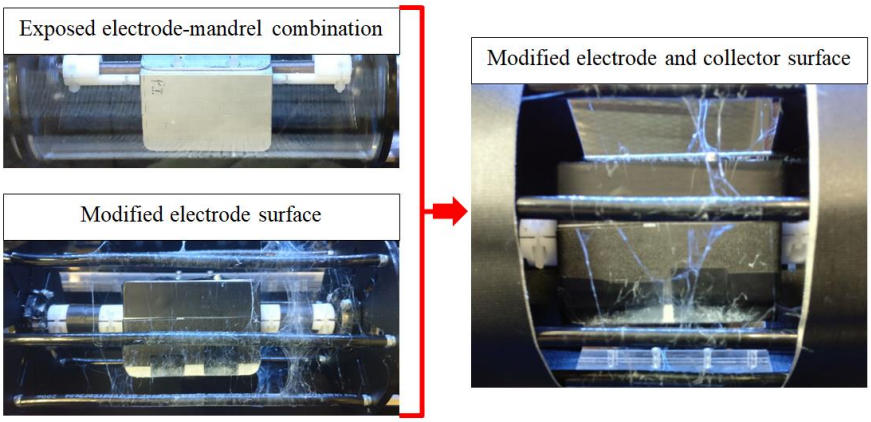

Figure 84: Images depicting the progression of electrode-mandrel combined electrospinning optimisation

This section demonstrated the inability of experimentation to adequately increase the ability to generate sufficient quantities of accessible fibre via electric field modification. As such the more traditional approach of modifying the temperature and humidity of the electrospinning region was investigated within the context of the developed machine.

4.8 Temperature and humidity control

For a large portion of the development within the project, experiments were conducted in New Zealand's summer period. Here temperature and relative humidity is known to be within the range of 20-30^{o}C and 70-75% respectively. The seasonal shift from these relatively high temperatures to colder temperatures occurred quite rapidly within 2019. This combined with the temperature sensitive nature of the biopolymer (collagen) utilised in experiments at this stage in the project yielded a sudden and unexpected cessation of machine functional fibre generation. Whilst temperature and humidity have been highlighted as having influence over the resultant fibres [79], development within the project seeked to identify a plausible way to modulate fibre production without the need for the complexities associated with environmental control. This was in part due to the large processing region within the machine as well as the unwanted complexity derived from the addition of multiple sensors and components. Given the inability to adequately modify fibre production through alternative means, a simple system for temperature and humidity user-based control was attempted. This took the form of a hot air emitter device which was suspended within the electrospinning chamber. By activating this device prior to and during the electrospinning process, the internal chamber could be heated. This demonstrated a dramatic increase in collagen fibre generation, Thus from this evaluation a simple control system utilising a temperature control unit, sensor and 240V relay was utilised [Figure 85].

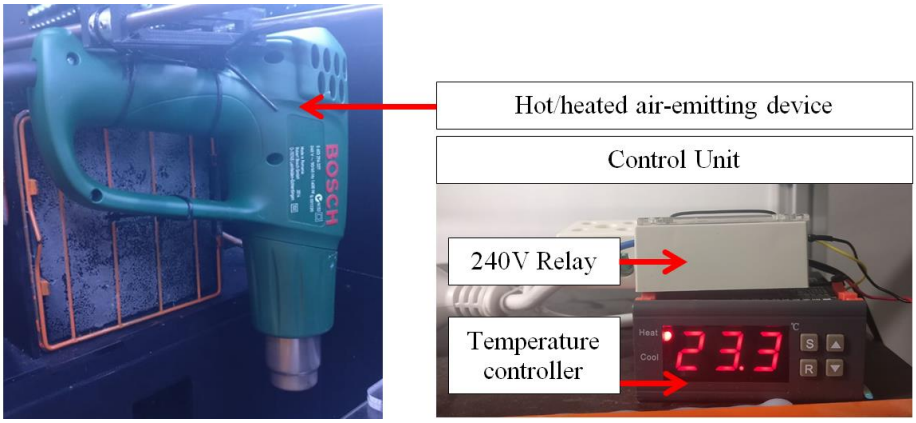

Figure 85: Simple control system utilised in an attempt to control the local environmental conditions for electrospinning to occur

It was hypothesised that the application of this control system allowed for the chamber temperature as well as the related relative humidity to be modified according to the desired set temperature. It is worth noting that the components utilised were not optimal, as such an error range of approximately 5^{o}C was associated with the use of this system. One concern with this system was that the resultant change in fibre formation was not a product of the effects of chamber temperature but rather the effects of this heating on the extruder. This logic was derived from the established understanding of Melt electrospinning, whereby the fibre generation productivity is directly related to the heat of the extruder utilised. As such to further investigate this, a small chamber was crafted to surround the extruder [Figure 86]. This chamber could be heated and the results of this more localised heating reviewed. Whilst this technique did demonstrate a beneficial relationship with the resultant fibre formation, the added chamber was not able to completely insulate the component resulting in cooling from the colder environment. Additionally the cooler environment resulted in a higher relative humidity and thus reduction in fibre formation. The potential for the use of an embedded heating control system was evaluated

[Figure 87], however this was not feasible due to the interactions/damage which would occur to the components from the exposure to the high voltage source.

Figure 86: Extruder surrounded with housing allowing this to be heated separate to the greater electrospinning environment

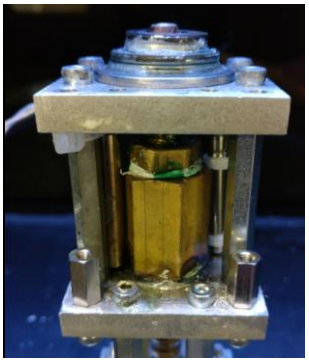

Figure 87: Heating element and sensor fixed directly to extruder

Given the restrictions on localized extruder based heating, an alternative method which could enable the heating of the environment as well as directly affect extruder temperature was investigated. This took the form of a fan-based heater which was situated underneath the extruder attachment plate. Vents were created through which heated air could be added to the environment with the fan acting to heat the extruder via the attachment plate. To allow for some control of this a thermometer was connected to the extruder. This would allow for reading prior to and post electrospinning (as this had to be disconnected during the operation of the High Voltage). Additional methods to control the environment included the use of a small-scale dehumidifier device as well as a commercial humidity and temperature sensor device. It is worth noting that the heater was switched off during machine operation to reduce any unwanted effects from the additional airflow provided by this component. These mechanisms for environment control/conditioning are annotated and illustrated in Figure 88.

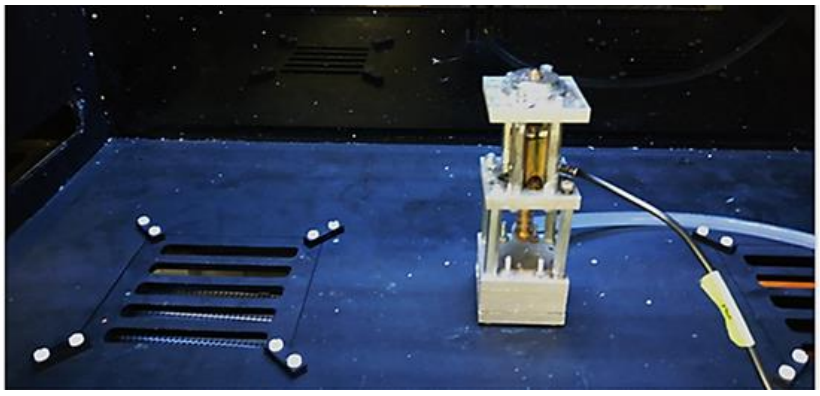

Figure 88: Extruder plate modification to include heating vents as well as means to evaluate extruder temperature.

4.9 Electronics based development

As many of the desired research equipment including a desired final machine were to be generated locally, some means to control the electronic systems within these was required. A decision was made to utilize a microcontroller for this work as these are typically more affordable than programmable logic controllers (PLCs) and would allow for a high degree of flexibility within the project. It is worth noting that the electronics utilized within this project were not of an industrial nature. This allowed for a reduction in costing and avoidance of complications derived from the integration of systems requiring different proprietary hardware or software.

The Arduino microcontrollers are an affordable, readily available and well documented product line. Whilst there are impressive alternatives to this technology such as the Trinamic TMCM-6110 or Nucleo boards, the Arduino was preferred. This was due to the increased user capabilities, as it was not restricted by proprietary software such as the Trinamic software and its integrated development environment (IDE) not requiring internet access. This device is also open source resulting in a higher prominence/accessibility of this device and a higher degree of familiarity with this product line. The Arduino Mega 2550 was chosen for this project as this board is popularly utilized within hobbyist 'do it yourself' (DIY) 3D printers having a desirable fifty two digital pins which can be assigned to various tasks. These microcontrollers as well as related characteristics are depicted in Table 18.

Table 18: Three major microcontroller alternatives evaluated within the project

Trinamic	Nucleo	Arduino
	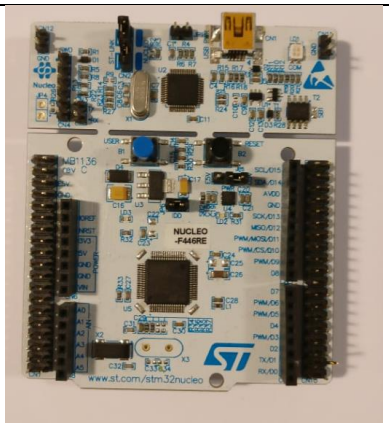	
• Robust microcontroller capable of complex motor control • Proprietary IDE • Undesirable Limits on the control/functionality	• Well documented competitor to Arduino • Utilised in opensource 3D Printer development • Proprietary online based IDE	• Very popular within hobbyist utilisation • Large established code resources • Completely opensource (including IDE)

Whilst the pins of microcontroller products are typically available for direct connection to electronic componentry, often a separate printed circuit board (PCB) is utilized to allow for a reduction in the complexity of wiring. One such unit typically utilized within the hobbyist construction of 3D printers is the RAMPs v1.4 [Figure 89]. These boards are capable of controlling up to five stepper motors through Pololu motor controller units and have ports for both input (i.e. sensors such as cantilever switches and buttons) and outputs (i.e. liquid crystal display (LCD) screens).

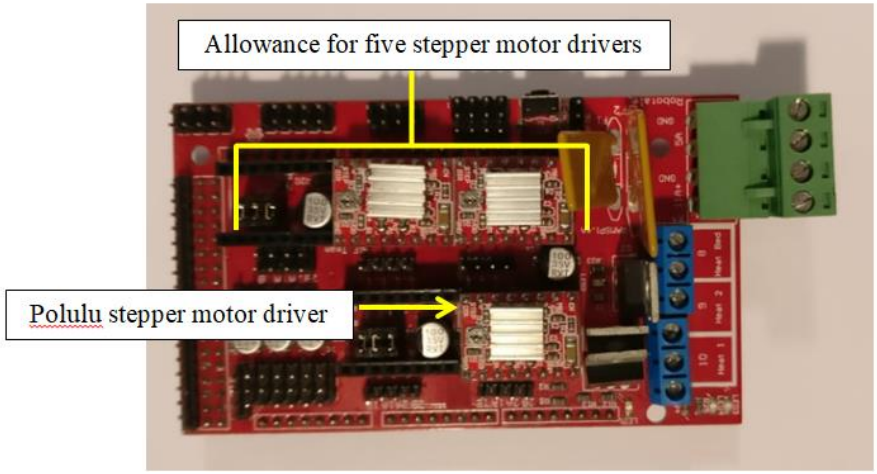

Figure 89: Example of a RAMPS v1.4 board with equipped Polulu stepper drivers

The RAMPs v1.4 solution was unfortunately not able to adequately service the continual project development, with a major limitation relating to the assigning of pins to components not actively used in the project (e.g. LCD screen). Following this breadboard was utilized for further prototyping. It is worth noting that whilst breadboard offers a simple and easy way to rapidly prototype with electronic componentry, this is susceptible to limitations relating to voltages above 5V and current above 2A. Due to the requirements of the project, the increasing number of electrical componentry for which this prototyping technique is not well suited became apparent. This limitation sometime resulting in inaccuracies in reading or assigning signals. As such for the testing of multiple motor and sensors a combination of perf-board (vero-board) and breadboard was utilized. This however resulted in a highly complicated mass of electrical wiring with troubleshooting of faulty connections tedious and time consuming. As such to simplify this work and increase system stability/reliability a decision was made to utilize a PCB board. It is worth noting that a fundamental flaw of this board related to the positioning of the output terminals for much of the components as such while this operated as required, the serviceability of this was greatly restricted by the amassed complex nature of the resultant wiring. The evolution of the electronic circuitry is demonstrated in Table 19.

Table 19: The evolution of the circuitry required for the project's machine/mechanisms

Breadboard	Veroboard-Breadboard	PCB board
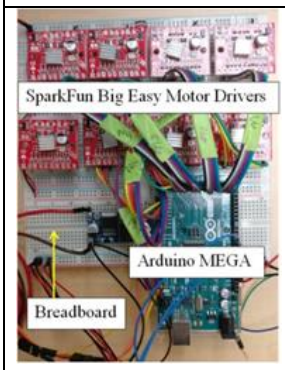	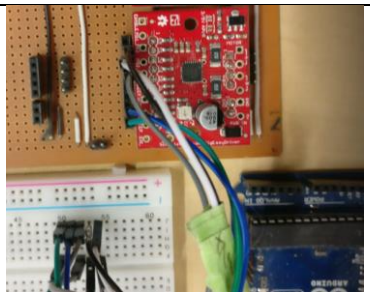	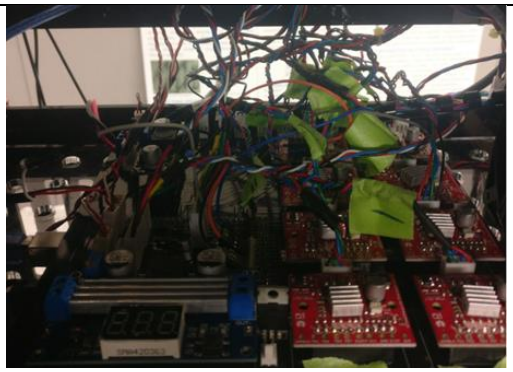
• Simple, effective prototyping unit • Limitations related to current and voltage	• Effective way to overcome restrictions • Allowed for mechanism testing • Complex wiring	• All –in-one solution • Bad output terminal design resulting in complex wiring

4.9.1 PCB Limitations

A major limitation to research and development of novel mechanisms and machines with respect to electronics relates to the continual and rapid development/modifications to control requirements. Standard PCB boards are particularly restricted in this capability as they are designed to incorporate all the required componentry as a final solution (i.e. they are built for purpose units). In the case of the PCB board utilized three major situations resulted in the requirement for modification. The first being a redundancy in the requirement for a PCB integrated and driven unit to control a 24V step up transformer. The second related to the vulnerability of the Arduino and potential for certain parts on this device to loose functionality and thus requirements for rewiring. The third change related to limitations in the design for the addition of new components/mechanisms. The modifications made to account for these limitations are presented in Table 20.

Table 20: PCB modifications required due to project development

PCB regulator	Port accessibility	Terminal addition
	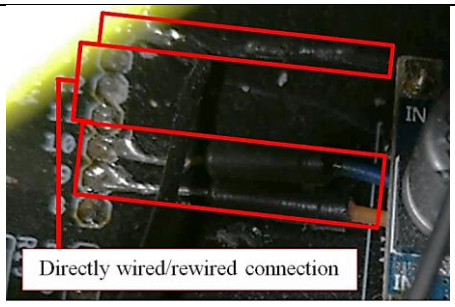	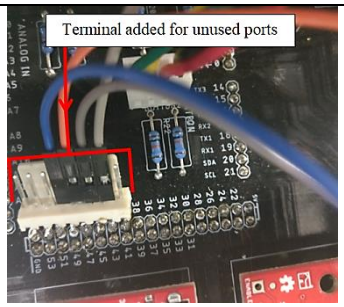
• Redundant component • Replaced with required component	• Problematic signals • Rectified through direct wiring/modification to connectors	• Terminal soldered onto existing PCB • Allowed for additional components to be added

Of these limitations the third is perhaps the most significant with respect to this project as the final outcome for it is intended to be a continual research and development machine. This would require the capability to add or remove componentry and mechanisms relative to the user's requirements. This limitation led to the ideation of a modular PCB orientated technique. This concept included the design of multiple boards containing the electronic parts (e.g. resistors, diodes, capacitors etc.) required for the desired component (e.g. relay, motor, switch etc.). An example of which could be utilized for a relay would be a PCB equipped with input (Arduino signal) and output (relay signal) terminals with a diode connected to the ground. These boards would be stacked like a building with the number of floors correlating to the required number of relays for the system. The wiring of this could be wrapped and neatly connect to an Arduino terminal. Due to time constraints and the capability to implement the desired functionality with the prior developed equipment, this concept (illustrated in Figure 90) was not deemed within the scope of the project and is instead recommended for future work in this field.

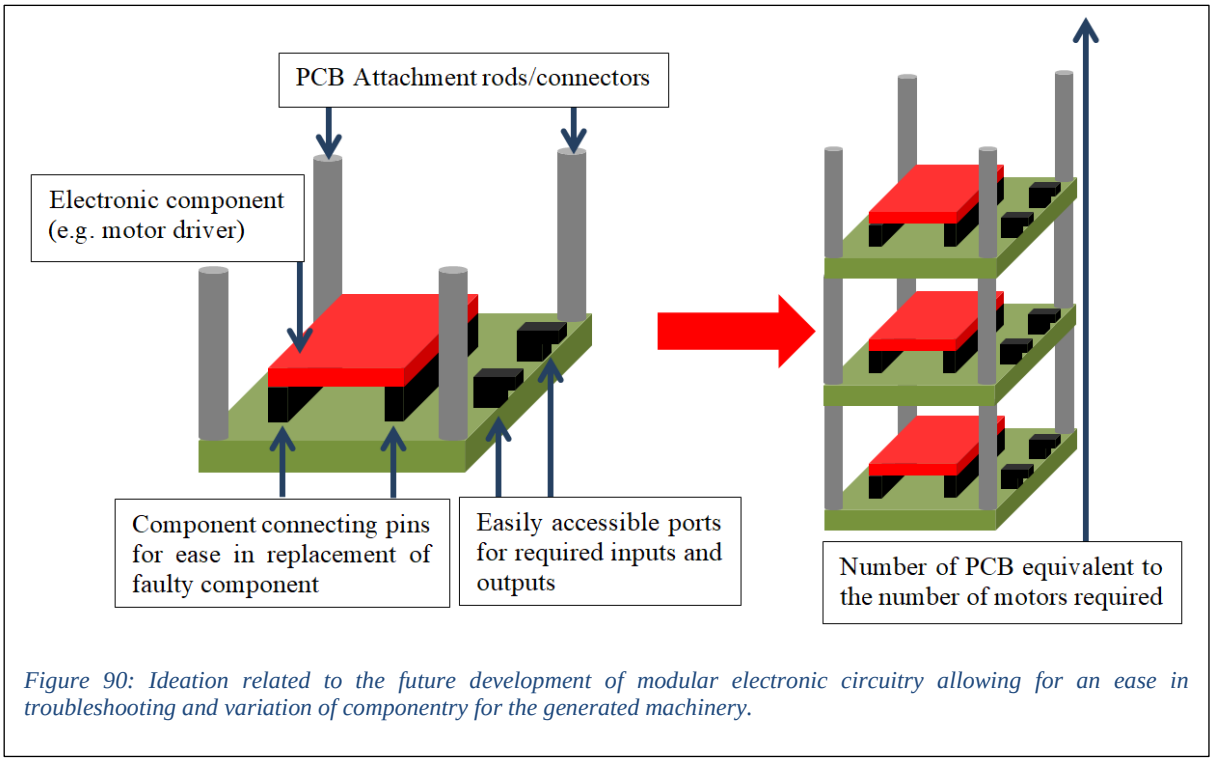

Figure 90: Ideation related to the future development of modular electronic circuitry allowing for an ease in troubleshooting and variation of componentry for the generated machinery.

Chapter 5 FINAL DEVELOPMENT OF A NOVEL FIBRE BASED MANUFACTURING RESEARCH AND DEVELOPMENT MACHINE

This project aimed to identify the potential for manufacturing of fibre based constructs such as the cornea. Research and subsequent investigation was highly motivated by the principles of 3D printing and automated additive manufacturing. Thus in order to adequately test the plausibility of the hypothesis some form of automated fibre based manufacturing system was required. This chapter discusses the development of the final research machine within this project namely progression associated with the Hardware, Machine Operation/Procedure and Software/Code.

5.1 Prior machine-based developments

The final machine developed within the project was a product of prior attempts to generate a means for the implementation of the post literature review hypothesis. The first embodiment took the form of a relatively simplistic acrylic chamber within which stepper motor leadscrews were mounted vertically to actuate a platform to a desired height. Additional elements to this machine included the use of an extractor fan, and a chamber in which the High Voltage Power supply could be situated [Figure 91]. Many fundamental evaluations relating to electrospinning were achieved through the implementation of the initial renditions of mechanisms relating to the syringe pump, collectors and extruders. A major limitation within this design related to the undesirable arcing of the electrostatic potential to the power supply (as such further testing required this to be placed externally) as well as the occurrence of electrostatic interference in the devices actuators. This led to the development of a simplified form in which clear acrylic was utilized to further evaluate the implemented processes [Figure 92]. This provided a more accessible method for the evaluation of rotating mandrel orientated techniques. The clear nature of the device helped to identify issues regarding the fibre formation on actuator lead screws that had previously been thought of as sufficiently protected. Revelations regarding the positioning of actuators as well as a requirement to add grounding to motor housings to prevent undesirable disruptions or inaccuracies were achieved through experimentation with this device.

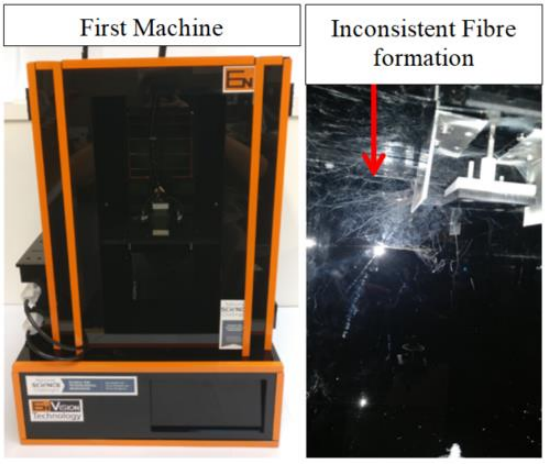

Figure 91: Initial attempts at machine development with issues relating to undesirable fibre accumulation

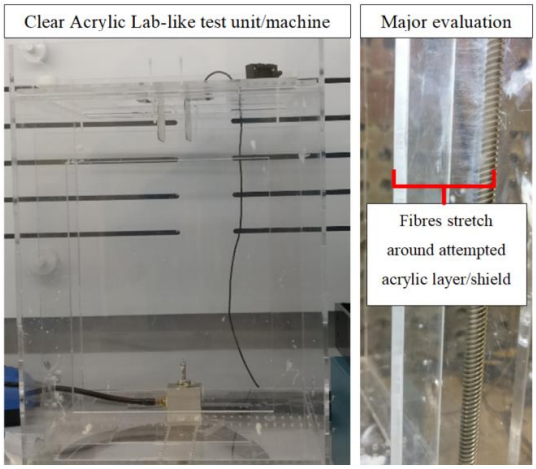

Figure 92: Simplified testing unit with an increased ability to identify limitations within actuation

5.2 Machine Operation/Procedure Development

From experimentation and developments within the work related to the previous machine renditions, processes which would be required in the final machine were identified. These processes are expressed as three distinct phases of machine operation and include the Machine Initialization, User Interface, and Machine Manufacturing phases. It is worth noting that given the desirability for this machine to allow for variation through modularity, the following described stages solely to the standardized use of the machine (i.e. the use of syringe pumps, peristaltic pumps etc.) and as such are subject to variation through the machine code. The following sections will discuss the desirable outcomes of each stage and illustrate these via flowcharts which aided in the later development of required functions to be coded in C. Whilst these functions are displayed alongside related flowchart headings, and a brief description for each delivered via a table, the fundamental code based functionality within these is discussed later within the chapter.

5.2.1 Machine Initialization phase

The first intended interaction that the user would have with the machine related to the powering on of the device, identification of certain mechanisms positions and the servicing/priming of devices. Once started a prompt to 'home' the motor components, namely return the actuated elements to the desired beginning position, would be issued. This would ensure positional control for following operations for the seven stepper motors as well as three servomotors. Upon completion of the 'homing' phase, the user will be prompted to service the vapour generating process. This is intended to involve the removal of any residual contaminant within the piping of this mechanism via the peristaltic actuation of cleaning agent (e.g. water or other suitable agent) through the system. The user will then be expected to purge the system of the cleaning agent and then prime/load the piping with the desired agent to be vaporized. The user will then be prompted to load a syringe of the desired solution and prime the related piping (in some cases until a meniscus is formed on the extruder) for electrospinning. Figure 93 illustrates the desired progression of this operation alongside the utilized code-based functions which are described in Table 21.

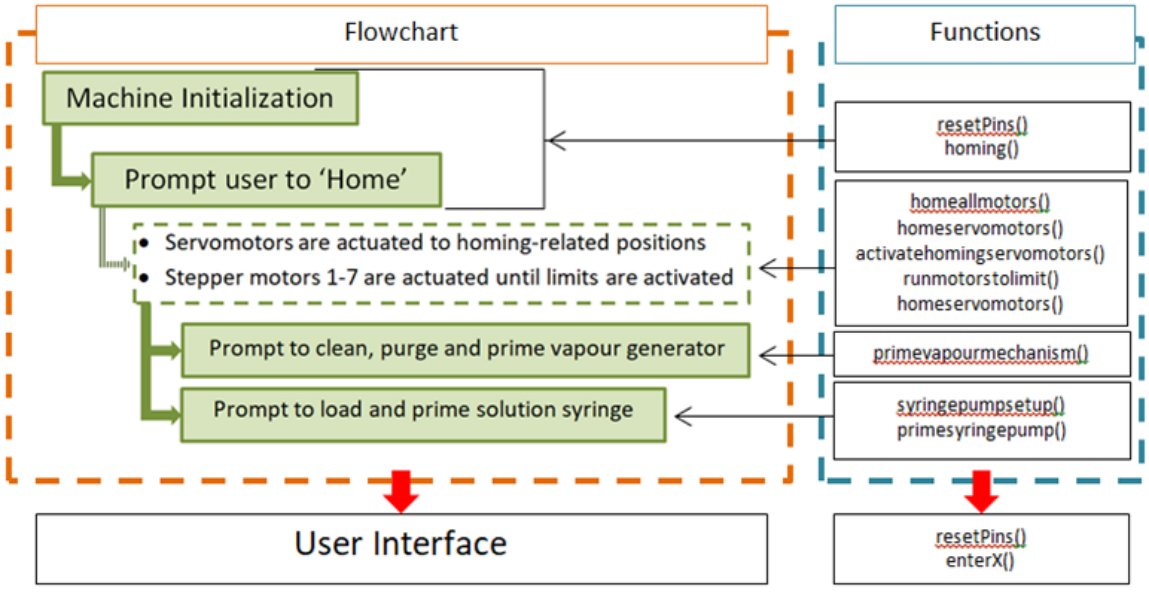

Figure 93: Flowchart showing the progression of the Machine initialization phase

Table 21: List and description of the implemented homing functions within the machine code

Homing Functions – these operations relate to the movement and servicing of components to allow for further accuracy in automation.	
Function	Description
resetPins()	This acts as a method in which modified variables can be reset to a defined value allowing for accuracy in further code.
homing()	An operation in which functions which set values/components to the desired initial state are utilized.
homeallmotors()	This will be utilized to results in the movement of all the motors towards the defined home positions (at limits).
homeservomotors()	An operation which utilizes functions within the Arduino Servo.h library to move all of the servomotor arms to a defined starting position
activatehomingservomotors()	When required this process will enable the movement of specific servomotors to ensure sensors are positioned to allow for further positional detection of mechanisms.
runmotorstolimit()	When this is used, the relative stepper motor will be actuated until the variable derived from its 'limit' sensor becomes the desired value.
primevapourmechanism()	An operation similar to primesyringepump() in which a button component is utilized to trigger the actuation of a motor component to allow for the desired loading of material.
syringepumpsetup()	This operation requests the millilitre per millimetre capability of the utilized syringe as well as prompts the user to begin the loading phase for this component.
primesyringepump()	The user is requested to utilize two button components each relaying a signal which is processed and results in the actuation of the syringe pump stepper motor to enable the desired loading of electrospinning solution

5.2.2 The User Interface phase

Whilst interaction by the user was required in the previous phase of the project this was primarily of a servicing nature, this subsequent stage requires information from the user to define how the machine will operate. This communication is responsible for the later implementation of various modules/technologies in the process and is largely responsible for leveraging of the modular nature of the machine to generate variations in novel results. This data is communicated by utilizing the Arduino's premade serial based control functions. The communication baud rate is defined as 9600bps by setting this through `Serial.begin(9600);`. The Arduino serial monitor is then set to this value and will display desired program information/prompts through applications of the `Serial.println("information/prompt");` or `Serial.print("information/prompt");` command. Information presented by the user is processed through `Serial.readString();` and assigned to a variable which is compared to the desired input and processed accordingly. An example of how this is implemented within the code is demonstrated in the annotated Figure 94.

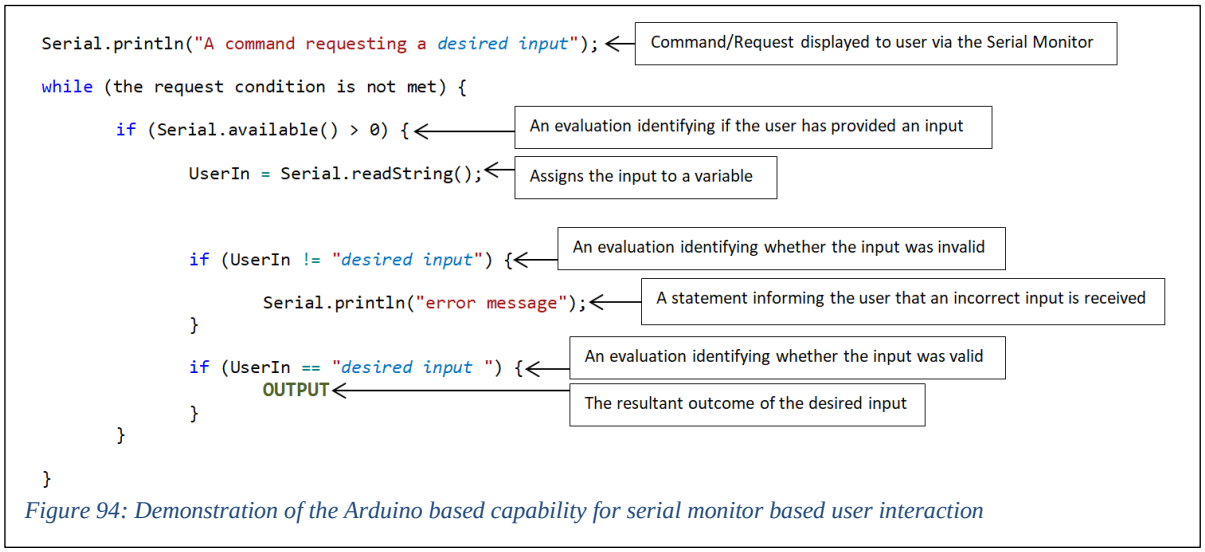

Figure 94: Demonstration of the Arduino based capability for serial monitor based user interaction

The first set of data requested relates to the heights/distances associated with the utilized extruder and collector. The utilized point of extrusion based mechanism might not always have an associated standardized height. As such to account for this variation relative to the machine limitations, the input value must be processed to identify the possible minimum and maximum values possible for the collector height. Thus the further input collector height will be able to provide feedback (if necessary) regarding the machine limitations. This simple calculation is depicted in Figure 95.

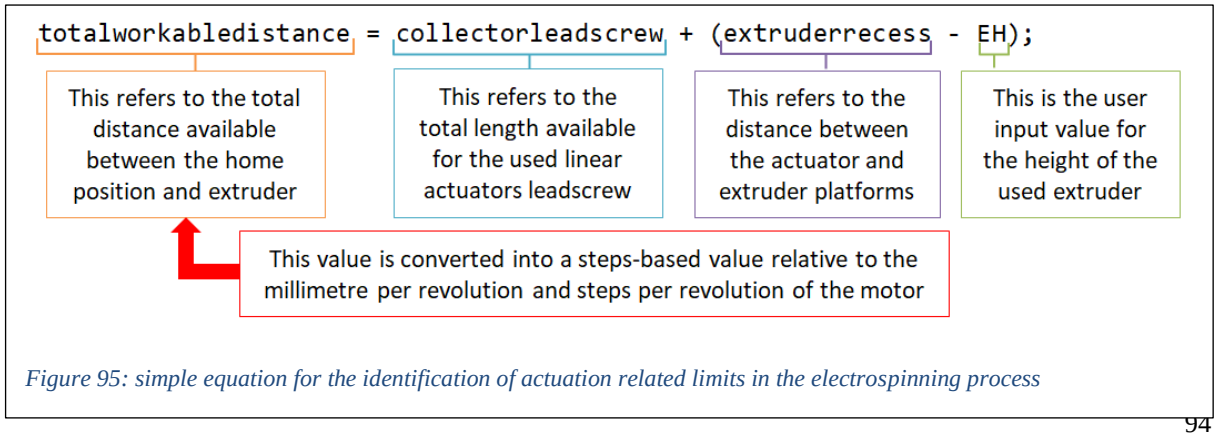

Figure 95: simple equation for the identification of actuation related limits in the electrospinning process

Following this, information important to the desired pump flowrate is requested for both the syringe pump and vapour based mechanisms. As mentioned initially, these components may vary, however this portion of operations is intended to allow for the input of information regarding the control of motor-based mechanisms utilized in both the electrospinning and sequential processing modules. The user is then asked to define the desired time for the electrospinning to occur as well as to identify the desired variation in collection angles for the collecting surfaces (note: this is for the subsequent retrieval of fibre from the utilized collector). The next stage presents the user with the choice of which additional process they require the retrieved fibre to be exposed to. For each process activated, the user will be requested to provide information relative to the desired exposure/activation characteristics (e.g. time, flowrate, or rpm). The final required user inputs relate to the method/nature of the implementation of the machines processes. Here two options are presented with a request regarding the number of operational iterations required being presented once the desired method has been chosen. To ensure that the user has not made a mistake throughout this process, all input data is then presented for final inspection prior to the Manufacturing phase. If the user is in agreement with the input values, they many now enter a value to begin entering the next phase. Prior to this phase however the user will be requested to manually set the desired electrospinning voltage on the now active high voltage power supply. It is worth noting that this will not occur and the user will not be able to enter the manufacturing phase if associated safety mechanisms identify potential danger/user error. Figure 96 illustrates the desired progression of this operation alongside the utilized code-based functions which are described in Table 22.

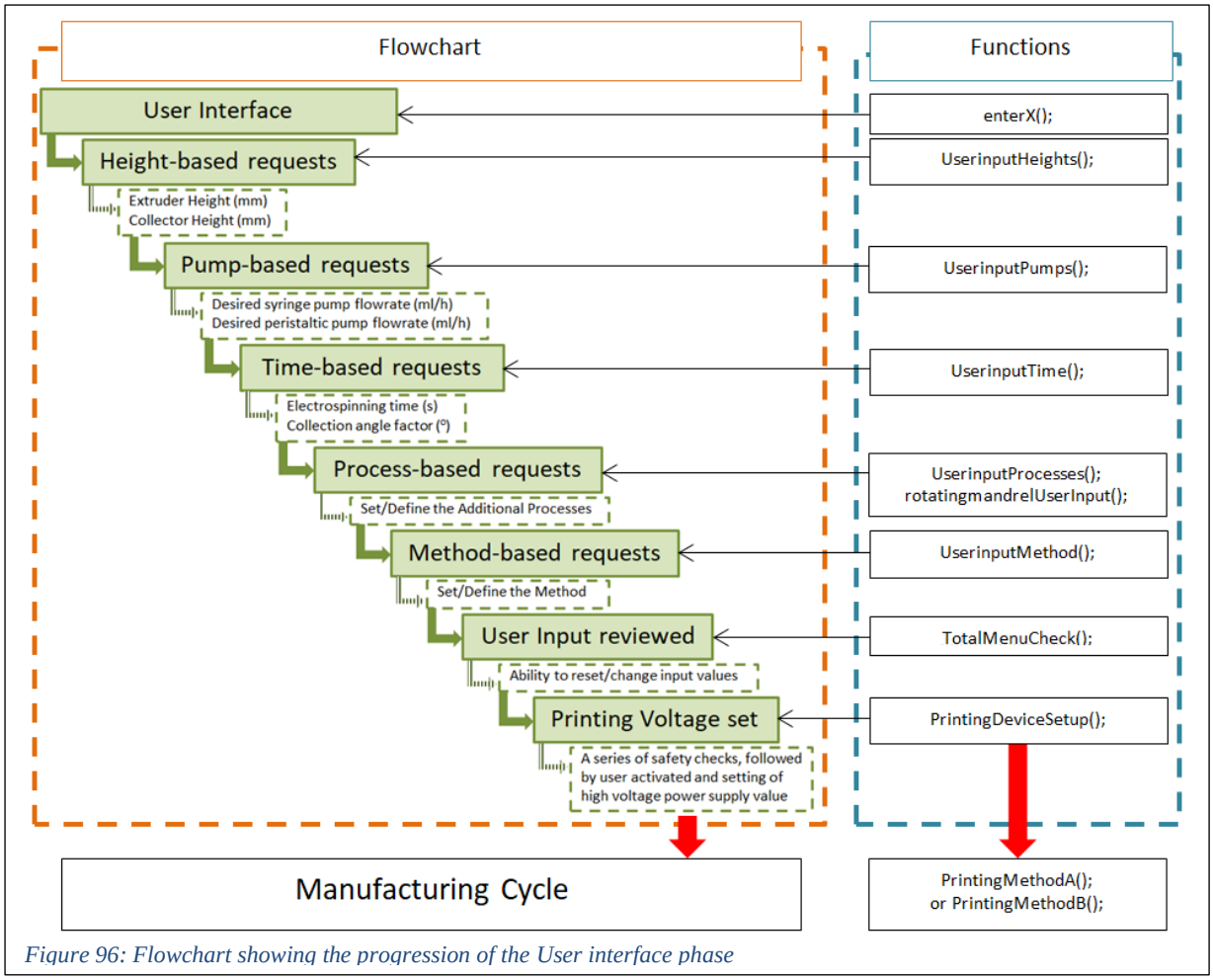

Figure 96: Flowchart showing the progression of the User interface phase

Table 22: List and description of the implemented User interface functions within the machine code

User Interface Functions – These processes relate to the stage at which the user must enter desired values which in turn are processed and implemented through motor actuation.	
enterX()	An operation in which functions which request user dependent information are utilized.
resetTimmers()	This process acts to control time-orientated variables which are fundamental for accurate actuation.
UserInputHeights()	Prompts requesting the extruder and collector heights are requested and compared allowing for accuracy in the desired distance between these.
UserInputPumps()	This requests the flowrates for the syringe pump and vapour (peristaltic pump) mechanisms.
UserInputTime()	An operation which will set a variable related to the length of desired time for the electrospinning process as well as set a variable for the desired rotational alteration in collection instances.
UserInputProcesses()	In this process the user will define which processes are to be utilized in the fabrication cycle. It also acts to retrieve the desired operational time for some of these.
rotatingmandrelUserInput()	Values are evaluated relative to the experimentally derived maximum revolutions per minute capability of the utilized motor and set accordingly.
UserInputMethod()	Values which control whether ‘Method A’ or ‘Method B’ are utilized are set.
TotalMenuCheck()	This allows the user to review all information set and modify values if required.
PrintingDeviceSetup()	This stage involves the setting of the High voltage power supply as such there is a monitoring the health and safety sensor value. If all conditions are appropriately met the user is able to set the desired values for the fabrication and proceed with the printing process.

5.2.3 The Manufacturing cycle phase

This phase no longer requires user interaction with the serial monitor of the control unit. Here the machinery/mechanisms employed will proceed to perform actions relative to the prior input information. The electrospinning process will initially actuate the collector platform to the desired collection distance derived from the user inputs. If the collector has been assigned a rotating/actuating mechanism, this will be activated to ensure the collector occurs in its desired form at the start of the fibre generating processes. Once this arrives at the desired position, the processes associated with electrospinning fibre generation will begin, namely the application of the input high voltage to the point of extrusion and the actuation of the syringe pump(or alternative) at the desire flowrate. This will occur for the user input electrospinning time after which all of these processes will cease (including collector related actuators) and the collector will be moved to a desired position for fibre transferal. Now the actuators associated with transferring the generated fibre media upon collecting surfaces will move to pre-assigned collector specific locations. If a desired collection angle has been specified, the collecting surface will rotated accordingly before it is actuated into the generated fibre (thereby collecting this onto its surface). At this stage, the machine operations are allowed to vary according to the user input methodology. If 'Method A' was selected the electrospinning and fibre transferal/retrieval processes would repeat a user defined number of times, following which the resultant structure of accumulated fibre will be subjected to the desired processing. Alternatively if 'Method B' was selected, the transferred layers of fibre would be subjected to additional processing after which this technique of electrospinning, fibre transferal/retrieval and fibre processing would be repeated a user defined number of times. Through these methods the following structures are intended to be generated: structures comprising solely of fibre, multi-material structures having varied proliferation of processing effects (namely a structure in which only the top layer has been processed) and structures with embedded and repeated layers of processing. Figure 97 illustrates the desired progression of this operation alongside the utilized code-based functions which are described in Table 23.

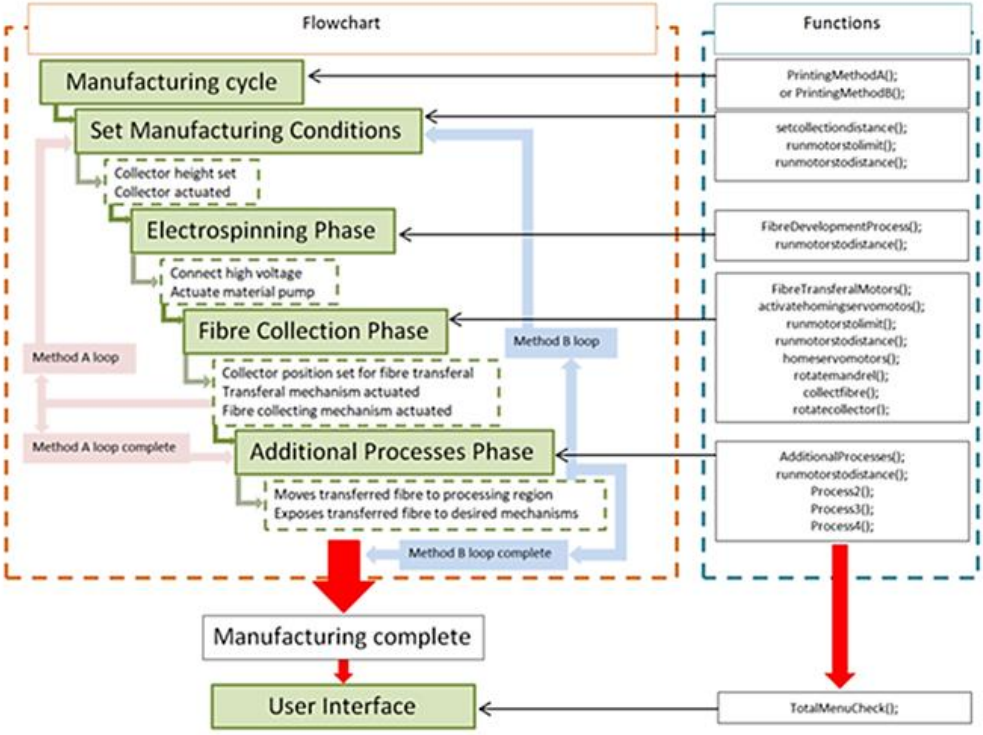

Figure 97: Flowchart showing the progression of the Manufacturing phase

Table 23: List and description of the implemented Printing functions within the machine code	
Printing Functions – These processes involve the automation and nature of the fabrication.	
PrintingMethodA()	An operation in which functions are initiated relative to the desired fabrication methodology.
PrintingMethodB()	An operation in which functions are initiated relative to the desired fabrication methodology.
setcollectiondistance()	This positions the collector at the previously set distance by actuating the relative motors.
FibreDevelopmentProcess()	The actuation of the high voltage connection controlled servomotor, syringe pump motor and rotating mandrel process motor are all subject to this function and activated accordingly.
FibreTransferalMotors()	This controls the actuation of the motors to regions required for the collection of fibre.
collectfibre()	
rotatecollector()	Here the motors utilized to control the positions and angle at which fibre is collected are controlled.
rotatemandrel()	This function will actuate the rotating collector to allow for the transferal of material at each of the defined areas of the collector.
AdditionalProcesses()	The additional processes are controlled by this operation, namely this ensures that only the desired processing methodologies are used for the defined time.
StopElectrospinning()	This function ensures that the high voltage power supply is disconnected and returns all components to the defined starting positions.

5.3 Hardware/componentry ideation

In order to implement the desired processes/phases of operation, some combination of mechanical and electronic componentry was required. The initial concept for which was illustrated and then converted into the annotated diagram depicted in Figure 98. The majority of the actuation based mechanisms are equipped with stepper motors which would actuate attached leadscrews thus generating the linear motion required. To control this motion cantilever switches would act as sensors and be fundamental for the implementation of the Homing phase. Additional mechanical actuator included the use of servomotors which would act to connect the high voltage for the extruder and provide additional functionalities to collector and homing-based mechanisms. Solid-state relays were also identified as potential control-orientated components which were implemented in the actuation of the additional process phase. The concept also included an extractor fan and LED floodlight, which were intended to be user controlled mechanisms to aid in the use of the machine. All other componentry displayed is mechanisms specific with greater discussion relating to these occurring in Chapter 4.

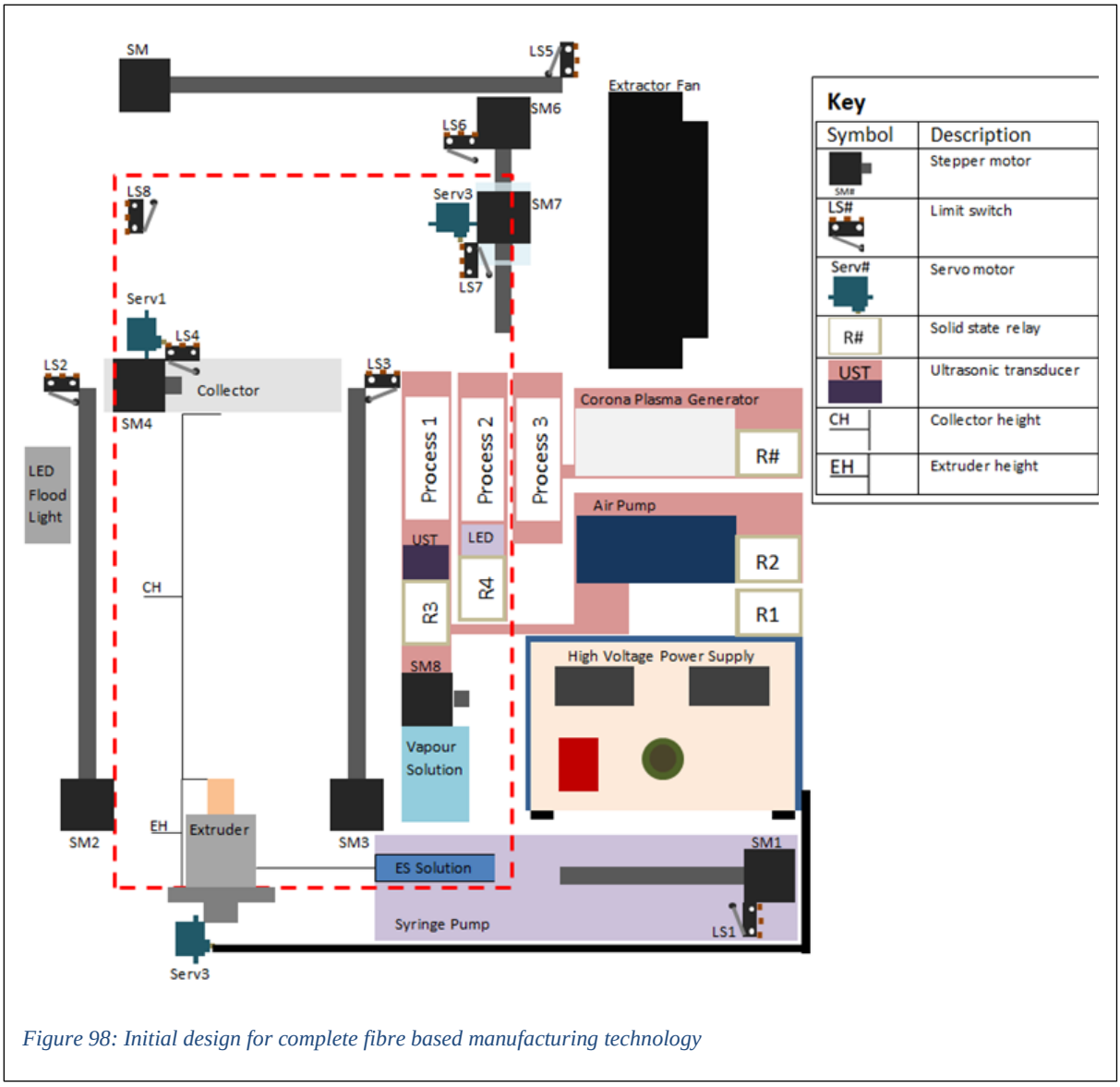

Figure 98: Initial design for complete fibre based manufacturing technology

5.4 Software/Code development

This project required code capable of producing time dependent control of asynchronous operations to enable the desired automated machine. This had to be able to store relevant values, update and monitor these values and ensure accuracy for multiple tasks. As an Arduino MEGA 2325 was utilized, the control system could be coded utilizing the C programming language. This type of programming is useful in its ability to utilize functions (titled segments of code) which can be repeated when required. Whilst every line of the code was deemed necessary within the project, this section will focus on certain fundamental sections and predominant functions (the full code is attached as Appendix D: Code). These include an evaluation of code relating to motor control and time based events. Whilst the implemented programming did account for certain factors of modularity (specifically those of the extruder heights), this was not feasible for all possible iterations of future developments. As such this is intended to be both utilized and modified according to user requirements. Thus in order to adequately utilize and modify this code the user must become familiar with the fundamental feature implemented in the program, namely the direct control of multiple stepper motor characteristics within defined intervals.

5.4.1 Stepper Motor Control

Stepper motors are widely utilized within many varied projects in which actuation is required. These components consist of a shaft connected to a magnetized rotor that is surrounded by stator coils (coils of copper wiring). Through the application of charge within these coils, a magnetic field is produced. This field will cause a reaction with the magnetic rotor and result in rotational actuation the amount of which is directly proportional to the rotational/sequential activation of neighbour coils. This staggered activation and deactivation is referred to as a step. Stepper motors come in a variety of forms, however for the scope of this research the hybrid stepper motors known as Nema 14 which are popular within hobbyist machine research and development were utilized. These motors have a standard step resolution of 1.8^{o} and thus require 200 steps to generate a full revolution of the motor shaft. To simplify the control of stepper motors, motor drivers are utilized. This project made use of Big Easy Motor drivers due to their capabilities of operating at voltages up to 30V, ability to operate under current of up to 2A and well documented resources. These components aid in the simplification of code required in actuating a motor, namely requesting logic inputs (0-5V equating to on or off) to enable the motor, set it's direction, result in a motor step and define the required micro-stepping. For most of the implemented motors, full-step actuation was utilized, with the exceptions being the syringe pump and peristaltic pump components. Rather than individually assign code to control this however the connections for the microstepping of these motors were connected either directly to 5V (for motors requiring micro-stepping) or ground (full-step motors).

Stepper motors were utilized within this project to perform two kinds of tasks. The first being the actuation of leadscrew units to provide linear motion thereby positioning mechanisms in desired locations and the second being the actuation of materials and mechanisms at a desired speed. Positional control was achieved simply through the evaluation of the relationship between the resultant millimetre-based linear motion and the number of motor shaft rotations. This yielded the number of steps required for 1mm worth of actuation. With respect to motor speed however, it is worth noting that code required to run a stepper motor always has some form of a delay between activating and deactivating the coils. This delay relates to time required for the rotor unit to appropriately align itself with the activated stator unit and is a fundamental limitation for applications requiring

motor outputs having high rotational speed (rpm). This project did however not require high speeds, rather the motors were expected to deliver a means for actuating material.

One of the benefits of utilizing the Sparkfun Big Easy Motor Drivers is that these components have been thoroughly documented by the manufacturer. This includes guides as well as example code which ensures ease in the rapid evaluation of motors and mechanisms. Figure 99 depicts the component (motor driver) alongside the example code identifying the relationship between connecting pins [130]. Of importance within stepper motor code like this example is the occurrence of a delay between the activation and deactivation of the step variable. This relates to the requirement for relates to time required for the rotor unit to appropriately align itself with the activated stator unit and is a fundamental limitation for applications requiring motor outputs having high rotational speed (rpm).

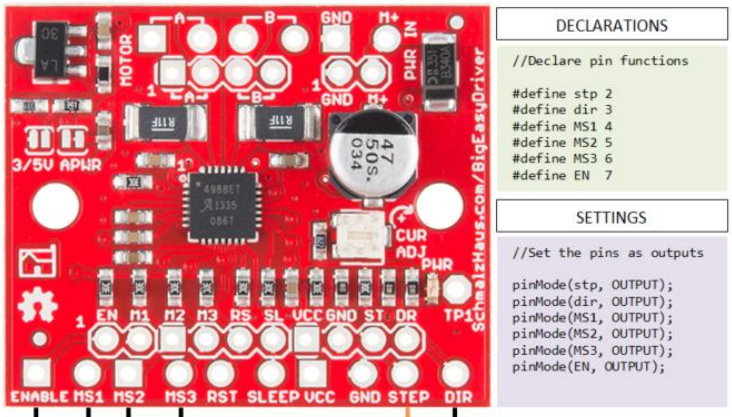

Figure 99: Sparkfun Big Easy motor driver with annotations related to example code provided by Sparkfun relative to the component ports

Prior Chapters have discussed the need to induce a solution flowrate for components such as peristaltic and syringe-based pumps. This was achieved through the identification of critical values which when computed would yield the required delay between the drivers coil activation and deactivation. The user is expected to ensure that the coded/assigned values for the utilized syringe and peristaltic pump are updated for when required. The first variable `SyrMLitrePerMmitre` refers to the output millilitre amount per millimetre of syringe actuation and the second variable relates to the denominator value for the `NoRevV` which refers to the output millilitre amount per rotation of the peristaltic pump motor. The following will describe the computation involved for syringe pump, however this is much the same for the peristaltic pump and only requires one additional conversion, namely the integration of syringe and motor outputs. The provided value of millilitre per millimetre of syringe actuation is compared to the millimetre output per revolution of the motor thus yielding a millilitre per revolution value. The user input value of millilitre per hour is then compared with this value which computes to the required revolutions per hour. This is now related to the defined number of steps per revolution of the motor (note this is micro-stepping dependent) and will provide the number of steps needed for this output per hour of operation. In order to identify the required step-based delay this value is then represented in the form of milliseconds passed per step. A final computation dividing this by two occurs as the delay will be situated between moments of activation and deactivation. Figure 100 depicts an annotated progression of the equation/computation utilized.

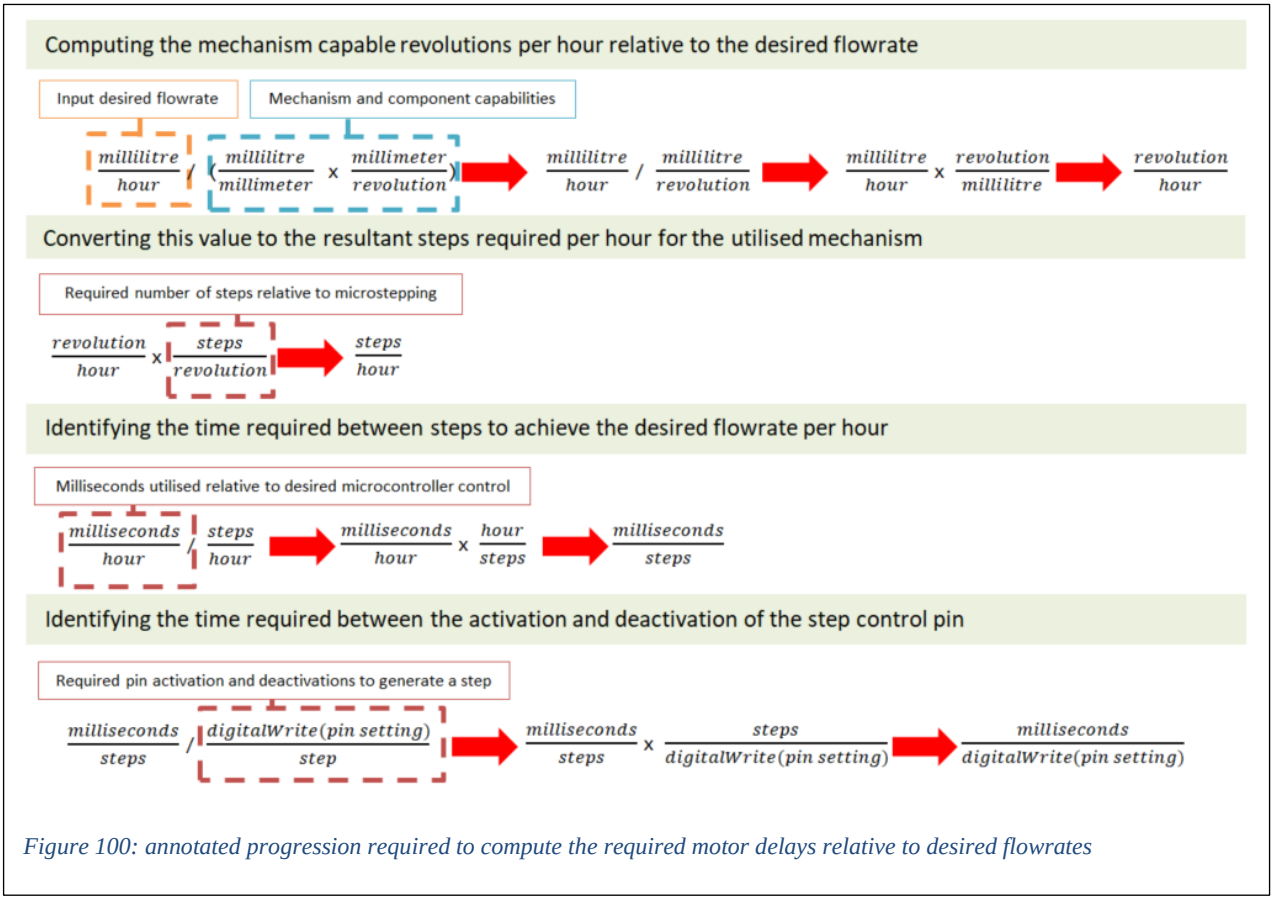

Figure 100: annotated progression required to compute the required motor delays relative to desired flowrates

It is worth noting that these can be utilized for more than just flowrate applications, an example for which is the use of this formula in generating the delay associated with the rotating mandrel. The only additional work required relates to the variation in microstepping and revolution per hour amounts (e.g. for the rotating mandrel collector, 200 steps per revolution are utilized and the required rpm is converted).

5.4.2 Operational efficiency

To increase efficiency within automation, often multiple actuators are activated/utilized at the same time. This is particularly relevant for situations in which diagonal motion is required such as those seen in many 3D printing gantry systems. A similar parallel actuation requirement existed within the desired machines movement of the two parallel linear platforms as well as the implementation of both rotating mandrel and syringe pump mechanisms in the electrospinning phase. This could not be readily achieved via the previously described code which operates in a ladder/stair-like sequential manner. Here the processor/compiler will perform tasks sequentially downward and thus is not immediately ideal for situations in which a potential compounding of delays could occur. An example of which would be the accumulation of prior and subsequently programmed delays affecting the implementation of code. This case is demonstrated in Figure 101 where 'actionD' can only occur/be processed after the time associated with the action and delay times of A, B and C have occurred.

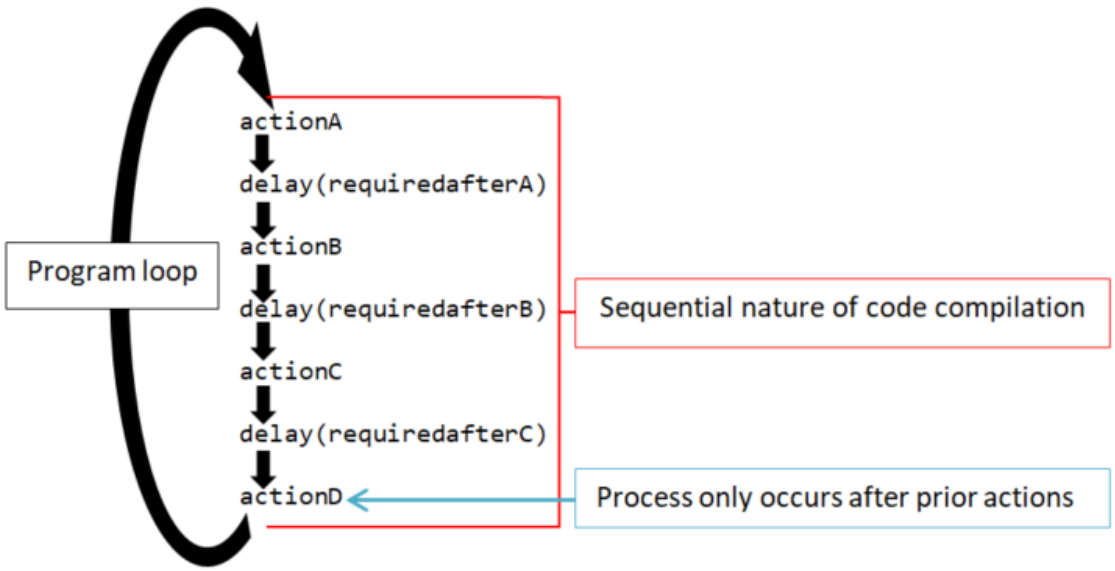

Figure 101: Illustration of the sequential nature of code compilation and the effects of prior action-based delays on later operations

The well documented and thoroughly utilized nature of the Arduino microprocessor unit device proved highly beneficial in providing a potential solution for this limitation. This was in the form of a forum post (https://forum.arduino.cc/index.php?topic=223286.0) by the user Robin2 entitled "*Topic: Demonstration code for several things at the same time*". Here an example of a methodology to aid in the processing of multiple outputs/instances (each having varied delay times) was outlined. This solution was based on the Arduino `millis()` function which will provide a value equal to how much time (in milliseconds) has elapsed at this instance of the codes operation. Through the manipulation of this information utilizing comparison statements and loop structures, events can be triggered relative to time. Figure 102 demonstrates how through the modification of a while loop structure a localized time has been generated against which the triggering condition for operations is evaluated.

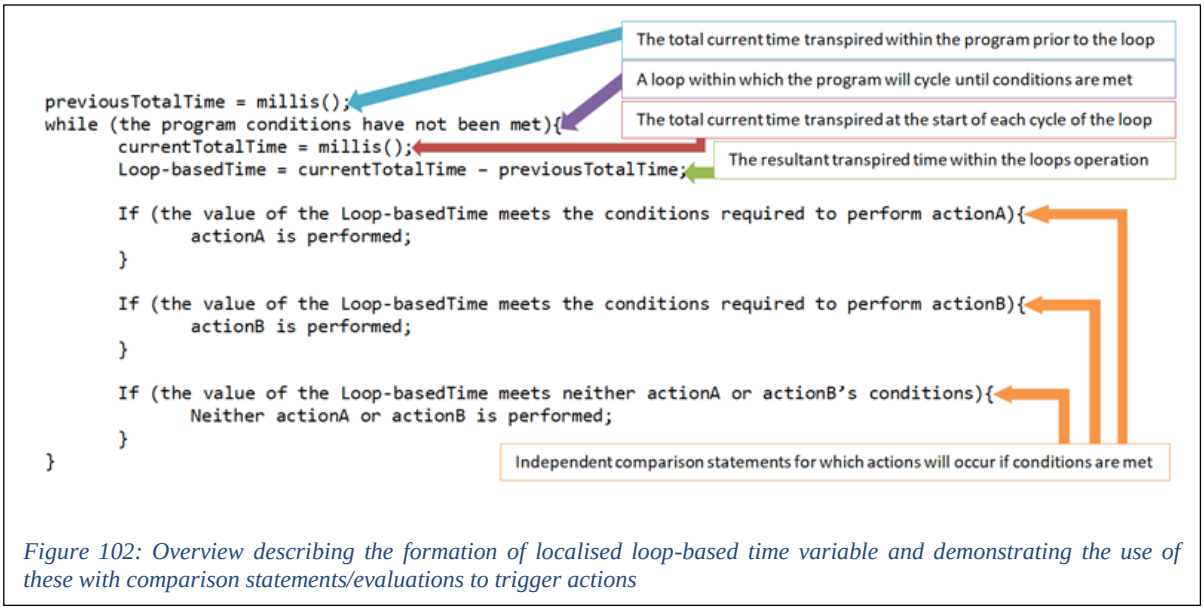

Figure 102: Overview describing the formation of localised loop-based time variable and demonstrating the use of these with comparison statements/evaluations to trigger actions

Through this the time between instances in which the multiple motor driver step controls are activated and deactivated can be controlled allowing for a practically parallel operation/processing of the actuators. It is worth noting that this technique does not yield true parallel processing. It does remove the effects of compounded `delay()` functions, however there will still be a processing delay relative to the operational speed of the microprocessor. This however is relatively minor in relation to the operation of the actuators and as such was deemed negligible for this project. Thus, this methodology was utilized to generate variables and conditions within the program to operate components and mechanisms within the machine for both defined periods of time as well as actuate these with respect to the relative elapsed operational time.

5.4.3 Fundamental program functions

The Arduino microprocessor can be controlled via the C programming language and as such allows for the segmentation of code into groupings. These groups are known as functions and often will compute specific tasks at various stages of the program. With respect to this project two fundamental functions relating to motor control were generated, namely *runmotorstolimit()* and *runmotorstodistance()*[Figure 103]. Both of these are similar (both resulting in actuation if the a/the condition (*variable*) is not met) with the major variation being that the later takes into account the current position of the motor and will set its direction accordingly.

```
void runmotorstodistance(const int motordirect, const int motorenable, const int motorpin, float PriorTime, float &resetcondition, float delay_speed, float &currentdistance, float variable) {
    float overwritetime = millis();
    float Time = overwritetime - PriorTime;

    float stepvalue = 0;
    if (currentdistance != variable) {
        digitalWrite(motorenable, LOW);
        if (variable - currentdistance > 0) {
            digitalWrite(motordirect, HIGH);
            stepvalue = 0.5;
        }
        else {
            digitalWrite(motordirect, LOW);
            stepvalue = -0.5;
        }
    }
    if (currentdistance != variable && (Time - resetcondition) >= delay_speed) {
        if (digitalRead(motorpin) == HIGH) {
            digitalWrite(motorpin, LOW);
            currentdistance = currentdistance + stepvalue;
        }
        else {
            digitalWrite(motorpin, HIGH);
            currentdistance = currentdistance + stepvalue;
        }
        resetcondition = resetcondition + delay_speed;
    }
    if (currentdistance == variable) {
        digitalWrite(motordirect, LOW);
        digitalWrite(motorpin, LOW);
        digitalWrite(motorenable, HIGH);
        resetcondition = 0;
    }
}
```

Figure 103: Implemented function through which motors are actuated to desired distances

The functions require information related to the status of the motor driver control elements (direction, enable, and step), the time-based control elements (previously expired operational time, delay/trigger time associated with the motor, and a trigger reset-based variable) and operational elements (current motor actuation/location and function control variable). It is important to note that the location variable refers to the amount of times a motor step has occurred relative to the origin (at which this value is 0). Within the function variables are defined for the time-based operations (*overwriteTime* and *Time*) and a variable for computation of the final location (*stepvalue*). Through computing the difference between the prior elapsed time variable (*PriorTime* which is set before the loop) and the time set within the function (*overwriteTime*), a counter-like variable (*Time*) is created. As the *PriorTime* value will not change, the value associated with the subtraction of this from the updated *overwriteTime* will equate to the time elapsed within the loop. Thus *Time* can be described as a localized form of *millis()*. Within the distance orientated function an evaluation of the current position of the actuator (*currentdistance*) relative to the desired value (*variable*) is conducted. For the occurrence of variation, the motor driver enable control will be activated (allowing for actuation) and the nature of this variation investigated. Through this the required direction of the motor and required value for computation (*stepvalue*) is identified. To perform actuation the position is once again evaluated and a further condition relating to the defined time-based restrictions of the motor evaluated. This additional comparison ensures that the motor driver step control will not be modified unless the desired interval of the motor (time related delay) has passed. As the `Time` variable will continue to increase relative to the duration of the loop, a resetting variable (`resetcondition`) having an assigned value relative to the delay is required. This will ensure that

motor actuation will only occur after a given time has elapsed between activation of the step control. Thus for every instance in which activation occurs the desired delay time must be subtracted from the elapsed loop time with respect to this comparison. It is worth noting that the nature of step control activation is relative to the prior status of this, thus ensuring the variable toggles appropriately. With respect to the distance related function the variable associated with the motor position (`currentdistance`) is updated relative to the `stepvalue`. The last segment within the function will return the motor control variables to their default values once the condition for actuation has been met (e.g. `currentdistance` equals `variable`).

Through the understanding of the above described functions and the manipulation of the variables within these, the majority of the mechanisms within the machine were made to function. It is worth noting that to allow for modifications within the code to function, an established understanding of C and manipulation of functions is required. Additionally the Arduino `Servo.h` library was utilized to control the machines servomotors and the serial output capabilities of the board utilized to provide a user interface.

5.5 Research and development characteristics/properties of the final machine

The final rendition of the machine was intended to allow for ease in further research and development of mechanisms and processing techniques. It is worth noting that the final construction of the machine was comprised predominantly of 4.5mm matt black acrylic, which can be easily machined, and was laser cut into the shapes required for assembly. The resultant machine has external dimensions 375mm (Width) by 1150mm (Length) by 1180mm (Height)and is situated within an aluminium frame of dimension 590mm (Width) by 1300mm (Length) by 2180mm (Height), which is equipped with wheels allowing for ease in mobility. In order for future development of technology within this machine to occur, the following design considerations need to be accounted for:

5.5.1 Electrospinning-based design characteristics

The two utilised linear actuators within the electrospinning section have an operating distance of 450mm in which they move two platforms upon which the collector (or potential collectors are attached). These platforms occur at a horizontal distance of 537mm from one another with the entire linear actuator elements occurring 168.5mm above the point of extrusion attachment plate. The total operating region for the electrospinning process in which the extruder and collector mechanism must be situated has dimensions 366mm (Width) by 575mm (Length) by 721mm (Height)[Figure 104].

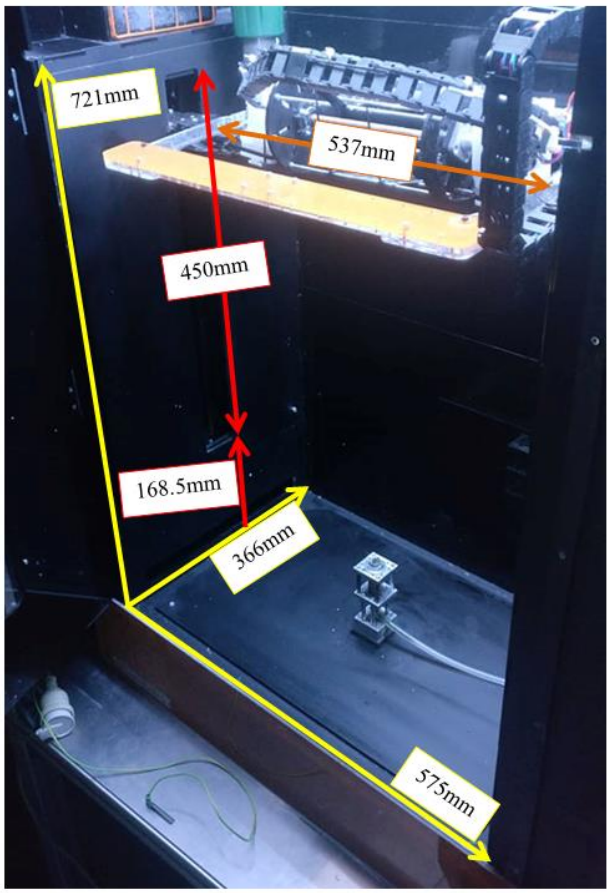

Figure 104: Final dimensions of the electrospinning region

5.5.2 Additional Processing-based design characteristics

The mechanisms implemented within the additional processing of the fibre are limited to the current size of the tower attached alongside the electrospinning based unit. The current form of this region predominantly acts as a housing unit in which the components required for mechanisms and machine functionality are housed. The core region in which the transferred fibres are to be modified by the additional processes has an area of dimensions 366mm (Width) by 366mm (Length) by 405.5mm (Height) and includes an 4.5mm attachment plate positioned 67.5mm from the back wall. This component is currently equipped with three aluminium-sliding components and allows for an ease in the addition and removal of processing mechanisms. Below this region, there are four compartments in which the high voltage power supply, syringe pump mechanism, electronics, peristaltic pump, and air pump components are currently stored [Figure 105].

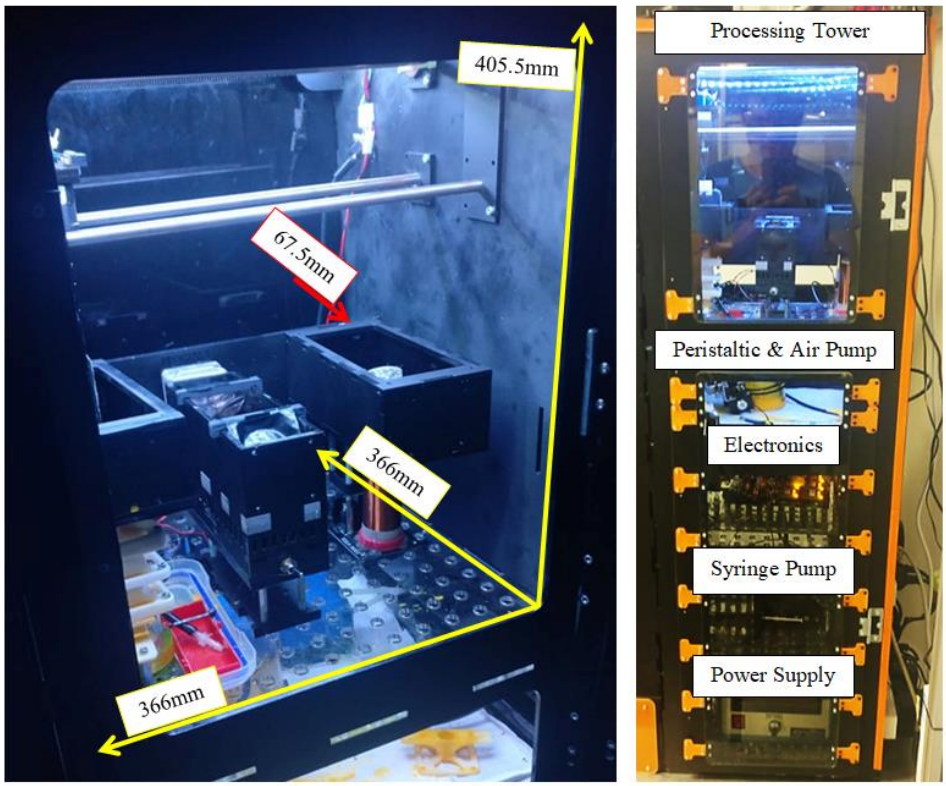

Figure 105: Processing region and equipment of the final machine

5.5.2.1 Fibre collection and transferal design characteristics

The current method for retrieving the generated fibre from the collector makes use of a linear actuator having a total operating distance of 950mm and the current the fibre transferal mechanism is capable of an operating distance of 143mm. Through these components, fibres are collected in the electrospinning phase and subjected to mechanisms in the additional processing phase. The development of these mechanisms is currently constrained to an area having dimensions 190.5mm (Width) by 950mm (Length) by 204.5mm (Height). It is worth noting that due to the method of actuation the current operating region for a collecting surface is 48.75mm (Width) by 48.75mm (Length) by 204.5mm (Height), however this can be altered through modifying the attachment to the fibre transferal actuator [Figure 106].

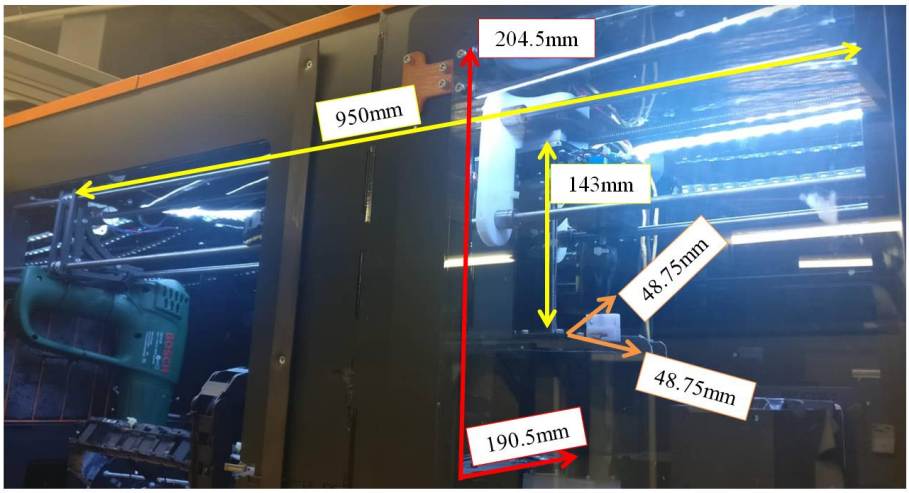

Figure 106: Fibre-handling system realised in the final machine with associated dimensions

5.5.3 Code based characteristics

The implemented code currently functions through the assignment of current mechanism-specific variables. These relate to the maximum traversal limits for the syringe pump mechanism (*SM1_SPstepperlimit* currently set to *10050* steps), and vertical linear stage components (*collectorleadscrew* currently set to *420* steps) as well as defined distances for the fibre retrieval unit (77500 steps) and the fibre collecting surface unit (*10000* steps),. The function-based nature of the developed code is highly beneficial for situations requiring the addition or modification of implemented technology. For the variation or addition of mechanisms within the additional processing phase consult with the *AdditionalProcesses();* function and associated *Process2/3/4();* functions. It is worth noting that the nature of the fibre retrieval and transferal is highly collector specific and as such much of the information related to transferal distances and number of collections is required to be accounted for within the *FibreTransferalMotors();, collectfibre(float desiredFTUpos();, rotatecollector();,* and *rotatemandrel();* functions of the machines code. Currently the program acts to repeat the transferal of fibre onto collecting surfaces at varied angles repeating for the length of the rotating mandrel. This will occur by traversing the mechanism in back and forth along the mandrel which will rotate for each direction ensuring the collecting surface is presented with generated fibre for each collection. This motion is achieved by the 'for loop' utilising the, *rotatecollector();,* and *rotatemandrel();* functions [Figure 107].

```
for (int rm = 0; rm <= 3; rm++) {

            rotatemandrel();

            for (int c = 0; c <= 4; c++) {
                  collectfibre((77000 - (c * 3000)));
            }

            rotatemandrel();

            for (int cf = 0; cf <= 4; cf++) {
                  collectfibre((65000 + (cf * 3000)));
            }

}
```

Figure 107: Coded 'for-loop' utilised to generate the rotating mandrel-based collection stratergy

Chapter 6 DISCUSSION OF EVALUATIONS RELATED TO THE HYPOTHESIS

This chapter discusses the studies which were conducted in order to identify the feasibility of elements within the hypothesis. These directed the development of technology within the project from which the final research and development machine was constructed. As such, the work discussed within this chapter relates to the use of technology within various stages of the project in an attempt to realise goals related to the main hypothesis derived in Chapter 3: Post Literature Review Hypothesis. Initial experimentation focussed on the ability to form electrospun fibres onto pre-existing structures. Following the outcome of this work, developments related to the ability to transfer fibre onto desired forms and the technology through which this occurs are described. The ability to modify the samples generated by the machine and potential technology namely vapour and plasma exposure are explored. Utilising revelations from this work, the ability to conduct this form of research and development within the confines of the created machine are evaluated. Finally research relating to the potential outcome of this developed technology to generate a three-dimensional form is discussed. It is worth noting that for many evaluations/studies conducted within this chapter, accessible and cost effective techniques (e.g. fused deposition modelling 3D printing) and materials (e.g. ABS, Acetone, expired resins) were initially utilised.

Many of the understandings developed through the evaluations within this chapter were utilised in the generation of published conference papers. These papers are attached within Appendix A: Papers Published.

6.1 Fibre distribution/forming strategies

Initial investigations involved the analysis of the effects related to the modification of collector surface topology to generated/accumulated fibre.

6.1.1 Wrapping/Molding of Fibres generated in Electrospinning

The utilisation of mold-based manufacturing is a popular technique for the production of three-dimensional fibre-based constructs. This technique typically involves a manufactured shape(mold) onto which the fibre material can be placed/wrapped. The structure is then exposed to agents and processes which result in the bonding of the fibre into the desired form. The mold is removed after the bonding is completed, yielding a form comprised solely of the implemented fibre-agent matrix. The electrospinning process has been thoroughly documented as capable of generating fibre upon electrode surfaces. The utilisation of structures such as rotating mandrels as collecting interfaces between the point of material extrusion and grounded collecting rod have been proven as capable of shaping the resultant distributed fibre (albeit a relatively planar distribution wrapped upon the mandrel). From this was hypothesised that through the modification of the collector surface topography, the distributed fibre can be accumulated upon mold like structures after which post processing (such as exposure to adhesive agents) can be utilised to generate controlled three-dimensional structures.

6.1.2 Experiment methodology

Experimentation occurred at Revolution Fibres, utilising a relatively simplistic electrospinning device in which and provided Nylon-Formic Acid solution. The major limitations of this device related to the manual adjustments of critical distances related to the electrospinning distance, solution beaker(flowrate) and collector height. This device was a derivative of Electrospinz's ES1a device which can be seen in Figure 109 and Figure 108 (acquired from [3]). The machines components were adjusted until electrospinning of fibres occurred and the utilised distances were measured as: distance to collector = 120mm, solution beaker height = 256mm, collector height = 250mm. The system relied on a purely gravitational system to induce the flow of solution there was no feasible or practical method for determining or controlling flow rate.

Figure 109: Revolution Fibres electrospinning device

Figure 108: Electrospinz ES1a device from [3]

7 mold-based surfaces were designed in SolidWorks and an UP!2 3D printer, loaded with white ABS filament and a set printing resolution of 0.25mm, was used to manufacture these. Of interest were the effects of surface collector extrusions and cavities on resultant electrospun fibre placement. For this study, a relatively flat collector surface was used as a control for comparison against three distinctive forms namely a semi-sphere, patterned semi-sphere and dog-bone analogue. The sphere based forms were intended to yield information regarding the fibre collection on organic/smooth surfaces with relatively few hard edges, whilst the dog-bone analogue forms were utilised to determine collection characteristics on relatively complex surfaces containing hard(90^o) edges. These shapes were extruded or cut into collecting surfaces with base dimension 50mmx50mm. Further dimensions for each surface are shown in the accompanying Figure 110**.**

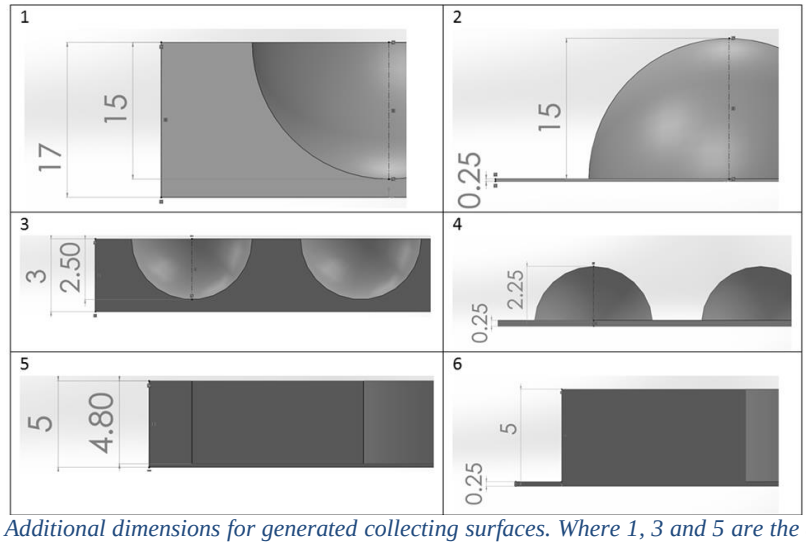

Figure 110: Additional dimensions for generated collecting surfaces. Where 1, 3 and 5 are the cavity and 2, 4 and 6 are the extruded versions of the semi-sphere, patterned semi-sphere and dog-bone analogue[7]

Each collecting surface was attached to the grounded collector plate via double sided tape. Collectors were positioned with the extruder nozzle directed approximately at their respective centres. The high voltage source was then activated and set to approximately 32kV for 5 minutes, after which the collector and unwanted fibre 'overspray' were removed and the process repeated. Each fibre-coated collector was then subjected to sputter coating (an average of 25 angstrom/2.5nm gold sputter coating applied through the use of Nanostructured coatings DSR1 device) and then evaluated via scanning electron microscopy using a Hitachi TM3030Plus.

6.1.2.1 Results

Figure 112 and Figure 111 demonstrate the resultant fibre distributions that occurred as a film on all surfaces.

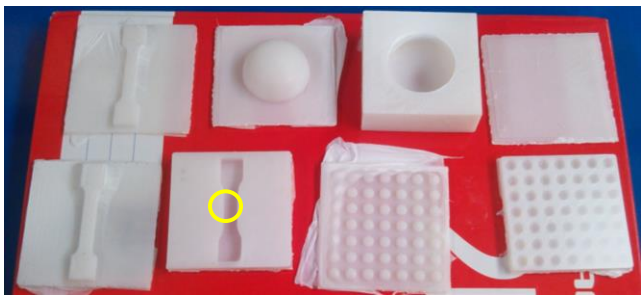

Figure 112: Image of collecting surfaces covered in film of nylon fibre (transparent fibres circled in yellow)[7]

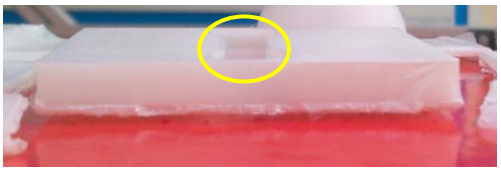

Figure 111: Image magnified and highlighting transparent fibres (circled in yellow)

Other than the expected generation of a film of fibre, no immediate fibre properties or characteristics could be determined from a macro evaluation of the flat collector. SEM imaging of this yielded the expected information, namely that fibres were spread out randomly at varying orientations [Figure 113], and these fibre characteristics were repeated for all cases where fibre made direct contact to flat surfaces [Figure 115]. A note should be made that even though the testing device was rudimentary, nanofibres were produced upon all of the surfaces including this simplistic surface [Figure 114].

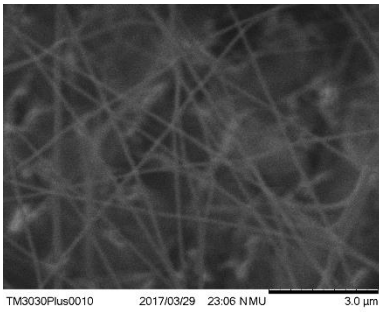

Figure 113: Flat surface SEM showing randomised fibre layout[7]

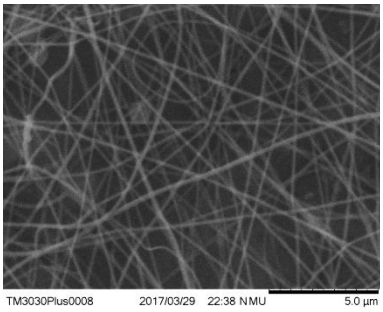

Figure 115: Example SEM illustrating randomised fibrils at base of dog-bone [7][7][5]collector [7]

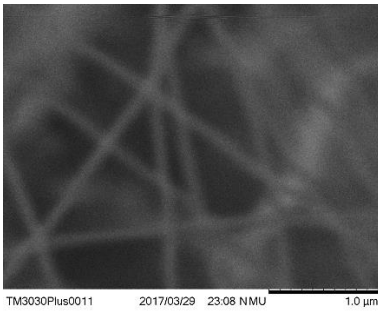

Figure 114: Flat surface SEM showing nano-scale fibre[7]

A macro evaluation of the surfaces containing extruded forms identified that the film of fibres appeared to stretch across gaps rather than wrap around extrusions and the film appeared more prominently on surfaces perpendicular to the direction of extrusion [Figure 116]. There is an apparent lack of fibre formation on the top/dome portion of the large semi-sphere; this is likely due to the greater distance of the spherical summit to

that of the grounded plate [Figure 118]. Unlike with this surface, the fibres seemed to stretch across and accumulate on top of the patterned semi-spheres instead of occurring at the base, this is potentially due to the proximity of the patterned extrusions resulting in interference between fibre and grounded plate (thus catching the fibres). The fibres stretched along the hard edges of the dog-bone analogue and did not seem to occur on the areas parallel to the direction of material extrusion (although this was difficult to evaluate under SEM).

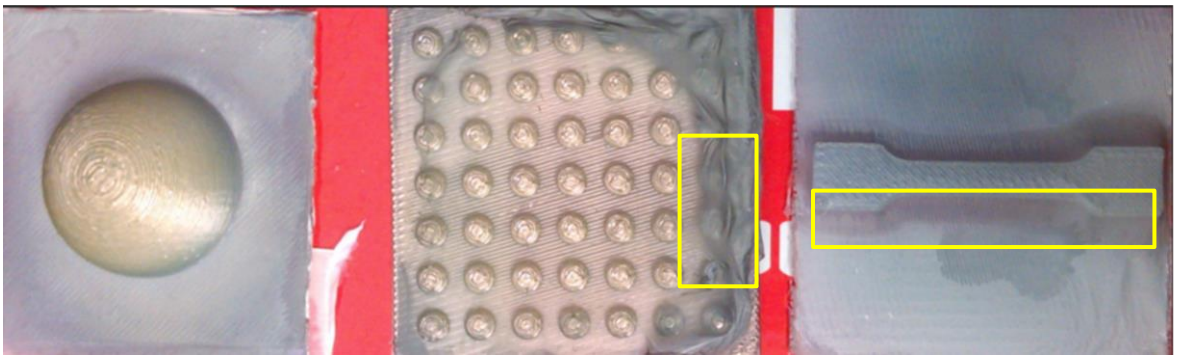

Figure 116: Image of the 3 extruded forms with yellow highlighting areas where the fibres have stretched across surfaces

SEM imaging of the areas at which fibres stretched across gaps yielded interesting results, namely that a relative alignment of fibre could be identified on the patterned semi-sphere collector [Figure 119] however this alignment was not present in the dog-bone analogue collector (it is hypothesised that this is due to the angle and distance of separation between surfaces) [Figure 117].

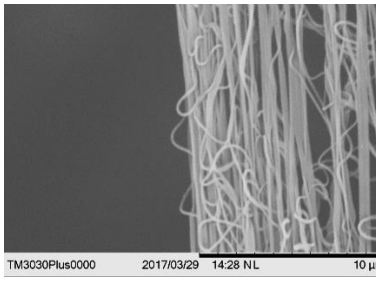

Figure 119: SEM of aligned fibres from the many semisphere [7]

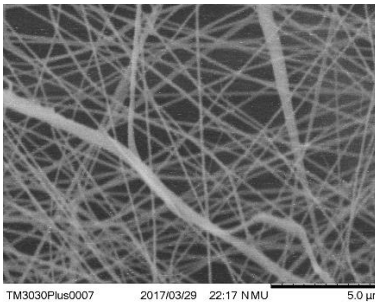

Figure 117: randomised fibres stretching along the edge of the dog-bone analogue [7]

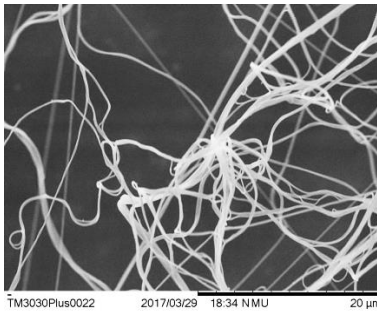

Figure 118: SEM showing relative lack of fibres at semi-sphere collector summit [7]

A macro evaluation of the surfaces containing cavities identified similar features found in the extruded surfaces, namely that the film of fibres appeared to stretch across gaps rather than conglomerate inside the cavities [Figure 123]. For the semi-sphere cavity, fibres did not stretch over the entirety of the gap; in fact this only occurred at the edge of the cavity. As with the extruded forms, an inspection of the areas parallel to the direction of extrusion indicates a lower amount of fibre collection (again this is difficult to evaluate through SEM). Much like with the extruded form, the proximity of the cavities of the patterned semi-spheres could potentially resulted in interference between fibre and grounded plate (thus suspending the fibres above the cavity). Unlike the in the extruded form, the fibres did not seem to stretch along/against the hard edges of the dog-bone analogue, with an exception being the area where these fibres stretched across the airgap.

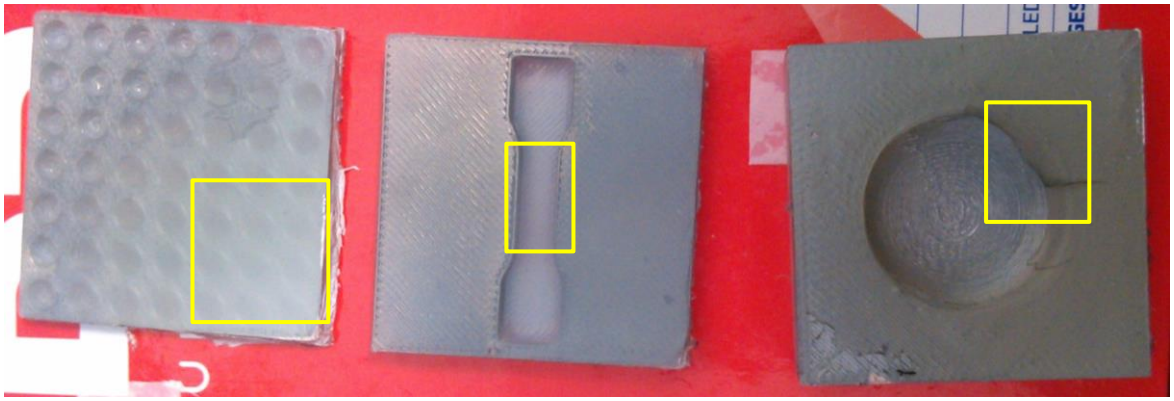

Figure 123: Image of the 3 surfaces containing cavities, with yellow highlighting areas where the fibres have stretched across surfaces

SEM imaging of the areas at which fibres stretched across gaps yielded similar alignment characteristics for the dog-bone and semi-sphere cavities [Figure 122 and Figure 120] interestingly the fibres stretching over the patterned semi-sphere cavities were randomly arranged [Figure 121] this is possibly due to the distance between surfaces being too small.

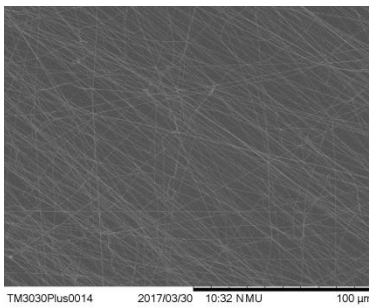

Figure 122: SEM showing alignment of fibre across the dog-bone cavity [7]

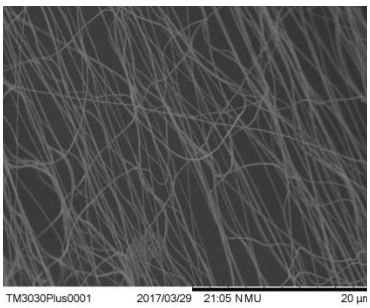

Figure 120: SEM showing alignment across semi-sphere gap [7]

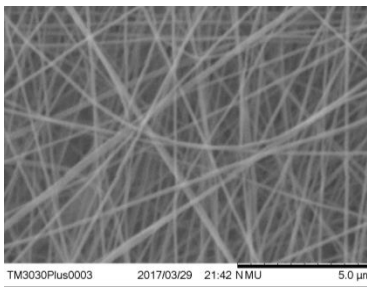

Figure 121: SEM showing randomisation of fibres above patterned sem-sphere cavity [7]

6.1.2.2 Evaluation of experimentation

The experimentation helped to re-inforce the previously discussed analogy of spider web generation (Chapter 2: Literature Review). Namely, that fibres colliding with interference will stick to this with the subsequent length of the fibres wrapping around the topography in the direction of actuation until collision with subsequent interference/ground. In the case of a spider's webbing (actuated by airflow) colliding with foliage (e.g. a tree), often this webbing collides with multiple points of interference forming a bridge of webbing from/upon which the spider constructs its web. Similarly, in electrospinning fibres actuated by electrostatic actuation collide with a collecting surface. This study demonstrated that the modification of the topology of this surface had significant affect upon generated fibres. These modifications however did not result in the occurrence of fibre structures in a controlled manner and was not optimal (variation in shape, diameter and general alignment). The testing was beneficial in highlighting some potential concerns for electrospinning onto three dimensional surfaces and hints that mold based fabrication through electrospinning is not a viable option. A major limitation within this study related to the simplistic ground/collector structure utilised. To further evaluate the potential for a mold based approach a more refined/controlled grounding method, such as the parallel electrode configuration needed to be investigated.

6.1.3 Parallel electrode Electrospinning

A further attempt to generate the desired fibre formation upon a surface during the electrospinning process related to the use of the parallel electrode technique. The previously implemented large grounded plate situated behind the desired surfaces is hypothesised to have yielded a relatively randomised electrostatic attraction. Thus, it was hypothesised that the influence of the now more accurately defined ground would be able to form the fibres on top of the surface/mold in not only the desirable form but also yield desirable fibre properties of alignment. Whilst literature had defined a minimal distance of 30mm between parallel electrode electrospinning, an attempt was made to utilize a large surface to support fibres stretching between electrodes. Whilst fibres did accumulate upon the large collecting plate through this technique [Figure 125] an inspection (SEM) of this identified that these no longer retained the desired alignment [Figure 124].

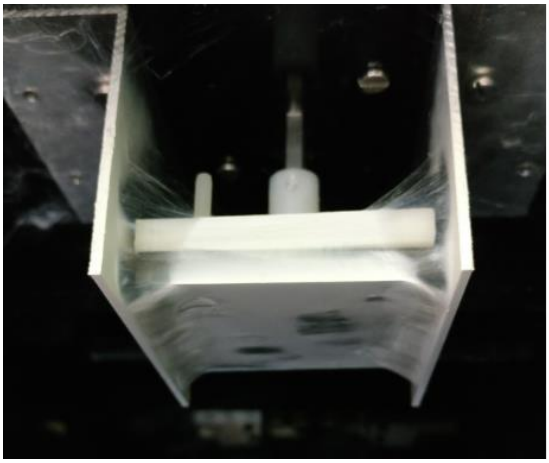

Figure 125: attempt at supported large distance parallel electrode electrospinning

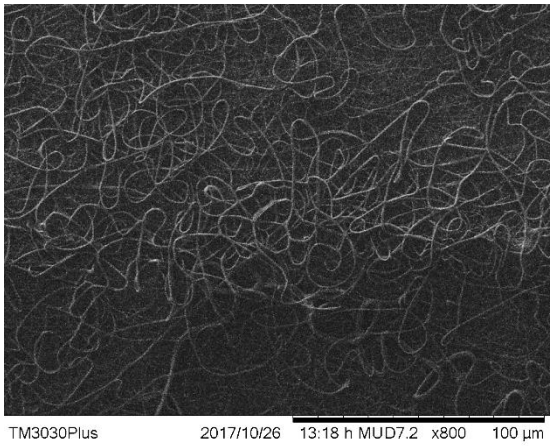

Figure 124: Randomised fibre accumulation on target of large distance parallel electrode electrospinning

This was hypothesised to be a result of the proximity of the electrodes to the collecting surface, namely that this distance resulted in an interception of whipping fibre restricting its ability to adequately stretch towards the alternative electrode. As such the distance between the surface and electrode was extended [Figure 126]. Further SEM evaluation of this surface indicated a tendency towards alignment at the surface edges; however, this was lost in the central regions [Figure 127]. From this, it was hypothesised that the interference of the surface structure was too large to allow for the further stretching of the fibre towards the parallel situated electrode.

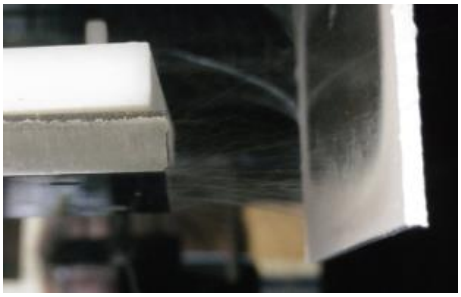

Figure 126: Extended distance between large flat surface and parallel electrode

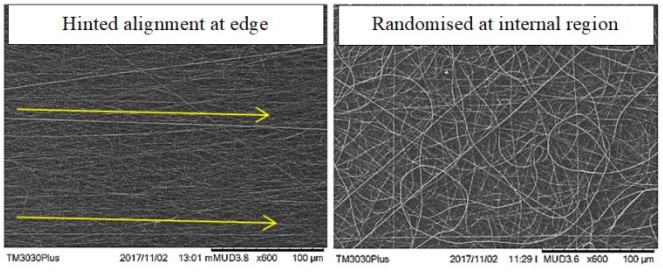

Figure 127: SEM images demonstrating a hinted alignment occurring at the surface edge whilst the internal region is randomised

An attempt seeking to leverage of the previous relationship of parallel fibres occurring at the point of connection /interference whilst reducing the surface area of the interference involved the use of a 3D printed semi-sphere surface [Figure 128]. It is worth noting that once again fibre stretching from the electrode to the surface could be seen. This was not identified as ideal as it was more desirable to have the fibre wrap/stretch along the surface towards the base of the semi-sphere. Additionally the SEM imaging of this highlighted that the intercepted fibres would wrap around the form resulting in a predominantly randomised orientation thus losing the desired alignment [Figure 129]. This indicated that a form placed within the regions of fibre generation within an electrospinning process would result in a modification to the trajectory of these thus negating attempts such as the parallel electrode technique to generate alignment.

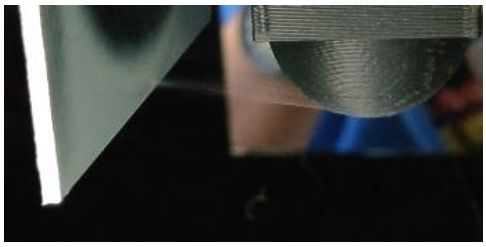

Figure 128: Image demonstrating the fibres suspended between the electrode an semi sphere-based collector.

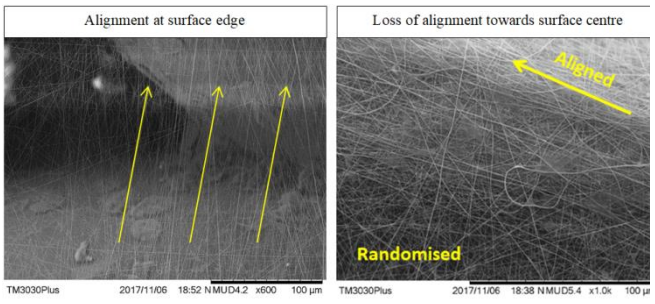

Figure 129: SEM evaluation of fibre distribution upon collector

This led to a decision to no longer attempt to generate fibre upon the mold/desired surface during the electrospinning process. Thus, a requirement for a separate collecting phase would allow for more control over the placed fibre (no longer subject to the nature of jet whipping instabilities) and ensure coating of the entire surface. To evaluate the process by which this collection would occur, structures were pushed through fibre generated at 90^{o} angles this resulted in a clearly identifiable cross-hatching of fibres upon the collector [Figure 130]. This yielded a dramatic improvement in the ability to acquire aligned fibre in various orientations upon a collector.

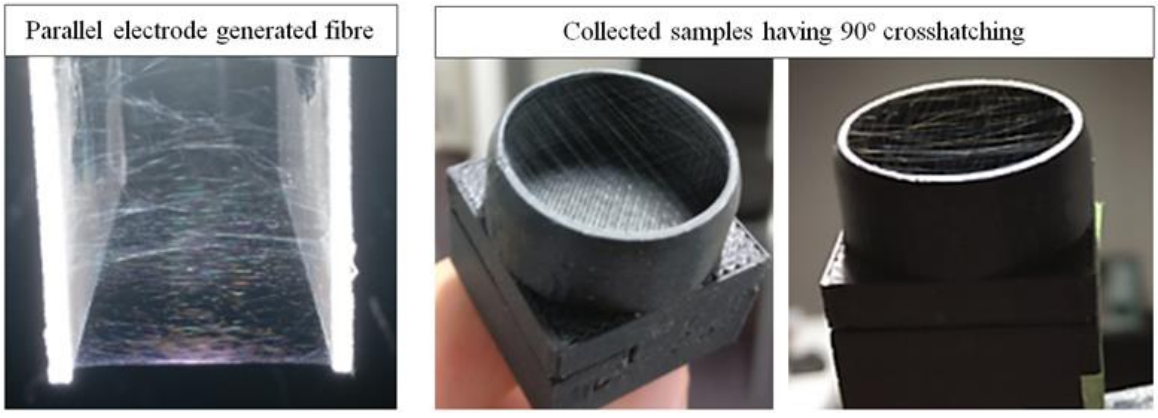

Figure 130: Samples generated by the collection of fibre at 90^{o} intervals for parallel electrode electrospinning.

6.1.4 Final Parallel Electrode Collector

Given the simplicity of the parallel electrode and the ease in use of this to troubleshoot the occurrence and prominence of fibre generation a mechanism for this was made to be implemented in the final machine allowing for further parallel electrode based studies. The function of this component and sample transferal is demonstrated in Figure 131.

Figure 131: Transferal process of fibre from the implemented parallel electrode technique

One of the major concerns relating to the automated transferal of material post electrospinning is the potential variation in fibre quantity upon the collectors. This can be seen in Figure 132 where in the case of the parallel electrode configuration the generated fibre has not filled the desired collection region. This anomaly can be attributed to many factors including but not limited to the imprecision in actuation and variation in electric field due to componentry (e.g. actuators). Following this work, experimentation utilising the above collector to generate collagen based samples was conducted.

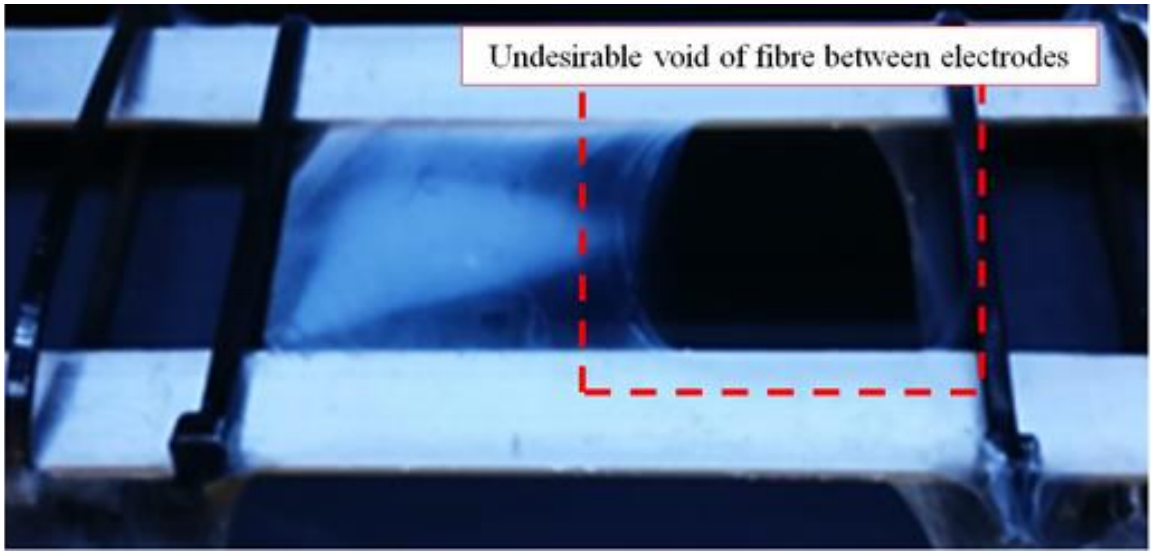

Figure 132: Displayed inconsistency in electrode gap coverage

6.1.5 Parallel electrode electrospinning of collagen

The electrospinning of collagen yielded far greater complexity in comparison to the nylon based studies. A sample of collagen was constructed from the electrospinning of RevolutionFibres collagen solution at 45kV at a distance of 125mm onto a parallel electrode configuration for 10minutes with the chamber temperature heated to 40°C, the extruder initially set to 35°C and the relative humidity set to 10%. Whilst the resulting fibres did not form a uniform sheet of distributed fibre between the plates (Figure 133), this experiment was continued to allow for the further analysis of the resulting collagen. The collection of collagen occurred a total of 5 times with the collecting surface being rotated at 90° intervals.

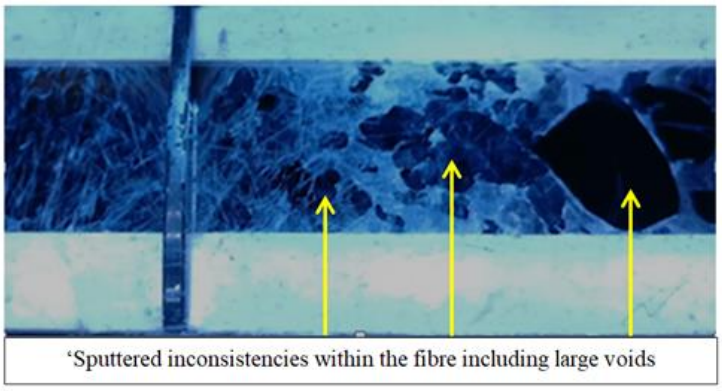

Figure 133: Inconsistencies in electrospun collagen fibres including voids

Further to this the ability to generate layers of fibres at controlled orientations was also subject to difficulties. Figure 134 demonstrates an SEM image of a collagen sample in which a region having somewhat alignment could be identified, however this region was surrounded by fibres which appeared to be arranged in random orientations.

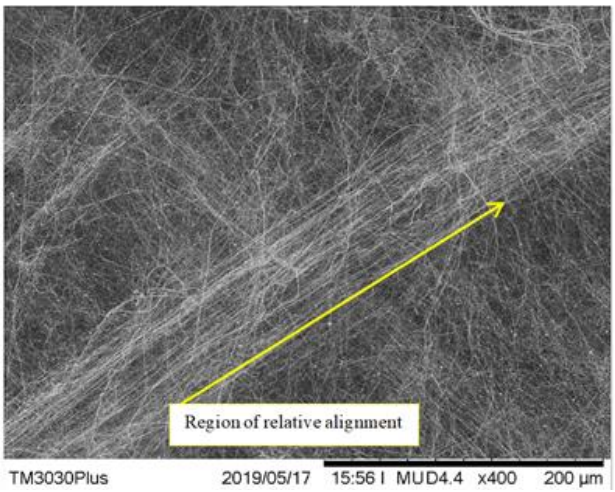

Figure 134: Collected electrospun collagen having a region of aligned fibre surrounded by non-aligned fibre

Further evaluation of this sample identified a predominance of randomly arranged fibre as well as a surface appearing to have regions of concentrated fibre and voids (Figure 135). This did not indicate a promising use of biopolymer to achieve similar results to the nylon-based tests. This led to experimentation in which the potential for the implementation of the rotating-mandrel based approach to increase the alignment of the fibre was evaluated.

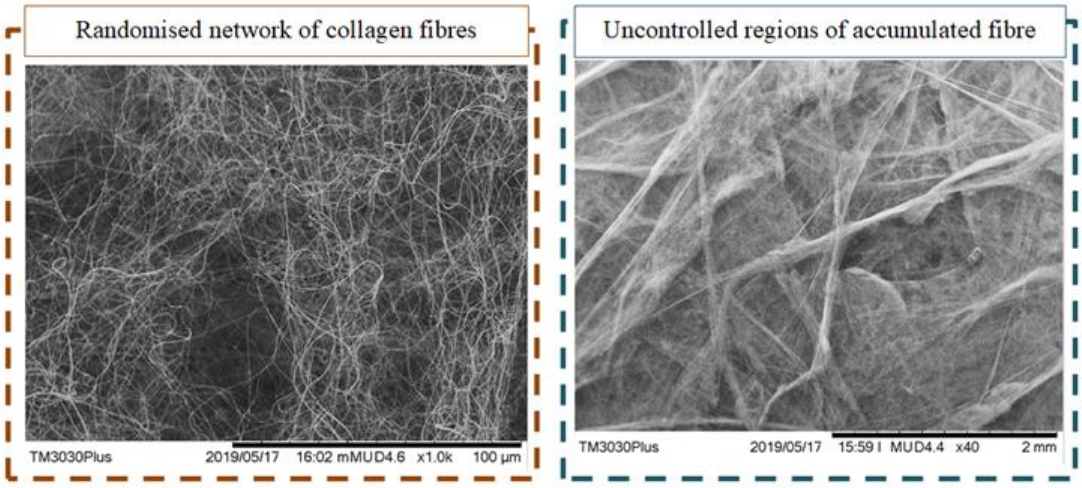

Figure 135: Additional regions/images of interest regarding the collagen-based SEM evaluations

6.1.6 Rotating Mandrel-based electrospinning of collagen

Much like the parallel electrode technique, the designed rotating mandrel mechanism had previously demonstrated the ability to generate aligned electrospun fibre. It was hoped that the generation of significant collagen fibres would be aided through the implementation of a version of this collector, along with modifications relating to the electric field of the electrospinning process and the inclusion of temperature and humidity control. Figure 136 depicts the original collector and its ability to be coated by Nylon 6,6 as well as the implemented, modified, version of this.

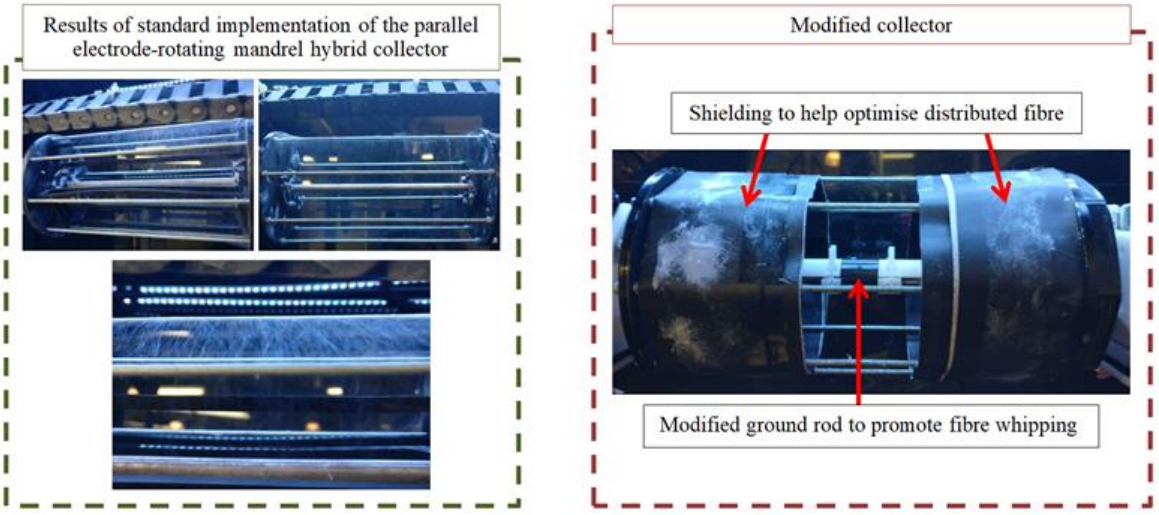

Figure 136: Depiction of the collector utilised in this experiment

Electrospinning was trialled using a voltage of 45kV, a flowrate of 1ml/h, a collector rpm of 100, within a chamber of 40^{o}C having a relative humidity of 10% and extruder temperature of 35^{o}C. These initial attempts to were met with limited success [Figure 137] and much work was done in attempting to identify a suitable height based parameter (modifications in the range of 90-15omm), however this did not yield any substantial change in productivity.

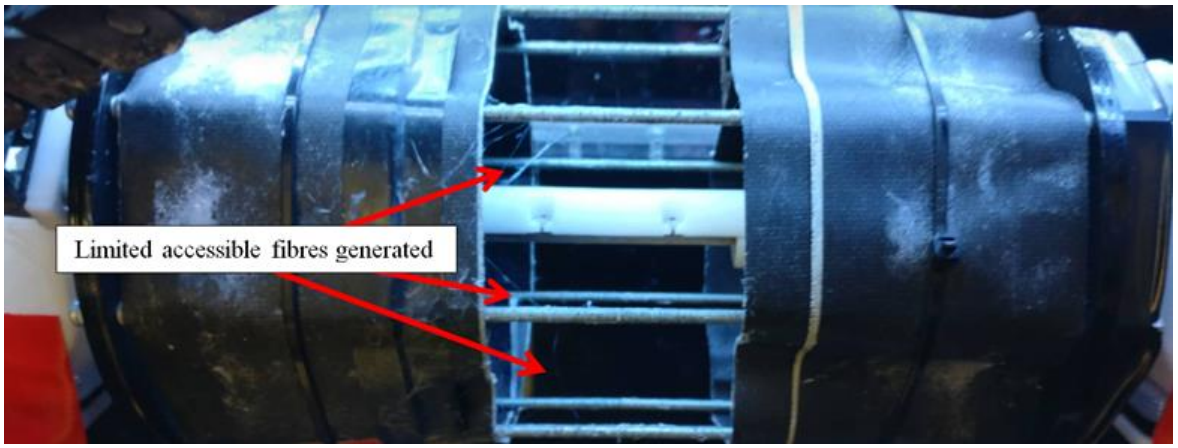

Figure 137: Initial electrospinning yielding limited success

Literature has discussed a method whereby an air assisted form of electrospinning has been implemented as a means to further increase fibre productivity. Given the current embodiment/restrictions of the generated system, this could potentially be realised by activating the heater element during the spinning process. This was trialled and yet the resultant productivity did not differ greatly. Finally, the rotating speed of the collector was dramatically reduced (from 100rpm to 50rpm). This dramatically increased the collection of fibre allowing for sample generation and further evaluation by SEM. It is worth noting that the fibres predominantly occurred upon the left region of the collector, this is thought to be due to this being closer to the airflow produced by the heater. Additionally certain regions of this generated fibre experienced voids/breakages, this is assumed to be a result of both the near proximity (95mm) as well as the high temperature and low humidity yielding dry and brittle fibres. These regions of interest along with the fibre coated collector are displayed in Figure 138.

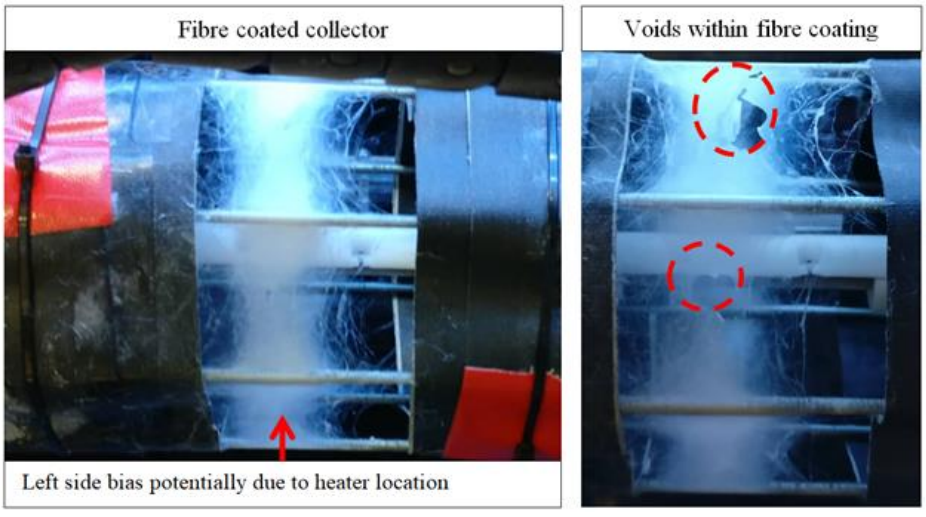

Figure 138: Improved coating of collagen upon the rotating collector with characteristics and non-conformities highlighted in red

The SEM evaluations of the sample generated from this process did not act to display any dramatic variation in alignment of collagen relative to the parallel electrode configuration. Whilst the surface of the sample could be described as somewhat more consistent (a characteristic attributed to the reduction in voids from the production process), the fibres did not demonstrate a dramatic increase in alignment. Whilst once again regions of alignment could be identified, these were still subject to non-conformance and nearby regions of fibres having randomised orientations. Finally it is worth noting that the average diameter of the generated fibres was approximately 300nm, however there was somewhat variance (between 500-100nm). This sample and the related SEM images is depicted in Figure 139.

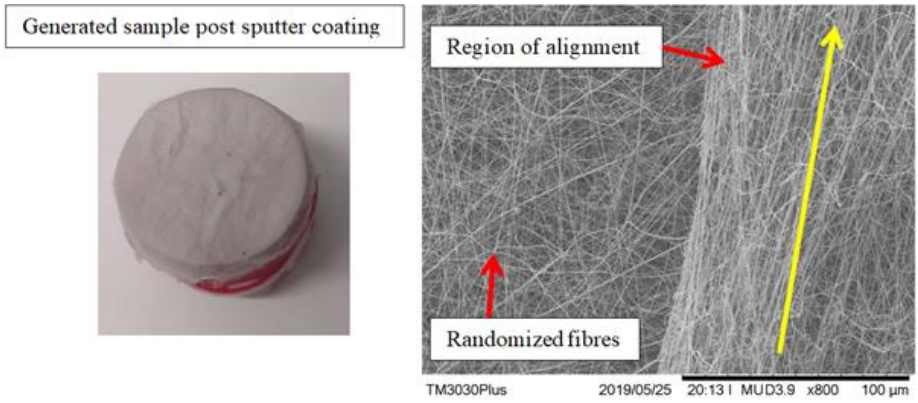

Figure 139: Collagen sample and associated SEM generated utilising the rotating mandrel approach

6.1.7 Review of fibre generation utilising the developed machine

Whilst the generated collagen samples did not demonstrate idealised characteristics of alignment, it is not within the scope of this research project to optimise this. However, it must be noted that the developed research machine now provides a framework in which this materials based optimisation can occur. As such the established relative regions of alignment within samples generated by each technique were deemed an acceptable method of validating the developed machines ability to generate controlled electrospinning based samples. Following this evaluation, strategies capable of functionalisation relative to the generated samples were investigated.

6.2 Sequential Functionalisation Strategies

Now that fibres could be collected, evaluations relating to the potential methods for the sequential functionalisation of these were conducted. This portion of research took into account the feasibility of potential technology for the integration of this within a larger automated system.

6.2.1 Vapour based functionalisation

Literature highlighted the use of vapour bath systems to affect generated fibre. Whilst it was deemed possible to include such systems within automation, a technique capable of actively depositing vapour generated via technology was desirable. A mechanism highlighted as particularly relevant to the scope of this project was the use of ultrasonic transducers to transform solution into vapour. This could allow for the generation of vapour from a wide range of solutions without the need for high temperatures or volatile chemistry.

One of the limitations associated with research related to submicron/nano-resolution fabrication relates to the methods of evaluation for this work. Given the institution-based available technology was not readily capable of handling such novel sample types; alternative means to validate techniques were investigated. One such methodology aimed to utilise the accessible FDM 3D printing technology to generate samples from cost effective ABS. The structural limitations of electrospinning generated fibres, derived from a lack of bonding, can be made comparative to the structural limitations of FDM generated samples derived from weak inter-layer bonding. Hence, it was hypothesised that a methodology yielding benefits to the tensile properties of 3DP ABS would have benefits to the desired fibre constructs. An additional benefit to experimentation utilising ABS was the popularly implemented post processing of this with Acetone vapour bath systems (similar to those utilised in electrospinning functionalisation). The desired outcome for this processing related to the interlayer characteristics of FDM printed parts is illustrated in Figure 140.

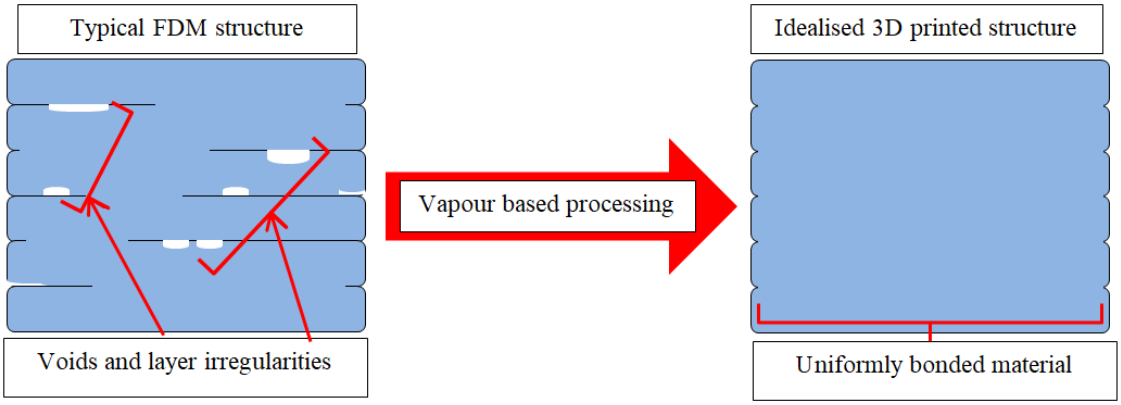

Figure 140: Illustration of the desired effects of applied vapour processing on the internal strctures of 3D printed material

Experimentation related to this initial experimentation was aided by a Masters of Engineering student whose project 'Implementing a control system for vapour based crosslinking/bonding of object' was briefly described within Chapter 1: Introduction. Prior to conducting experimentation utilising ultrasonic transduction to generate vapour a benchmark (comparative dataset) was generated. This required the 3D printing of twenty-five ABS ASTM D635 'dogbone' which samples were grouped and suspended at varied levels of print completion over a bath of Acetone solution. It is important to note that the varied print completion was intended to simulate the desired sequential processing of the functionalisation technique and that the vapour bath did not require additional actuation to generate vapour due to Acetones volatile nature allowing it to evaporate at room temperatures. This study did make use of a computer fan to circulate the vapour in an attempt to ensure adequate coating of the agent upon the samples. This relatively uncontrolled exposure study was then followed by a study in which the same number of samples were similarly generated and positioned within a controlled vapour chamber. Here a system of sensors and actuators was utilised to control the delivery of ultrasonically transduced acetone vapour onto the samples. Of interest was that the ultimate tensile strength of the samples seemed to degrade with the increase in exposure intervals for the benchmark study this relationship was relatively inverted for the later controlled exposure study. The data of these studies is displayed in Table 24 with the relationship of exposure to ultimate tensile strength displayed graphically in Figure 141.

Table 24: Table containing Ultimate Tensile strength data from both the benchmark and controlled exposure studies [1, 2]

Period of printing at which exposure occurred	Average Ultimate Tensile Strength (MPa): (benchmark study)	Average Ultimate Tensile Strength (MPa)(controlled exposure study)
0% exposure to Acetone	41.2	42.9
Exposure at 25% increments	33.7	45.1
Exposure at 50% increments	39.4	43.4
Exposure at 100% increments	29.1	30.7
Printing pause at 50% not exposed	40	41.1

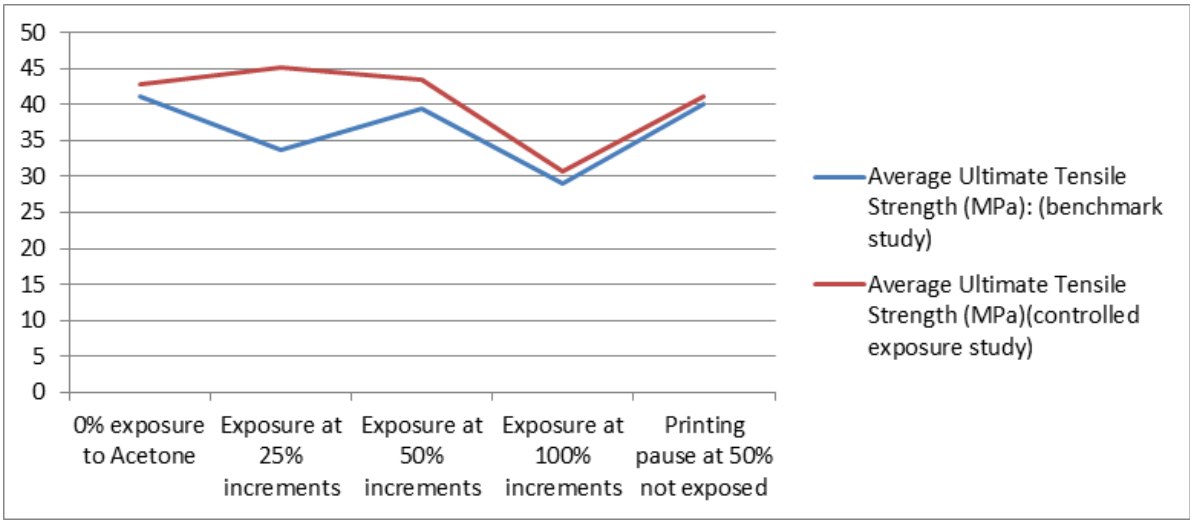

Figure 141: Graphical display of resultant reaction of ABS samples to acetone exposure. [1, 2]

This dramatic variation was attributed to the differences in the positioning of the samples during the exposure interval. For the benchmark study these were suspended above the solution bath with the assumption that the vapour/evaporated particulate would have a lower density to air and thus aided by the propulsion of the fan would accumulate on the samples. Prior work with the ultrasonic transducer mechanisms (Chapter 4**:** Experimental Component Development) identified that the generated vapour was denser than air and thus would sink/move downwards post generation, as such for the control study the samples were placed beneath the inlet. This would suggest further investigation related to the benchmark study, however for the purpose of this research the resultant effects as well as the demonstrated decrease in cavitation (thereby the increase in inter layer bonding) of the samples treated by the controlled [demonstrated in the SEM images of Figure 142] proved adequate enough to motivate further fibre based evaluations.

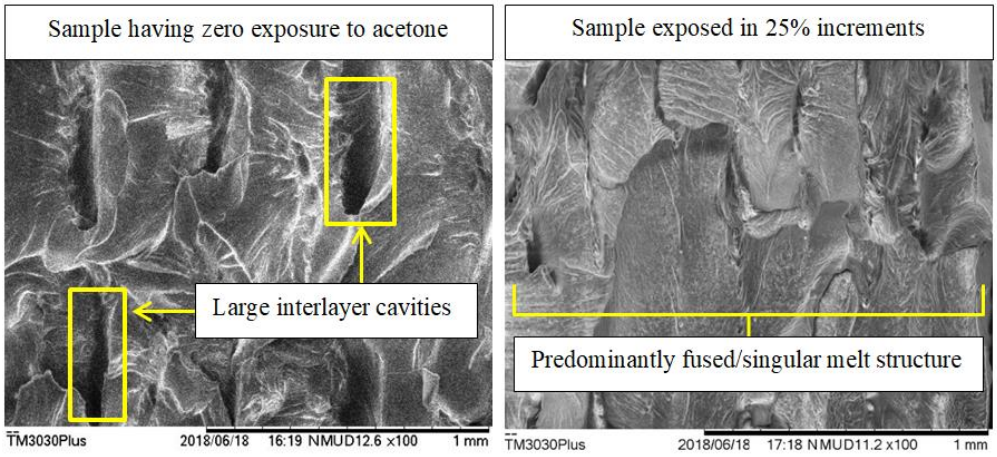

Figure 142: SEM comparisons of the topographical characteristics of a sample having no exposure and a sample being exposed to controlled acetone vapour in 25% intervals [1]

This technique was now identified as a plausible means to generate viable alteration to material via deposited vapour agents. It was hypothesised that through the implementation of solutions such as photo-curable resins, a functionalised structure consisting of a resin-fibre matrix could be generated. This ideology is illustrated in Figure 143.

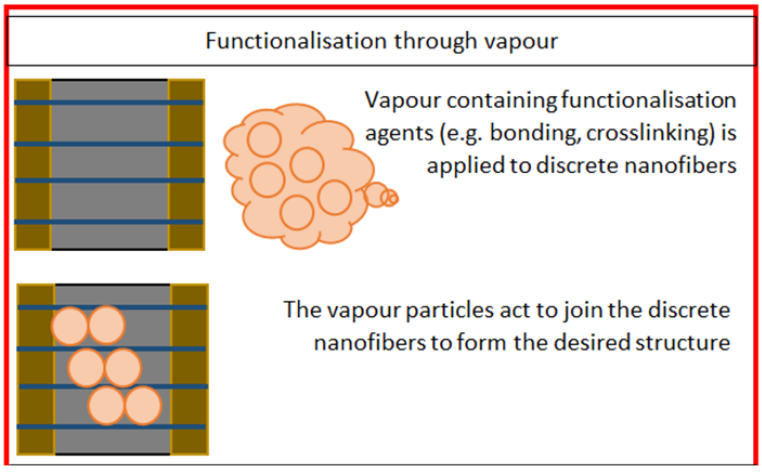

Figure 143: Hypothesised relationship of fibre exposed to functionalising vapour agent

To validate this hypothesis a simple study was conducted utilising Nylon 6,6 solution and expired 3D Systems photo-curable resin. A sample of collected fibre was generated through a sequential process of electrospinning for five minutes followed by collection upon a ABS 3D printed circular form. This occurred 5 times with the orientation of collection varied at 90^{o} per collection. Following the procurement of fibre, this sample was subjected to generated vapour for an additional 2 minutes with the resultant matrix exposed to UV light for 5 minutes at a distance of 50mm. The complete sample was then subjected to gold sputter coating (50angstron delivered via the Nanostructured coatings DSR1 device) and evaluated utilising a Hitachi TM3030Plus SEM. The derived SEM images demonstrated in Figure 144 depicted a highly promising resultant matrix of fibre joint by photo-curable resin. It is worth noting that from these images it was hypothesised that the depicted regions of resin occurred as spheroids thus encasing multiple levels/layers of fibre. This demonstrated the ability to join/bond fibres generated via electrospinning through this technique.

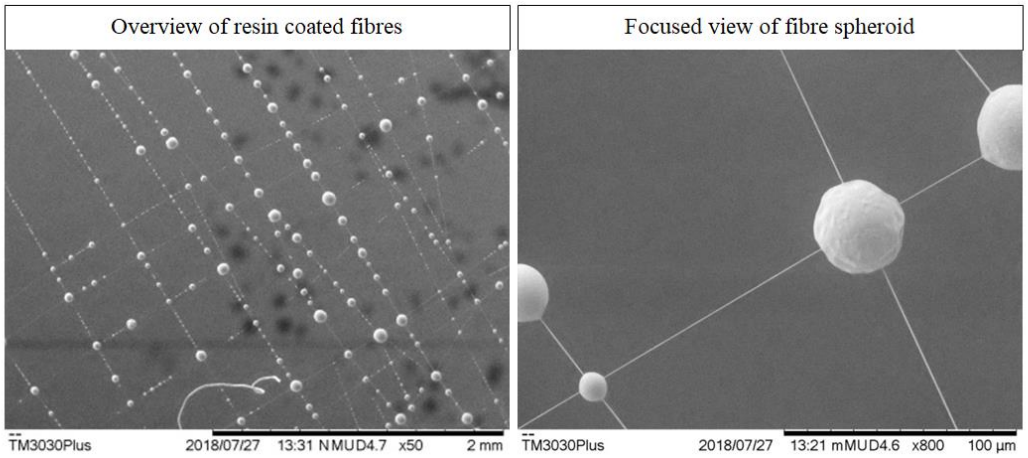

Figure 144: SEM image depicting the capability to utilise ultrasonic transduction to generate vapour agents and functionalise collected fibres.

Utilising the generated SEM images in conjunction with SolidWorks software, information relating to the relative fibre orientations within the sample was generated. This evaluation allowed for the generation of two datasets, namely the relatively vertical lines and horizontal lines. Figure 145 depicts how this data was attained with it being fully represented in Table 25.

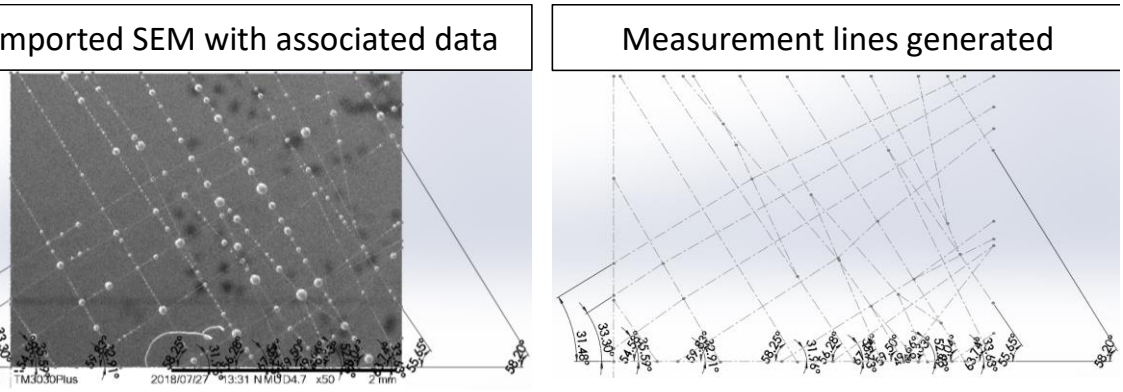

Figure 145: The methodology for generating datasets relating to fibre orientations

Table 25: Data relating to the resultant fibre alignment relative to the horizontal of the SEM utilised

Vertical Lines	Horizontal lines (inverted)	Horizontal lines (corrected)	Angled variance between Horizontal and Vertical lines
54.58	31.48	148.52	93.94
59.83	33.3	146.7	86.87
58.25	35.59	144.41	86.16
56.28	32.91	147.09	90.81
67.14	31.96	148.04	80.9
59.5	35.73	144.27	84.77
49.66	52.23	127.77	78.11
66.33	33.63	146.37	80.04
58.04			
63.74			
55.65			
58.2			
Average vertical		**Average horizontal**	**Average variance**
58.93333333		144.14625	85.2

It is important to note that the vertical lines and horizontal lines were measured relative to the image horizontal axis, additionally the horizontal values were measured from the inverted orientation (counter-clockwise) and this had to be accounted for. Utilising the data valuable information related to the angle variation between horizontal and vertical lines, namely the offset between fibres could be generated. This yielded an average value of 85.2^{o} which strongly indicated adherence to the collection angle utilised of 90^{o}. A major concern within this evaluation related to the potential of fibre-interactions to offset and disrupt the dataset through each new addition of the fibre/resin. Thus a further statistical-based analysis was conducted regarding these data sets to determine the evaluations validity. This was achieved through the use of the Minitab software implementation of a one-way Anova to generate graphical representations of the datasets (Figure 146). These graphs demonstrated a condition of normality (Normal Probability plot) and a justified versus-fits relationship with identified outliers highlighted in red. Additionally the histogram demonstrated a uniform distribution of the data around the mean (zero) and the versus order further validated the datasets by demonstrating a non-continuous trend.

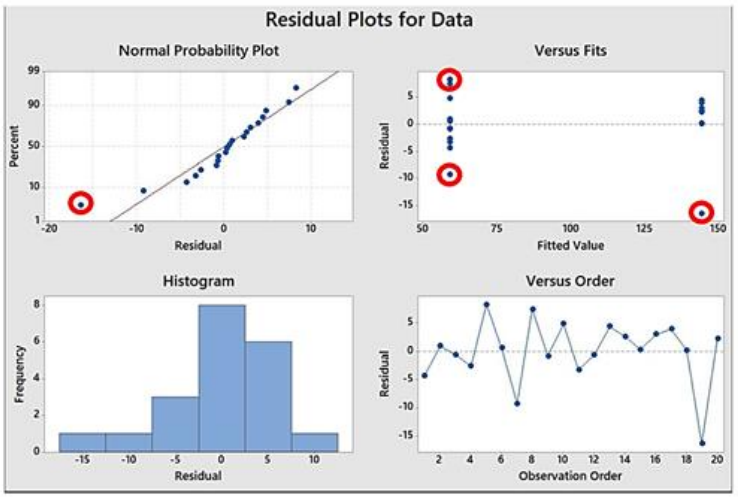

Figure 146: Graphical output from Minitab one-way Anova to evaluate dataset validity

6.2.2 Application of vapour on Collagen fibre Samples

One of the major limitations of manipulating electrospun collagen relates to it's dramatically hydrophilic characteristics. Namely the fibres will distort and react to moisture which in turn has the potential to yield undesirable affects for generated samples. The main limitation to the application of vapour to any sample (including the implemented collagen samples) will relate to a pre-existing understanding of both the proximity and vapour quantity required. Proximity relates to the potential for the vapour stream to actively damage the samples though the force at which they pass through/deposit onto the fibres. The vapour quantity relates to both the threshold at which the deposited solution becomes too heavy for the fibre to support. It is also important to recognise that the accumulation of solution upon the fibre could allow for the movement of the fibre within this and as such the quantity should not be great enough to allow for this distortion.

Thus in order to determine the effects of vapour upon this material a threshold distance between the point of vapour production and the fibre coated surfaces was investigated. To accomplish this goal, 6 fibre coated 'cookie cutter' samples were generated. The fibre was formed via the electrospinning of the collagen solution at 45kV at a distance between the extruder and collector of 150mm. The implemented extruder was the single nozzle unit and the collector was the parallel electrode-rotating mandrel variation. The collector was spun at a rate of 100rpm and the process occurred for 10minutes per sample. Following this the samples were generated by the transferal of the fibres onto the surfaces occurring 8 times with each transferal occurring at a 90^{o} offset from the prior collection, with the resultant samples demonstrated in Figure . It is worth noting that these samples did not appear to have a uniform thickness as such two of the samples having the most drastic differences were removed from the sample set (highlighted in yellow in Figure 147).

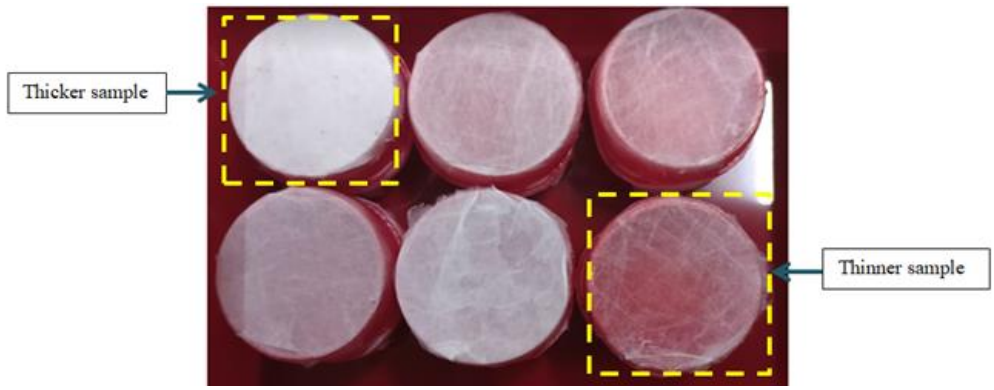

Figure 147: Samples generated for vapour based analysis

The samples were situated at 50, 100, 150, 200mm for each trial with the results demonstrated in Figure 148. The exposure to vapour had significant modifications to the transparency of the fibre samples.

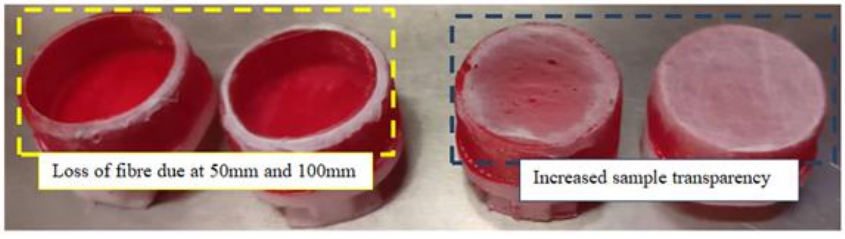

Figure 148: Vapour proximity experiment effects on sample fibres

Attempts made to further analyse the sample through the use of an SEM demonstrated yielded complications in the form of sample degradation. This occurred in both attempts to sputter coat the sample as well as in the viewing process of the electron microscope. It is hypothesised that these processes acted to continue the now riboflavin coated collagen cross-linking process. This could have resulted on too much train on the surrounding fibre and due to the unsupported nature of this sample result in the breakages seen in Figure 149. It is also worth noting that an SEM of this collection demonstrated a significantly different more fused-like structure to that of the standard fibre sample, additionally a spheroid object (plausibly a residual vapour droplet) could be identified [Figure 150]. Given the complexities in applying solution to the hydrophilic collagen samples and the undesirable affects this could have on the orientations of fibres within these, a non-solution based approach to modify samples, namely plasma irradiation was investigated.

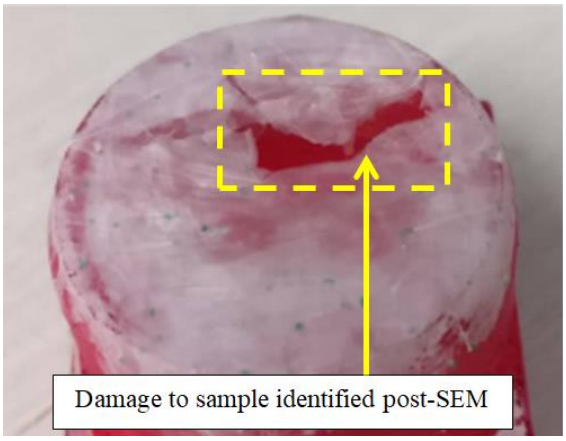

Figure 149: Example of damage to sample identified during and post-SEM imaging

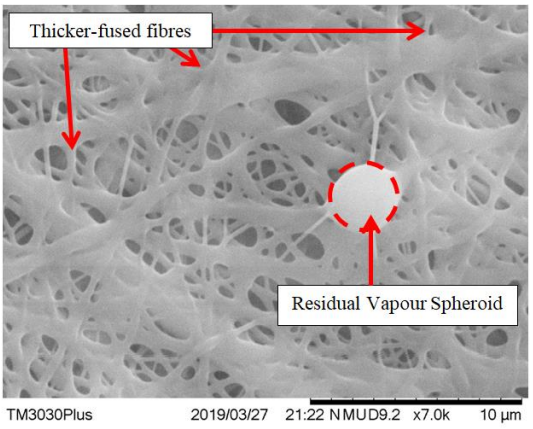

Figure 150: Changes to the structure of the sample's collagen fibres

6.2.3 Plasma based functionalisation

The use of vapour introduced an additional element within the process which was reliant on additional material which thus would result in the final structure being composed of multiple materials (a composite structure), additionally this coating technique was quite time intensive. Chapter 4: Experimental Component Development discussed the potential utilisation of plasma surface modification technology which lead to the development of a corona discharge plasma system specifically suited for this projects requirements. One of the major limitations of this newly developed mechanisms was the lack of knowledge relating to the ideal operating conditions/parameters, namely the required distance between sample and point of plasma production. Much like with the initial vapour orientated investigations, FDM 3D printed ABS samples were utilised as cost effective analogues to determine the effects of the desired processing technique.

To investigate the processing nature of the mechanism an acrylic stand with a manoeuvrable platform was created. Additionally acrylic components utilised to position the sample and mechanism plasma outlets/production points were made. Similar to previous studies, thirty ABS ASTM D635 'dogbone' samples were 3D printed. These were grouped and positioned accordingly at varied distances from the point of plasma generation. Utilising the above experimental setup samples were processed with the corona discharge mechanism and then evaluated through tensile testing, the results of which are displayed in Table 26 (as well as graphically demonstrated in Figure 151).

Table 26: Resultant mean ultimate tensile strength for each sample set exposed to corona plasma surface modification[10]

Sample	Mean Ultimate Tensile Strength (MPa)	Improvement of Ultimate Tensile Strength (MPa) (Relative to Benchmark)
Benchmark	18.27	NA
Sample 1 (36 mm)	18.85	0.58
Sample 2 (30 mm)	18.83	0.56
Sample 3 (24 mm)	19.01	0.74
Sample 4 (18 mm)	18.7	0.43
Sample 5 (12 mm)	17.3	-0.97

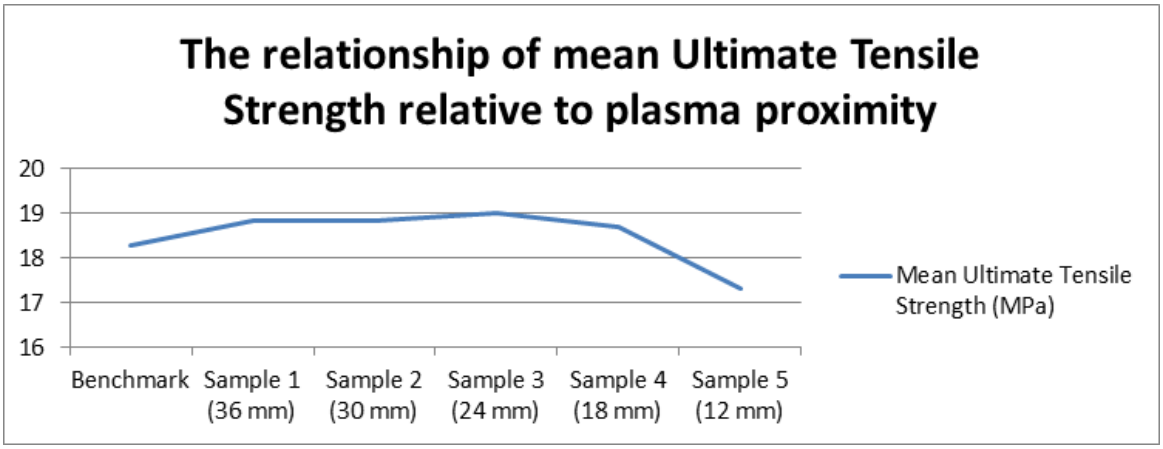

Figure 151: Graphical display of the effects of plasma proximity on ultimate tensile strength of ABS samples[10]

This study demonstrated that alterations yielding benefits to the crosslinked nature and thus improving the tensile properties of polymer-based structures could be achieved through processing with this mechanism. Additionally for the ABS samples an optimal operating window of 24mm from the point of plasma generation could be identified. It must be noted that at this distance there was a only a 0.74MPa increase in tensile strength which is relatively low in comparison to the 2.2MPa improvement of the optimal controlled vapour based processing. Additionally this technique has the potential to thermally degrade the sample for situations in which the sample is too close to the plasma. Finally, it is worth noting that additional studies should be conducted to further evaluate the effectiveness of this processing relative to mechanisms such as focused UV exposure. Whilst this study did demonstrate beneficial results, the lack of easily identifiable topographical alterations by this technique as well as the lack in pre-exiting knowledge related to proximity/exposure-optimisation indicated limit the potential future evaluation of this within fibre based studies.

6.2.4 Implementation of plasma treatment on Fibres

A simple investigative analysis regarding the use of plasma involved the exposure of a developed sample to the simplified (single point) end-effector. This allowed for an ease in manipulation of proximity between sample and plasma [Figure 152].

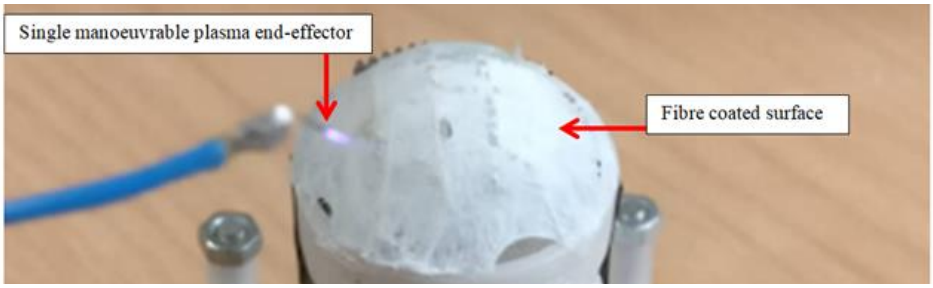

Figure 152: Simple hand-held experimentation of plasma based exposure on functionalising collagen sample

Much like in the previous synthetics-based experiments, plasma occurring too close to the fibres resulted in thermal degradation. Importantly, the tendency for the plasma stream to arc to the more conductive 'cutting edge' of the collector yielded dramatic damage/distortion to the fibres at the samples edge [Figure 153].

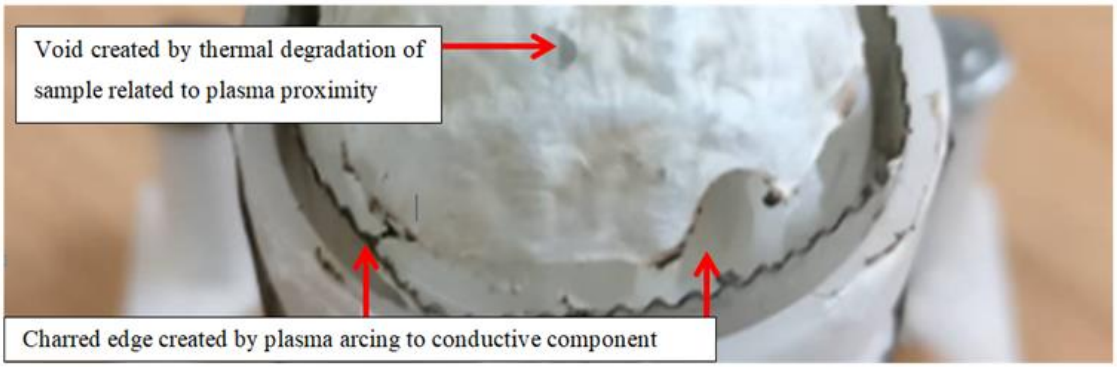

Figure 153: Damage to sample from plasma exposure

The plasma was capable of modifying the sample surface. This was identifiable as a colour/transparency change in the regions where thermal degradation did not occur [Figure 154].

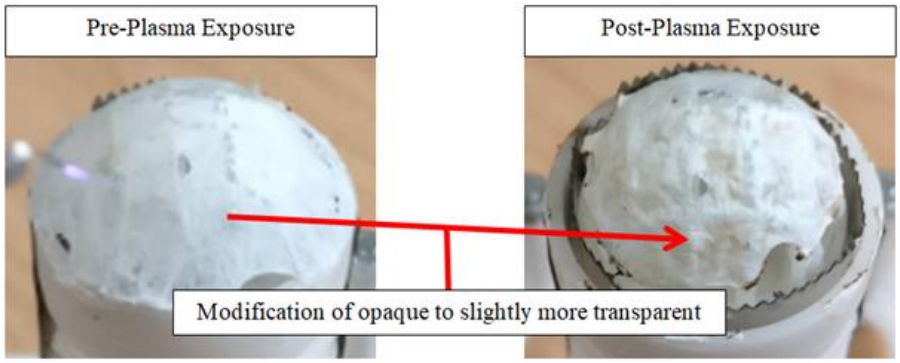

Figure 154: Demonstration of the modification of sample surface from opaque to transparent

Another limitation for this technology related to the uncontrolled modification of collector-fibre relationships due to the exerted energy from the plasma. This is hypothesised as being capable of modifying the surface of the collector in a fashion which may result in the additional bonding of this to the fibres of the sample. This potential occurrence could explain/justify the difficulties in removing the sample [Figure 155].

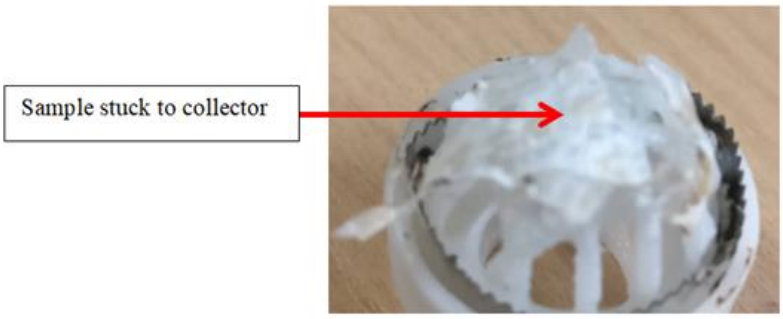

Figure 155: Depiction of difficulties in removing fibre from collector

The effect of plasma irradiation upon generated fibre-based samples was much more difficult to identify/characterize in comparison to the vapour-processed samples. As such to further validate the effectiveness of the developed technology within the project, an automated sample was generated in which vapour-processing technology was utilised.

6.3 Automated machine generated samples

The evaluation of the automated procedure to generate a functionalised fibre-based construct utilising the machine made use of Nylon 6, 6 solution which was functionalised with expired 3D Systems photo-curable resin. Within this test, the electrospinning was conducted for 5 minutes at a flowrate of 1ml/h, with generated fibres collected on a parallel electrode-based rotating mandrel actuated at 100rpm. The resultant collection was transferred onto a circular surface which was rotated at 45^{o} prior to each collection. This occurred 20 times after which the sample was moved to the vapour mechanism and exposed to vapour for a further five minutes and then transferred to the lithography mechanism and the coated resin made to cure for 5 minutes. The resultant annotated SEM images of this process are displayer in Figure 156.

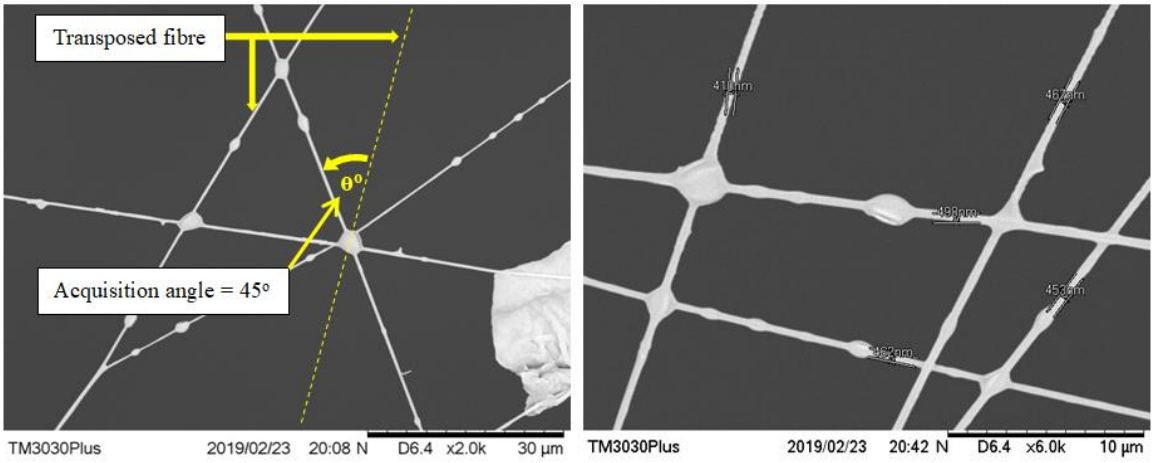

Figure 156: SEM images of the first sample electrospinning-vapour generated through the automated machine

Much like the previous hypothesis-validating experiment, an SEM depicting a range of fibres from this sample was imported into SolidWorks for further evaluation of the fibre collection orientations. The chosen SEM as well as the generated data is depicted in Figure 157 and Table 27.

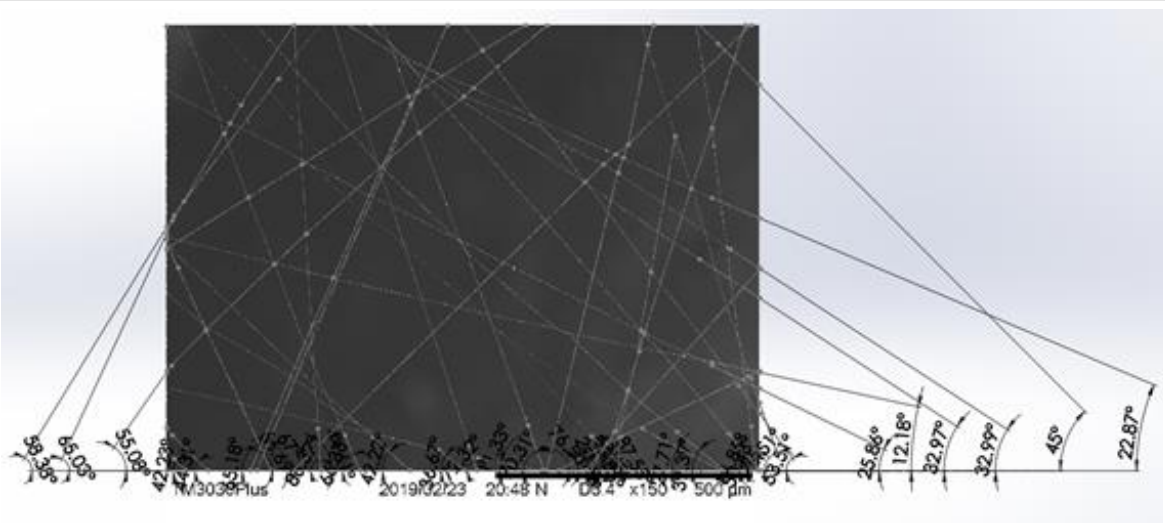

Figure 157: Chosen SEM for fibre angle-based evaluation including derived measurements.

The angle based analysis of this sample required some thresholding, namely the grouping of data into sets having associations with the idealised variation (0^o, 45^o, 90^o, and 135^o). For each of these sample sets a mean value was generated. These mean values were then compared with one another and then subtracted from one another to identify the collection resultant angle between the fibres. Of the datasets, Groups 1 and 2 differed quite significantly relative to the expected 45-degree angle, to ensure the data still retained some statistical relevance, a further evaluation of the data set was required.

Table 27: Data representing the angular characteristics of the fibre generated utilising the developed machine

Group 1(0/180)	**Group 2 (45)**	**Group 3 (90)**	**Group 4 (135)**
Range (157.8-22.5)	Range (22.5-67.5)	Range (67.5-112.5)	Range (112.5-157.5)
11.33	42.23	86.32	121.62
12.18	44.31	72.32	114.97
22.87	65.18	70.31	124.92
	42.22	81.85	113.31
	36.67	70.51	113
	44.58	103.5	135.39
	27.71	92.45	151.28
	39.39		127.15
	50.46		117.32
	53.51		
	25.86		
	32.91		
	32.99		
	45		
	66.36		
Average	**Average**	**Average**	**Average**
15.46	43.292	82.46571429	124.3288889
Calculated variance angle			
71.1311111	27.832	39.17371429	41.8631746

A one-way Anova (conducted using Minitab) of the data allowed for an evaluation of the validity of this data. The Normality graph generated from this demonstrated that the data was arranged in close proximity to the normality line, with some outliers clearly distinguishable. The data demonstrated a good conformity within the versus mean plot with a mean-based variation of approximately $^{+}/_{-}10$, however once again the outliers could be clearly identified. The associated histogram whilst being slightly skewed to the left could be described as having a bell curve like appearance (if the residuals occurring to the right (near 20) are ignored. Finally the versus order line graph further validates the data by demonstrating a non-continuous trend line. All of these graphs are depicted in Figure 158 where the outliers have been highlighted via a red circle.

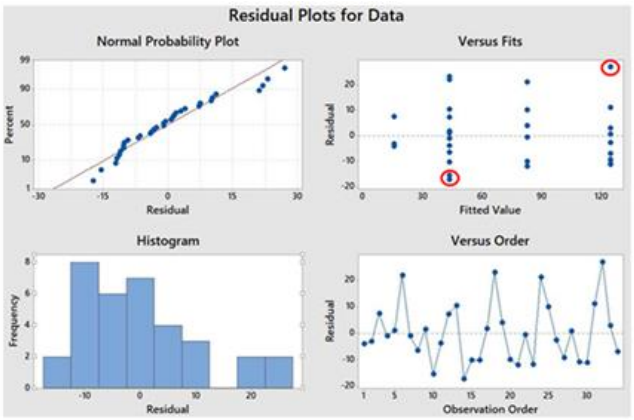

Figure 158: Graphical results from the one-way Anova demonstrating sample set validity

6.4 Generating a 3D fibre based object

One of the greatest challenges in identifying the potential for the developed machine to generate a self-sustaining 3D object relates to the nature of the output of the fundamental process electrospinning. This technique typically generates very thin layers of material and whilst the machine developed makes use of a sequential collection and building up of these layers to generate a relatively thicker construct, the threshold at which this will allow for a self-sustaining object is unknown. This leads to complications related to the fragility of developed samples where by attempts to remove these from the collecting surface may lead to undesirable breaking/fracturing of the material. Attempts to reduce the strain on the samples during the removal process utilised thin pieces of wire through which attempts to lift the edges of the material were made [Figure 159].

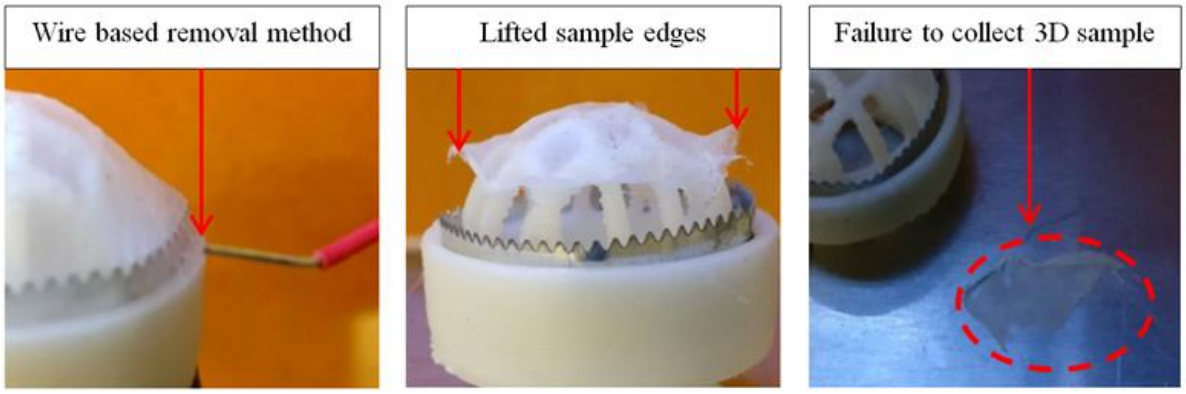

Figure 159: Wire based process to remove fibre based structures from 3D collector

This project was able to generate a self-sustaining 3D dome structure, however this was achieved through much trial and error. The major difficulties associated with this process related to the failures occurring from exposure of processing elements and the failure to remove the sample from the collector. This process is illustrated as a flowchart in which examples of the failure and success are provided in Figure 160.

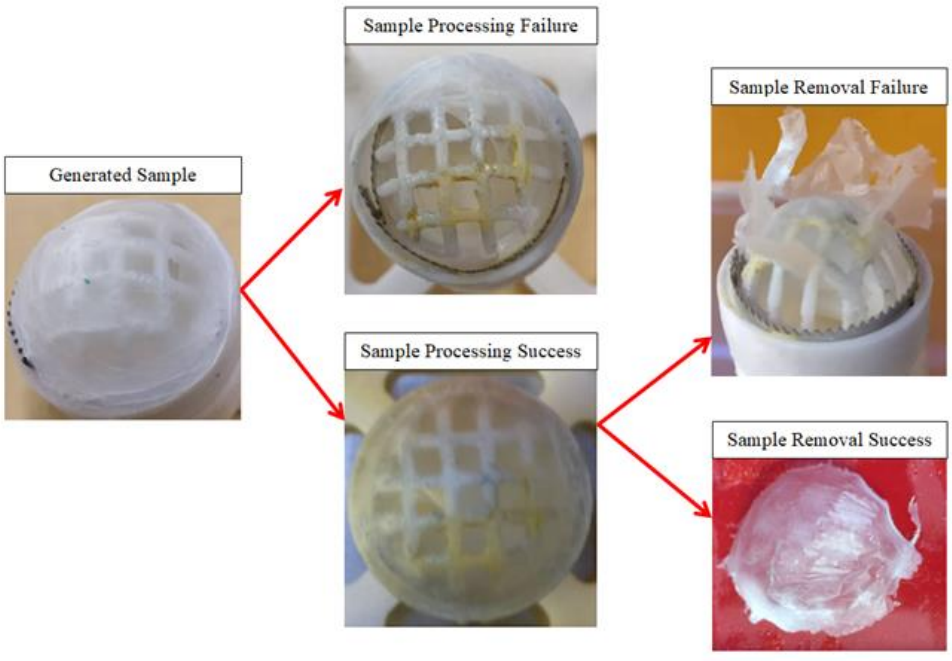

Figure 160: Process of trial and error demonstrating the difficulties associateed with the generation of a self-sustaining three dimensional fibre based object.

The successful structure was comprised of collected collagen fibres which were then exposed to riboflavin solution for 10 minutes and then functionalised by UV exposure for 15minutes. One of the key features of this sample is the retention of the features of the collector utilised, namely it is both a semi-sphere as well as retaining an indentation derived from the supporting crosshatched structure [Figure 161].

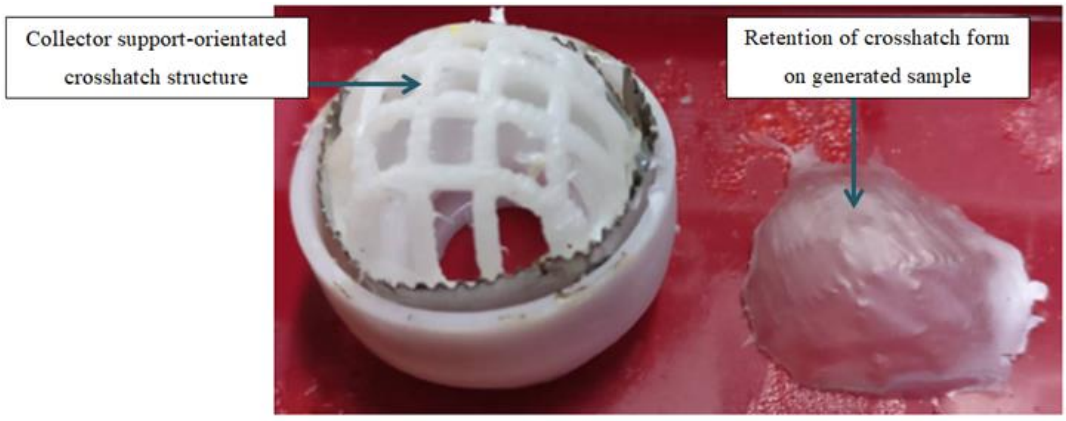

Figure 161: Demonstration of 3D fibre-based object having retained structural elements of the collector utilised

This sample aided to further validate the hypothesis as well as yield a dramatic new potential for future research utilising this developed machine. Given the ability to modify the parameters and mechanisms of the machine, testing specific to both synthetic and biopolymer based fibre constructs can be conducted with a new degree of simplicity. Prior to this work no simple and automated means of conducting such electrospinning based manufacturing research existed.

Chapter 7 FUTURE WORK AND RECOMMENDATIONS

This section relates to the recommended future work relating to this project. It must be noted however that whilst much work relating to the implementation and optimisation of the materials implemented within this study as well as novel materials can (and should) be conducted utilising the gained knowledge from this project, here a focus is made on discussing the future Mechatronics-based developments related to the machine.

7.1 Vapour-orientated recommendations:

A greater control and optimisation of the vapour-based functionalisation can be achieved through the further development of the transducer component. It is encouraged that future renditions of this mechanisms do not make use of a commercial product, but rather incorporate a more adjustable system. This could take the form of a method in which control of the implemented frequency and wavelength will be made possible thus further allowing the potential materials to be vaporised as well as the resultant characteristics of the generated particulate. An additional field of interest includes the future stereo-lithography printing potential of vapour deposited photo-curable resin.

7.2 Plasma-orientated recommendations:

The effects and potential for the implemented corona discharge plasma mechanism have yet to be fully realised. Of interest is the further analysis of both the proximity and the intensity at which this process functions. Additional work should be conducted to yield a comparison of this technology to the effects of prolonged UV on sample ultimate tensile strength.

7.3 Environmental control recommendations:

A more robust system for the active control and retention of parameters relating to temperature and humidity is encouraged. Of interest is the potential for the implementation of vacuum or near-vacuum conditions within the electrospinning region and the effects of these on fibre displacement.

7.4 Code recommendations:

The implemented code took the form of C and utilised many functions to perform the operations required by the machine. Future work could aim to optimise this through the conversion of the established program to class driven embedded programming. This would both allow for an increase degree in the control and implementation of operations as well as potentially enable the control of transducers such as the ultrasonic piezoelectric disk which requires a signal having a frequency in the MHz range.

7.5 Electronics recommendations:

Whilst a modular electronics system was developed through this project, it was not fully realised. It is highly encouraged that this be implemented for ease in the future variation and introduction of mechanisms.

7.6 High Voltage isolation recommendations:

To ensure a higher degree of safety the further isolation of high voltage related components through the implementation insulator mechanisms (e.g. glass housings) is recommended. Additionally components such as the implemented syringe system should investigate the use of a glass-orientated system to allow for active heating of the implemented material.

7.7 Electric Field manipulation recommendations:

Much work was conducted within this project in an attempt to increase the electrospinning productivity via the utilisation of electric field modifying conductive or insulating elements. This was in an attempt to derive a methodology inspired by hydrodynamic 3DP that would negate a dependency on a high degree of temperature, humidity, or vacuum-based control. One technique that was hypothesised within this project related to the use of a secondary high voltage source. Given that the developed system would allow for the potential electrospinning of material at distances of up to 450mm from the extruder, investigations into some technique capable of manipulating the field at these varied distances is encouraged. It is worth noting that within this project single nozzle experiments demonstrated that any material charged via the same power supply and positioned sufficiently higher than the nozzle outlet would nullify the occurrence of Taylor cones and subsequent electrospinning. As such, a secondary high voltage power supply (capable of 25kV output) must be utilised in the further development of electric field manipulating techniques. The intended outcome for which is illustrated in Figure 162 whereby all external potential electric interference is negated by this component.

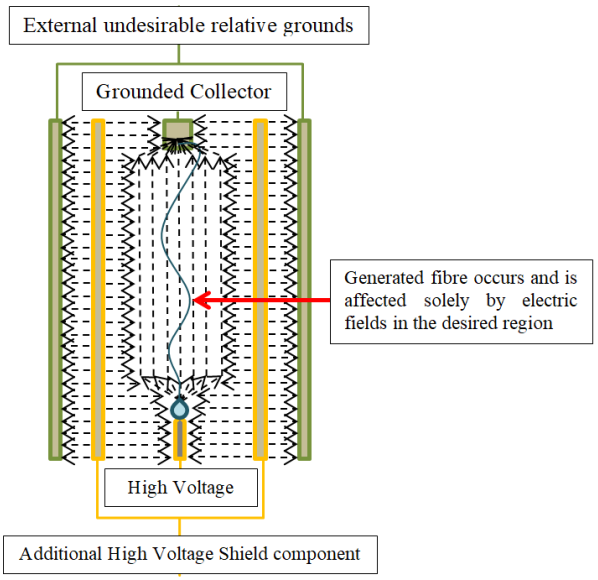

Figure 162: Illustration in which the creation of a secondary electric field will negate the effects of undesirable attraction towards auxiliary components

7.7.1 Variability within automated electrospinning

As the developed machine allows for a programmable variation in the distance between extruder and collector, an ideal implementation of the hypothesised field manipulation would account for this. One idea that could achieve this includes the use of cylindrical aluminium pieces having staggered sizes. Where each segment of aluminium could be connected to the next size up or down allowing the formation of a funnel when extended

similar to that of a telescope. A limitation of this concept relates to the amount of material required (which might limit the minimum possible distance between extruder and collector) as well as the potential for the electrospun fibre jets to collide with the funnel and form blockages. Another alternative potential solution was inspired by concepts of electromagnetism and the 'slinky' toy. In this version, copper wire would travel in a circular loop towards the collector with gaps between the wire expanding and contracting relative to the distance required. This spiral of copper wire would have an additional benefit of generating a magnetic field in the direction of the flow of current. Literature has discussed the potential benefits of magnetic fields in target fibre formation, as such this potential mechanism property is deemed worth investigating. It should be noted however that the use of this technique would result in non-uniform field manipulation at various distances. These ideologies and notable features are displayed in Figure 163.

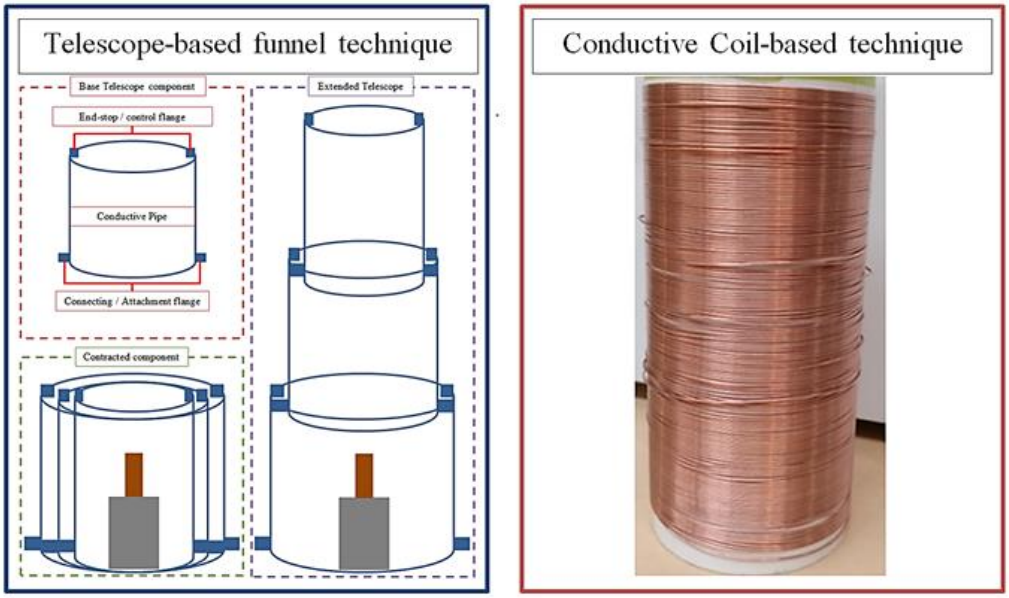

Figure 163: Ideation for the implementation of a secondary high voltage component to modify the electrospinnnig electric field

7.8 Future Funded work recommendations

Given the novelty within this field of research, many future initiatives utilising the technology derived within this project (as well as variations thereof) could relate strongly to research entities associated with manufacturing and additive manufacturing. This work has already been pivotal to the current and future success of a New Zealand Ministry of Business Innovation and Employment funded Smart Ideas project. The success of this application further justifying the demand and interest associated with this form of technology. This project strongly relates to the use of the technology developed herein for bio-fabrication as such it is recommended that work relating to the development of novel biomaterials which are able to leverage off this form of processing should be developed.

Chapter 8 PROJECT CONCLUSION

This project aided in the development of the field and capabilities of Additive Manufacturing technology. It was motivated by the needs within industry such as to fibre-reinforcement, biotechnology and tissue engineering in the ability to additively manufacture objects constructed from fibres is highly desirable. An analysis of the relative literature highlighted a potential methodology through which the generation of such items could be achieved. A deficiency in technology capable of facilitating this research resulted in the need to develop a novel form of technology capable of electrospinning-additive manufacturing research and development. Following these realisations, much design-based experimentation, and development was conducted in order to generate a novel technology capable of furthering this field of engineering relative to the aforementioned industry. The currently implemented technology and the ability to vary this, due to the project outcomes emphasis on modularity, allowed for the evaluation of potential new forms of manufacturing. These evaluations aided in the validation of the final machine and its automated methodology. Finally, an additively manufactured, self-sustaining three-dimensional biopolymer fibre-based object was created through implementation of this research technology. This aided in the promotion of this works relevance to the future facilitation and development of research to overcome limitations within fibre and biotechnology orientated fields. The final rendition of the modular mechatronics research and development machine is displayed in Figure 164.

Figure 164: Developed modular mechatronics technology for fibre-based manufacturing and biofabrication research

Chapter 9 REFERENCES

[1] J. Schutte, P. Wijisundira, M. Harris, and J. Potgieter, "Evaluation of the effects of controlled ultrasonic acetone vapourisation on Fused Deposition Modelling 3D Printed Acrylonitrile Butadiene Styrene," *25th International Conference on Mechatronics and Machine Vision in Practice (M2VIP)*, p. 5, 2018 2018.

[2] P. Wjesundira, J. Schutte, and J. Potgieter, "The effects of acetone vapour inter-layer processing on fused deposition modelling 3D printed acrylonitrile butadiene styrene," *24th International Conference on Mechatronics and Machine Vision in Practice (M2VIP)*, p. 6, 2017 2017.

[3] Electrospinz. (5/04). *Electrospinz Laboratory ES Family*. Available: http://www.electrospinz.co.nz/products.php

[4] Contipro. (2015 22/09/2018). *4SPIN*. Available: https://www.4spin.info/

[5] K. M. Meek, "The Cornea and Sclera," in *Collagen: Structure and Mechanics*, P. Fratzl, Ed., ed New York: Springer Science +Business Media, 2008.

[6] D. Li, Y. Wang, and Y. Xia*, "Electrospinning of Polymeric and Ceramic Nanofibres as Uniaxially Aligned Arrays," *Nano Letters*, vol. 3, pp. 1167 -1171, 2003.

[7] J. Schutte, J. Potgieter, S. Dirven, and X. Yuan, "The effects of electrospinning collection surface modification on nylon 6-6 placement," *24th International Conference on Mechatronics and Machine Vision in Practice (M2VIP)*, p. 6, 2017 2017.

[8] J. Schutte, X. Yuan, S. Dirven, and J. Potgieter, "The opportunity of electrospinning as a form of additive manufacturing in biotechnology," *24th International Conference on Mechatronics and Machine Vision in Practice (M2VIP)*, p. 6, 2017 2017.

[9] N. Ismail, F. J. Maksoud, N. Ghaddar, K. Ghali, and A. Tehrani-Bagha, "Simplified modeling of the electrospinning process from the stable jet region to the unstable region for predicting the final nanofibre diameter," *Journal of Applied Polymer Science*, vol. 133, 2016.

[10] J. Schutte, J. Leveneur, X. Yuan, and J. Potgieter, "Evaluation of the effects of corona discharge plasma exposure proximity to Fused Deposition Modelling 3D Printed Acrylonitrile Butadiene Styrene," *25th International Conference on Mechatronics and Machine Vision in Practice (M2VIP)*, p. 6, 2018 2018.

[11] R. Nayak, R. Padhye, I. Kyratzis, Y. B. Truong, and L. Arnold, "Recent advances in nanofibre fabrication techniques," *Textile Research Journal*, vol. 82, pp. 129-147, Jan 2012.

[12] S. A. M. Tofail, E. P. Koumoulos, A. Bandyopadhyay, S. Bose, L. O'Donoghue, and C. Charitidis, "Additive manufacturing: scientific and technological challenges, market uptake and opportunities," *Materials Today*, vol. 21, pp. 22-37, Jan-Feb 2018.

[13] J. Gardan, "Additive manufacturing technologies: state of the art and trends," *International Journal of Production Research*, vol. 54, pp. 3118-3132, 2015.

[14] K. V. Wong and A. Hernandez, "A Review of Additive Manufacturing," *ISRN Mechanical Engineering*, vol. 2012, pp. 1-10, 2012.

[15] F. Calignano, D. Manfredi, E. P. Ambrosio, S. Biamino, M. Lombardi, E. Atzeni, *et al.*, "Overview on Additive Manufacturing Technologies," *Proceedings of the IEEE*, pp. 1-20, 2017.

[16] Y. S. Zhang, K. Yue, J. Aleman, K. Mollazadeh-Moghaddam, S. M. Bakht, J. Yang, *et al.*, "3D Bioprinting for Tissue and Organ Fabrication," *Ann Biomed Eng*, vol. 45, pp. 148-163, Jan 2017.

[17] B. Duan, "State-of-the-Art Review of 3D Bioprinting for Cardiovascular Tissue Engineering," *Ann Biomed Eng*, vol. 45, pp. 195-209, Jan 2017.

[18] "Artificial Cornea," ed, 2015.

[19] "The Need is Real: Data," ed: Health Resources & Services Administration, , 2013.

[20] R. R. Jose, M. J. Rodriguez, T. A. Dixon, F. Omenetto, and D. L. Kaplan, "Evolution of Bioinks and Additive Manufacturing Technologies for 3D Bioprinting," *Acs Biomaterials Science & Engineering*, vol. 2, pp. 1662-1678, Oct 2016.

[21] C. K. Chua and W. Y. Yeong, "Chapter 3 Bioprinting Techniques," in *Bioprinting Principles and Applications*, ed Singapore: World Scientific Publishing Co. Pte. Ltd., 2015, pp. 63-111.

[22] C. K. Chua and W. Y. Yeong, "Chapter 1 Introduction to Tissue Engineering," in *Bioprinting Principles and Applications*, ed Singapore: World Scientific Publishing Co. Pte. Ltd., 2015, pp. 1-12.

[23] S. V. Murphy and A. Atala, "3D bioprinting of tissues and organs," *Nat Biotechnol*, vol. 32, pp. 773-785, Aug 2014.

[24] P. G. Campbell and L. E. Weiss, "Tissue engineering with the aid of inkjet printers," *Expert Opin Biol Ther*, vol. 7, pp. 1123-7, Aug 2007.

[25] D. J. S. Hulmes, "Collagen Diversity, Synthesis and Assembly," in *Collagen Structure and Mechanics*, ed New York: Springer Science+Business Media, 2008, pp. 15-22.
[26] V. R. Sherman, W. Yang, and M. A. Meyers, "The materials science of collagen," *J Mech Behav Biomed Mater,* vol. 52, pp. 22-50, Dec 2015.
[27] K. P. Mashige, "A review of corneal diameter, curvature and thickness values and influencing factors* " *The South African Optometrist* vol. 4, pp. 186-189, 2013.
[28] K. M. Meek, "The Cornea and Sclera," in *Collagen Stucture and Mechanics*, ed New York: Springer Science+Business Media LLC, 2008, pp. 359-362.
[29] "Facts About the Cornea and Corneal Disease," ed: Department of Health and Human Services, 2013.
[30] "How Does The Human Eye Work?," ed: National Keratoconus Foundation, 2016.
[31] C. Boote, S. Dennis, R. H. Newton, H. Puri, and K. M. Meek, "Collagen Fibrils Appear More Closely Packed in the Prepupillary Cornea: Optical and Biomechanical Implications," *Investigative Ophthalmology & Visual Science,* vol. 44, pp. 2941-2942, 2946, 2003.
[32] "Give the Gift of Sight...", ed: New Zealand National Eye Bank 2013.
[33] J. P. Whitcher, M. Srinivasan, and M. P. Upadhyay, "Corneal blindness: a global perspective," *Bulletin of the World Health Organization,* vol. 79, pp. 214-215, 2001.
[34] L. G. Blok, M. L. Longana, H. Yu, and B. K. S. Woods, "An investigation into 3D printing of fibre reinforced thermoplastic composites," *Additive Manufacturing,* vol. 22, pp. 176-186, Aug 2018.
[35] M. Harris, J. Potgieter, R. Archer, and K. M. Arif, "Effect of Material and Process Specific Factors on the Strength of Printed Parts in Fused Filament Fabrication: A Review of Recent Developments," *Materials,* vol. 12, p. 34, 2019 2019.
[36] Y. Sano, R. Matsuzaki, M. Ueda, A. Todoroki, and Y. Hirano, "3D printing of discontinuous and continuous fibre composites using stereolithography," *Additive Manufacturing,* vol. 24, pp. 521-527, Dec 2018.
[37] H. J. Levis, A. K. Kureshi, I. Massie, L. Morgan, A. J. Vernon, and J. T. Daniels, "Tissue Engineering the Cornea: The Evolution of RAFT," *J Funct Biomater,* vol. 6, pp. 50-65, Jan 22 2015.
[38] M. Miotto, R. M. Gouveia, and C. J. Connon, "Peptide Amphiphiles in Corneal Tissue Engineering," *J Funct Biomater,* vol. 6, pp. 687-707, Aug 06 2015.
[39] A. Shah, J. Burgnano, S. Sun, A. Vase, and E. Orwin, "The Development of a Tissue-Engineered Cornea: Biomaterials and Culture Methods," *International Pediatric Research Foundation, Inc.,* vol. 63, p. 535, 2008.
[40] M. E. Gomes, M. T. Rodrigues, R. M. A. Domingues, and R. L. Reis, "Tissue Engineering and Regenerative Medicine: New Trends and Directions-A Year in Review," *Tissue Eng Part B Rev,* vol. 23, pp. 211-224, Jun 2017.
[41] F. P. W. Melchels, M. A. N. Domingos, T. J. Klein, J. Malda, P. J. Bartolo, and D. W. Hutmacher, "Additive manufacturing of tissues and organs," *Progress in Polymer Science,* vol. 37, pp. 1079-1104, Aug 2012.
[42] B. Zhang, Y. Luo, L. Ma, L. Gao, Y. Li, Q. Xue, *et al.*, "3D bioprinting: an emerging technology full of opportunities and challenges," *Bio-Design and Manufacturing,* vol. 1, pp. 2-13, 2018.
[43] C. Mandrycky, Z. Wang, K. Kim, and D. H. Kim, "3D bioprinting for engineering complex tissues," *Biotechnol Adv,* vol. 34, pp. 422-34, Jul-Aug 2016.
[44] I. T. Ozbolat and M. Hospodiuk, "Current advances and future perspectives in extrusion-based bioprinting," *Biomaterials,* vol. 76, pp. 321-43, Jan 2016.
[45] A. D. Dias, D. M. Kingsley, and D. T. Corr, "Recent advances in bioprinting and applications for biosensing," *Biosensors (Basel),* vol. 4, pp. 111-36, Jun 2014.
[46] K. Barton, S. Mishra, K. A. Shorter, A. Alleyne, P. Ferreira, and J. Rogers, "A desktop electrohydrodynamic jet printing system," *Mechatronics,* vol. 20, pp. 611-616, Aug 2010.
[47] S. N. Jayasinghe, A. N. Qureshi, and P. A. Eagles, "Electrohydrodynamic jet processing: an advanced electric-field-driven jetting phenomenon for processing living cells," *Small,* vol. 2, pp. 216-9, Feb 2006.
[48] J. E. Kelly, "Collagen: ubiquitous, unsung protein," ed: Protein Data Bank, 2009.
[49] M. J. Fullana and G. E. Wnek, "Electrospun collagen and its applications in regenerative medicine," *Drug Deliv Transl Res,* vol. 2, pp. 313-22, Oct 2012.
[50] P. Fratzl, "Cellulose and collagen: from fibres to tissues," *Current Opinion in Colloid & Interface Science,* vol. 8, pp. 32-39, Mar 2003.
[51] M. D. Shoulders and R. T. Raines, "COLLAGEN STRUCTURE AND STABILITY," *Annu Rev Biochem,* vol. 78, pp. 1-2, 11, 34-35, 2009.
[52] P. Fratzl and R. Weinkamer, "Nature's hierarchical materials," *Progress in Materials Science,* vol. 52, pp. 1263-1334, Nov 2007.

[53] C. E. Ghezzi, J. Rnjak-Kovacina, and D. L. Kaplan, "Corneal tissue engineering: recent advances and future perspectives," *Tissue Eng Part B Rev*, vol. 21, pp. 278-87, Jun 2015.
[54] C. Boote, C. S. Kamma-Lorger, S. Hayes, J. Harris, M. Burghammer, J. Hiller, *et al.*, "Quantification of collagen organization in the peripheral human cornea at micron-scale resolution," *Biophys J*, vol. 101, pp. 33-42, Jul 06 2011.
[55] C. Boote, S. Dennis, R. H. Newton, H. Puri, and K. M. Meek, "Collagen fibrils appear more closely packed in the prepupillary cornea: optical and biomechanical implications," *Invest Ophthalmol Vis Sci*, vol. 44, pp. 2941-8, Jul 2003.
[56] D. F. Holmes, C. J. Gilpin, C. Baldock, U. Ziese, A. J. Koster, and K. E. Kadler, "Corneal collagen fibril structure in three dimensions: Structural insights into fibril assembly, mechanical properties, and tissue organization," *Proc Natl Acad Sci U S A*, vol. 98, pp. 7307-12, Jun 19 2001.
[57] B. Kong and S. L. Mi, "Electrospun Scaffolds for Corneal Tissue Engineering: A Review," *Materials*, vol. 9, p. 614, Aug 2016.
[58] H. S. Dua, L. A. Faraj, D. G. Said, T. Gray, and J. Lowe, "Human corneal anatomy redefined: a novel pre-Descemet's layer (Dua's layer)," *Ophthalmology*, vol. 120, pp. 1778-85, Sep 2013.
[59] J. W. Ruberti and J. D. Zieske, "Prelude to corneal tissue engineering – Gaining control of collagen organization," *Prog Retin Eye Res* vol. 27, pp. 549-577, 2008.
[60] J. W. Ruberti, A. S. Roy, and C. J. Roberts, "Corneal biomechanics and biomaterials," *Annu Rev Biomed Eng*, vol. 13, pp. 269-95, Aug 15 2011.
[61] K. M. Meek and A. J. Quantock, "The Use of X-ray Scattering Techniques to Determine Corneal Ultrastructure," *Progress in Retinal Eye Research*, vol. 20, pp. 97-98 , 106-108, 2001.
[62] K. M. Meek, "The Cornea and Sclera," in *Collagen: Structure and Mechanics*, ed New York: Springer Science+Business Media LLC, 2008, pp. 359-396.
[63] L. A. Hapach, J. A. VanderBurgh, J. P. Miller, and C. A. Reinhart-King, "Manipulation of in vitro collagen matrix architecture for scaffolds of improved physiological relevance," *Phys Biol*, vol. 12, p. 061002, Dec 21 2015.
[64] J. W. Ruberti and J. D. Zieske, "Prelude to corneal tissue engineering - gaining control of collagen organization," *Prog Retin Eye Res*, vol. 27, pp. 549-77, Sep 2008.
[65] F. N. Syed-Picard, Y. Du, A. J. Hertsenberg, R. Palchesko, M. L. Funderburgh, A. W. Feinberg, *et al.*, "Scaffold-free tissue engineering of functional corneal stromal tissue," *J Tissue Eng Regen Med*, Nov 15 2016.
[66] C. J. Lowe, I. M. Reucroft, M. C. Grota, and D. I. Shreiber, "Production of Highly Aligned Collagen Scaffolds by Freeze-drying of Self-assembled, Fibrillar Collagen Gels," *ACS Biomater Sci Eng*, vol. 2, pp. 643-651, Apr 11 2016.
[67] J. Zhang, A. M. Sisley, A. J. Anderson, A. J. Taberner, C. N. McGhee, and D. V. Patel, "Characterization of a Novel Collagen Scaffold for Corneal Tissue Engineering," *Tissue Eng Part C Methods*, Dec 28 2015.
[68] F. Tabassum and D. M. Mondal, "Scientific Aspects of Lever " *INTERNATIONAL JOURNAL OF SCIENTIFIC RESEARCH*, 2016.
[69] T. R. F. MD. (2012, 05/04). *What is eye pressure?* Available: https://www.aao.org/eye-health/ask-ophthalmologist-q/eye-pressure-glaucoma
[70] K. T. Kanawa, "Māori weaving and tukutuku – te raranga me te whatu," 22 Oct 2014.
[71] J. A. Matthews, G. E. Wnek, D. G. Simpson, and G. L. Bowlin, "Electrospinning of Collagen Nanofibres," *Biomacromolecules*, vol. 3, pp. 232-238, 2002.
[72] M. Mirjalili and S. Zohoori, "Review for application of electrospinning and electrospun nanofibres technology in textile industry," *Journal of Nanostructure in Chemistry*, vol. 6, pp. 207-213, Sep 2016.
[73] D. Li and Y. Xia, "Electrospinning of Nanofibres:Reinventing the Wheel?**," *ADVANCED MATERIALS*, vol. 16, pp. 1151-1167, 2004.
[74] T. D. Brown, P. D. Daltona, and D. W. Hutmacher, "Melt electrospinning today: An opportune time for an emerging polymer process," *Progress in Polymer Science*, vol. 56, pp. 116-166, May 2016.
[75] W. Cui, Y. Zhou, and J. Chang, "Electrospun nanofibrous materials for tissue engineering and drug delivery," *Sci Technol Adv Mater*, vol. 11, p. 014108, Feb 2010.
[76] K. Garg and G. L. Bowlin, "Electrospinning jets and nanofibrous structures," *Biomicrofluidics*, vol. 5, pp. 1-16, 2011.
[77] K. Garg and G. L. Bowlin, "Electrospinning jets and nanofibrous structures," *Biomicrofluidics*, vol. 5, p. 13403, Mar 30 2011.
[78] R. Stepanyan, A. V. Subbotin, L. Cuperus, P. Boonen, M. Dorschu, F. Oosterlinck, *et al.*, "Nanofibre diameter in electrospinning of polymer solutions: Model and experiment," *Polymer*, vol. 97, pp. 428-439, 2016.

[79] A. Haider, S. Haider, and I.-K. Kang, "A comprehensive review summarizing the effect of electrospinning parameters and potential applications of nanofibres in biomedical and biotechnology," *Arabian Journal of Chemistry,* vol. 11, pp. 1165-1188, 2018.

[80] A. Moheman, M. S. Alam, and A. Mohammad, "Recent trends in electrospinning of polymer nanofibres and their applications in ultra thin layer chromatography," *Adv Colloid Interface Sci,* vol. 229, pp. 1-24, Mar 2016.

[81] P. D. Dalton, C. Vaquette, B. L. Farrugia, T. R. Dargaville, T. D. Brown, and D. W. Hutmacher, "Electrospinning and additive manufacturing: converging technologies," *Biomaterials Science,* vol. 1, pp. 171-185, 2013.

[82] S. Thenmozhi, N. Dharmaraj, K. Kadirvelu, and H. Y. Kim, "Electrospun nanofibres: New generation materials for advanced applications," *Materials Science and Engineering B-Advanced Functional Solid-State Materials,* vol. 217, pp. 36-48, Mar 2017.

[83] P. McClellan and W. J. Landis, "Recent Applications of Coaxial and Emulsion Electrospinning Methods in the Field of Tissue Engineering," *Biores Open Access,* vol. 5, pp. 212-27, 2016.

[84] N. Duan, X. Geng, L. Ye, A. Zhang, Z. Feng, L. Guo, *et al.*, "A vascular tissue engineering scaffold with core-shell structured nano-fibres formed by coaxial electrospinning and its biocompatibility evaluation," *Biomed Mater,* vol. 11, p. 035007, May 20 2016.

[85] S. B. Orr, A. Chainani, K. J. Hippensteel, A. Kishan, C. Gilchrist, N. W. Garrigues, *et al.*, "Aligned multilayered electrospun scaffolds for rotator cuff tendon tissue engineering," *Acta Biomater,* vol. 24, pp. 117-26, Sep 2015.

[86] L. Persano, A. Camposeo, C. Tekmen, and D. Pisignano, "Industrial Upscaling of Electrospinning and Applications of Polymer Nanofibres: A Review," *Macromolecular Materials and Engineering,* vol. 298, pp. 504-520, May 2013.

[87] Dan Li, Gong Ouyang, Jesse T. McCann, and Younan Xia, "Collecting Electrospun Nanofibres with patterned electrodes," *NANO LETTERS,* vol. 5, pp. 913-916, 2005.

[88] S. Zhong, W. E. Teo, X. Zhu, R. W. Beuerman, S. Ramakrishna, and L. Y. L. Yung, "An aligned nanofibrous collagen scaffold by electrospinning and its effects on in vitro fibroblast culture," *Journal of Biomedical Materials Research Part A,* vol. 10.1002, pp. 456-462, 2006.

[89] F. Yuan, L. Wang, C. C. Lin, C. H. Chou, and L. Li, "A cornea substitute derived from fish scale: 6-month followup on rabbit model," *J Ophthalmol,* vol. 2014, p. 914542, 2014.

[90] B. Dong, O. Arnoult, M. E. Smith, and G. E. Wnek, "Electrospinning of Collagen Nanofibre Scaffolds from Benign Solvents," *Macromolecular Rapid Communication,* vol. 30, pp. 539-542, 2009.

[91] G. P. Huang, S. Shanmugasundaram, P. Masih, D. Pandya, S. Amara, G. Collins , *et al.*, "An investigation of common crosslinking agents on the stabilityof electrospun collagen scaffolds," *Journal of Biomedical Materials Research Part A,* vol. 103A, pp. 762-771, 2014.

[92] C. Dhand, S. T. Ong, N. Dwivedi, S. M. Diaz, J. R. Venugopal, B. Navaneethan, *et al.*, "Bio-inspired in situ crosslinking and mineralization of electrospun collagen scaffolds for bone tissue engineering," *Biomaterials,* vol. 104, pp. 323-325, 2016.

[93] D. A. Castilla-Casadiego, H. V. Ramos-Avilez, S. Herrera-Posada, B. Calcagno, L. Loyo, J. Shipmon, *et al.*, "Engineering of a Stable Collagen Nanofibrous Scaffold with Tunable Fibre Diameter, Alignment, and Mechanical Properties," *Macromolecular Materials and Engineering,* vol. 301, pp. 1064-1075, Sep 2016.

[94] B. Dong, O. Arnoult, M. E. Smith, and G. E. Wnek, "Electrospinning of collagen nanofibre scaffolds from benign solvents," *Macromol Rapid Commun,* vol. 30, pp. 539-42, Apr 01 2009.

[95] T. J. Sill and H. A. von Recum, "Electrospun materials for affinity-based engineering and drug delivery," *Journal of Physics: Conference Series,* vol. 646, pp. 1-3, 2015.

[96] B. S. Jha, C. E. Ayres, J. R. Bowman, T. A. Telemeco, S. A. Sell, G. L. Bowlin, *et al.*, "Electrospun Collagen: A Tissue Engineering Scaffold with Unique Functional Properties in a Wide Variety of Applications," *Journal of Nanomaterials,* vol. 2011, pp. 1-15, 2011.

[97] L. H. Meng, O. Arnoult, M. Smith, and G. E. Wnek, "Electrospinning of in situ crosslinked collagen nanofibres," *Journal of Materials Chemistry,* vol. 22, pp. 19412-19417, 2012.

[98] C. Dhand, S. T. Ong, N. Dwivedi, S. M. Diaz, J. R. Venugopal, B. Navaneethan, *et al.*, "Bio-inspired in situ crosslinking and mineralization of electrospun collagen scaffolds for bone tissue engineering," *Biomaterials,* vol. 104, pp. 323-38, Oct 2016.

[99] D. Le Corre-Bordes, K. Hofman, and B. Hall, "Guide to electrospinning denatured whole chain collagen from hoki fish using benign solvents," *Int J Biol Macromol,* vol. 112, pp. 1289-1299, Jun 2018.

[100] B. Kong, W. Sun, G. Chen, S. Tang, M. Li, Z. Shao, *et al.*, "Tissue-engineered cornea constructed with compressed collagen and laser-perforated electrospun mat," *Sci Rep,* vol. 7, p. 970, Apr 20 2017.

[101] S. L. Mi, B. Kong, Z. J. Wu, W. Sun, Y. Y. Xu, and X. Su, "A novel electrospinning setup for the fabrication of thickness-controllable 3D scaffolds with an ordered nanofibrous structure," *Materials Letters*, vol. 160, pp. 343-346, Dec 1 2015.
[102] J. I. Kim, J. Y. Kim, and C. H. Park, "Fabrication of transparent hemispherical 3D nanofibrous scaffolds with radially aligned patterns via a novel electrospinning method," *Sci Rep*, vol. 8, p. 3424, Feb 21 2018.
[103] Q. Yao, W. Zhang, Y. Hu, J. Chen, C. Shao, X. Fan, *et al.*, "Electrospun collagen/poly(L-lactic acid-co-epsilon-caprolactone) scaffolds for conjunctival tissue engineering," *Exp Ther Med*, vol. 14, pp. 4141-4147, Nov 2017.
[104] L. Duque Sanchez, N. Brack, A. Postma, P. J. Pigram, and L. Meagher, "Surface modification of electrospun fibres for biomedical applications: A focus on radical polymerization methods," *Biomaterials*, vol. 106, pp. 24-45, Nov 2016.
[105] M. J. Fullana and G. E. Wnek, "Electrospun collagen and its applications in regenerative medicine," *Drug Deliv. and Transl. Res.*, vol. 2, pp. 313-322, 2012.
[106] B. S. Jha, C. E. Ayres, J. R. Bowman, T. A. Telemeco, S. A. Sell, L. G. Bowlin, *et al.*, "Electrospun Collagen: A Tissue Engineering Scaffold with Unique Functional Properties in a Wide Variety of Applications," *Journal of Nanomaterials* vol. 2011, pp. 1-14, 2011.
[107] G. Wollensak, E. Spoerl, and T. Seiler, "Riboflavin/ultraviolet-a-induced collagen crosslinking for the treatment of keratoconus," *Am J Ophthalmol*, vol. 135, pp. 620-7, May 2003.
[108] S. Hayes, C. S. Kamma-Lorger, C. Boote, R. D. Young, A. J. Quantock, A. Rost, *et al.*, "The effect of riboflavin/UVA collagen cross-linking therapy on the structure and hydrodynamic behaviour of the ungulate and rabbit corneal stroma," *PLoS One*, vol. 8, p. e52860, 2013.
[109] S. Kling, A. Hammer, A. Conti, and F. Hafezi, "Corneal Cross-Linking with Riboflavin and UV-A in the Mouse Cornea in Vivo: Morphological, Biochemical, and Physiological Analysis," *Transl Vis Sci Technol*, vol. 6, p. 7, Jan 2017.
[110] A. S. McCall, S. Kraft, H. F. Edelhauser, G. W. Kidder, R. R. Lundquist, H. E. Bradshaw, *et al.*, "Mechanisms of corneal tissue cross-linking in response to treatment with topical riboflavin and long-wavelength ultraviolet radiation (UVA)," *Invest Ophthalmol Vis Sci*, vol. 51, pp. 129-38, Jan 2010.
[111] T. Xu, K. W. Binder, M. Z. Albanna, D. Dice, W. Zhao, J. J. Yoo, *et al.*, "Hybrid printing of mechanically and biologically improved constructs for cartilage tissue engineering applications," *Biofabrication*, vol. 5, p. 015001, Mar 2013.
[112] W. Liu, D. Wang, J. Huang, Y. Wei, J. Xiong, W. Zhu, *et al.*, "Low-temperature deposition manufacturing: A novel and promising rapid prototyping technology for the fabrication of tissue-engineered scaffold," *Mater Sci Eng C Mater Biol Appl*, vol. 70, pp. 976-982, Jan 01 2017.
[113] H. Gudapati, M. Dey, and I. Ozbolat, "A comprehensive review on droplet-based bioprinting: Past, present and future," *Biomaterials*, vol. 102, pp. 20-42, Sep 2016.
[114] M. Hospodiuk, M. Dey, D. Sosnoski, and I. T. Ozbolat, "The bioink: A comprehensive review on bioprintable materials," *Biotechnol Adv*, Jan 03 2017.
[115] M. Parhizkar, P. Sofokleous, E. Stride, and M. Edirisinghe, "Novel preparation of controlled porosity particle/fibre loaded scaffolds using a hybrid micro-fluidic and electrohydrodynamic technique," *Biofabrication*, vol. 6, pp. 1-12, 2014.
[116] W. C. Wilson, Jr. and T. Boland, "Cell and organ printing 1: protein and cell printers," *Anat Rec A Discov Mol Cell Evol Biol*, vol. 272, pp. 491-6, Jun 2003.
[117] P. L. Chandran, D. C. Paik, and J. W. Holmes, "Structural mechanism for alteration of collagen gel mechanics by glutaraldehyde crosslinking," *Connect Tissue Res*, vol. 53, pp. 285-97, 2012.
[118] Z. Tian, C. Li, L. Duan, and G. Li, "Physicochemical properties of collagen solutions cross-linked by glutaraldehyde," *Connect Tissue Res*, vol. 55, pp. 239-47, Jun 2014.
[119] N. N. Kumbhar and A. V. Mulay, "Post Processing Methods used to Improve Surface Finish of Products which are Manufactured by Additive Manufacturing Technologies: A Review," *Journal of The Institution of Engineers (India): Series C*, 2016.
[120] T. Kudo, K. Sekiguchi, K. Sankoda, N. Namiki, and S. Nii, "Effect of ultrasonic frequency on size distributions of nanosized mist generated by ultrasonic atomization," *Ultrason Sonochem*, vol. 37, pp. 16-22, Jul 2017.
[121] H. Kim, J. Lee, and Y. Y. Won, "A simple derivation of the critical condition for the ultrasonic atomization of polymer solutions," *Ultrasonics*, vol. 61, pp. 20-4, Aug 2015.
[122] D. Briceño-Gutierrez, V. Salinas-Barrera, Y. Vargas-Hernández, L. Gaete-Garretón, and C. Zanelli-Iglesias, "On the Ultrasonic Atomization of Liquids," *Physics Procedia*, vol. 63, pp. 37-41, 2015.
[123] V. P. Secasanu, C. K. Giardina, and Y. Wang, "A novel electrospinning target to improve the yield of uniaxially aligned fibres," *Biotechnol Prog*, vol. 25, pp. 1169-75, Jul-Aug 2009.

[124] Elmarco. (2004-2019, 10/12/2018). *Nanospider™ equipment*. Available: http://www.elmarco.com/gallery/nanospider-equipment/

[125] J. R. Rocca-Smith, T. Karbowiak, E. Marcuzzo, A. Sensidoni, F. Piasente, D. Champion, *et al.*, "Impact of corona treatment on PLA film properties," *Polymer Degradation and Stability*, vol. 132, pp. 109-116, Oct 2016.

[126] D. Hetemi and J. Pinson, "Surface functionalisation of polymers," *Chem Soc Rev*, vol. 46, pp. 5701-5713, Oct 2 2017.

[127] Z. M. Huang, Y. Z. Zhang, M. Kotaki, and S. Ramakrishna, "A review on polymer nanofibres by electrospinning and their applications in nanocomposites," *Composites Science and Technology*, vol. 63, pp. 2223-2253, Nov 2003.

[128] F.-G. Chizoba Ekezie, D.-W. Sun, and J.-H. Cheng, "A review on recent advances in cold plasma technology for the food industry: Current applications and future trends," *Trends in Food Science & Technology*, vol. 69, pp. 46-58, 2017.

[129] F.-H. Kuok, K.-Y. Kan, I.-S. Yu, C.-W. Chen, C.-C. Hsu, I. C. Cheng, *et al.*, "Application of atmospheric-pressure plasma jet processed carbon nanotubes to liquid and quasi-solid-state gel electrolyte supercapacitors," *Applied Surface Science*, vol. 425, pp. 321-328, 2017.

[130] TONI_K. *Big Easy Driver Hookup Guide*. Available: https://learn.sparkfun.com/tutorials/big-easy-driver-hookup-guide

APPENDIX A: PAPERS PUBLISHED

DRC 16

MASSEY UNIVERSITY
GRADUATE RESEARCH SCHOOL

STATEMENT OF CONTRIBUTION
DOCTORATE WITH PUBLICATIONS/MANUSCRIPTS

We, the candidate and the candidate's Primary Supervisor, certify that all co-authors have consented to their work being included in the thesis and they have accepted the candidate's contribution as indicated below in the *Statement of Originality*.

Name of candidate:	Juan Schutte
Name/title of Primary Supervisor:	Prof. Johan Potgieter
Name of Research Output and full reference:	
Evaluation of the effects of controlled ultrasonic acetone vaporisation on Fused Deposition Modelling 3D Printed Acrylonitrile Butadiene Styrene	
In which Chapter is the Manuscript /Published work:	Chapter 6
Please indicate:	
• The percentage of the manuscript/Published Work that was contributed by the candidate:	70
and	
• Describe the contribution that the candidate has made to the Manuscript/Published Work:	
The candidate has written the majority of the manuscript. The candidate has contributed to the experimentation and provided the analysis required for this publication.	
For manuscripts intended for publication please indicate target journal:	
Candidate's Signature:	Digitally signed by Juan Schutte Date: 2019.06.04 15:23:23 +12'00'
Date:	04/06/2019
Primary Supervisor's Signature:	Johan Potgieter Digitally signed by Johan Potgieter Date: 2019.06.06 11:07:16 +12'00'
Date:	06/06/2019

(This form should appear at the end of each thesis chapter/section/appendix submitted as a manuscript/ publication or collected as an appendix at the end of the thesis)

GRS Version 4– January 2019

Evaluation of the effects of controlled ultrasonic acetone vaporisation on Fused Deposition Modelling 3D Printed Acrylonitrile Butadiene Styrene

Juan Schutte
School of Engineering and advanced technology
Massey University
Auckland, New Zealand
J.Schutte@massey.ac.nz

Pamitha Wijisundira
School of Engineering and advanced technology
Massey University
Auckland, New Zealand

Muhammad Harris
School of Engineering and advanced technology
Massey University
Auckland, New Zealand
M.Harris@massey.ac.nz

Johan Potgieter
School of Engineering and advanced technology
Massey University
Auckland, New Zealand
J.Potgieter@massey.ac.nz

***Abstract*— The application of vapour exposure systems upon 3D printed objects as a means for surface modification is a thoroughly established technique. This study investigated the utilization of a generated controlled vapour chamber device to further derive the relationship between surface modification exposure to that of part structural properties, namely interlayer bonding. This controlled utilization of vapour is intended to identify potential for future sequential 3D printing methodologies. The study mirrored previous work as such an UPBox Fused deposition modelling printer was required to produce thirty acrylonitrile butadiene styrene ASTM D638 Type IV dog-bone samples. Each of these was subjected to controlled vapour exposure relative to defined sample sets, namely groups of 5 representing exposure intervals at 0%, 20%, 25%, 50%, and 100% printing completion. Analysis for these was conducted via Instron 5967 tensile testing and a Hitachi TM3030Plus Scanning electron microscopy. These samples depicted an directly proportional increase in ultimate tensile strength and layer fusion with increased vapour exposure. These values contradicted the previous uncontrolled study.**

Keywords—Additive Manufacturing, 3D Printing, Surface modification, Coating

I. INTRODUCTION

Fused Deposition Modelling (FDM) 3D Printing (3DP) has achieved widespread popularity due to its simplicity and affordability. Typically these systems are comprised of a 3-axis gantry system upon one of which is fastened an extruder system, namely a heated nozzle through which polymer filament is directed/fed[1-3]. One of the major drawbacks of this technology is its relative tendency towards poor surface finish quality (namely the striated appearance caused by the layers)[4, 5] . A popular and common method amongst both industry and hobbyist markets is the utilisation of acetone exposure on Acrylonitrile Butadiene Styrene (ABS) FDM 3D printed parts[6, 7]. The apparent nature of this technique is that it chemically initialises a reactivity within ABS which promotes the merging of the distinctive extruded pathways and layering common in this form of additive manufacturing (AM)[3, 8, 9]. As such this seemingly has an effect upon the bonding/bonded features of the material/part. One of the fundamental weaknesses of 3D printing (3DP) or AM parts is delamination, namely the separation/splitting of generated parts/objects along a layer commonly due to forces applied. It is generally accepted that these failures are derived from weak interlayer bonding (ILB) [7, 10], namely the strength of the merged/linked material with prior and subsequent layering. Typically the application of acetone either as uncontrolled rubbing or simplistic vapour bath systems which do not actively monitor how much of the exposure occurs. Given these techniques have the apparent ability to merge ABS polymer layers, there is interest to investigate the possibility and potential benefits for the controlled application of these agents at defined stages of the printing process.

One technique to accomplish this would be to submerge printed parts into acetone solution (immersion treatment)[6], however, this will not guarantee a uniform exposure due to run-off and acetones low rate of evaporation. A more precise implementation could take the form of an inkjet sequential 3D printing process however this will result in a high degree of complexity[11]. Thus this research was inclined to investigate the potential utilisation and control of vapour bath systems. Namely, this research aims to identify a plausible methodology for the controlled application of initialiser (e.g. Acetone) or adhesive elements to promote ILB within a 3DP process.

Vapour is unique in that it can comprise of submicron and nanoparticulate which can be manipulated as a gas. Controlled vapour production has occurred through many physical and chemical techniques [12]. Often these require relatively high temperatures, pressures and complexities uncommon in typical FDM 3DP systems [9]. As such this study was driven to utilise simplistic vapour generation technology capable of operation at lower temperatures and pressures.

A technology particularly suited for this type of work is ultrasonic atomisation/vaporisation. This functions through the application of high frequency signals to a piezoelectric transducer (generally a stretched film which contracts when exposed to an electric signal) yielding high-frequency mechanical actuation[13-15]. The coating of the surface of these devices in liquid yields a high degree of surface agitation. This stems from the generation of waves which at a

critical frequency collide, resulting in the dispulsion of liquid particulate in the form of vapour. The rate of vapour generation and size of vapour particulates have been associated with modification of the delivered signal frequency [13]. This manner of control will allow for device output variability.

This study will leverage off previously identified evaporant orientated Acetone-ABS studies[6, 7, 16]. Through the utilisation of a derived device for controlled vapour addition, the following will be investigated:

- The relationship between Acetone vapour exposure to ABS ILB.
- The effect on internal structures through the controlled implementation of vapour at varied stages of a printing process

II. Methodology

Generated samples within the study took the form of the ASTM D638 Type IV testing standard and these were exposed to consumer grade 100% Acetone (Amazing Haste).

A. Sample Production

Desired samples were produced through the utilisation of a commercial grade Tier Time FDM 3D Printer (UpBox). Of importance for this study was the capability of these printers to pause and resume printing operations at desired layers. 25 Samples were produced from this device with an implemented printing resolution of 0.25mm and infill of 99% additionally these were printed without support material/raft. In total 5 sample sets were generated corresponding to 0%NA, 25%, 50%, 100% and 50%NA (where NA refers to not applied).

B. Developed Controlled Vapour Addition Chamber

A device capable of monitoring the vapour content of a chamber was designed in Solidworks where structural components were laser cut out of 4.5mm black acrylic and the processing chamber constructed from waterjet 3mm clear glass [Fig. 1]. An Arduino Mega controlled transducers and air pumps relative to sensors and displayed the results upon an LCD screen. Utilising this technology the glass chamber was kept at a controlled vapour level being 20ml for the duration of the process. This control took the form of a feedback loop system in which the controlled removal or addition of vapour material was dependant on the set values from a user and values read by sensors within the chamber.

C. Manual Sequential Printing Process

To determine the effects of Acetone vapour as a sequential process within 3DP the FDM process was halted at 25% and 50% intervals. This cessation was followed by a transferal of the printed parts to the developed controlled Vapour Addition Chamber. Here samples were subjected to 20ml of acetone vapour for 20 minutes. A completely printed (100%) part was also subjected to this treatment. Additionally, a sample set was generated for a pause and resume at 50% without acetone exposure to identify the effects of printing cessation of structural integrity. All of these samples were evaluated with respect to a 0% exposure with zero pauses sample set.

Fig. 1: Image depicting the constructed controlled vapour delivery device

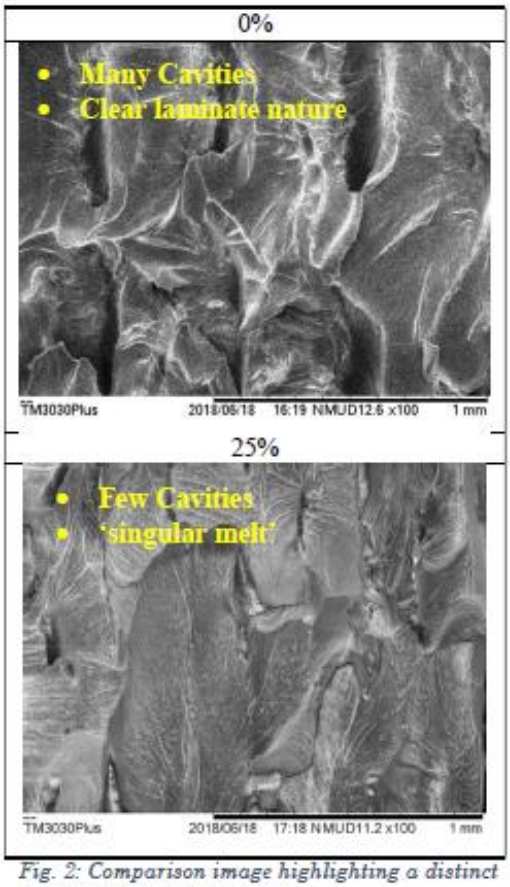

Fig. 2: Comparison image highlighting a distinct change in internal structuring

D. *Tensile testing*

The Ultimate tensile strength (UTS) was derived for each sample set through the utilisation of an Instron 5967 equipped with a 30kN load cell. Samples were positioned and fastened centrally with a distance of 65mm between the clamps.

E. *Microscopy*

Topographical analysis occurred through the utilisation of a Hitatchi TM3030Plus Scanning electron microscope (SEM). This analysis was conducted post tensile testing to avoid unwanted effects from the electron beam irradiation. Of interest here were regions near the points of fracture and regions at which additional layer merging due to vapour processing could be established.

III. Results & Discussions

The UTS of the sample sets was proportional to the number of instances of exposure. This relationship is described graphically in Fig. 3 with the data for each sample present in Table 1. It is plausible to suggest then that the controlled addition of the acetone vapour within a 3DP process is beneficial to the ILB of a part. Exposure at every 25% of a printing process yielded higher UTS than at every 50%. These points of exposure within the process relate to intermediary layers as such the application of acetone vapour here can be described as aiding in the formation of bonding between layers. From this, a linear relationship between the number of intervals at which acetone is applied and the proportional increase in UTS can be inferred. Of interest is the decrease in UTS for the 100% sample. This sample was also dramatically weaker than the 0% sample. This is likely due to the formation of a solid external structure without much internal fusing, however, it is concerning that the UTS value for this was significantly lower than the benchmark (12.2MPa).

Topographical analysis through SEM imaging revealed an increasing degree of resultant extruded pathway merging for an increase in vapour exposure. Fig. 2 demonstrates the extremes from 0% exposure which contains many regions of large cavitation and distinct layering compared to 25% the samples receiving the most Acetone treatment. These samples demonstrated a clear fusing of the internal structures of the object generating more of a 'singular melt' than comprising of separate layers. It is important to note that this sample still had some slight cavitation. Additionally, a cross-sectional fracture SEM image was generated for each sample set in an attempt to generate an understanding of the internal structural modifications from this process. Distinctive forms present in these images and a comparison of these is depicted in Table 2. Note here the 100% sample has distinctive layering, thus reiterating previous statements that the nature of solely external vapour exposure generates an outer core.

A. *Relevance to previous work*

In 2017, a paper titled "The effects of Acetone vapour inter-layer processing on Fused Deposition Modelling 3D Printed Acrylonitrile Butadiene Styrene" was presented at M2VIP. The results of this study compared to this work demonstrated a significant increase in UTS for both the 25% and 50% both demonstrating a significantly desirable outcome/justification for controlled vapour based sequential systems (Table 1). Namely, these generated an increase of 11.4MPa and 4MPa respectively. It is worth noting that the 2017 25% sample demonstrated a decrease in UTS whereas a more logical trend line is generated in the 2018 results. When comparing these studies one dramatic difference must be noted, namely the placements of processed samples within the respective vapour chambers. In the 2017 experiments, the density of evaporated Acetone was assumed to be less than the density of air this assumption together with intended actuation from a fan meant that exposure occurred against the direction of gravity. Alternatively, recent work has situated the parts below the point of vapour introduction thus deposition of particulates in this study was aided by gravity. As such it will be of interest to repeat the previous study.

IV. Conclusions and Recommendations

Ultrasonic Atomisation yielded a sufficiently useful technique in controlling the Acetone vapour within this study. This technique has the potential to be implemented as a parallel or sequential within 3D Printing. A beneficial relationship between Acetone exposure for FDM ABS 3DP at specified intervals was established. The study also indicated the potential to introduce sequential elements within this technology without the risk of decreasing part quality. The UTS and supporting SEM data supports the requirement to automate and have a controlled delivery of acetone vapour to

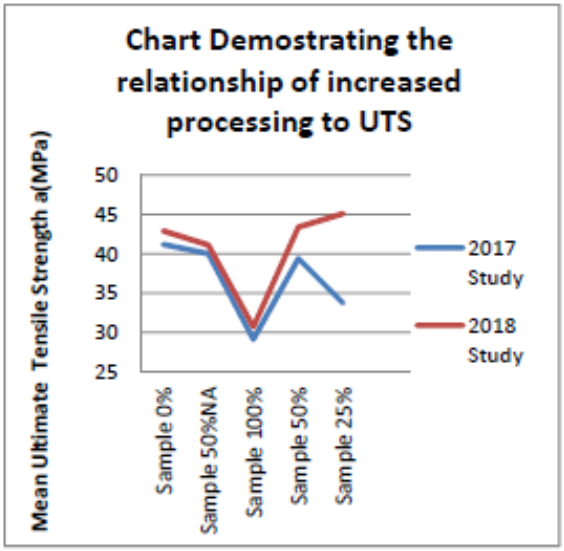

Fig. 3: Image graphically representing the relationship controlled acetone vapour to ultimate tensile strength

Table 1: Table containing data from both the 2017 evaporant and current controlled studies

Sample	Average UTS(MPa) (2017 study)	Average UTS(MPa) (current study
0%	41.2	42.9
25%	33.7	45.1
50%	39.4	43.4
100%	29.1	30.7
50% NA	40	41.1

ABS during the 3DP process as this will allow for beneficial bonding of internal structures. It should however be noted that additional investigative testing will be conducted to further validate this technology and the resultant relationships.

Future Recommendations include:

- Investigations into less volatile adhesive/bonding agent alternatives
- Further investigations regarding the effects of halting and processing parts within the 3DP process.
- Further investigations in 100% Sample cases.
- The 3DP of samples of varied orientations to identify optimal printing for vapour exposure
- An analysis of the chemical and material science relating to the interactions of utilized polymers and agents.
- Investigation into the potential for implementation of FDM with a chamber of controlled vapour saturation.
- Derivation of a model relating to ABS interlayer exposure to acetone vapour within a 3DP process.

This work forms part of fundamental investigations for future research regarding the addition of processing elements within 3DP technology.

V. ACKNOWLEDGEMENTS

The authors would like to thank the New Zealand National Science Challenge for funding this research as well as Assoc.

VI. REFERENCES

[1] A. Ferreira, K. M. Arif, S. Dirven, and J. Potgieter, "Retrofitment, open-sourcing, and characterisation of a legacy fused deposition modelling system," *The International Journal of Advanced Manufacturing Technology*, 2016.

[2] W. Gao, Y. B. Zhang, D. Ramanujan, K. Ramani, Y. Chen, C. B. Williams, *et al.*, "The status, challenges, and future of additive manufacturing in engineering," *Computer-Aided Design*, vol. 69, pp. 65-89, Dec 2015.

[3] T. D. Ngo, A. Kashani, G. Imbalzano, K. T. Q. Nguyen, and D. Hui, "Additive manufacturing (3D printing): A review of materials, methods, applications and challenges," *Composites Part B: Engineering*, vol. 143, pp. 172-196, 2018.

[4] J. R. C. Dizon, A. H. Espera, Q. Y. Chen, and R. C. Advincula, "O Mechanical characterization of 3D-printed polymers," *Additive Manufacturing*, vol. 20, pp. 44-67, Mar 2018.

[5] E. J. McCullough and V. K. Yadavalli, "Surface modification of fused deposition modeling ABS to enable rapid prototyping of biomedical

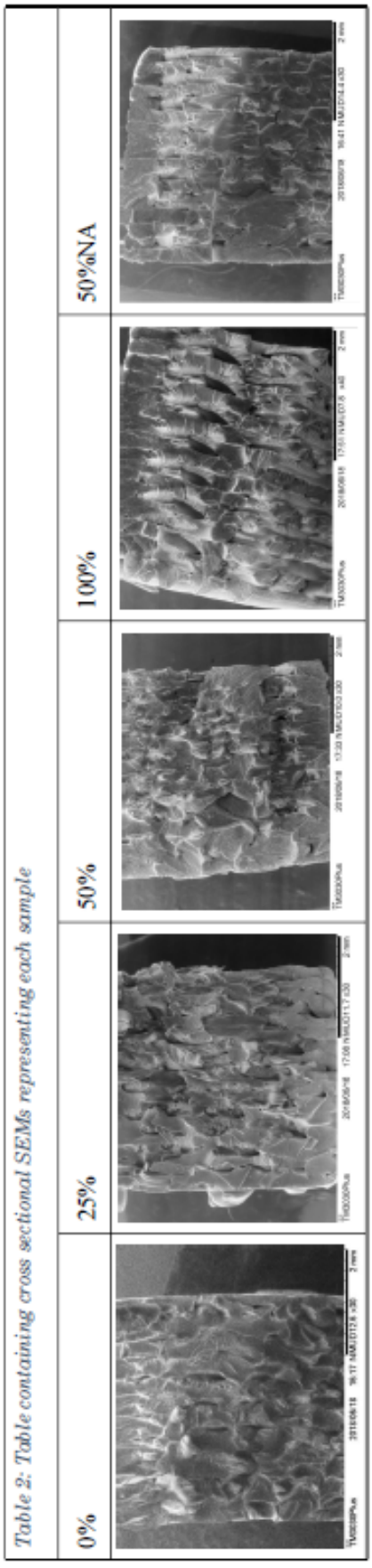

Table 2: Table containing cross sectional SEMs representing each sample

microdevices," *Journal of Materials Processing Technology,* vol. 213, pp. 947-954, Jun 2013.

[6] N. Jayanth, P. Senthil, and C. Prakash, "Effect of chemical treatment on tensile strength and surface roughness of 3D-printed ABS using the FDM process," *Virtual and Physical Prototyping,* vol. 13, pp. 155-163, 2018.

[7] A. Garg, A. Bhattacharya, and A. Batish, "Chemical vapor treatment of ABS parts built by FDM: Analysis of surface finish and mechanical strength," *The International Journal of Advanced Manufacturing Technology,* vol. 89, pp. 2175-2191, 2016.

[8] F. Calignano, D. Manfredi, E. P. Ambrosio, S. Biamino, M. Lombardi, E. Atzeni, *et al.*, "Overview on Additive Manufacturing Technologies," *Proceedings of the IEEE,* pp. 1-20, 2017.

[9] J. Gardan, "Additive manufacturing technologies: state of the art and trends," *International Journal of Production Research,* vol. 54, pp. 3118-3132, 2015.

[10] P. K. Gurrala and S. P. Regalla, "Part strength evolution with bonding between filaments in fused deposition modelling," *Virtual and Physical Prototyping,* vol. 9, pp. 141-149, 2014.

[11] H. Gudapati, M. Dey, and I. Ozbolat, "A comprehensive review on droplet-based bioprinting: Past, present and future," *Biomaterials,* vol. 102, pp. 20-42, Sep 2016.

[12] T. S. S. Jong-Hee Park, *Chemical Vapor Deposition*: ASM International 2001.

[13] T. Kudo, K. Sekiguchi, K. Sankoda, N. Namiki, and S. Nii, "Effect of ultrasonic frequency on size distributions of nanosized mist generated by ultrasonic atomization," *Ultrason Sonochem,* vol. 37, pp. 16-22, Jul 2017.

[14] H. Kim, J. Lee, and Y. Y. Won, "A simple derivation of the critical condition for the ultrasonic atomization of polymer solutions," *Ultrasonics,* vol. 61, pp. 20-4, Aug 2015.

[15] D. Briceño-Gutierrez, V. Salinas-Barrera, Y. Vargas-Hernández, L. Gaete-Garretón, and C. Zanelli-Iglesias, "On the Ultrasonic Atomization of Liquids," *Physics Procedia,* vol. 63, pp. 37-41, 2015.

[16] C.-C. Kuo, C.-M. Chen, and S.-X. Chang, "Polishing mechanism for ABS parts fabricated by additive manufacturing," *The International Journal of Advanced Manufacturing Technology,* vol. 91, pp. 1473-1479, 2016.

DRC 16

MASSEY UNIVERSITY
GRADUATE RESEARCH SCHOOL

STATEMENT OF CONTRIBUTION
DOCTORATE WITH PUBLICATIONS/MANUSCRIPTS

We, the candidate and the candidate's Primary Supervisor, certify that all co-authors have consented to their work being included in the thesis and they have accepted the candidate's contribution as indicated below in the *Statement of Originality*.

Name of candidate:	Juan Schutte
Name/title of Primary Supervisor:	Prof. Johan Potgieter
Name of Research Output and full reference:	
Evaluation of the effects of corona discharge plasma exposure proximity to Fused Deposition Modelling 3D Printed Acrylonitrile Butadiene Styrene	
In which Chapter is the Manuscript /Published work:	Chapter 6
Please indicate:	
• The percentage of the manuscript/Published Work that was contributed by the candidate:	100
and	
• Describe the contribution that the candidate has made to the Manuscript/Published Work:	
The candidate has written the majority of the manuscript. The candidate has conducted the experimentation and provided the analysis required for this publication.	
For manuscripts intended for publication please indicate target journal:	
Candidate's Signature:	Digitally signed by Juan Schutte Date: 2019.06.04 15:23:23 +12'00'
Date:	04/06/2019
Primary Supervisor's Signature:	Johan Potgieter Digitally signed by Johan Potgieter Date: 2019.06.06 11:06:26 +12'00'
Date:	06/06/2019

(This form should appear at the end of each thesis chapter/section/appendix submitted as a manuscript/ publication or collected as an appendix at the end of the thesis)

Evaluation of the effects of corona discharge plasma exposure proximity to Fused Deposition Modelling 3D Printed Acrylonitrile Butadiene Styrene

Juan Schutte
School of Engineering and advanced technology
Massey University
Auckland, New Zealand
J.Schutte@massey.ac.nz

Jerome Leveneur
Ion BeamMaterial Science
GNS Science
Wellington, New Zealand
J.Leveneur@gns.cri.nz

Xiaowen Yuan
School of Engineering and advanced technology
Massey University
Auckland, New Zealand
XW.Yuan@massey.ac.nz

Johan Potgieter
School of Engineering and advanced technology
Massey University
Auckland, New Zealand
J.Potgieter@massey.ac.nz

***Abstract*— Plasma derived cross-linking of polymer surfaces is an established technique within industry. This study investigated how the utilization and proximity of an atmospheric plasma generating device affects the ultimate tensile strength and surface quality of 3D printed Acrylonitrile Butadiene Styrene. The study made use of a linear stage device to accurately modify the distance between parts and devices. We aimed to evaluate the potential of atmospheric plasma treatment to improve the mechanical performance of 3D printing systems. 3D printed samples were generated by a Tier Time UPBox Fused deposition modelling printer. Thirty ASTM D638 Type IV dog-bone samples were generated. They were grouped into 6 categories corresponding to varied heights from the generated plasma, namely 36 mm (Sample 1), 30 mm (Sample 2), 24 mm (Sample 3), 18 mm (Sample 4), 12 mm (Sample 5) as well as an unprocessed Benchmark Sample. Optimal ultimate tensile strength occurred at 24 mm being 19.01 MPa whilst the surface quality of the samples experienced little change.**

Keywords—Additive Manufacturing, 3D Printing, Surface modification, Coating, Plasma irradiation

I. INTRODUCTION

Recently 3D printing (3DP) as a means of rapid prototyping has experienced a dramatic increase in popularity. The fundamental process within this technology is the sequential processing and bonding of additional material to priorly processed material. Within 3DP this additive sequence is repeated to form a three dimensional part. This form of additive manufacturing (AM) has occurred through the application of various techniques which are largely dependent on the type of material to be processed, namely solids, liquids and powders [1, 2]. The Fused Deposition Modelling (FDM) technique of 3DP has achieved widespread popularity due to it's accessability (relative ease of use) [3, 4]. This form of AM transforms solid wire polymer filament material into deposited layers of polymer melt via thermal and mechanical actuation. Whilst the positional nature of of this deposition is robustly controlled through mechanically actuated gantry systems, the same control cannot be associated with the deposited melt. The uniformity of the extrusion can be controlled through the optimisation and modification of the extrusion mechanisms, however once deposited there is a lack of direct control manipulation of the polymer. As the melt retains thermal energy during the interval before solidification, it is susceptible to the forces of gravity as well as non-uniform cooling. As such the surface quality as well as the inter-layer consistencies are likely to contain anomolies such as regions of cavitation. These irregularities may lead to issues regarding inter-layer bonding and polymer cross-linking which in turn affect the structural integrity of the part.

It is worth noting that the application of surface modifications techniques to FDM 3DP parts made from popular materials such as ABS and PLA is being used to modify a part's properties. A popular method for this includes the use of volatile chemicals such as acetone which initiate elements within the polymer to further fuse/melt the layers together. Typically such application of chemical solutions or vapours occurs as a post-process dependant on additional vapour bath systems [5, 6]. Thus an alternative technique having lower material and equipment requirements whilst yielding benefits to structural strength and surface quality were investigated.

Given that most generic forms of 3D printers utilise polymers in their additive manufacturing processes, alternative methods of polymer surface modification not reliant on such complexities were investigated. One of the most popular technologies for the surface treatment of polymers is plasma irradiation. Plasma treatment of products has been implemented as a form of surface modification within many polymer based industries [7-9]. Technologies such as Plasmatec-X by Tantec provide monouvreable benchtop device purpose built for this form of processing [Figure 1]. Plasma generation systems come in a variety of forms but can be classified as either operating under low pressure (partial vacuum) or at atmospheric pressure. It should be noted that some of these techniques are prone to high temperature or complexities not well suited for 3DP[10] . One particular form of plasma generation which shows promise for this form of process is corona plasma generation[7, 8, 11, 12]. This atmospheric-based technique does not require specific gas elements and does necessarily produce excessively high

temperatures. The plasma is generated through the application of low voltages at high frequencies to sharp end effectors/electrodes [8]. This results in the ionisation of surrounding gas, generating a small volume of plasma. Finally the technollogy has been described as relatively inexpensive[11]. This technique was identified as well suited for implemetation within polymer 3DP technology. Application of plasma treatment for 3DP is in its infancy, while commercial outlets that propose plasma enhanced 3DP systems [13], only a few studies can be found that investigate the improvements from plasma in the 3DP process [14].

A robust and portable version of a corona plasma generatind device was created by the Institute for Geological and Nuclear Science (GNS Science) in New Zealand for the purpose of further investigating the potential benefits of plasma technology in 3DP. Currently the desirable/optimal working parameters of this device have yet to be identified/established for this type of work, as such this study will attempt to derive this content experimentally and will primarily investigate the effect of proximity of generated plasma to acrylonitrile butadiene styrene 3D printed parts. Through this study there is a potential for the identification of a new form of either sequential or post processing of 3DP parts not requiring significantly more material or equipment.

II. Methodology

The ASTM D638 Type IV sample-testing standard (DatapointLabs) was utilised for this study. The dimensions for this were translated into a Solidworks CAD 3D model and utilised in the generation of 30 ABS samples.

A. 3D Printed Sample Generation

An UPBox commercial grade 3D Printer (Tier Time) loaded with white ABS filament was utilised to manufacture thirty samples. These were printed with a resolution of 0.2mm and an infill of 99% (note these refer to UPStudio settings). Each set of 5 samples were printed simultaneously in identical orientations (Figure 2) in order to attempt to achieve regularity within the sample sets.

B. Linear Stage Development

A simple apparatus containing an adjustable vertical stage with multiple mounting points for devices and samples was modelled utilising Solidworks. This was then manufactured via laser cutting of clear acrylic [Figure 3]. This testing equipment allowed for the manual vertical movement of the stage in 20 mm intervals. Additional Sample positioning and Spacer parts were laser cut utilising 3 mm acrylic to allow for increase accuracy in sample placement and variation in sample height Figure 4.

C. Experimental Protocol

The testing stage was set with a distance of 45 mm between the manoeuvrable platform and the fixed (top) platform. The plasma device was located upon the top panel above the samples with the rationale that this might aid in negating unwanted accumulation of hot air from the plasma rising and getting trapped at the sample. The experiment utilised a set machine output voltage of 26 V. Given that plasma represents a charged beam of ionised gas seeking

Figure 1: The handheld plasma surface modification product by Tantec

Figure 2: The final printed sample set.

Figure 3: Developed manual acrylic testing stage

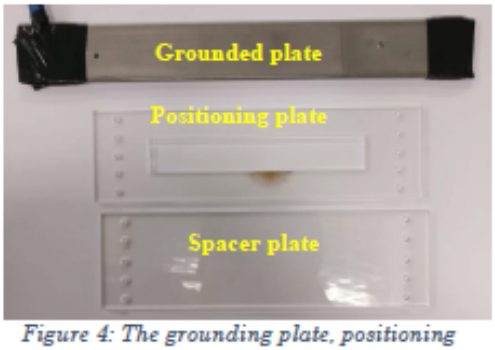

Figure 4: The grounding plate, positioning plate and spacer plat used in this study.

ground, to aid in the trajectory of this, a grounded plate was incorporated beneath each sample.

The limitations for the parameter to be modified were derived experimentally, namely adjustments were made until a distance at which severe plasma induced sample degradation was reached. This distance was found to be approximately 5mm at which sample ignition and breakdown was prevalent.

Following this evaluation 5 sample sets were allocated for locations 36 mm (Sample 1), 30 mm (Sample 2), 24 mm (Sample 3), 18 mm (Sample 4), and 12 mm (Sample 5) away from the exposure point/s (One Sample set acted as the 'control' being unexposed to plasma irradiation). Each sample was placed within the positioning part and the desired height adjusted through spacer parts.

D. *Plasma Irradiation*

Each Sample was exposed to plasma irradiation twice, with each period of exposure being equal to 10 minutes. Due to the nature of the linear stage, the plasma exposure was off centre by 5 mm. Thus the second exposure to Plasma was intended to cover a greater region ensuring uniform irradiation.

The first processing occurred via an exposed and twisted aluminium wire having an outer diameter of approximately 2 mm. This was positioned centrally to the right of the sample. The second plasma processing occurred as 4 smaller diameters (1 mm) exposed and wrapped aluminium points. These were located at 5 mm and 15 mm offset from the centre on either side.

E. *Result evaluation*

Two stages of evaluation occurred for these parts, namely a non-destructive microscopy, followed by destructive tensile testing and scanning electron microscopy.

Tensile Testing

An Instron 5967 was utilised to generate data relating to fatigue analysis. This device was loaded with a 30 kN load cell ad a strain gauge was utilised allowed for the aided derivation of values such as ultimate tensile strength (UTS). The samples were placed centrally within the devices clamps with the upper and lower clamps set at 65 mm apart.

SEM Microscopy

Samples were finally reviewed post Instron testing via a Hitachi TM3030Plus. This was not done prior to tensile testing due to potential unwanted effects from electron beam exposure and spatial limitations of the SEM chamber. As such post Instron evaluation samples were further reduced in size with care placed on regions of interest such as the point of fracture as these were analysed in this device.

III. RESULTS & DISCUSSIONS

A major impacting feature within this study was the tendency towards plastic deformation of samples closer to the point of plasma production. The bending of these samples can

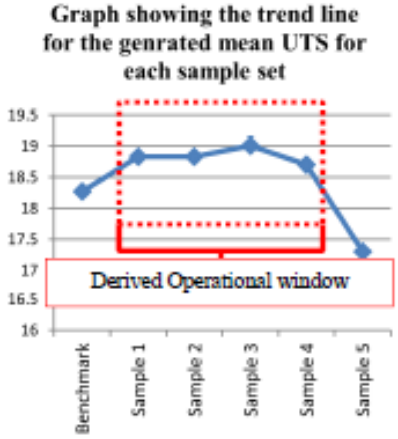

Figure 5: Variation in UTS for various distance to plasma source.

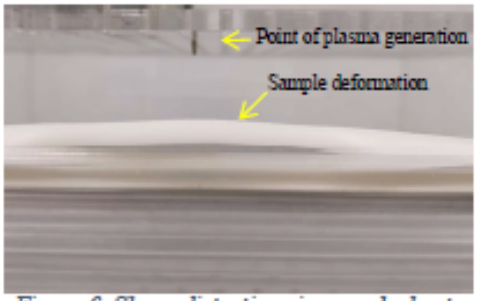

Figure 6: Shape distortions in sample due to delivered heat

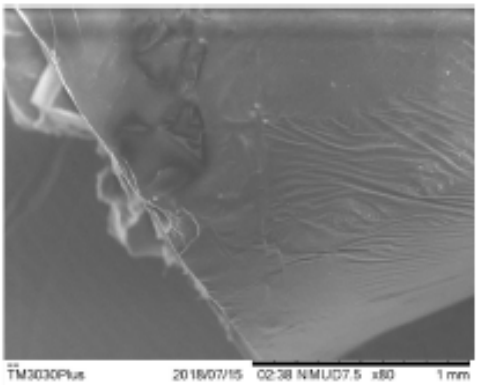

Figure 7: SEM image demonstrating effects of melting on sample

Table 1: Table containing the mean ultimate tensile strength for each sample set

Sample	Mean UTS (MPa)
Control/Benchmark	18.27
Sample 1	18.85
Sample 2	18.83
Sample 3	19.01
Sample 4	18.7
Sample 5	17.3

New Zealand National Science Challenge

be seen in Figure 6 and is a clear indicator of sufficiently high energy contact with Samples 3, 4 and 5. Due to this, samples were taped down to the testing station to retain proximity accuracy.

A. Identification of a beneficial operational window

The mean results for tensile testing are described in Table 1. The highest tensile strength (19.01 MPa) was found for Sample 3 which was located 24 mm away from the plasma generating wire. This value indicated that with appropriate proximity between part and corona plasma an increase in approximately 0.7 MPa can be achieved. The derived mean UTS values also identified a depreciating trend when the samples were too close to the plasma, namely Sample 5 having a UTS approximately 1 MPa lower than the control. This trend, graphically illustrated in Figure 5, allowed for the formation of an operational window within which future work regarding corona plasma should be conducted. It can be hypothesised that this increase in UTS is derived from the additional cross-linking of polymer chains present on the surface of the sample (similar to that of established plasma based polymer treatments [7, 10]).

B. Further statistical analysis of study

Analysis of additional Instron generated data in relation to sample group standard deviation (σ) highlighted a potential cause for concern in non-conformity. Samples 1, 2 and 4 had a $\sigma < 0.4$ whilst Samples 3, 5 and the Benchmark had $\sigma > 0.9$. Thus, further investigations where required and conducted through a statistical analysis software (MiniTab18). A one-way Anova of the data yielded the graphs depicted in Figure 8. These depicted a normally distributed value set for the Normal Probability Plot highlighting an acceptable trend in results. The Versus Fits output was helpful in identifying certain values within the data in close proximity to the lower limit (highlighted in red as < 17.5). This likely explains the variability in standard deviation. These values however are not considered detrimental outliers as they were still located within the limit boundaries. The histogram depicted a clear trend (occurring as a bell curve) within the data. It is worth noting that this one-way Anova yielded a *p* value of 0.055 (greater than a = 0.05) for Sample 5 indicating that the process having a distance of 12 mm did not reject the null hypothesis and thus can be declared not practically significant. Given that this value was not significantly different to the *a* value, this sample set will still be discussed.

C. Topographical Analysis

The major surface topography of each sample remained relatively unchanged. The plasma irradiation did not act to seal the cavities of the samples. Sample 5 differed and had a much greater reduction in these voids but also suffered thermal degradation (yielding detrimental surface melting) [Figure 7]. It is worth noting that the sample surfaces appeared very rough and this is plausibly due to the plasma exposure however, the benchmark surface had similar distortions (albeit that these were slightly more prominent) [Figure 4]. Thus this study could not identify plausible and

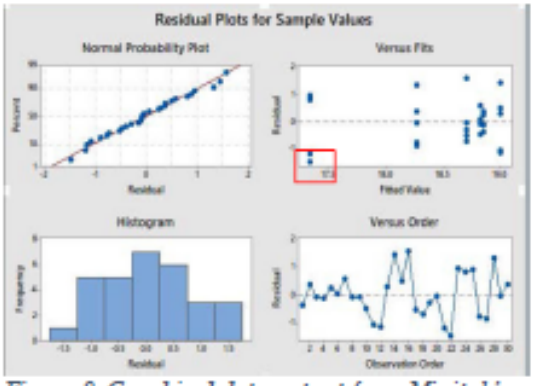

Figure 8: Graphical data output from Minitab's one-way ANOVA

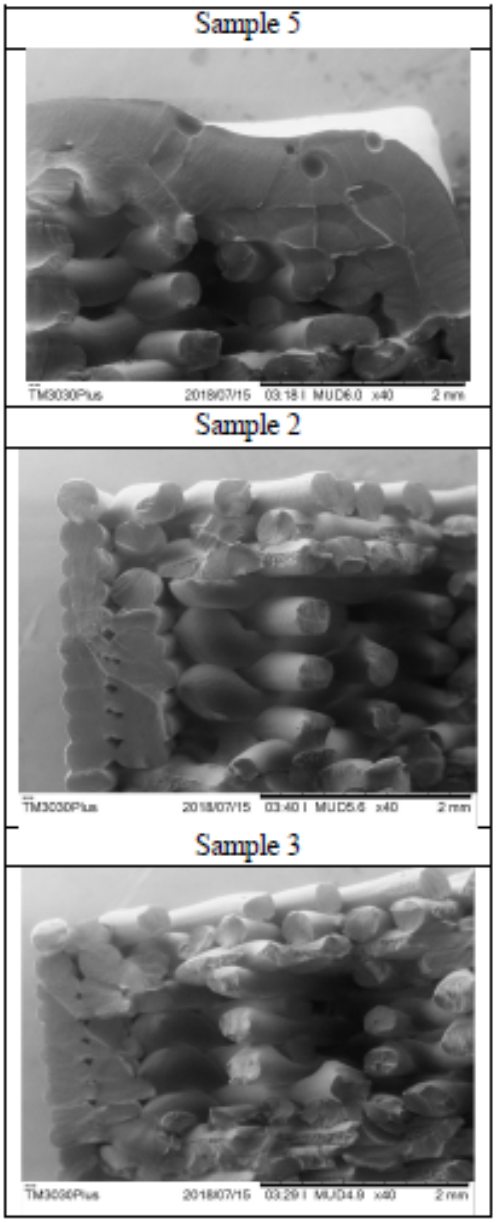

Figure 9: SEM images depicting a comparative view of the cross-sectional fracture microscopy for the generated Samples.

significant surface quality improvement due to plasma irradiation. Additional cross sectional microscopy of the fracture points for Sample 2 and Sample 3 did not identify any significant distortions to justify the 0.2 MPa increase in UTS between these. Additionally no major structural differences could be identified when comparing the sample sets to the benchmark. As such, the modifications made to the samples due to plasma interaction are highly likely to be of a slight cross-linking nature affecting the polymer chains without yielding sufficient energy for these to result in structural deformation.

IV. CONCLUSIONS AND RECOMMENDATIONS

This study was successful at demonstrating the potential benefits of implementing corona discharge plasma generation to a 3D printing process. The current study demonstrated that this device was capable of modifying the properties of 3DP, sometimes drastically so when the enforced 5 mm proximity limit is not considered and as such, a processing window to be utilised in related future work. Additionally, to further scope the limitations and range of the processing window described herein, additional proximity based studies should be conducted utilising more precise actuation mechanisms.

The following research recommendations are made regarding future work involving this research:

- The use of higher end 3DP to attain samples of a higher standard/quality.
- The automation of a linear-stage testing device to enable higher precision in proximity manipulation.
- Improvement of sample clamping/holding mechanisms to increase precision and avoid unwanted distortions from heat/exposure.
- Work to derive fewer irregularities within the plasma stream, and methods to identify a uniform plasma yield for multiple extrusion points.
- A centralised sample esc grounding plate to ensure attraction solely to the sample.
- Formation of more advanced clamping mechanisms to limit the effects of structural distortion on experimental parameters.
- Studies related to the further integration of this technique within intervals of a 3DP process.

This work forms part of fundamental investigations for future research regarding the addition of processing elements within 3DP technology.

V. ACKNOWLEDGEMENTS

The authors would like to thank the New Zealand National Science Challenge for funding this research. We also acknowledge the technical contribution of John Futter and Bruce Crothers from GNS Science.

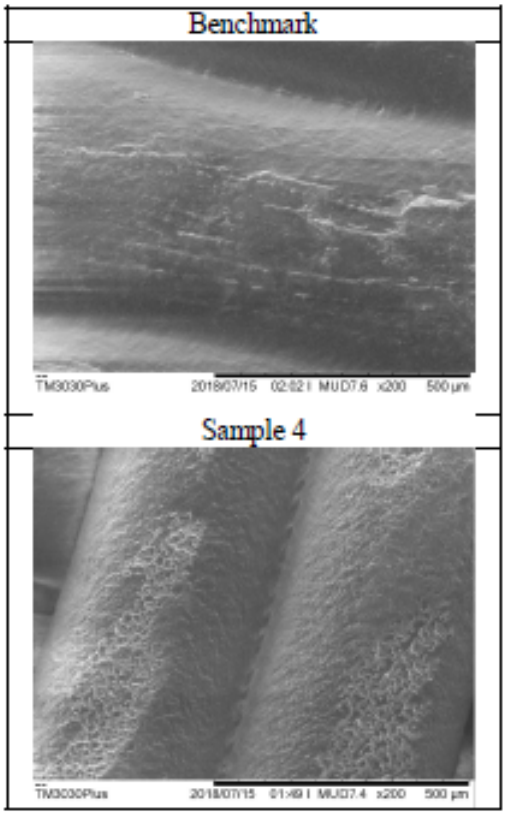

Figure 10: Comparison of SEM images showing the different surface features between the benchmark and Sample 4

VI. REFERENCES

[1] F. Calignano, D. Manfredi, E. P. Ambrosio, S. Biamino, M. Lombardi, E. Atzeni, *et al.*, "Overview on Additive Manufacturing Technologies," *Proceedings of the IEEE*, pp. 1-20, 2017.

[2] T. D. Ngo, A. Kashani, G. Imbalzano, K. T. Q. Nguyen, and D. Hui, "Additive manufacturing (3D printing): A review of materials, methods, applications and challenges," *Composites Part B: Engineering*, vol. 143, pp. 172-196, 2018.

[3] J. Gardan, "Additive manufacturing technologies: state of the art and trends," *International Journal of Production Research*, vol. 54, pp. 3118-3132, 2015.

[4] O. A. Mohamed, S. H. Masood, and J. L. Bhowmik, "Optimization of fused deposition modeling process parameters: a review of current research and future prospects," *Advances in Manufacturing*, vol. 3, pp. 42-53, 2015.

[5] A. Garg, A. Bhattacharya, and A. Batish, "Chemical vapor treatment of ABS parts built by FDM: Analysis of surface finish and mechanical strength," *The International Journal of Advanced Manufacturing Technology*, vol. 89, pp. 2175-2191, 2016.

[6] N. Jayanth, P. Senthil, and C. Prakash, "Effect of chemical treatment on tensile strength and surface roughness of 3D-printed ABS using the FDM process," *Virtual and Physical Prototyping*, vol. 13, pp. 155-163, 2018.

[7] J. R. Rocca-Smith, T. Karbowiak, E. Marcuzzo, A. Sensidoni, F. Piasente, D. Champion, *et al.*, "Impact of corona treatment on PLA film properties," *Polymer Degradation and Stability*, vol. 132, pp. 109-116, Oct 2016.

[8] D. Hetemi and J. Pinson, "Surface functionalisation of polymers," *Chem Soc Rev*, vol. 46, pp. 5701-5713, Oct 2 2017.

[9] Z. M. Huang, Y. Z. Zhang, M. Kotaki, and S. Ramakrishna, "A review on polymer nanofibers by electrospinning and their applications in nanocomposites," *Composites Science and Technology*, vol. 63, pp. 2223-2253, Nov 2003.

[10] S. Samal, "Thermal plasma technology: The prospective future in material processing," *Journal of Cleaner Production*, vol. 142, pp. 3131-3150, 2017.

[11] F.-G. Chizoba Ekezie, D.-W. Sun, and J.-H. Cheng, "A review on recent advances in cold plasma technology for the food industry: Current applications and future trends," *Trends in Food Science & Technology*, vol. 69, pp. 46-58, 2017.

[12] F.-H. Kuok, K.-Y. Kan, I.-S. Yu, C.-W. Chen, C.-C. Hsu, I. C. Cheng, *et al.*, "Application of atmospheric-pressure plasma jet processed carbon nanotubes to liquid and quasi-solid-state gel electrolyte supercapacitors," *Applied Surface Science*, vol. 425, pp. 321-328, 2017.

[13] D. Mathijsen, "Bigger, stronger, faster… pushing the envelope of 3D printers to turn them into true production tools," *Reinforced Plastics*, vol. 62, pp. 194-202, 2018.

[14] H. Abourayana, P. Dobbyn, and D. Dowling, "Enhancing the mechanical performance of additive manufactured polymer components using atmospheric plasma pre-treatments," *Plasma Processes and Polymers*, vol. 15, p. 1700141, 2018.

DRC 16

MASSEY UNIVERSITY
GRADUATE RESEARCH SCHOOL

STATEMENT OF CONTRIBUTION
DOCTORATE WITH PUBLICATIONS/MANUSCRIPTS

We, the candidate and the candidate's Primary Supervisor, certify that all co-authors have consented to their work being included in the thesis and they have accepted the candidate's contribution as indicated below in the *Statement of Originality*.

Name of candidate:	Juan Schutte
Name/title of Primary Supervisor:	Prof. Johan Potgieter
Name of Research Output and full reference:	
The effects of acetone vapour inter-layer processing on fused deposition modelling 3D printed acrylonitrile butadiene styrene	
In which Chapter is the Manuscript /Published work:	Chapter 6
Please indicate:	
• The percentage of the manuscript/Published Work that was contributed by the candidate:	70
and	
• Describe the contribution that the candidate has made to the Manuscript/Published Work:	
The candidate has written the majority of the manuscript. The candidate has contributed to the experimentation and provided the analysis required for this publication.	
For manuscripts intended for publication please indicate target journal:	
Candidate's Signature:	Digitally signed by Juan Schutte Date: 2019.06.04 15:23:23 +12'00'
Date:	04/06/2019
Primary Supervisor's Signature:	Johan Potgieter Digitally signed by Johan Potgieter Date: 2019.06.06 11:07:55 +12'00'
Date:	06/06/2019

(This form should appear at the end of each thesis chapter/section/appendix submitted as a manuscript/ publication or collected as an appendix at the end of the thesis)

GRS Version 4– January 2019

The effects of Acetone vapour inter-layer processing on Fused Deposition Modelling 3D Printed Acrylonitrile Butadiene Styrene.

Juan Schutte, Pamitha Wjesundera, Assoc. Prof. Johan Potgieter
School of Engineering and Advanced Technology, Massey University
Auckland, New Zealand
j.schutte@massey.ac.nz

Abstract—**The characteristics of the interlayer bonding within 3D Printed objects is a fundamental feature determining the capabilities of the resultant object. This study set out to identify the opportunity for additional inter layer processing within 3D Printing. Inter layer processing is the addition of processes before a new layer can be printed upon a previous layer. Thirty Acrylonitrile butadiene styrene ASTM D638 Type IV dog-bone samples were generated using an UPBox Fused deposition modelling printer. These were segmented into five groups associated with exposure at 0%, 20%, 25%, 50%, and 100% printing intervals. Tensile testing was conducted through the utilization of an Instron 5967 and a Hitachi TM3030Plus Scanning electron microscope was used for topographical analysis of sample layer fusion/bonding. Samples showed a inversely proportional change in characteristics relative to inter-layer processing, namely an increase in processing decreased the ultimate tensile strength at elongation and decreased the distinguishable layering and cavities within the sample.**

Keywords—Additive Manufacturing, 3D Printing, Surface modification, Coating

I. INTRODUCTION

3D printing (3DP) is a form of additive manufacturing (AM) in which 'layer-based' processing of material results in the generation of three-dimensional objects [1, 2]. Thus these parts are fundamentally laminate in nature. Many 3DP methodologies rely on the application of pressure or heat to deposit/process the material into the desired form.

The technology has been associated with restrictions occuring from weak inter-layer bonding resulting in delamination as well as poor aesthetic quality, this is prevalent in Fused Deposition Moddelling (FDM) 3DP) [3] (Figure 1). The most prominent form of this technology makes use of polymer filament which is actuated to an extrusion point at which the material is subjected to thermal actuation. This thermal actuation results in the occurance of a polymer melt being extruded upon a colecting surface. In a FDM 3DP process the polymer is deposited as 'pathways' of material both alongisde previously extruded material (forming part of a layer as well as on top of previously placed material. The thermal characteristics of the heated polymer encourage the fusion of adjacent polymer streams. As such, the control of this is a major contributing factor to the objects inter-layer bonding.

The degree of inter-layer bonding of 3DP parts relates to the capability of the material processing technique to result in the joining/fusing of new layers. The strength of the material bonding is generally proportional to the degree of fusion [4]. Another key factor associated with good bonding is the surface area interaction between material [4]. If the surface finish of a printed layer does not match with the subsequent layers addition of material cavities can occur and result in a weaker bond. Due to a lack of complete quantity control in 3DPs addition of material, areas vacant of material can occur. These vacancies not only reduce surface contact and subsequently inter-layer bonding but also result in areas of potential stress concentrations.

Whilst much work has been conducted in ensuring controlled thermal/environmental conditions within 3DP (seen in devices such as the proffessional Fortus 250mc and consumerist UPBox, much less interest has been directed at methodologies eliminating generated layer voids. As such there is incentive to investigate potential methodologies for improvement of inter-layer surface quality. The enhancement of external surface characteristics/quality of 3DP parts has already been achieved through the implementation of many post-processing methodologies including abrasive polishing and chemical exposure [5]. A popular technique for the surface modification of 3DP Acrylonitrile butadiene styrene (ABS) FDM parts is through the utilization of Acetone vapor in a vapor-bath exposure system [6].

Vapour the the occurance of material particulate in a gaseous phase at a temperature lower than the materials critical temperature (at which evaporation would occur) [7].Vapour has been utilized within coating proceedures and is generally the result of different chemical reactions. This process is known as a chemical vapour deposition [5]. It is a popular coating methodology due to it's ability to evenly distribute material upon a surface and is capable of processing many

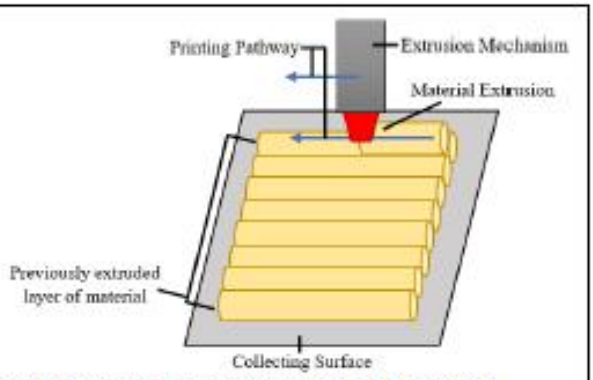

Figure 1: Illustrating the standard components of a FDM 3DP

forms and object features. Given this understanding of the effectiveness of vapour as a surface modification agent, it will be of interest in the processing of internal object layers.

The following paper will investigate whether inter-layer surface modification will have a functional alteration to the characteristics of both 3D Printed parts as well as the internal layer fusion/bonding will be altered. This study forms part of ongoing work relating to the application of inter-layer processing within 3DP processes.

II. Methodology

The UPBox by Tier time uses a FDM form of 3DP to generate objects from polymer filament. This printer is utilized for this study due to the ability to pause the process at a defined layer. The cessation of printing at defined intervals will allow for the controlled removal and processing of samples.

A. Sample Generation

Thirty ASTM D638 Type IV dog-bone samples were generated from 3DP ABS filament, from these six groups were generated. The longest and thickest side of each object was printed parallel to the printing platform. The printing process was halted at 20%, 25%, 50% intervals of the total printing layers to allow for processing. A note is made that the printing was halted again at the 50% interval for an evaluation of the effects of printing interruption on a sample. Additional information regarding printing properties is described in Table 1.

B. Acetone exposure

Three sample groups were subjected to levels of exposure to acetone vapour namely at 20%, 25% and 50% intervals. One sample group was only exposed to vapour post printing, namely at the 100% interval. The final two groups were not exposed to acetone, these being the 0% and 50%NA (where NA refers to not applied).

Vapour processing was implemented through the utilisation of a vapour bath system, with samples suspended 50mm above

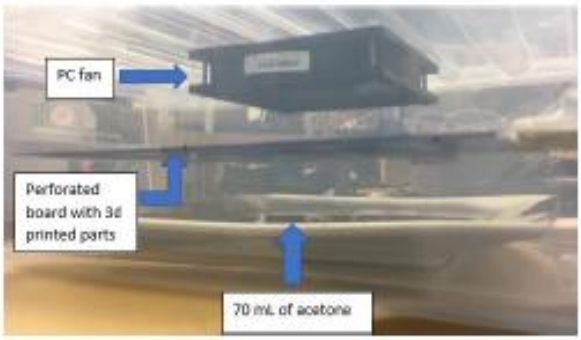

Figure 2: Acetone vapour bath system

Table 1: UP!BOX Settings utilized

Object infill	99%
Layer thickness	0.25mm
Print temperature	230° C
Quality	Normal
Nozzle diameter	0.4mm
Filament diameter	1.75mm
Raft material	No
Printing platform	275 X 225

Table 2: Vapour bath settings

Acetone, ml	70
Vapor bath container, mm	494 L X 322W X 138H
PC fan, V	5
Perforated board, mm	275X 225
3D printed Type IV dogbanes	5
Minutes	20

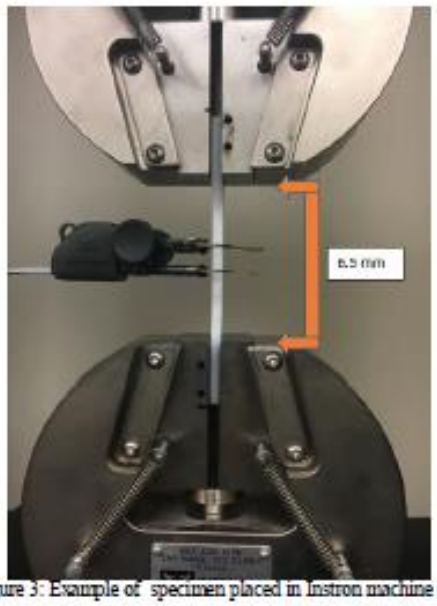

Figure 3: Example of specimen placed in Instron machine

acetone solution (Figure 2). This arrangement exploited the solutions characteristic of evaporation at room temperature (23°C) in an attempt to control the quantity of vapour within the chamber.

Table 3: Average ultimate tensile strength and respective standard deviation for samples

Sample	Average UTS(MPa)	Standard deviation
0%	41.2	1.013
20%	32.0	1.518
25%	33.7	1.295
50%	39.4	0.933
100%	39.7	1.871
50% NA	40	1.272

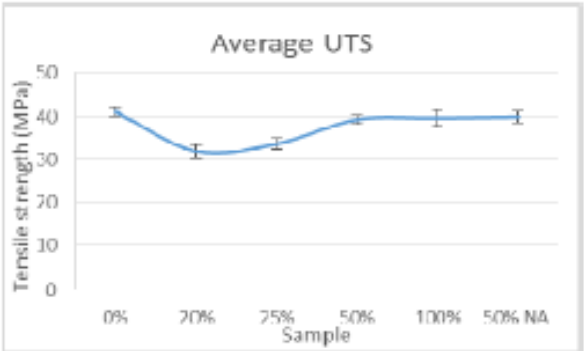

Figure 5: Average tensile strength for each sample

C. *Sample Analysis*

Sample groups were labelled as 'Sample X%' where 'X%' refers to the percentage interval for processing (e.g., Sample 25% relates to the group of which vapour exposure occurred at every 25% of the total printing layers). An Instron 5967 was utilized with a load cell of 30kN to determine the ultimate tensile strength (UTS) at extension as well as each sample groups standard deviation (SD). This value will determine sample uniformity and statistical consistency of the obtained results; as such, this value will be presented to demonstrate the reliability of the data received. The testing grippers were positioned 65mm apart, between which samples were fastened and the extension actuation was set at 0.2 mm/mm/min (Figure 3). An Hitachi TM30303Plus scanning electron microscope (SEM) was utilized to generate images for topographical analysis. The input voltage was set at 5k with Standard Reduction at magnification of 100,500and 1000.

III. RESULTS & DISCUSSIONS

As expected the external surface quality of the samples were altered by the exposure to acetone, namely the distinctive layering of ABS became less distinct. It should also be noted that with increased intervals of exposure there was an apparent decrease in sample thickness (this is potentially due to the material movement into cavities). These physical alterations are demonstrated in Figure 5.

The following SEM analysis refers to Figure 6 in which two examples (A and B) of each sample group are displayed with yellow circles identifying cavities and red lines identifying regions of interest.

The presence of distinguishable layering diminished with the increase in acetone exposure with hardly any distinctive layering identifiable in the 'Sample 20%' group. The occurrence of cavities seemed to be inversely proportional to that of the vapor processing. It is interesting to note the occurrence of distinctive deformation in regions of the object which seem to coincide with the intervals of inter-layer processing (highlighted by the red arrow), these could be indicative of a chemical alteration made by the acetone to the ABS surface. In general, the topographical imaging suggests a higher degree of fusion with increased exposure to acetone. Typically, this would indicate a higher strength however by analyzing the data from the Instron tensile testing an opposite relationship becomes apparent.

Table 3 and Figure 4 contain the results of average UTS and the SD for different experiments performed. It must be noted that all SD values fall under the threshold of 5% [8], the highest variation being 1.871 occuring in the 100% sample group. The average ultimate tensile strength improves with increase in percentage of acetone treatment. The highest average UTS among acetone treated samples was recorded as 39.7 MPa for sample 100%, followed by 39.4 MPa, 33.7 MPa and 32 MPa for samples 50 %, 25% and 20% respectively. This showed a relatively linear decrease in UTS with increased exposure to inter layer processing. The unprocessed samples which yielded the highest strength also indicate that the interruption of printing (namely the 50%NA sample) showed a negative relationship to strength. It must be noted that both the 100% and 50% sample showed a decrease of 1.5 MPa and 0.6 MPa respectively thus reaffirming that the exposure to acetone had a negative effect on UTS.

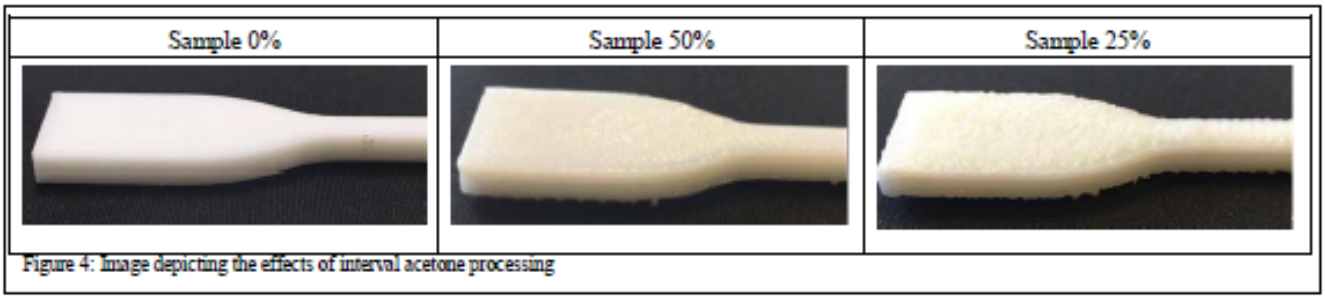

Figure 4: Image depicting the effects of interval acetone processing

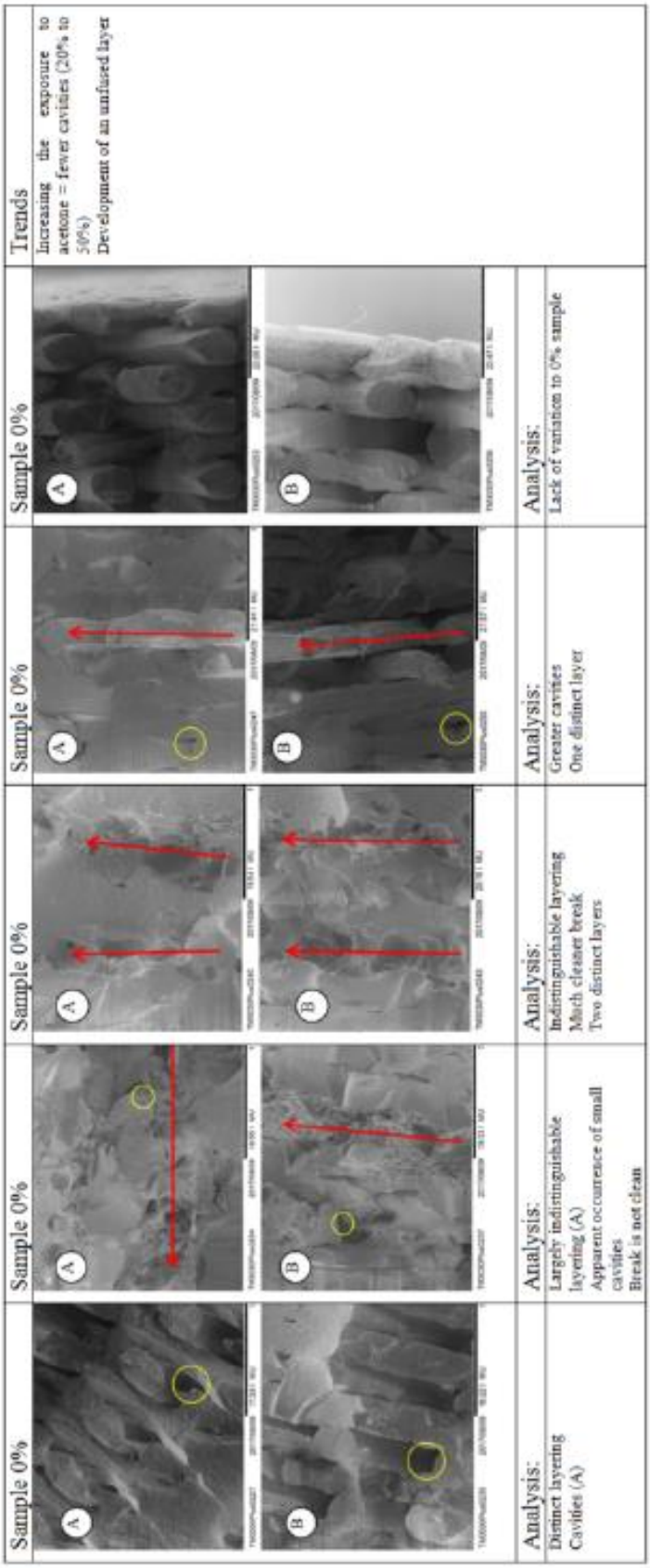

Figure 6: SEM images and the respective analysis for these where A and B represent two samples from each group

Current literature records the strength of similar parts as approximately 28.5 – 33.96 MPa [9, 10], thus it is interesting to note a much higher recording in this study (an increase of 7.74 MPa). This is potentially due to an increase in 3DP capabilities as well as potentially the result of raft-less printing and should undergo further investigation.

The relationship between inter layer processing and tensile extension strength showed a linear decrease in strength proportional to the quantity of inter layer processing (the average UTS for each sample group is summarised in the graph depicted in Figure 4). This apparent proportional decrease in strength to increase in acetone exposure supports the previous notion regarding the possible changes to polymer chemistry.

From this discussion, the following hypothesis have been made regarding the effects of acetone inter-layer processing on ABS parts:

- Acetone alters the polymer chain structure of ABS resulting in a more brittle structure having lower ductility and thus yielding an inversely proportional relationship between ultimate tensile stress and quantity of vapor exposure.
- Alterations to the polymer chains in ABS due to acetone affect the reactivity of this to future/following attempts of thermal fusion (subsequent FDM layering).
- A threshold exists in inter-layer processing of FDM ABS to Acetone in which the optimal/critical interval of vapor application yields optimal tensile strength.

IV. CONCLUSION/SUMMARIZATION

This study helped to highlight the potential of inter-layer processing within 3DP. This study has successfully yielded an analysis of the effects of Acetone vapour inter-layer processing on Fused Deposition Modelling 3D Printed Acrylonitrile Butadiene Styrene, namely that this produced a negative impact on the UTS of the resultant object. This study also highlighted the decrease in strength of interrupted printed samples. From the following recommendations are made regarding future work:

- An analysis of the effects of interruptions at varied intervals of an FDM process should be conducted.
- The chemical nature of ABS and Acetone interaction and the effect this has on polymer chain length should be evaluated.
- The application of proven bonding agents at varied printing intervals should be conducted.
- A study should be conducted regarding the current UTS capabilities of FDM 3DP, this should include the various options in printing including orientation and raft-less printing.

This work will form a fundamental ground work for the future research regarding the addition of processing elements within 3DP.

V. ACKNOWLEDGEMENTS

The authors would like to thank the New Zealand National Science Challenge for funding this research as well as Assoc. Prof John Harrison for his guidance in the use of liquid nitrogen to prepare the samples for topographical analysis.

REFERENCES

[1] F. Calignano, D. Manfredi, E. P. Ambrosio, S. Biamino, M. Lombardi, E. Atzeni, *et al.*, "Overview on Additive Manufacturing Technologies," *Proceedings of the IEEE,* vol. 105, pp. 593-612, 2017.

[2] J. Gardan, "Additive manufacturing technologies: state of the art and trends," *International Journal of Production Research,* vol. 54, pp. 3118-3132, 2015.

[3] H. Bikas, P. Stavropoulos, and G. Chryssolouris, "Additive manufacturing methods and modelling approaches: a critical review," *The International Journal of Advanced Manufacturing Technology,* vol. 83, pp. 389-405, 2015.

[4] A. Garg, A. Bhattacharya, and A. Batish, "Chemical vapor treatment of ABS parts built by FDM: Analysis of surface finish and mechanical strength," *The International Journal of Advanced Manufacturing Technology,* vol. 89, pp. 2175-2191, 2016.

[5] T. S. S. Jong-Hee Park, *Chemical Vapor Deposition*: ASM International 2001.

[6] N. N. Kumbhar and A. V. Mulay, "Post Processing Methods used to Improve Surface Finish of Products which are Manufactured by Additive Manufacturing Technologies: A Review," *Journal of The Institution of Engineers (India): Series C,* 2016.

[7] C. E. Morosanu, *Thin Films by Chemical Vapour Deposition*: Elsevier, 2016.

[8] J. R.Davis, *Tensile Testing, 2nd Edition* ASM International, 2004.

[9] A. R. Torrado, C. M. Shemelya, J. D. English, Y. Lin, R. B. Wicker, and D. A. Roberson, "Characterizing the effect of additives to ABS on the mechanical property anisotropy of specimens fabricated by material extrusion 3D printing," *Additive Manufacturing,* vol. 6, pp. 16-29, 2015.

[10] A. R. Torrado Perez, D. A. Roberson, and R. B. Wicker, "Fracture Surface Analysis of 3D-Printed Tensile Specimens of Novel ABS-Based Materials," *Journal of Failure Analysis and Prevention,* vol. 14, pp. 343-353, 2014.

DRC 16

MASSEY UNIVERSITY
GRADUATE RESEARCH SCHOOL

STATEMENT OF CONTRIBUTION
DOCTORATE WITH PUBLICATIONS/MANUSCRIPTS

We, the candidate and the candidate's Primary Supervisor, certify that all co-authors have consented to their work being included in the thesis and they have accepted the candidate's contribution as indicated below in the *Statement of Originality*.

Name of candidate:	Juan Schutte
Name/title of Primary Supervisor:	Prof. Johan Potgieter
Name of Research Output and full reference:	
The effects of electrospinning collection surface modification on nylon 6-6 placement	
In which Chapter is the Manuscript /Published work:	Chapter 6
Please indicate:	
• The percentage of the manuscript/Published Work that was contributed by the candidate:	100
and	
• Describe the contribution that the candidate has made to the Manuscript/Published Work:	
The candidate has written the majority of the manuscript. The candidate has conducted the experimentation and analysis required for this publication.	
For manuscripts intended for publication please indicate target journal:	
Candidate's Signature:	Digitally signed by Juan Schutte Date: 2019.06.04 15:23:23 +12'00'
Date:	04/06/2019
Primary Supervisor's Signature:	Johan Potgieter Digitally signed by Johan Potgieter Date: 2019.06.06 11:08:37 +12'00'
Date:	06/06/2019

(This form should appear at the end of each thesis chapter/section/appendix submitted as a manuscript/ publication or collected as an appendix at the end of the thesis)

GRS Version 4– January 2019

The effects of electrospinning collection surface modification on nylon 6-6 placement

Juan Schutte, Johan Potgieter, Steven Dirven, Xiaowen Yuan,
School of Engineering and Advanced Technology, Massey University
Auckland, New Zealand
j.schutte@massey.ac.nz

***Abstract*—The nature of fibre placement/manipulation in electrospinning has been recorded through the utilization of surface actuation and electrostatic manipulation. This study investigates the potential of a simplistic approach to fibre placement manipulation through the utilization of non-uniform non-conducting collecting surfaces. A solution of Nylon 6,6 and Formic acid was electrospun with an ES1a device and through the use of SEM analysis submicron and nanofibre alignment was identified. This study achieved the generation of actuation-less and electrode-less alignment, reiterating current literatures rationale of alignment formation. The study noted limitations regarding the potential combination of mold/cavity and electrospinning based manufacturing. From this work future recommendations regarding surface modification have been derived.**

Keywords*— *Electrospinning, Surface Collector, Additive Manufacturing, 3D Printing, Surface deformation, orientation, Nylon 6-6

I. INTRODUCTION

Electrospinning (electrostatic spinning) is a relatively rapid, efficient and inexpensive process in which an electric field is utilized in the generation of micro- and nanofibres [1-3]. The technology has been applied to over 200 polymers [4] (both natural and synthetic) and can be described as the combination of three distinctive parts namely the Solution, the Charged Extruder and the Collecting Surface [2, 5-7] (Figure 1). The 'Solution' refers to a polymer-solvent mixture that is often subjected to actuation directing the fluid to a conductive extrusion point. This component, described here as the 'Charged Extruder', is connected to a high voltage (kV) – low current (μA) power supply and is responsible for generating the required electrostatic forces within the 'Solution'. An optimal process includes the formation of 'Solution' upon the extruder where only surface tension forces hold this material (e.g. the generation of a meniscus when using a syringe pump). The extruder is then charged which results in the buildup of electrostatic forces within the material and formation of a Taylor cone. At a critical voltage (this varies between polymers utilized), these forces will overcome the surface tension forces resulting in the expulsion of a stream/jet of material. Due to electrostatic instabilities, this material whips through the air evaporating the acidic solvent leaving the desired polymer fibre, which accumulates upon the 'Collecting Surface' (an oppositely charged area).

The New Zealand National Science Challenge funds this work

This process is limited to the fabrication of mats (two-dimensional objects) and does not actively control the orientations or placement of the collected nanofibre. Popular methods allowing for the manipulation of these parameters is through the modification of the 'Collecting Surface' utilized [8-10]. Through the actuation of this component alignment can be instilled in generated fibres. Two popular derivations of collecting surface modification include the splitting of the surface to generate a parallel electrode configuration with an airgap (sometimes filled with non-conductive collecting plate), and the actuated spinning/rotating of the surface (often in the form of a rotating drum, disk, or conveyor collector) [2, 6, 11].

The use of rotational actuation generates alignment of fibre in the direction of rotation; this alignment and relatively even distribution is due to the mutual electrostatic repulsion between deposited fibres [1, 12-14]. It must also be noted that by varying rotation speed, resultant fibre alignment can also be manipulated [1]. A major advantage of this mechanism is that it retains functionality when scaled for larger manufacturing requirements. This technique is however only able to produce aligned fibre in a singular direction. Control over the direction of alignment is achievable via the use of parallel electrodes [15, 16] This methodology exploits the electrostatic attraction of the formed nanofibre to oppositely charged areas, resulting in the stretching of the fibre between electrodes [1]. This mechanism has been recorded as relatively limited by scale (relative alignment lost at gaps greater than 30mm [9, 14, 16]. A recent study by Orr *et al* demonstrated that through the combination of alignment mechanisms these spatial limitations could be relatively overcome. In this study a combination of ceramic magnets, parallel copper electrodes and distilled water was utilized to allow for alignment over a 100mm distance [9].

In both the rotational and the parallel electrode configurations, the surface can be described as relatively planar/simple. These techniques do not actively control the location of fibre placement. Direct writing electrospinning is a largely underdeveloped method which allows for greater control of distributed fibre placement. This control is derived from the automation of either collector or extruder at short collection distances. These shorter distances allow for the reduction in randomized jet instabilities (allowing for greater

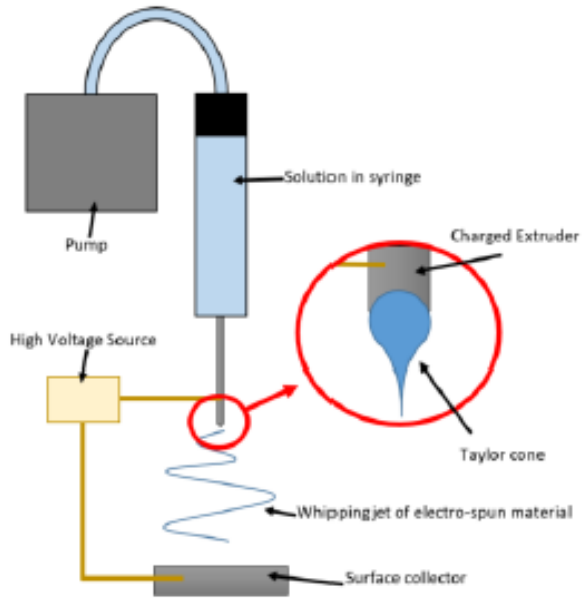

Figure 1: Figure illustrating the components and features of electrospinning

control of fibre deposition), however result in less evaporation yielding fibres coated in solvent [17]. This study will investigate the potential for the controlled placement of electrospun fibre onto and into molds for object generation, and thus further develop an understanding of the intricacies associated with electrospinning, namely the nature of fibre formation and placement.

II. METHODS

For this study, a relatively flat collector surface was used as a control for comparison against three distinctive forms namely a semi-sphere, patterned semi-sphere and dog-bone analogue. These shapes were extruded or cut into collecting surfaces with base dimension 50mmx50mm. Experimentation occurred at RevolutionFibres, utilizing their electrospinning device (a derivative of Electrospinz's ES1a device) (*Figure 2* acquired from [18]) and provided Nylon-Formic Acid solution.

A. Surface Generation

7 electrospinning surfaces (Figure 3) were designed in SolidWorks and an UP!2 3D printer, loaded with white Acrylonitrile butadiene styrene (ABS) filament and a set printing resolution of 0.25mm, was used to manufacture these. The dimensions of these and desired research outcomes are described below.

Semi-sphere (Figure 4, 1 and 2): A large dome (r= 15mm, h=15mm) shape was utilized to determine if electrospinning was capable of being utilized in a mold-based manufacturing methodology whereby fibres coating the extrusion and cavity regions would generate the desired three-dimensional object.

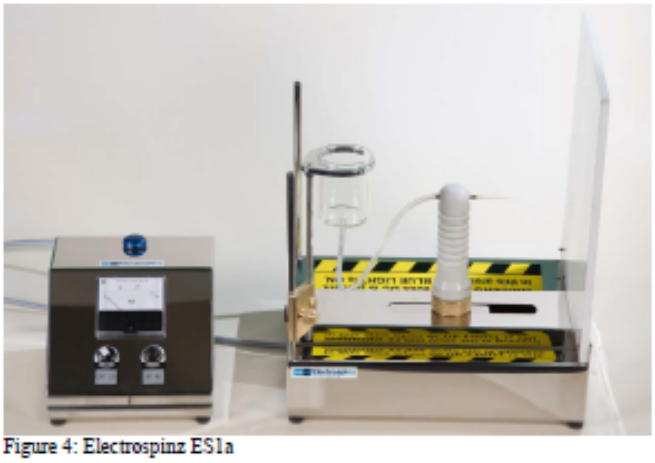

Figure 4: Electrospinz ES1a

Patterned semi-sphere (Figure 4, 3 and 4): A pattern

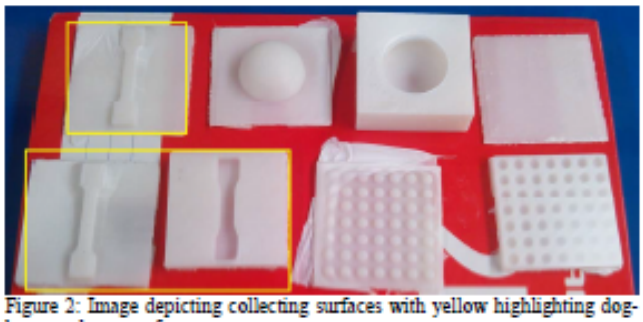

Figure 2: Image depicting collecting surfaces with yellow highlighting dog-bone analogue surface

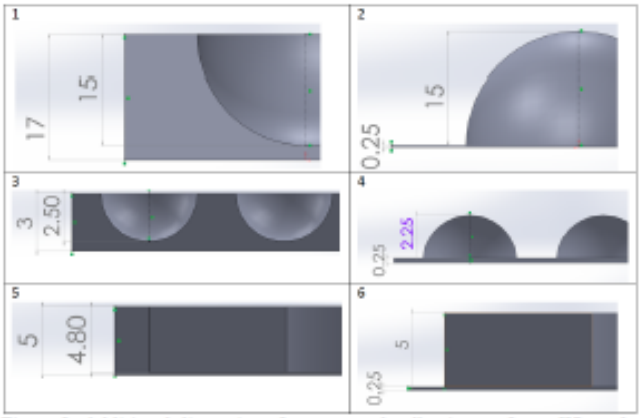

Figure 3: Additional dimensions for generated collecting surfaces. Where 1, 3 and 5 are the cavity and 2, 4 and 6 are the extruded versions of the semi-sphere, patterned semi-sphere and dog-bone analogue

consisting of 49 extrusions (r= 2.5mm, h= 2.5mm) was utilized to determine the ability to generate an array of fibre between the extruded material (which will have a lower degree of conductivity). This pattern was also utilized in a cavity-based approach in an attempt to retain the cavity-derived alignment

over the entire region of the collecting surface. This degree of control is ideal for scaffold generation [1, 6, 9, 19, 20].

Dog-bone analogue (Figure 4, 5 and 6): A dog-bone analogue extrusion (outer width= 10mm, inner width= 6mm, transition radius= 10mm, length= 45mm, *Figure 3*) was utilized to determine the relationship of electrospun fibres on surfaces having non-uniform width as well as perpendicular areas/walls (containing hard (90°) edges).

B. *Electrospinning*

Each collecting surface was attached to the grounded collector plate via double-sided tape. Collectors were positioned with the extruder nozzle directed approximately at their respective centers. Components were manually adjusted until electrospinning of fibres occurred and the utilised distances measured as: distance to collector = 120mm, solution beaker height = 256mm, collector height = 250mm. The high voltage source was set to approximately 32kV for 5 minutes, after which the collector and unwanted fibre 'overspray' were removed and the process repeated.

C. *Analysis*

Each fibre-coated sample was then subjected to sputter coating (an average of 25 angstrom/2.5nm gold sputter coating applied through the use of Nanostructured coatings DSR1 device) after which the topographical characteristics were evaluated via scanning electron microscopy images generated by an Hitachi TM3030Plus.

III. Results and Discussions

SEM image analysis was conducted to determine the relationship between the types of deformation namely extrusions and cavities with the resultant fibre orientations. To understand the deviations occurring from surface modification, this analysis was conducted on the flat surface collector as a control. This collector demonstrated the expected occurrence of relative randomness in fibre orientation (Figure 7)[1].

A. *Extrusion-Fibre relationships*

The electrospun fibres did not coat the large semi-sphere extrusion as intended; rather the electrostatic forces seemed to attract these fibres away (towards the more conductive

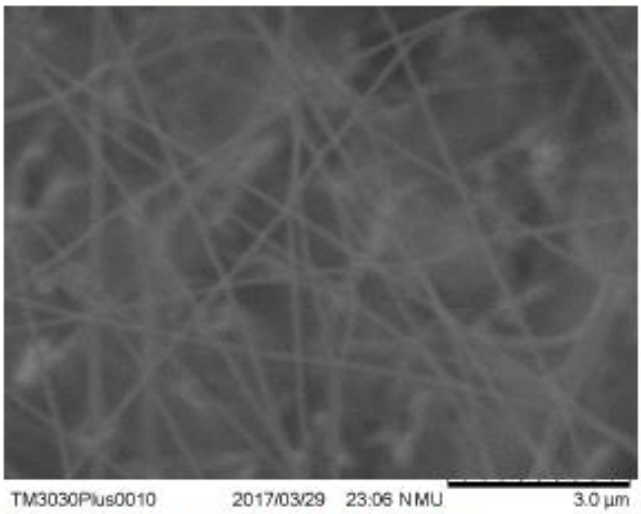

Figure 7: Randomly orientated fibers upon flat collector

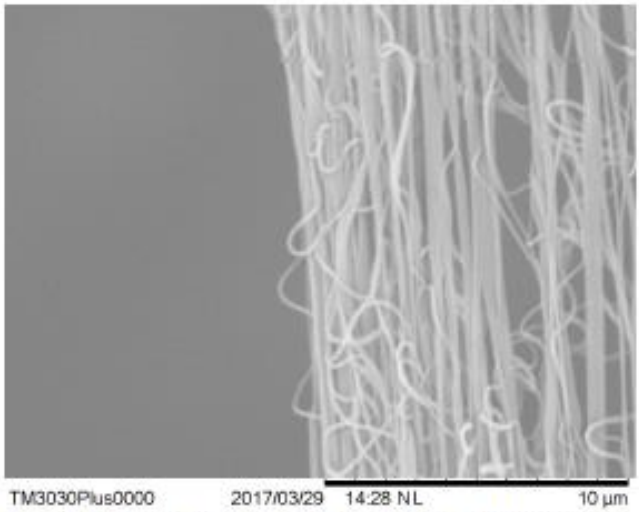

Figure 5: SEM image of relatively aligned fibre stretching the gap between extrusions

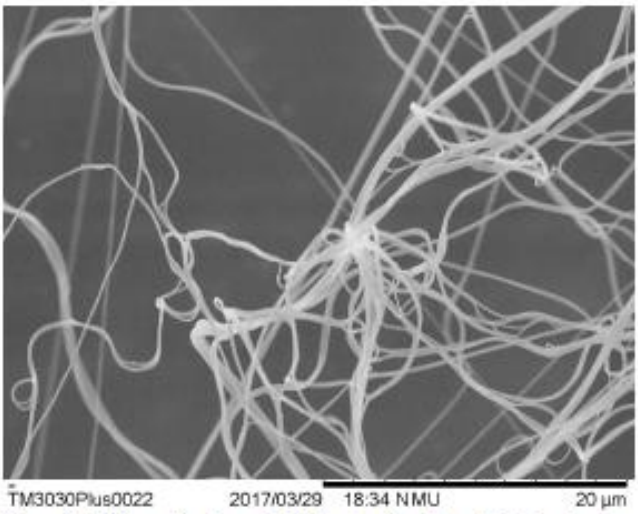

Figure 6: SEM imaging of summit (highest area) of the extruded semi-sphere

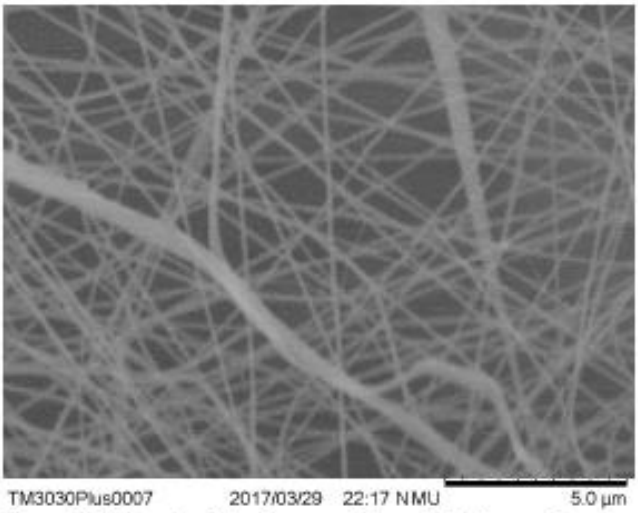

Figure 8: SEM imaging of the electrospun fiber at the dog-bone analogue edge

surfaces) leaving few fibres on the summit of the relatively nonconductive area (Figure 6). This relationship of fibre to conductive regions seemed to differ in the patterned semi-sphere extrusions, namely this sample yielded a majority of fibre occurring at the extrusion summits. Instead of the expected embedded array of fibre between extrusions, the material seemed to stretch across the gaps between the patterns (Interestingly this material seemed to occur in a relatively aligned formation (Figure 5)). Fibre also occurred on the summit of the dog-bone analogue, with modifications to the width of this yielding little effect on the resultant fibres. Of interest was the nature of the material along the edge of the extrusion (Figure 8), this seemed to stretch away from the edge towards the base (forming an apparent hypotenuse) and is potentially due to the latent momentum from the material whipping within the electrospinning process. This apparent movement of fibre reiterated the understanding generated from the large extrusion, namely the attraction of material to a more conductive areas. Generally, collection surfaces that are too close to the extrusion point result in 'wet' electrospinning in which the solvent from solution has not evaporated completely [1]. It should be noted that no wet electrospinning characteristics could be identified in this study. From these samples, a relationship to both the degree of extrusion as well as proximity of extrusions is hypothesized, namely:

- At a critical extrusion height from a conductive base, fibres will no longer occur on the surface summit. This coincides with literature in which optimal electrospinning is described as occurring at specific distances between collection and extrusion regions (relative to voltage and solution utilized) [1, 21].
- At a critical distance between extrusions, fibres will proceed to stretch across this distance.

B. *Cavity-Fibre relationship*

Electrospun material did not actively seem to conglomerate in the large semi-sphere cavity, rather material began to stretch across the gap and resulted in the partial covering of the opening (once again this stretched fibre resulted in the formation of a relative alignment as can be seen in Figure 9). A similar effect occurred on the patterned sample with the

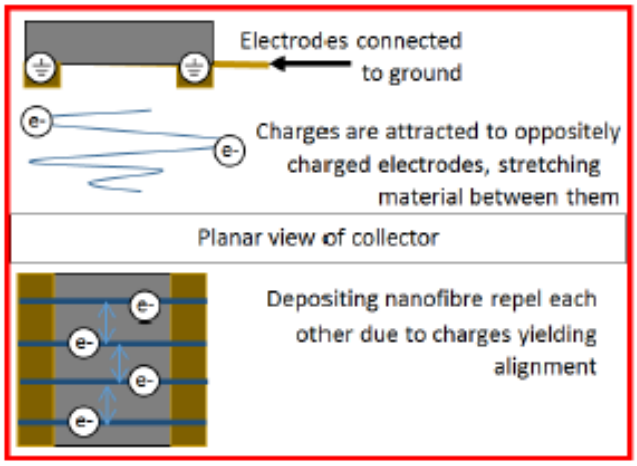

Figure 11: Figure illustrating the repulsion of charged fibres in a parallel electrode configuration

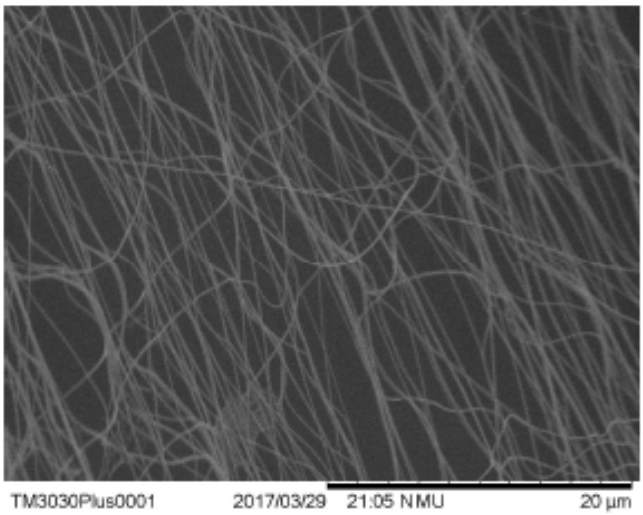

Figure 9: SEM of Large semi-sphere cavity highlighting the relative alignment of fibres spanning the gap.

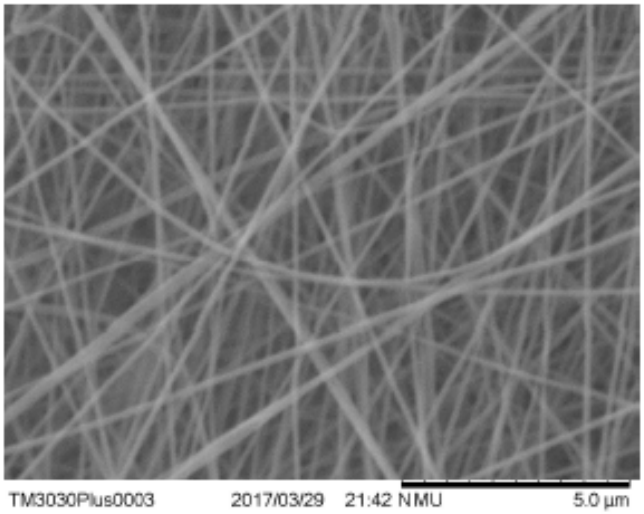

Figure 10: Relatively randomized fibers upon patterned semi-sphere collector

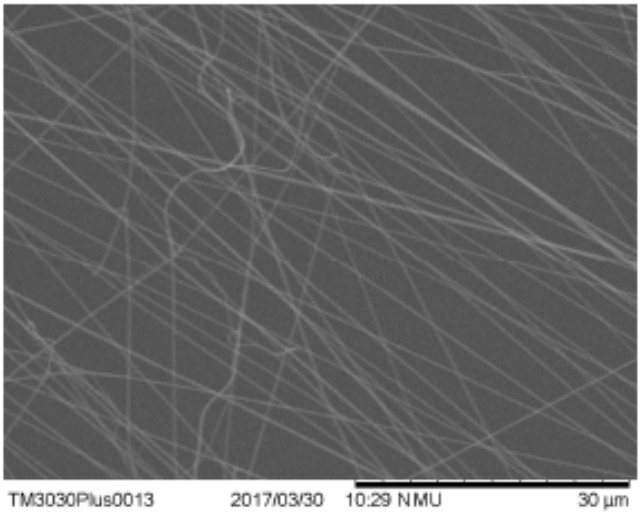

Figure 12: Relative alignment demonstrated by fibers spanning the smaller gap of the dog-bone analogue cavity

material completely covering the gaps. Interestingly no discernable change to fibre alignment/placement could be identified, with the resultant fibres echoing those seen in the control (flat collector) (Figure 10). The dog-bone analogue demonstrated a partial covering of the cavity as well. This occurred only at the central and smaller gap of the cavity and once again demonstrated relative alignment (Figure 12). These samples reiterate the previous hypothesis regarding the critical distance between extrusions and the stretching of fibres between them, however there is an apparent disparity in the understanding regarding the collection of material in more conductive regions. This inconsistency is derived from fibre occurring on the large semi-sphere surfaces. In the case of the extrusion the lack of fibre was associated with a lower conductivity whereas in the case of the cavity regions presumably with similar conductivity were coated in fibre. Potentially this is due to the nature of the occurring grounded areas, namely the relatively grounded area in the cavity sample was much smaller than that of the extrusion.

C. *Alignment*

Whilst this study did not actively pursue the generation of alignment it is interesting to note the occurrence of this feature within the patterned extrusion, large semi-sphere cavity, and dog-bone analogue cavity. Alignment within electrospinning studies has been recorded as the result of the electrostatic repulsion of distributed fibres upon subsequent fibre [11](an example of this is shown in Figure 11). This study utilized no active encouragement of alignment via mechanical or electrostatic actuation; as such, the formation of alignment is reliant on current literatures understanding of inter-fibre electrostatic repulsion yielding alignment. Additionally the loss of relative alignment was present for the air gap of 30mm present in the Semi-Sphere cavity thus coinciding with statements found in [9, 14, 16].

IV. Conclusion and Recommendations

The results from this study demonstrated the submicron and nanofibre fabrication capability of this technology (these occurring on each surface). Although the results of this study demonstrated, appealing characteristics (nanofibre and fibre alignment), these did not occur in a controlled manner yielding variation in diameter and general placement. This study was beneficial in highlighting some potential concerns for electrospinning onto three dimensional surfaces and hints that mold based fabrication through electrospinning is not a viable option. It should however be noted that some of the characteristics discovered in the study could potentially be a result of the equipment utilized and as such further investigation into the methodologies employed for fibre placement/control is required. The following recommendations are made for future work involving similar collecting surface modifications:

- *Large semi-sphere extrusion and cavity*: Future work regarding a mold/coating based approach should investigate the use of a uniformly conductive surface.
- *Patterned semi-sphere extrusions and cavities*: An increase in the patterned objects dimensions as well as increase the extrusion distances should be implemented in an attempt to force the fibre to the more conductive areas.
- *Dog-bone analogues/Parallel edges*: To attain electrospun material on parallel surfaces future work should investigate the use of deformed conductive surfaces. Of interest is the scaling capability of the fibres occurring analogous to the hypotenuse from the summit and base of the parallel edge.

V. Acknowledgements

The author would like to thank Ian Hosie (C.T.O. of Revolutions Ltd.) for providing the electrospinning apparatus and solution required for this study. Thanks are given to the New Zealand National Science Challenge for funding this work.

References

[1] M. Mirjalili and S. Zohoori, "Review for application of electrospinning and electrospun nanofibers technology in textile industry," *Journal of Nanostructure in Chemistry*, vol. 6, pp. 207-213, Sep 2016.

[2] D. Li and Y. Xia, "Electrospinning of Nanofibers:Reinventing the Wheel?**," *ADVANCED MATERIALS*, vol. 16, pp. 1151-1167, 2004.

[3] T. D. Brown, P. D. Daltona, and D. W. Hutmacher, "Melt electrospinning today: An opportune time for an emerging polymer process," *Progress in Polymer Science*, vol. 56, pp. 116-166, May 2016.

[4] B. Kong and S. L. Mi, "Electrospun Scaffolds for Corneal Tissue Engineering: A Review," *Materials*, vol. 9, p. 614, Aug 2016.

[5] M. J. Fullana and G. E. Wnek, "Electrospun collagen and its applications in regenerative medicine," *Drug Deliv Transl Res*, vol. 2, pp. 313-22, Oct 2012.

[6] W. Cui, Y. Zhou, and J. Chang, "Electrospun nanofibrous materials for tissue engineering and drug delivery," *Sci Technol Adv Mater*, vol. 11, p. 014108, Feb 2010.

[7] J. A. Matthews, G. E. Wnek, D. G. Simpson, and G. L. Bowlin, "Electrospinning of Collagen Nanofibers," *Biomacromolecules*, vol. 3, pp. 232-238, 2002.

[8] B. S. Jha, R. J. Colello, J. R. Bowman, S. A. Sell, K. D. Lee, J. W. Bigbee, *et al.*, "Two pole air gap electrospinning: Fabrication of highly aligned, three-dimensional scaffolds for nerve reconstruction," *Acta Biomater*, vol. 7, pp. 203-15, Jan 2011.

[9] S. B. Orr, A. Chainani, K. J. Hippensteel, A. Kishan, C. Gilchrist, N. W. Garrigues, *et al.*, "Aligned multilayered electrospun scaffolds for rotator cuff tendon tissue engineering," *Acta Biomater,* vol. 24, pp. 117-26, Sep 2015.

[10] V. P. Secasanu, C. K. Giardina, and Y. Wang, "A novel electrospinning target to improve the yield of uniaxially aligned fibers," *Biotechnol Prog,* vol. 25, pp. 1169-75, Jul-Aug 2009.

[11] K. Garg and G. L. Bowlin, "Electrospinning jets and nanofibrous structures," *Biomicrofluidics,* vol. 5, p. 13403, Mar 30 2011.

[12] J. Cheng, Y. Jun, J. Qin, and S. H. Lee, "Electrospinning versus microfluidic spinning of functional fibers for biomedical applications," *Biomaterials,* vol. 114, pp. 121-143, Jan 2017.

[13] A. Haider, S. Haider, and I.-K. Kang, "A comprehensive review summarizing the effect of electrospinning parameters and potential applications of nanofibers in biomedical and biotechnology," *Arabian Journal of Chemistry,* 2015.

[14] L. Persano, A. Camposeo, C. Tekmen, and D. Pisignano, "Industrial Upscaling of Electrospinning and Applications of Polymer Nanofibers: A Review," *Macromolecular Materials and Engineering,* vol. 298, pp. 504-520, May 2013.

[15] D. Li, Y. Wang, and Y. Xia*, "Electrospinning of Polymeric and Ceramic Nanofibers as Uniaxially Aligned Arrays," *Nano Letters,* vol. 3, pp. 1167 - 1171, 2003.

[16] Dan Li, Gong Ouyang, Jesse T. McCann, and Younan Xia, "Collecting Electrospun Nanofibers with patterned electrodes," *NANO LETTERS,* vol. 5, pp. 913-916, 2005.

[17] G. Luo, K. S. Teh, Y. Liu, X. Zang, Z. Wen, and L. Lin, "Direct-Write, Self-Aligned Electrospinning on Paper for Controllable Fabrication of Three-Dimensional Structures," *ACS Appl Mater Interfaces,* vol. 7, pp. 27765-70, Dec 23 2015.

[18] Electrospinz. (5/04). *Electrospinz Laboratory ES Family*. Available: http://www.electrospinz.co.nz/products.php

[19] P. D. Dalton, C. Vaquette, B. L. Farrugia, T. R. Dargaville, T. D. Brown, and D. W. Hutmacher, "Electrospinning and additive manufacturing: converging technologies," *Biomaterials Science,* vol. 1, pp. 171-185, 2013.

[20] C. Dhand, S. T. Ong, N. Dwivedi, S. M. Diaz, J. R. Venugopal, B. Navaneethan, *et al.*, "Bio-inspired in situ crosslinking and mineralization of electrospun collagen scaffolds for bone tissue engineering," *Biomaterials,* vol. 104, pp. 323-38, Oct 2016.

[21] K. Garg and G. L. Bowlin, "Electrospinning jets and nanofibrous structures," *Biomicrofluidics,* vol. 5, pp. 1-16, 2011.

DRC 16

MASSEY UNIVERSITY
GRADUATE RESEARCH SCHOOL

STATEMENT OF CONTRIBUTION
DOCTORATE WITH PUBLICATIONS/MANUSCRIPTS

We, the candidate and the candidate's Primary Supervisor, certify that all co-authors have consented to their work being included in the thesis and they have accepted the candidate's contribution as indicated below in the *Statement of Originality*.

Name of candidate:	Juan Schutte
Name/title of Primary Supervisor:	Prof. Johan Potgieter
Name of Research Output and full reference:	
The opportunity of electrospinning as a form of additive manufacturing in biotechnology	
In which Chapter is the Manuscript /Published work:	Chapter 6
Please indicate:	
• The percentage of the manuscript/Published Work that was contributed by the candidate:	100
and	
• Describe the contribution that the candidate has made to the Manuscript/Published Work:	
The candidate has written the majority of the manuscript. The candidate has conducted the experimentation and analysis required for this publication.	
For manuscripts intended for publication please indicate target journal:	
Candidate's Signature:	Digitally signed by Juan Schutte Date: 2019.06.04 15:23:23 +12'00'
Date:	04/06/2019
Primary Supervisor's Signature:	Johan Potgieter Digitally signed by Johan Potgieter Date: 2019.06.06 11:09:11 +12'00'
Date:	06/06/2019

(This form should appear at the end of each thesis chapter/section/appendix submitted as a manuscript/ publication or collected as an appendix at the end of the thesis)

GRS Version 4– January 2019

The opportunity of Electrospinning as a form of Additive Manufacturing in Biotechnology

Juan Schutte, Xiaowen Yuan, Steven Dirven, Johan Potgieter
School of Engineering and Advanced Technology, Massey University
Auckland, New Zealand
j.schutte@massey.ac.nz

***Abstract*—3D Printing additive manufacturing is a rapidly developing form of technology. Currently able to manipulate many polymers (both synthetic and organic), this technique is quickly becoming an integral part of biotechnological developments. This paper highlights the fundamentals of this technology namely the mechanisms employed in standard 3D printing, it then introduces tissue engineering a field in which current versions of this technology have been employed as bioprinting. The limitations with respect to tissue engineering are discussed outlining the current technologies inability to produce nanofibre based structures common in tissue such as tendon, cartilage and cornea. From this requirement for nanofibre production, electrospinning is introduced as a potential pathway for future tissue engineering 3D printing technologies and finally the current combination of this technology with 3D Printing is discussed yielding current limitations in retaining required nano-resolutions.**

Keywords— 3D Printing, Additive manufacturing, Tissue Engineering, Bioprinting, Nanofibre, Electrospinning

I. INTRODUCTION

Additive manufacturing(AM) is described as the successive introduction of material in a specific order to develop/generate a final structure [1]. One of the most prominent forms of this technology is 3D Printing (3DP). This is a rapidly growing prototyping and manufacturing technology that occurs in many different forms for various materials and functionalities. Variation in mechanism employed are due to differences in the properties of various materials (e.g. viscosity, thermal reactivity etc.) three distinct processing methodologies have been developed namely: material deposition, processing of powders or processing of liquids [2] (the range of this technology is depicted in *Figure 1*). The fundamental feature of this technology is the layer-by-layer introduction and processing of material to generate three-dimensional objects. 3DP has developed to be capable of processing both synthetic and organic polymers as such it has found uses in many industries including biotechnology, particularly in the field of Tissue engineering (TE). This discipline has been described as the result of a combination of biomimicry, autonomous self-assembly and grouping of mini-tissue building blocks to generate desirable organic material/tissue [3]. In this instance, biomimicry refers to the desire for replication of biological constructs. Successful biomimicry is dependent on the understanding and replication of the fundamental aspects/constituents of biological constructs. Early cellular components are capable of self-induced/generated organizational development that allows for the formation of required micro-architecture and biological function, and is referred to as autonomous self-assembly. This capability is due to the inherent capabilities of early cellular components to generate extracellular matrix (ECM) components, appropriate cell signaling, autonomous organization and patterning. Additionally tissues can often be segmented into small functional parts or mini-tissues, which can be appropriately placed and through the aid of tissue/cellular properties such as self-assembly the larger functional tissue/organ can be mimicked/produced [3]. These fundamental properties of TE together with an adept understanding within the fields of engineering, imaging, biomaterials, cell biology, biophysics and medicine with respect to the desired biological construct are manipulated through the utilization of 3DP technology in the form of Bioprinting (BP) to manufacture desirable tissue [4-6]. Whilst proven in its capability to produce tissue for TE, this technology is currently restricted by its inability to generate certain desirable features found in vivo. One such feature relates to the occurrence of fibre-based constructs within tissue such as cartilage, tendon, muscle and cornea. This limitation of BP has led researchers to identify a plausible technology capable of fibre production. One such technology of increasing prominence within AM and TE is Electrospinning (ES). This is a relatively rapid, efficient and inexpensive process which exploits the characteristics of electric fields, surface charge and Coulombic forces to generate nanofibers from polymer-solvent solutions [7-10]. Nano- and micro-scale fibres have been electro-spun from over 200 polymers (both natural and synthetic polymers) [11]. This process can occur through the utilization of a controlled or uncontrolled extrusion/feed system [12]. Given that controlled systems allow for greater control of fibre properties (quality and diameter) as well as having a higher success rate in ES, these will be of predominant interest in this paper as these are fundamental features of AM [9, 13-15].

This work is funded through the New Zealand National Science Challenge.

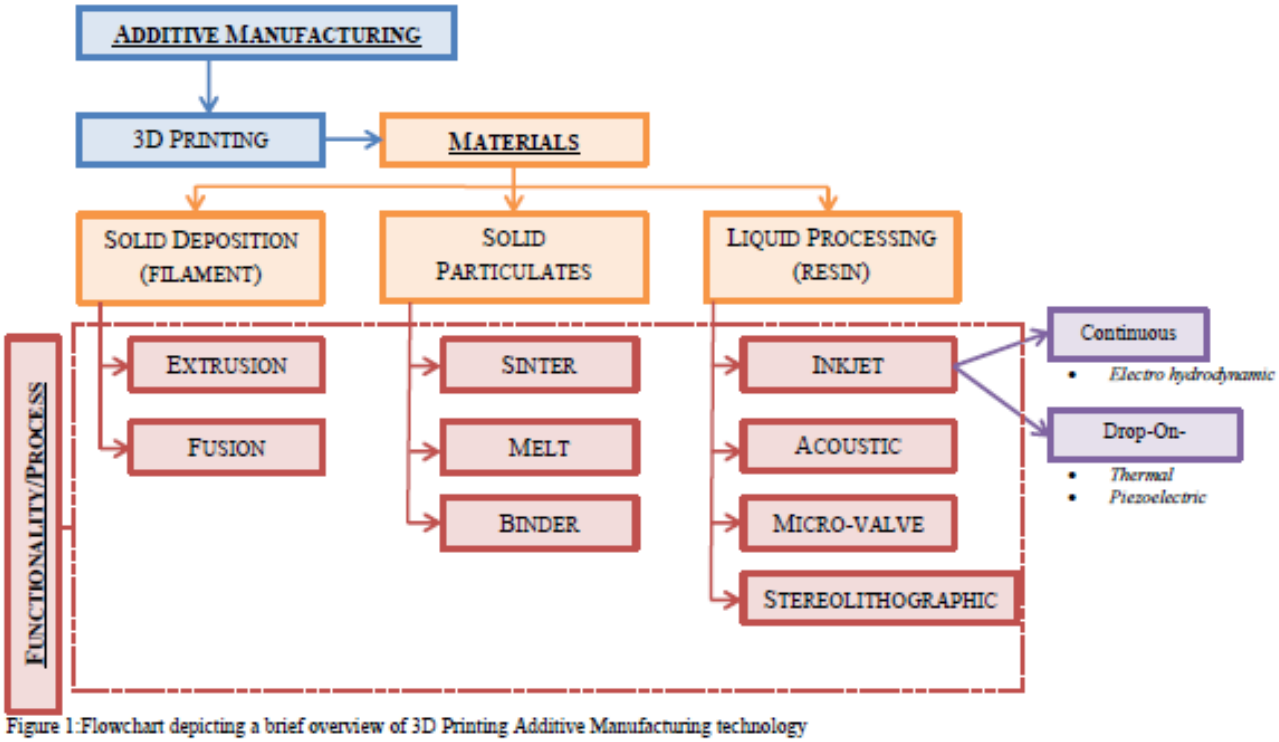

Figure 1:Flowchart depicting a brief overview of 3D Printing Additive Manufacturing technology

This paper will serve as a brief overview of topics concerning the practices of 3DP, the relevance of these to TE, the application of 3DP in TE as BP, the unmet requirements of TE, ES as a resolution to TE requirements, and finally the application of 3DP in ES. This work forms part of ongoing research regarding the developments of AM in TE.

II. 3D PRINTING MECHANISMS AND LIMITATIONS

In order to understand the opportunity for developments within any form of 3DP an analysis must first be conducted regarding the current capabilities and mechanisms employed by the technology.

Standardized 3DP AM is generally classified into three forms relating to the types of material processed [1], namely filaments, particulates and liquids. Within these groups there are many different variations of 3DP mechanisms (for more information regarding these see [1, 16, 17]). Whilst there are many forms of the technology, fundamentally all 3DP can be described by the following process steps [16]:

- Controlled and actuated (often mechanical or pneumatic) introduction of material to a processing region.
- Material is processed (generally through thermal actuation) at a controlled region (this region typically becomes the previously processed region if subsequent layers exist).
- Once the above steps have repeated enough to yield the desired object, it is then ready to be removed from the processing region.
- The removal of 3DP parts often requires the post process removal of support material (either in the form of printed support structures or unprocessed material).

A. Viscosity, support material and resolution

Material viscosities restrict the type of methodology utilized. Higher and lower viscosities are better processed by deposition and liquid processing methodologies respectively [1, 16]. Both deposition and droplet-based liquid processing methodologies often require support structures/material when complex objects containing overhangs are produced. This must be removed through some form of post processing to yield the desired object [16]. Stereolithographic and powder processing AM involves the layer-by-layer introduction of a bed/layer of powder material through a powder spreading/roller mechanism allowing previous layers to act as support material, thus this requires less post processing (material removal). Material deposition AM in the form of extrusion techniques have relatively limited resolutions when compared to other forms of AM [1] (it is due to this limitation that post processing to improve the surface quality of material deposition AM is often required). Currently the highest printing resolution occurs in liquid processing AM [16]. The above 3DP technologies typically utilize common manufacturing materials (Synthetic polymers and Metals) however recently similar AM methodologies have been utilized in TE.

The a fundamental feature of TE relates to the successive introduction of cellular building blocks to generate tissue is echoed in 3DP fundamental ordered introduction of material to generate objects. It must be noted however that due to the high temperatures and pressures employed by some 3DP mechanisms (e.g. fused deposition modelling, selective laser melting and inkjet printing) this technology will require modifications when dealing with biopolymer.

III. Bioprinting in Tissue Engineering

Bioprinting (BP) is an AM based practice, which utilizes organic material to generate organic objects and tissues that are highly sought after in the medical field [3, 18, 19]. The most prominent forms of BP technology are extrusion-based, droplet-based and laser assisted printing. These techniques are classified as either direct or indirect, where direct refers to the printing of the final organic structure and indirect refers to the formation of sacrificial molds/scaffolds into which material is distributed and allowed to mature ,after which these can require post-processing to remove [19]. Given that BP is a form of 3DP it shares similarities in both fundamental process steps and the nature of technological variation to overcome material processing requirements, namely a variation in the processing of macro (cell aggregate), micro (single cell) and nano(cells and proteins) [20].

Of specific TE interest are the differences between process able biomaterial, acceptable viscosities, cell viability, vertical print quality, and resultant cell density[21]. These differences are described below:

Laser assisted BP is capable of processing biomaterials in a moderate range of 1-300mPa/s whereas inkjet techniques are associated with lower viscosity ranges (3.5-12mPa/s [3, 21]). This differs with extrusion techniques which require bio-material to have relatively high viscosity (ranging from 30mPa/s-over 6x10^7mPa/s [21]) to restrict the unwanted leaking of material from the extrusion mechanism [18]. Both inkjet and laser assisted techniques are associated with poor and fair vertical structure quality whilst having high print resolution (with some inkjet techniques such as electrohydrodynamic printing capable of resolutions <10µm) whereas extrusion techniques have good vertical structure quality with moderate resolution (generally unable to accurately produce biological objects smaller than 100µm [22]). Typically resolutions in the range of 10-1000µm are utilized. Inkjet, Laser assisted and extrusion techniques have low (<10^6 cells/mL), medium (<10^8 cells/mL) and High (in the case of cell spheroids) resultant cell densities. The resultant cell viability of extrusion techniques are lower than that of droplet-based BP, where cell survival rates are dependent on extrusion pressure and nozzle size [3]. Inkjet BP has been recorded as capable of producing droplet sizes ranging from <1pL to >300pL with deposition rates from 1 - 10000 droplets per second, these capabilities have allowed for the production of 50µm wide lines (produced via patterned drops) of one or two cells [3]. Both the inkjet and extrusion BP processes are limited by the depositing mechanism namely issues associated with nozzle size, nozzle clogging (through material sedimentation and aggregation), spatial accuracy, exertion of shear stress on material [3, 23, 24]. Current BP practices predominantly focus on the accurate placement of a cell or group of cells. Most of these 3DP practices are limited by the predominant reliance on the utilization of heat and pressure for higher resolutions (an exception being that of electrohydrodynamic printing [25, 26]) which can yield complications and damages(known as denaturing) to the biological material (illustrated in *Figure 2*).

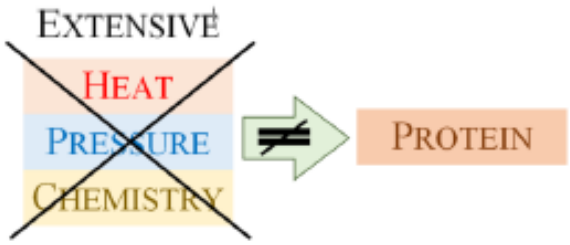

Figure 2: The fundamental restrictions associated with biological material manipulation.

An understanding of the current technology for the generation of biological constructs is not sufficient for the reproduction of tissues as there is a lack of 3DP and BP methodologies for the production of fibre for the generation of fibre based constructs which can be seen in biological constructs such as tendon, cornea and muscle. These limitations reveal a requirement to further investigate the development of a biopolymer friendly form of nanofiber production based AM technology.

A. Deriving Nano-fibres

Many technologies exist to produce nanofibres, some of which include: Forcespinning, Melt blowing, flashspinning, biocomponentspinning, phase separation, drawing and ES. This technique (with the exception of melt ES) does not expose material to the high temperatures associated with processes such as Meltblowing and Forcespinning allowing for fabrication utilizing temperature sensitive polymers or proteins. When compared to Template synthesis or Self-assembly, the ES process is relatively simple, potentially yielding less room for error. Other techniques such as Phase-separation (limited to certain polymers) or drawing (a discontinuous process) are relatively simplistic, however these lack the scalability and control associated with ES [12]. In general, for nanofibre production ES, whilst not perfect and limited by timeous/productivity and solvency recovery issues, it appears as an optimal methodology for the future progression of AM in TE.

IV. ELECTROSPINNING

The typical ES procedure is similar to that of certain 3DP techniques in that both systems incorporate the mechanical actuation of material to a point of processing. The techniques differ in that instead of thermal actuation the use of a high voltage exposure (generally above 20 kV) [8, 27] results in a malleability and movement/deposition of material (the standardized electrospinning apparatus is depicted in *Figure 3*). Standard ES occurs through the utilization of a single nozzle charged extruder, which produces a single jet/stream of material. *Nayak et al* sited this as a cause for relatively low production of fibre over a given time period and stated an average production of 300mg/h [12]. To overcome this productivity based issue multiple needles, and needless systems forms of extruders have been utilized.

As with 3DP technology the mechanisms employed in this process vary according to the requirements of both the material being processed as well as the desired outcome. Two prominent features resulting in variation are the nature of solvent toxicity and desirability for alignment.

A. ES solvent toxicity

Solvents utilized within this process are acidic and can result in toxicity yielding complications in biocompatibility[9]. Melt ES is an alternative form of ES that utilizes heat to melt polymers allowing for ES with less concern for toxicity from solvents. This is however a relatively underdeveloped process (limited to approximately 100 published articles) and currently is recorded as only capable of producing fibres much larger than those seen in traditional ES [10]. This technique is reliant on the utilization of high temperatures which can be detrimental to biological material as such is highly unlikely to be implemented in biotechnology. Coaxial ES refers to ES, which utilizes a 'needle within a needle' system to overcome solvent limitations. This technique allows for the introduction of an additional material into the ES process and yields sheath-core fibres where the inner and outer materials of the fibres differ. The outer/sheath material assists or carries the inner material in the ES process. This technique is used to electrospin material that either resists the process or requires hazardous solvents. Emulsion ES can yield similar results, however instead of requiring complex needle components this form of ES utilizes a chemical means of separation between the materials within a single solution [28]. Coaxial and emulsion electro-spun fibres tend to be larger than those generated by traditional ES [28, 29].

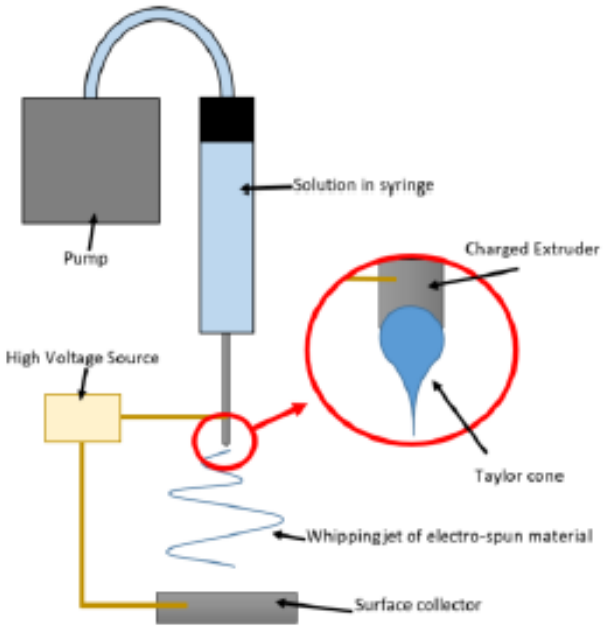

Figure 3: Figure illustrating the components and features of electrospinning

B. ES aligned fibre

Standardized ES utilizing a flat surface as the collecting area, yields networks of randomized fibrils [7, 30]. The alignment of which can be altered through the application of strain, thermodynamics or magnetism during polymerization [30]. Within ES, techniques the modification and actuation of the collecting surface can help generate alignment in produced fibres. The collecting surface has been split to generate a parallel electrode configuration with an airgap (sometimes filled with non-conductive collecting plate), and has been actuated to form rotating drum, disk, and conveyor collectors [7, 9, 14]. The use of rotational actuation generates alignment of fibre in the direction of rotation; this alignment and relatively even distribution is due to the mutual electrostatic repulsion between deposited fibres [7]. It must also be noted that by varying rotation speed, resultant fibre alignment can also be manipulated [8]. A major advantage of this mechanism is that it retains functionality when scaled for larger manufacturing requirements. For even greater control of the direction of fibre alignment collecting areas utilizing a split-electrode/air-gap configuration have been utilized [31]. This methodology exploits the electrostatic attraction of the formed nanofibre to oppositely charged areas, resulting in the stretching of the fibre between electrodes[8]. It must be noted that this mechanism is relatively restricted by scale (relative alignment lost at gaps greater than 30mm [32-34]. A recent study by Orr *et al* demonstrated that through the combination of alignment mechanisms these spatial limitations could be relatively overcome. In this study a combination of ceramic magnets, parallel copper electrodes and distilled water was utilized to allow for alignment over a 100mm distance [32]. Another relatively underdeveloped method, which allows for even greater control of distributed fibre is that of direct writing ES. This control is derived from the automation of either collector or extruder at short collection distances. These shorter distances allow for the reduction in randomized jet instabilities this will however result in less evaporation yielding wet ES [35].

C. *Functionality of ES material*

One of the major differences between a 3DP and a ES process relates to the nature of the resultant material. Once processed printed material can be easily manipulated, this is not the case for ES fibre mats. Often functionalization procedures are utilized to generate additional crosslinks and bonding between the fibres to reinforce the connection and allow for greater manipulation. This has occurred through the exposure of vapour bath systems as well as more direct application methodologies. Predominantly this application of agents has occurred as a post process separate to the ES procedure, however recently advances have been made to incorporate forms of 3DP within the process to accomplish this in a more automated fashion.

D. *ES limitations*

Currently ES is limited to the fabrication of mats (two dimensional objects). Due to the accumulation of charge from electrospun fibres on the collecting surface, resultant material is restricted to a thickness of approximately 3-4mm [36]. Additional ES limitations involve the hazardous nature of solvents utilized, efficiency/productivity and generated fibre control. In order to overcome these limitations as well as the functionality requirements of ES research has investigated the combination of this process with those of 3DP. Both extrusion and droplet based 3DP AM techniques have been employed alongside ES, generally in the form of a layer from one process being followed by a layer from the other process. This has enabled the construction of objects with a higher degree of three dimensionality as well as increased functionalization/bonding [36-38].

V. Conclusion

In conclusion, current AM technology has been thoroughly applied as a form of Biotechnology for scaffold and tissue fabrication at a micron scale. Current limitations in BP include the inability to produce complex fibre-based structures such as tendon. In order to fabricate these micron and nano-based fibres additional technology has been investigated, a promising process to accomplish this is through ES. This technology is similar to AM in that it is a depositional technology. Current research has implemented a combination of previously established 3DP technology and ES methodologies to develop fibre-based structures. This paper has yielded a good foundation for future research regarding the developments of AM in TE.

VI. Acknowledgements

The author would like to thank the New Zealand National Science Challenge for funding this work.

VII. References

[1] J. Gardan, "Additive manufacturing technologies: state of the art and trends," *International Journal of Production Research,* vol. 54, pp. 3118-3132, 2015.

[2] K. V. Wong and A. Hernandez, "A Review of Additive Manufacturing," *ISRN Mechanical Engineering,* vol. 2012, pp. 1-10, 2012.

[3] S. V. Murphy and A. Atala, "3D bioprinting of tissues and organs," *Nat Biotechnol,* vol. 32, pp. 773-785, Aug 2014.

[4] H. J. Levis, A. K. Kureshi, I. Massie, L. Morgan, A. J. Vernon, and J. T. Daniels, "Tissue Engineering the Cornea: The Evolution of RAFT," *J Funct Biomater,* vol. 6, pp. 50-65, Jan 22 2015.

[5] M. Miotto, R. M. Gouveia, and C. J. Connon, "Peptide Amphiphiles in Corneal Tissue Engineering," *J Funct Biomater,* vol. 6, pp. 687-707, Aug 06 2015.

[6] A. Shah, J. Burgnano, S. Sun, A. Vase, and E. Orwin, "The Development of a Tissue-Engineered Cornea: Biomaterials and Culture Methods," *International Pediatric Research Foundation, Inc.,* vol. 63, p. 535, 2008.

[7] K. Garg and G. L. Bowlin, "Electrospinning jets and nanofibrous structures," *Biomicrofluidics,* vol. 5, p. 13403, Mar 30 2011.

[8] M. Mirjalili and S. Zohoori, "Review for application of electrospinning and electrospun nanofibers technology in textile industry," *Journal of Nanostructure in Chemistry,* vol. 6, pp. 207-213, Sep 2016.

[9] D. Li and Y. Xia, "Electrospinning of Nanofibers:Reinventing the Wheel?**," *ADVANCED MATERIALS,* vol. 16, pp. 1151-1167, 2004.

[10] T. D. Brown, P. D. Daltona, and D. W. Hutmacher, "Melt electrospinning today: An opportune time for an emerging polymer process," *Progress in Polymer Science,* vol. 56, pp. 116-166, May 2016.

[11] B. Kong and S. L. Mi, "Electrospun Scaffolds for Corneal Tissue Engineering: A Review," *Materials,* vol. 9, p. 614, Aug 2016.

[12] R. Nayak, R. Padhye, I. Kyratzis, Y. B. Truong, and L. Arnold, "Recent advances in nanofibre fabrication techniques," *Textile Research Journal,* vol. 82, pp. 129-147, Jan 2012.

[13] M. J. Fullana and G. E. Wnek, "Electrospun collagen and its applications in regenerative medicine," *Drug Deliv Transl Res,* vol. 2, pp. 313-22, Oct 2012.

[14] W. Cui, Y. Zhou, and J. Chang, "Electrospun nanofibrous materials for tissue engineering and drug delivery," *Sci Technol Adv Mater,* vol. 11, p. 014108, Feb 2010.

[15] J. A. Matthews, G. E. Wnek, D. G. Simpson, and G. L. Bowlin, "Electrospinning of Collagen Nanofibers," *Biomacromolecules,* vol. 3, pp. 232-238, 2002.

[16] F. Calignano, D. Manfredi, E. P. Ambrosio, S. Biamino, M. Lombardi, E. Atzeni, *et al.*, "Overview on Additive Manufacturing Technologies," *Proceedings of the IEEE,* pp. 1-20, 2017.

[17] W. Gao, Y. B. Zhang, D. Ramanujan, K. Ramani, Y. Chen, C. B. Williams, *et al.*, "The status, challenges, and future of additive manufacturing in engineering," *Computer-Aided Design,* vol. 69, pp. 65-89, Dec 2015.

[18] F. P. W. Melchels, M. A. N. Domingos, T. J. Klein, J. Malda, P. J. Bartolo, and D. W. Hutmacher, "Additive manufacturing of tissues and organs," *Progress in Polymer Science,* vol. 37, pp. 1079-1104, Aug 2012.

[19] Y. S. Zhang, K. Yue, J. Aleman, K. Mollazadeh-Moghaddam, S. M. Bakht, J. Yang, *et al.*, "3D Bioprinting for Tissue and Organ Fabrication," *Ann Biomed Eng,* vol. 45, pp. 148-163, Jan 2017.

[20] C. K. Chua and W. Y. Yeong, "Chapter 3 Bioprinting Techniques," in *Bioprinting Principles and Applications*, ed Singapore: World Scientific Publishing Co. Pte. Ltd., 2015, pp. 63-111.

[21] C. Mandrycky, Z. Wang, K. Kim, and D. H. Kim, "3D bioprinting for engineering complex tissues," *Biotechnol Adv,* vol. 34, pp. 422-34, Jul-Aug 2016.

[22] I. T. Ozbolat and M. Hospodiuk, "Current advances and future perspectives in extrusion-based bioprinting," *Biomaterials,* vol. 76, pp. 321-43, Jan 2016.

[23] A. D. Dias, D. M. Kingsley, and D. T. Corr, "Recent advances in bioprinting and applications for biosensing," *Biosensors (Basel),* vol. 4, pp. 111-36, Jun 2014.

[24] P. G. Campbell and L. E. Weiss, "Tissue engineering with the aid of inkjet printers," *Expert Opin Biol Ther,* vol. 7, pp. 1123-7, Aug 2007.

[25] K. Barton, S. Mishra, K. A. Shorter, A. Alleyne, P. Ferreira, and J. Rogers, "A desktop electrohydrodynamic jet printing system," *Mechatronics,* vol. 20, pp. 611-616, Aug 2010.

[26] S. N. Jayasinghe, A. N. Qureshi, and P. A. Eagles, "Electrohydrodynamic jet processing: an advanced electric-field-driven jetting phenomenon for processing living cells," *Small,* vol. 2, pp. 216-9, Feb 2006.

[27] K. Garg and G. L. Bowlin, "Electrospinning jets and nanofibrous structures," *Biomicrofluidics,* vol. 5, pp. 1-16, 2011.

[28] P. McClellan and W. J. Landis, "Recent Applications of Coaxial and Emulsion Electrospinning Methods in the Field of Tissue Engineering," *Biores Open Access,* vol. 5, pp. 212-27, 2016.

[29] N. Duan, X. Geng, L. Ye, A. Zhang, Z. Feng, L. Guo, *et al.*, "A vascular tissue engineering scaffold with core-shell structured nano-fibers formed by coaxial electrospinning and its biocompatibility evaluation," *Biomed Mater,* vol. 11, p. 035007, May 20 2016.

[30] L. A. Hapach, J. A. VanderBurgh, J. P. Miller, and C. A. Reinhart-King, "Manipulation of in vitro collagen matrix architecture for scaffolds of improved physiological relevance," *Phys Biol,* vol. 12, p. 061002, Dec 21 2015.

[31] D. Li, Y. Wang, and Y. Xia*, "Electrospinning of Polymeric and Ceramic Nanofibers as Uniaxially Aligned Arrays," *Nano Letters,* vol. 3, pp. 1167 - 1171, 2003.

[32] S. B. Orr, A. Chainani, K. J. Hippensteel, A. Kishan, C. Gilchrist, N. W. Garrigues, *et al.*, "Aligned multilayered electrospun scaffolds for rotator cuff tendon tissue engineering," *Acta Biomater,* vol. 24, pp. 117-26, Sep 2015.

[33] L. Persano, A. Camposeo, C. Tekmen, and D. Pisignano, "Industrial Upscaling of Electrospinning and Applications of Polymer Nanofibers: A Review," *Macromolecular Materials and Engineering,* vol. 298, pp. 504-520, May 2013.

[34] Dan Li, Gong Ouyang, Jesse T. McCann, and Younan Xia, "Collecting Electrospun Nanofibers with patterned electrodes," *NANO LETTERS,* vol. 5, pp. 913-916, 2005.

[35] G. Luo, K. S. Teh, Y. Liu, X. Zang, Z. Wen, and L. Lin, "Direct-Write, Self-Aligned Electrospinning on Paper for Controllable Fabrication of Three-Dimensional Structures," *ACS Appl Mater Interfaces,* vol. 7, pp. 27765-70, Dec 23 2015.

[36] P. D. Dalton, C. Vaquette, B. L. Farrugia, T. R. Dargaville, T. D. Brown, and D. W. Hutmacher, "Electrospinning and additive manufacturing: converging technologies," *Biomaterials Science,* vol. 1, pp. 171-185, 2013.

[37] T. Xu, K. W. Binder, M. Z. Albanna, D. Dice, W. Zhao, J. J. Yoo, *et al.*, "Hybrid printing of mechanically and biologically improved constructs for cartilage tissue engineering applications," *Biofabrication,* vol. 5, p. 015001, Mar 2013.

[38] W. Liu, D. Wang, J. Huang, Y. Wei, J. Xiong, W. Zhu, *et al.*, "Low-temperature deposition manufacturing: A novel and promising rapid prototyping technology for the fabrication of tissue-engineered scaffold," *Mater Sci Eng C Mater Biol Appl,* vol. 70, pp. 976-982, Jan 01 2017.

[1]

APPENDIX B: POSTERS PUBLISHED

NZ Product Accelerator

Project title: The Potential for Biofabrication of complex collagen tissues through Bioprinting methodologies

PhD Student: Juan Schutte Year: 2016 Affiliation: Massey University
Supervisor(s): A.Prof. Johan Potgieter, Dr. Steven Dirven, Dr Xiaowen Yuan

Project Aim:
This project aims to achieve the development of requirements for the production of complex collagen based tissues

Collagen:
Collagen is the most abundant form of fibrous protein within the animal kingdom and can be found in connective tissue and the extracellular matrix.

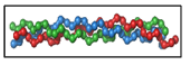

Corneas:
The cornea is an excellent example of a complex collagen tissue. This tissue is comprised of many layers containing collagen. One such layer is the Stroma, which makes up approximately 90% of the cornea. Research has shown a distinctive lack of viable Stroma analogue development.

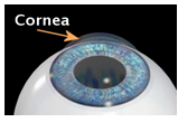

Stroma:
The Stroma provides an excellent example of a highly structured collagen based layer, consisting of predominantly Type I collagen. This layer provides much of the strength structure and transparency found in the cornea. The collagen within the Stroma occurs in the form of layers of interwoven sheets of aligned collagen called lamellae. Thus development of a means for replication of tissue similar to this could potentially allow for the generation of many fundamental collagen based constructs.

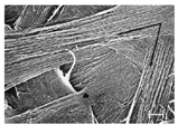

Relevant Technology:
Electrospinning is a capable methodology for the production of aligned nanofibers such as those found in the corneas Stroma. Unfortunately the process of electrospinning requires material to be exposed to solutions which are not biocompatible.
Traditional Bioprinting approaches deal predominantly with extrusion methodologies and heat. Issues regarding fibre control and delamination are prevalent within this technology which results in complications in the production of highly ordered tissue such as the Stroma.

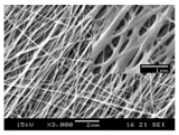

Research:
Within this project research including but not limited to biofabrication technologies, collagen properties, collagen processing methodologies, cornea production/processing technology, and fabricated collagen tissue biocompatibility will be conducted.

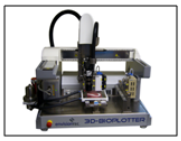

NZProduct Accelerator Research Meeting: 3rd August 2016

MASSEY UNIVERSITY
TE KUNENGA KI PŪREHUROA
UNIVERSITY OF NEW ZEALAND

The Potential of Bioprinting Technologies in the Production of Complex Collagen Tissues

Juan Schutte, Supervisor: A.Prof Johan Potgieter

School of Engineering and Advanced Technology (SEAT), Albany, Massey University, New Zealand

Collagen

Collagen is the most abundant form of fibrous protein within the animal kingdom and can be found in connective tissue and the extracellular matrix.

COLLAGEN STRUCTURE

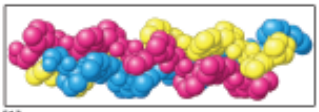

[1]

Corneas

One example of a collagen based tissue is the cornea. The cornea is comprised of clear dome-like layers which cover the front of the eye and enable vision. If the cornea is irreversibly damaged (be it from disease or injury) a corneal transplant is required. Often these transplants require donor corneas which are a finite resource in high demand. As such there is a need for the development of a method capable of producing complex collagen based tissues like the cornea.

CORNEA STRUCTURE

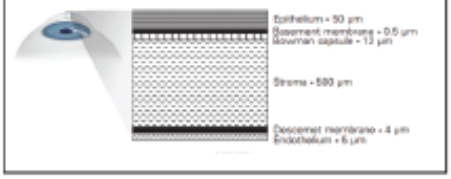

[2]

DESIRED OUTCOME

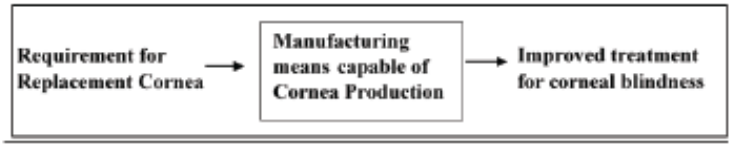

[3]

Bioprinting

One such method of production is bioprinting. Bioprinting involves the arrangement of biological matter in a manner that results in a useful organic structure. It should however be noted that for accurate bioprinting a thorough understanding of both the biological matter as well as the desired organic structure needs to be developed.

BIOPRINTER

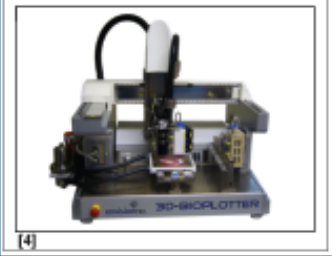

[4]

Research

Thus there is a need to develop a thorough understanding of collagen within complex collagen based tissue. research including but not limited to bioprinting technologies, collagen properties, collagen processing methodologies, cornea production/processing technology, and collagen bioprinting compatibility will be conducted.

BIOPRINTING

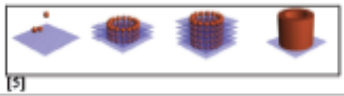

[5]

In closing it is the aim and objective of the above described project to achieve the development of requirements for the production of complex collagen based tissues.

[1] - Collagen Structure, Figure demonstrates the triple helix structure of collagen (Oregon State University, n.d.)
[2] - Cornea Structure, Figure demonstrates the commonly accepted layers of the cornealhelix structure of collagen (Vision Care Specialists, n.d.)
[3] - Desired Outcome, Figure demonstrates the current desired outcome for this project.
[4] - Bioprinter, Figure demonstrates Envisiontec's 3D Bioplotter Bioprinter (Chua & Yeong, 2015)
[5] - Bioprinting, Figure demonstrates an example of the implementation of Bioprinting to achieve a functional structure from cells (Chua & Yeong, 2015)

MASSEY UNIVERSITY
TE KUNENGA KI PŪREHUROA
UNIVERSITY OF NEW ZEALAND

The Potential for Biofabrication of complex collagen tissues through Bioprinting methodologies

Juan Schutte, Supervisor: A.Prof Johan Potgieter

School of Engineering and Advanced Technology (SEAT), Albany, Massey University, New Zealand

Collagen

Collagen is the most abundant form of fibrous protein within the animal kingdom and can be found in connective tissue and the extracellular matrix.

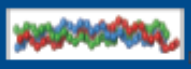

[1]

Corneas

The cornea is an excellent example of a complex collagen tissue. This tissue is comprised of many layers containing collagen. One such layer is the Stroma, which makes up approximately 90% of the cornea. Research has shown a distinctive lack of viable Stroma analogue development.

[2]

Stroma

The Stroma provides an excellent example of a highly structured collagen based layer, consisting of predominantly Type I collagen. This layer provides much of the strength structure and transparency found in the cornea. The collagen within the Stroma occurs in the form of layers of interwoven sheets of aligned collagen called lamellae. Thus development of a means for replication of tissue similar to this could potentially allow for the generation of many fundamental collagen based constructs.

[3]

Relevant Technology

Electrospinning is a capable methodology for the production of aligned nanofibers such as those found in the corneas Stroma. Unfortunately the process of electrospinning requires material to be exposed to solutions which are not biocompatible.

Traditional Bioprinting approaches deal predominantly with extrusion methodologies and heat. Issues regarding alignment and delamination are prevalent within this technology which results in complications in the production of highly ordered tissue such as the Stroma.

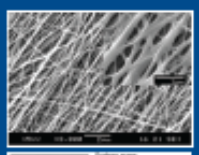

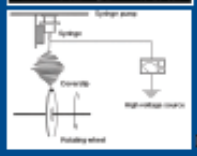

[4]

Research

Within this project research including but not limited to biofabrication technologies, collagen properties, collagen processing methodologies, cornea production/processing technology, and fabricated collagen tissue biocompatibility will be conducted.

In closing it is the aim and objective of the above described project to achieve the development of requirements for the production of complex collagen based tissues.

[1] - Collagen Structure, Figure demonstrates the triple helix structure of collagen
[2] - Cornea Structure, Figure demonstrates the location of the cornea
[3] - Desired Outcome, Figure demonstrates microscopy of the naturally occuring stroma which is to be used as a goal.
[4] - Electrospining, Figure demonstrates the basic principle of Elkectrospining and the results thereof.

National SCIENCE Challenges

MASSEY UNIVERSITY
TE KUNENGA KI PŪREHUROA
UNIVERSITY OF NEW ZEALAND

Spearhead 5: Biomaterial 3D Printing

The pathway to Composite nanofiber based 4D bioprinting

Juan Schutte, Supervisor: Prof Johan Potgieter
School of Engineering and Advanced Technology (SEAT), Albany, Massey University, New Zealand

Collagen

This is the most abundant protein within the animal kingdom, occuring as 28 different types. This research project has identified type I fibre associated (FASCIT) collagen as the fundamental structural element of many natuarally occuring tissues. As Figure 1 demonstrates, this occurance is often characterised by submicron and nanofibres containing D-banding.
Additionally this protein is highly relevant within New Zealand based biomaterials research as it can be locally sourced.

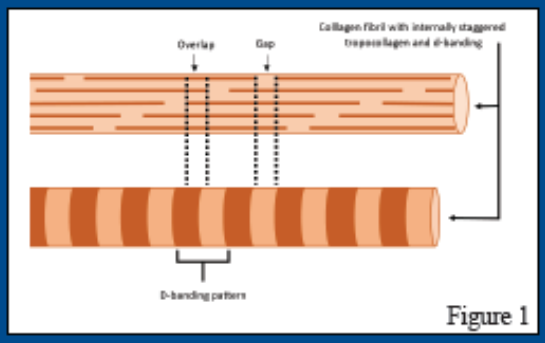

Figure 1

Additive Manufacturing

Within Additive Manufacturing's 3D Printing, there exists a relative dificiency in the capability to generate controlled fibre-based structures such as those seen in the cornea stroma or woven carbon fibre based industry. As Figure 2 indicates this technology has largely focussed on the manipulation of solid filament, powders and liquid resin manipulation ofen via thermal or extensive pressurised actuation. These traditional approaches are thus limited in their ability to process biomaterials.

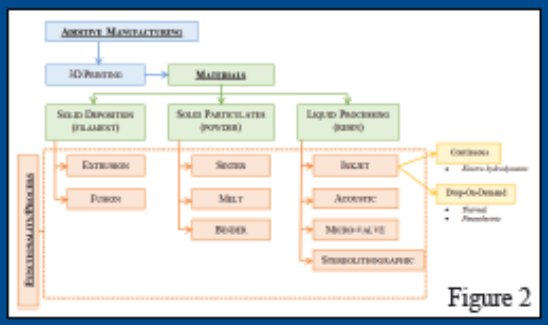
Figure 2

Electrospinning

A technique of increasing popularity for the production of submicron and nanofibres is electrospinning. There are many variations of this technology. Through a review of available literature, the parrallel electrode technique was highlighted due to its capability of sequentially controlling generated fibre orientation (Figure 3). One of the major drawbacks of this technique however is it's relative restriction to the generation of largely two dimentional structures as well as it's apparent low productivity, lack of functionality and potential for high toxicity. Current research is actively persuing the further development of techniques and technology within Massey University's Centre for Additive Manufacturing.

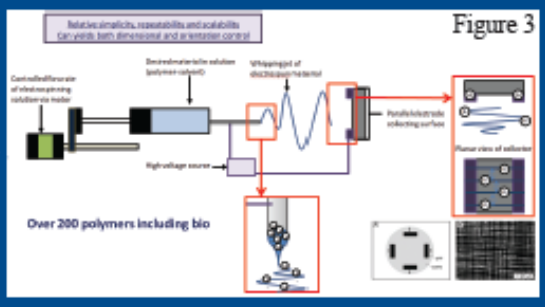

Figure 3

This research is conducted in collaboration with the members of Spearhead 5: Biomaterial 3D Printing, namely:

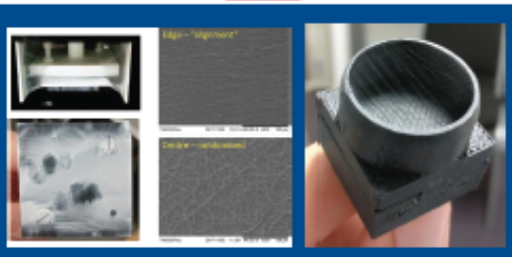

National SCIENCE Challenges

MASSEY UNIVERSITY
TE KUNENGA KI PŪREHUROA
UNIVERSITY OF NEW ZEALAND

Spearhead 5: Biomaterial 3D Printing

The pathway to Composite nanofiber based 4D bioprinting

Juan Sebuffe, Supervisor: Prof Johan Potgieter
School of Engineering and Advanced Technology (SEAT), Albany, Massey University, New Zealand

Device Development

Following fundamental evaluations of technology such as traditional 3D Printing, electrospinning, surface modification technology and the nature of naturally occuring biological structures, invaestigative research was conducted. This yielded results which promoted a requirement for the development of a more controlled automated method of manufacturing.

Mechatronics Engineering

Through a combination of systems Design, CAD, Manufacturing, Electronics and Programming an automated printing solution capable of extensive research and development was generated.

This research is conducted in collaboration with the members of Spearhead 5: Biomaterial 3D Printing, namely:

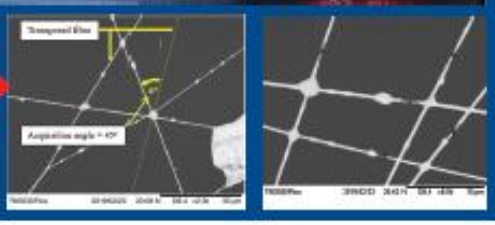

APPENDIX C: RELATED PATENT APPLICATION (PARTIALLY DISCLOSED)

Due to confidentiality the below excerpts are strictly indicative of the resultant patent application.

CONTROLLED ADDITIVE ELECTROSPINNING-BASED FIBRE ORIENTED THREE-DIMENSIONAL MANUFACTURING

ABSTRACT

Methods are disclosed which leverage of electrospinning and Additive manufacturing technology to produce three dimensional objects comprised of fibre occurring in a highly ordered/controlled fashion. Examples of such control include alignment, cross-linking, directional orientation, composite functionality and fibre diameter. The method includes the electrostatic, magnetic, thermal and physical manipulation of electrospinning polymer fibre (either synthetic or organic) to ensure controlled deposition upon a target. A layer generated through this is then subjected to the controlled addition of functionalisation agents resulting in inter-fibril cross-linking which can include the delivery of composite functionality. This sequence of controlled electrostatic-based deposition followed by the controlled addition of functionalisation is repeated as a form of sequential additive manufacturing. This technique has resulted in various objects disclosed herein.

FIELD

This disclosure related to methods of sequential additive manufacturing including electrospinning in particular the generation of three dimensional controlled fibre-based compositions such as isotropic fibrous forms and particularly functionalised fibrous forms.

BACKGROUND

Controlled properties of isotropy or anisotropy are fundamental for the manufacturing of both synthetic and organic structures. Whilst this level of control has been achieved in a two-dimensional fashion there exists an opportunity to derive a process which leverages off electrospinning and Additive Manufacturing technologies to generate similar fibre-based structures in a three dimensional form. Though current techniques exist in combining electrospinning and additive manufacturing, often these do not focus on the retension of dimensional properties(including features such as alignment and layer resolution), encourage inter-fibril bronding (via ccross-linking) or leverage off composite functionalities. The ability to bridge this research and manufacturing gap is highly relevant to both precision engineering as well as fields of biotechnology.

DESCRIPTION OF DRAWINGS

Figure 1 A-B illustrate the fundamental nature of the described process

Figure 2 illustrates the nature of the mechanisms employed within the process where A-C depict variations to collection mechanisms and C-E present variations to extrusion mechanisms.

Figure 3 is a schematic view of an embodiment of an apparatus configured to manufacture an article, where C-D demonstrate examples of this embodiment utilising the polymer Nylon 6, 6 (PA66);

Figure 4 is a schematic view of another embodiment of an apparatus configured to manufacture an article, where C-D demonstrate examples of this embodiment utilising the polymer Nylon 6, 6 (PA66);

Figure 5 demonstrates through microscopy the inter-fibre bonding of derived layers;

Figure 6 demonstrates through microscopy the nature of functionalisation and additive material strategies within derived layers, with A representing composite synthetic material and B representing inclusion of organic materials;

Figure 7 demonstrates an active(A, cantilever) and passive(B, dome) three dimensional structure;

Figure 8 demonstrates through fatigue testing data the relative properties of derived structures in relation to traditional forms of additive manufacturing (i.e. PA66 processed in the described technique versus selective laser sintering fabrication).

Figure 9 demonstrates the nature of melt electrospinning(of PA66), coaxial electrospinning(of keratin-collagen solution) and emulsion electrospinning(of XX-XX solution) through this technique;

Figure 10 details additional properties of derived examples including data for structure width, structure length, fibre diameter, transparency, cell proliferation;

SUMMARY

Disclosed herein are methods which combine techniques of electrospinning in combination with Additive Manufacturing and automation technology to yield functional three dimensional fibre-based structures. The inventors developed a variable technique to exploit the parameters of electrospinning and ultrasonic transduction in the proximity of modified additive manufacturing technology. The technique is typically sequential in nature with targeted electrospinning followed by targeted functionalisation delivered by ultrasonic transduction and additive manufacturing technology/actuation.

In some examples targeted functionalisation agent delivery is inclusive of additional material yielding composite properties to the electrospun layer.

Additional examples yielded from this technique include isotropic biopolymer and synthetic polymer structures for use in fields of tissue engineering (e.g. regenerative medicine) and advanced engineering. This technique has been achieved through the utilisation of multiple devices as well as a central/singular device.

An in depth example utilising Nylon 6-6 in combination with Formic Acid at 15 w/v% to generate aligned micro-fibres at varied angles.

DETAILED DESCRIPTION OF SEVERAL EMBODIMENTS

Disclosed herein are methods for fabricating micron and nano-resolution fibre based three dimensional structures. Embodiments of this technology may be utilised to produce both composite and non-composite styled materials/objects from either synthetic or organic polymers. A fundamental feature of the invention is the utilisation of electrostatic actuation to derive fibres in the form of electrospinning. This feature can be embodied in the forms associated with electrospinning namely: melt electrospinning, coaxial electrospinning or emulsion electrospinning. The embodiments of electrospinning contain the following highlighted fundamental features:

Solution: Electrospinning requires the material (from which the resultant fibres are to be generated) to be in a solution. These solutions are often in the form of a polymer (the desired material) dissolved in an acidic solvent. Solvents with a low boiling point are generally more favourable in electrospinning as this allows for dry formation of fibres.

Charged Extruder: A charge is induced through the use of a voltage source connected to the extruding mechanism through which the material introduced to the system. The characteristics of the electrospinning process as well as the resultant fibre are influenced by the applied voltage, distance from collecting surface and rate of extrusion/flow of solution. The following discusses these factors:

Applied Voltage: The applied voltage is often in the range of several kilovolts and varying this will have an effect on factors such as spinning current, beaded morphology, fibre morphology and fibre structure. Increasing the voltage results in longer and smaller (diameter) fibres, however beaded morphology is likely to occur reducing the surface area.

Distance from collecting surface: The distance between the extruder and the collecting surface influences the fibre evaporation rate, deposition time and inconsistency interval. These factors affect the properties of the resultant fibre e.g. decreasing of this distance results in a wet fibre containing a beaded structure.

Rate of extrusion/flow of solution: Increases in the extrusion/flow rate of the solution results in larger fibre diameters as well as beaded morphology as such for smaller diameters a low rate of extrusion/flow should be implemented.

Collecting surface: This surface will collect the material which is undergoing the electrospinning process. The resultant fibre will be affected by the type of collecting surface used as well as actuation of the surface (namely the speed of actuation). Factors such as the crystal orientation of fibres and evaporation of solvent are influenced by the speed of collecting surface rotation/actuation.

The above declared features and the relationships between them will be included in the discussion of the following embodiments.

In one embodiment an apparatus containing actuation to vary the distance from charged extruder to the collection region is utilised to allow for modifications to electrospinning parameters accounting for various materials.

In another embodiment of the apparatus the housing of components within or externally are of non-conductive material (minimising risks of internal electric fields on the user and external fields on the internal process.

One embodiment of the mechanisms of utilised apparatus allows for these to be variable yielding a modular apparatus.

In some embodiments material utilised to generate fibres is altered, some embodiments alter this during each layering-process whilst other embodiments have this occur sequentially.

In some embodiments the process will occur within a centralised housing together with a user interface system as an apparatus with other embodiments occurring as the described process occurring in multiple apparatus utilised sequentially;

In some embodiments the functionalisation strategy will implement a vapour or evaporation based (gaseous phase) application of material.

In some embodiments the functionalisation strategy will incorporate lithographic elements such as a controlled laser which can be embodied in the form of a UV source for cross linking.

In some embodiments the process works to electrospin aligned nanofiber across oppositely charged parallel electrode plates from which the fibres are manually removed via an insert between the electrodes.

In some embodiments this insert is rotated allowing for the collection of material at varying angles in respect to previous collections.

In some embodiments such collected fibre is exposed to functionalisation strategies such as cross-linking agents at an interlayer or post layering stage.

In some embodiments the process works to collect electrospun material upon a rotating collection plate.

CLAIMS

We Claim:

1. A method for the fabrication of fibre-based three dimensional structures comprising of the following steps:
    a. Electrospinning of material;
    b. Collection of electrostatically charged material in a controlled and aligned fashion;
    c. Collection of aligned material upon a defined processing surface;
    d. Subjecting collected fibres to functionalisation strategies in defined regions;
2. The method of claim 1 in which steps a-d are subjected to repetition to derive a defined three dimensional object;
3. The method of claim 1 in which the non-functionalised fibres are removed;
4. The method of claim 1 in which a functionalisation strategy is not utilised sequentially (step d is not incorporated in the methodology)
5. The method of claim 1 in which step d is embodied such that utilised material or agents are of a liquid, solid or gaseous nature are utilised.
6. The method of claim 1 in which step d is embodied as a method of lithographic actuation or polymerisation.
7. A method of claim 1 in which the functionalisation strategy is employed post multiple repetitions of steps a-c.
8. A method of claim 1 in which step c involved the modification to collection orientation allowing for variation in fibre orientation per collection layer.
9. A method of claim 1 in which step c can occur multiple times prior to requiring the repetition of step a.
10. A method of claim 1 in which melt electrospinning, coaxial electrospinning, emulsion electrospinning is utilised for step a;

TERMS

Additive Manufacturing:	*a form of manufacturing in which objects are fabricated through the layer-by-layer addition and processing of material*
3D Printing:	*An automated form of additive manufacturing*
Tissue engineering:	*An inter-disciplinary engineering approach which seeks to resolve issues in the replication and modification of biological matter.*
Matrix:	*Meshwork of proteins and/or carbohydrates, cells can be embedded or infiltrate into the network; extracellular matrix is structural component of tissues in vivo*
Gel:	*Solid comprised of(1) 3D polymer network and (2) enough liquid to ensure elastic material properties[15], can be embedded with cells and injected into tissues with/without cells incorporated*
Scaffold:	*3D and highly porous interconnected polymer network hydrated with a liquid allowing cell attachment, proliferation, and transport of nutrients and metabolic waste, generally embedded with cells or made to allow native cell infiltration if implanted*
Polymerization:	*A process of reacting monomer molecules together in a chemical reaction to form polymer chains or three-dimensional networks.*
Isotropy:	*implies identical properties in all directions*
Anisotropy:	*the property of being directionally dependent*
Functionalization:	*A process whereby an object is subjected to parameters which strengthen and allow for the later manipulation of the object*
Cross-linking:	*The process whereby chemical bonds are formed between fibres*
Coating:	*2D film of polymer on a substrate, cells can be added on top of coating (beyond the scope of this review, but often used to alter the stiffness of substrates upon which cells are seeded)*
Layering Process	*A process in which a defined layer of material is added to a defined region.*

11. A method for claim 1 in which variations to the point of electrospinnig (extrusion point/charged extruder) will occur. Alternatives including:
    a. Single needle/nozzle
    b. Multiple needle/nozzle
    c. Needle-less/nozzle-less
12. A method for claim 1 in which variation in the material utilised in step a occurs within the process;
13. A method for claim 1 in which synthetic polymers are utilised;
14. A method for claim 1 in which organic polymers are utilised;
15. A method for claim 1 in which synthetic or organic material is deposited upon the material;
16. A method for claim 1 in which the collection of material in step b and/or c occurs upon or between an actuated surface;
17. A method for claim 1 in which the collection of material in step b and/or c occurs upon or between a stationary surface;
18. A method for claim 1 in which the distance between the point of electrospinning and the regions of collection are variable both prior and during the fabrication process;
19. A method for claim 1 in which magnetic field manipulation is utilised to modify derived fibre properties;
20. A fibrous construct derived from a method of any of the claims 1-17;
21. The fibrous construct of claim 18 occurring comprising of organic or synthetic agents;
22. The fibrous construct of claim 18 being comprised of a composite material;
23. The fibrous construct fabricated through claims 1-X for utilisation as scaffolds;

APPENDIX D: CODE

```
/*
Name:    MachineProgram.ino
Created:  7/11/2018 12:42:55 PM
Author: jschutte
*/

//=========================================
// ---------- LIBRARIES ----------------
//=========================================
#include <Servo.h>

//=========================================
// ---------- ASSIGNED PINS -------------
//=========================================


//Stepper Motors //////////I THINK I AM GOING TO REMOVE ALL THE MICROSTEPPING, Have 2 Connectors i.e. a HIGH and A LOW
//Syringe Pump Motor
#define SM1_SP_Step        20
#define SM1_SP_Direction    21
#define SM1_SP_Enable       19

#define SP_MS 44

//Vapour Peristaltic Pump
#define SM8_VP_Step        17
#define SM8_VP_Direction    18
#define SM8_VP_Enable      16

#define VP_MS 46

//Z/Collector-Extruder Distance Motors ///-LOL use same pins!-PLEASE NOTE YOU NEED TO SET THE MICROSTEPPING AS LOW FOR THESE I.E. SET TO ONE INPUT LOW
//CEUMotor1
#define SM2_CEU_Step        25
#define SM2_CEU_Direction    27
#define SM2_CEU_Enable       23

//CEUMotor2
#define SM3_CEU_Step        24
#define SM3_CEU_Direction    26
#define SM3_CEU_Enable       22

//Rotating Mandrel Motor
#define SM4_RM_Step        31
#define SM4_RM_Direction    29
#define SM4_RM_Enable      33

//Fibre Transferal Unit
#define SM5_FTU_Step        37
#define SM5_FTU_Direction    35
#define SM5_FTU_Enable       39

//Fibre Collection Unit
#define SM6_FCU_Step        43
#define SM6_FCU_Direction    41
#define SM6_FCU_Enable       45

//Rotating Fibre collector unit
#define SM7_RFCU_Step       49
#define SM7_RFCU_Direction    47
#define SM7_RFCU_Enable      51

//Servo Motors //define servo motor pins
//Collector homing servo
Servo ServM1_RM;
int ServM1_RM_pos = 0;

//Rotating Fibre Collection Unit homing servo
Servo ServM2_RFCU;
int ServM2_RFCU_pos = 0;

//High Voltage Connection Control Servo
Servo ServM3_HVC;
int ServM3_HVC_pos = 0;

//LED Masking Servo
Servo ServLED;

//Limit Switches
#define LS1_LimSP 8
#define LS2_LimCEU1 7
#define LS3_LimCEU2 6
#define LS4_LimRM 5
#define LS5_LimFTU  4
#define LS6_LimFCU  3
#define LS7_LimRFCU 2
#define LS8_LimD  40

//Buttons
#define FwdSyringe  34
#define FwdLight 32
#define BwdSyringe  30
#define BwdLight 28
#define PeriP 36
#define PeriPLight 38

//Relays
#define R1_PS 50
#define R2_AP 13
#define R3_Vap  12
#define R4_LED  9
#define R5_CPG  10

#define vapourTrans 53
//=========================================
//---------- VARIABLES ----------------
//=========================================

String UserIn; //a variable used to temporarily store the input form the user in the user interface portion of the code
```

```
                                                    //user input values
float EH = 0, CH = 0, DF = 0, TC = 0, NC = 0, DR = 0, NoRevE = 0, NoRevV = 0, NoRevM = 0, SyrMlitrePerMmitre = 0, VapFrRev = 0, VF = 0, rpmIn = 0;
float MachineTimeOn = 0; //Time set for code to run

                                                                                                    //Control variables relating to the activation and duration of certain processes
float HasCollected = 0, Timeprocess = 0, P1 = 0, P2 = 0, P2var = 0, P2_FTUpos = 0, P3 = 0, P3var = 0, P3_FTUpos = 0, P4 = 0, P4var = 0, P4_FTUpos = 0, MA = 0, NPX = 0, MB = 0, NX = 0;
float P2timeset = 0, P3timeset = 0, P4timeset = 0;

//Cotrol variables for positional control
float desiredFTUpos = 0; //THIS IS THE DESIRED DISTANCE, MODIFY THIS IN LATER CODE!!!!
float desiredFCUpos = 0; //THIS IS THE DESIRED DISTANCE, MODIFY THIS IN LATER CODE!!!!
float totalworkabledistance = 0; //as above
int getMotorsInPosition = 0;  //control variables relating to FTU actuation
int deactivateSMLimits = 0;   //control variables relating to FTU actuation
int getCollectorInPosition1 = 0; //control variable for FCU
int getCollectorInPosition2 = 0; //control variable for FCU
int collected = 0; //collecting control variable 4 times collected
int Aproc = 0, AP2 = 0, AP3 = 0, AP4 = 0;

//variables which will control the limits On or Off for the motor
int CV_RM = 0, CV_FTU = 0, CV_FCU = 0, CV_RFCU = 0, CV_SP = 0, CV_CEU = 0, CV_CEU2 = 0;


// Varaibles which are used to control the time between High-Low activations for Steppers (THIS WILL RELATE TO SPEED!)
float delayTimeSM1_SP = 0;
float delayTimeSM2andSM3_ZS = 0;
float delayTimeSM4_RM = 0;
float delayTimeSM5_FTU = 0;
float delayTimeSM6_FCU = 0;
float delayTimeSM7_RFCU = 0;
float delayTimeSM8_VP = 0;

//Variables utilised to reset the time (required for delays) after an instance of High-Low
float ResetTimeSM1_SP = 0;
float ResetTimeSM2_ZS1 = 0;
float ResetTimeSM3_ZS2 = 0;
float ResetTimeSM4_RM = 0;
float ResetTimeSM5_FTU = 0;
float ResetTimeSM6_FCU = 0;
float ResetTimeSM7_RFCU = 0;
float ResetTimeSM8_VP = 0;

float TimeOn = 0;       // stores the value of millis() in each iteration of the program

int x = 0;            //general control/loop program variable
int homingval = 0;        //homing variables
int FirstInputRun = 0, userinputval = 0; //user interface value

float oldTime = 0;        //variables to reset time and prevent overflow
float currentTime = 0;

//Limit Variables containing the maximum actuation limitations
float SM1_SPstepperlimit = 0;   //A limit variable preventing syringepumpfrom overactuating
float limitSyr = 0;     //A comparison variable ensuring the syringe pump does not overactuate

float SPPos = 0;
float CUE1Pos = 0;
float CUE2Pos = 0;
float FTUPos = 0;
float FCUPos = 0;
float RFCUPos = 0;
float RMPos = 0;

//=========================================
//---------- PROGRAM CODE ----------
//=========================================


void setup() {
                    Serial.begin(9600);

                    //Set pin modes here

                    //Stepper Motor Setup
                    //Syringe Pump
                    pinMode(SM1_SP_Step, OUTPUT);
                    pinMode(SM1_SP_Direction, OUTPUT);
                    pinMode(SM1_SP_Enable, OUTPUT);

                    pinMode(SP_MS, OUTPUT);

                    //Collector-Extruder Distance Motors
                    //CEU1
                    pinMode(SM2_CEU_Step, OUTPUT);
                    pinMode(SM2_CEU_Direction, OUTPUT);
                    pinMode(SM2_CEU_Enable, OUTPUT);

                    //CEU2
                    pinMode(SM3_CEU_Step, OUTPUT);
                    pinMode(SM3_CEU_Direction, OUTPUT);
                    pinMode(SM3_CEU_Enable, OUTPUT);

                    //Rotating Mandrel
                    pinMode(SM4_RM_Step, OUTPUT);
                    pinMode(SM4_RM_Direction, OUTPUT);
                    pinMode(SM4_RM_Enable, OUTPUT);

                    //Fibre transferal unit
                    pinMode(SM5_FTU_Step, OUTPUT);
                    pinMode(SM5_FTU_Direction, OUTPUT);
                    pinMode(SM5_FTU_Enable, OUTPUT);

                    //Fibre collection unit
                    pinMode(SM6_FCU_Step, OUTPUT);
                    pinMode(SM6_FCU_Direction, OUTPUT);
                    pinMode(SM6_FCU_Enable, OUTPUT);

                    //Rotating Fibre collection unit
                    pinMode(SM7_RFCU_Step, OUTPUT);
                    pinMode(SM7_RFCU_Direction, OUTPUT);
                    pinMode(SM7_RFCU_Enable, OUTPUT);

                    //Rotating Fibre collection unit
                    pinMode(SM8_VP_Step, OUTPUT);
```

```
	pinMode(SM8_VP_Direction, OUTPUT);
	pinMode(SM8_VP_Enable, OUTPUT);

	pinMode(VP_MS, OUTPUT);

	//Limit Switch Setup
	pinMode(LS1_LimSP, INPUT_PULLUP);
	pinMode(LS2_LimCEU1, INPUT_PULLUP);
	pinMode(LS3_LimCEU2, INPUT_PULLUP);
	pinMode(LS4_LimRM, INPUT_PULLUP);
	pinMode(LS5_LimFTU, INPUT_PULLUP);
	pinMode(LS6_LimFCU, INPUT_PULLUP);
	pinMode(LS7_LimRFCU, INPUT_PULLUP);
	pinMode(LS8_LimD, INPUT_PULLUP);

	//Buttons
	pinMode(FwdSyringe, INPUT_PULLUP);
	pinMode(FwdLight, OUTPUT);
	pinMode(BwdSyringe, INPUT_PULLUP);
	pinMode(BwdLight, OUTPUT);
	pinMode(PeriP, INPUT_PULLUP);
	pinMode(PeriPLight, OUTPUT);

	//Relay Setup
	pinMode(R1_PS, OUTPUT);
	pinMode(R2_AP, OUTPUT);
	pinMode(R3_Vap, OUTPUT);
	pinMode(R4_LED, OUTPUT);
	pinMode(R5_CPG, OUTPUT);
	pinMode(vapourTrans, OUTPUT);

	//Servo Motor Setup and start position
	ServM1_RM.attach(42);
	ServM2_RFCU.attach(14);
	ServM3_HVC.attach(15);
	ServM1_RM.write(120);
	ServM2_RFCU.write(10);
	ServM3_HVC.write(70);
	ServLED.attach(48);
	ServLED.write(10);


	resetPins();

	//FirstInputRun = 5; //for testing quickly with total menu check
	//enterX();

	//homing();	//function which starts when machine started and requests homing operations


	//TESTING FUNCTIONS
	//FOR A

	CV_SP = 0;
	CV_CEU = 0;
	CV_CEU2 = 0;
	CV_RM = 0;
	CV_FTU = 0;
	CV_FCU = 0;
	CV_RFCU = 0;

	digitalWrite(SP_MS, HIGH);
	digitalWrite(VP_MS, HIGH);

	delayTimeSM1_SP = 1;
	delayTimeSM2andSM3_ZS = 1;
	delayTimeSM4_RM = 10;
	delayTimeSM5_FTU = 1;
	delayTimeSM6_FCU = 1;
	delayTimeSM7_RFCU = 10;
	delayTimeSM8_VP = 1;

	SM1_SPstepperlimit = 10050;			//value derived from manual measure measurement!!!!
	limitSyr = 0;

	EH = 123;
	CH =  95; //110 parrallello //95 single nozzle// rotat 150
	totalworkabledistance = 420 + (200 - EH);
	DF = 0.25;
	VF = 1;
	DR = 45;
	P1 = 1;
	rpmIn = 50;
	P2 = 0;
	P3 = 0;
	P4 = 0;
	SyrMlitrePerMmitre = 0.06;
	P2timeset = (180000);
	P3timeset = (180000);
	P4timeset = (180000);
	MachineTimeOn = (600000);
	NoRevM = rpmIn * 60; //rev/hour
	delayTimeSM4_RM = ((3600000 / (200 * NoRevM)) / 2);
	//Stepper Motor Process Variables
	NoRevE = DF / (SyrMlitrePerMmitre * 2); //THE DENOMINATOR RELATES TO THE Syringe ml/mm which then compared to the motor mm/rev (2mm/rev in standard) equals a ml/rev value. e.g.
	NoRevV = VF / 10; //denominator value indicative of motor ml per revolution output
	delayTimeSM1_SP = ((3600000 / (3200 * NoRevE)) / 2); // will provide the delay in microseconds for a flowrate in rev/hour for motor having 16th microstepping e.g. h/(stps*rev/h) = h^2/revsteps namely
How much time (h) is required between the steps necessary
	delayTimeSM8_VP = ((3600000 / (3200 * NoRevV)) / 2);
	MB = 1;
	NX = 10;
	SPPos = 0;
	CUE1Pos = 0;
	CUE2Pos = 0;
	FTUPos = 0;
	FCUPos = 0;
	RFCUPos = 0;
	RMPos = 0;


	//END
	testingfunctions();

}
```

```
void testingfunctions() {

		SM1_SPstepperlimit = 10050;			//value derived from manual measure measurement!!!!
		limitSyr = 0;
		Serial.println(digitalRead(LS1_LimSP));
		Serial.println(digitalRead(LS2_LimCEU1));
		Serial.println(digitalRead(LS3_LimCEU2));
		Serial.println(digitalRead(LS4_LimRM));
		Serial.println(digitalRead(LS5_LimFTU));
		Serial.println(digitalRead(LS6_LimFCU));
		Serial.println(digitalRead(LS7_LimRFCU));
		Serial.println(digitalRead(LS8_LimD));

		float Time_home = 0;
		float overwritetime_home = 0;

		delayTimeSM2andSM3_ZS = 1;
		delayTimeSM5_FTU = 1;
		delayTimeSM6_FCU = 1;
		delayTimeSM7_RFCU = 10;

		ResetTimeSM1_SP = 0;
		ResetTimeSM2_ZS1 = 0;
		ResetTimeSM3_ZS2 = 0;
		ResetTimeSM4_RM = 0;
		ResetTimeSM5_FTU = 0;
		ResetTimeSM6_FCU = 0;
		ResetTimeSM7_RFCU = 0;
		ResetTimeSM8_VP = 0;


		NoRevM = rpmIn * 60; // max rev/hour = 200 (numerator)
		delayTimeSM4_RM = ((3600000 / (200 * NoRevM)) / 2);

		DF = 0.25; // 0.25;

		NoRevE = DF / (SyrMlitrePerMmitre * 2); //THE DENOMINATOR RELATES TO THE Syringe ml/mm which then compared to the motor mm/rev (2mm/rev in standard) equals a ml/rev value. e.g.

		VF = 1000;

		NoRevV = VF / 10; //Denomination equals ml output per motor revolution (in this case 10).
		delayTimeSM1_SP = ((3600000 / (3200 * NoRevE)) / 2); // will provide the delay in microseconds for a flowrate in rev/hour for motor having 16th microstepping e.g. h/(stps*rev/h) = h^2/revsteps namely
How much time (h) is required between the steps necessary
		delayTimeSM8_VP = ((3600000 / (3200 * NoRevV)) / 2);



		int control = 0;

		digitalWrite(SP_MS, LOW);

		Serial.println("Function Tester");
		Serial.println(" ");
		Serial.println("H =  home omotors");
		Serial.println("A =  Electrospin");
		Serial.println("B =  Vapour");
		Serial.println("C =  PrimeVapourMechanism");
		Serial.println("D =  Lights");
		Serial.println("E =  Syringe/Plasma");
		Serial.println("");

		//homeservomotors();
		//delay(5000);
		//activateshomingservomotors();


		//ServM3_HVC_pos = 25;
		//ServM3_HVC.write(ServM3_HVC_pos);

		while (x == 0) {

			if (Serial.available() > 0) {
				UserIn = Serial.readString();

				if (UserIn != "H" && UserIn != "h" && UserIn != "A" && UserIn != "a" && UserIn != "C" && UserIn != "c" && UserIn != "B" && UserIn != "b"  && UserIn != "D" && UserIn
!= "d"  && UserIn != "E" && UserIn != "e") {
					Serial.println("That is not an option");
				}

				//HOMING MOTORS SECTION

				if (UserIn == "H" || UserIn == "h") {
					homeallmotors();
					SPPos = 0;
					CUE1Pos = 0;
					CUE2Pos = 0;
					FTUPos = 0;
					FCUPos = 0;
					RFCUPos = 0;
					RMPos = 0;
					testingfunctions();
				}

				if (UserIn == "A" || UserIn == "a") {
					x = 0;
					/*while (x == 0) {
					digitalWrite(R1_PS, HIGH);
					digitalWrite(R2_AP, HIGH);
					digitalWrite(R3_Vap, HIGH);
					digitalWrite(R4_LED, HIGH);
					digitalWrite(R5_CPG, HIGH);
					delay(1000);
					digitalWrite(R1_PS, LOW);
					delay(1000);
					digitalWrite(R2_AP, LOW);
					delay(1000);
					digitalWrite(R3_Vap, LOW);
					delay(1000);
					digitalWrite(R4_LED, LOW);
					delay(1000);
					digitalWrite(R5_CPG, LOW);
					delay(1000);
					}
```

```
                                        float priorTime_home = millis();
                                        delayTimeSM4_RM = 10;
                                        delayTimeSM1_SP = 1;
                                        digitalWrite(SP_MS, LOW);
                                        CV_SP = 0;
                                        CV_CEU = 0;
                                        CV_CEU2 = 0;
                                        CV_RM = 0;
                                        CV_FTU = 0;
                                        CV_FCU = 0;
                                        CV_RFCU = 0;
                                        */

                                        //temporary testing values

                                        setcollectiondistance();
                                        Serial.println("Collection Distance set");
                                        //Serial.println(oldTime);

                                        oldTime = millis();
                                        FibreDevelopmentProcess();
                                        Serial.println("Electrospinning Phase Over");

                                        homeservomotors();


                                        testingfunctions();

                                }

                                if (UserIn == "B" || UserIn == "b") {
                                                delayTimeSM7_RFCU = 50;
                                                digitalWrite(VP_MS, HIGH);
                                                VF = 25;
                                                NoRevV = VF / 0.5; //UPDATE THESE IN FUNC
                                                delayTimeSM8_VP = ((3600000 / (3200 * NoRevV)) / 2); //UPDATE THESE IN FUNC
                                                ResetTimeSM8_VP = 0;

                                                P2timeset = (60000);

                                                AP2 = 1;

                                                P2 = 1;

                                                Process2();

                                                testingfunctions();

                                }

                                if (UserIn == "C" || UserIn == "c") {
                                                primevapourmechanism();

                                }

                                if (UserIn == "D" || UserIn == "d") {

                                                P3timeset = (60000);

                                                AP3 = 1;

                                                P3 = 1;

                                                Process3();/*

                                                                homeservomotors();
                                                                ServM3_HVC_pos = 70; //25
                                                                ServM3_HVC.write(ServM3_HVC_pos);

                                                                testingfunctions();*/

                                }

                                if (UserIn == "E" || UserIn == "e") {
                                                primesyringepump();
                                                /*
                                                activateshomingservomotors();
                                                ServM3_HVC_pos = 40; //25
                                                ServM3_HVC.write(ServM3_HVC_pos);
                                                /*P4timeset = (60000);

                                                AP4 = 1;

                                                P4 = 1;

                                                Process4();*/
                                                //testingfunctions();
                                }

                        }
                }
}

//=======================================
//---------- HOMING INTERVAL ------------
//=======================================

void resetPins() {

                //Stepper Motor Setup
                //Syringe Pump
                digitalWrite(SM1_SP_Step, LOW);
                digitalWrite(SM1_SP_Direction, LOW);
                digitalWrite(SM1_SP_Enable, HIGH);

                digitalWrite(SP_MS, HIGH);

                //Collector-Extruder Distance Motors
```

```
	//CEU1
	digitalWrite(SM2_CEU_Step, LOW);
	digitalWrite(SM2_CEU_Direction, LOW);
	digitalWrite(SM2_CEU_Enable, HIGH);

	//CEU2
	digitalWrite(SM3_CEU_Step, LOW);
	digitalWrite(SM3_CEU_Direction, LOW);
	digitalWrite(SM3_CEU_Enable, HIGH);

	//Rotating Mandrel
	digitalWrite(SM4_RM_Step, LOW);
	digitalWrite(SM4_RM_Direction, LOW);
	digitalWrite(SM4_RM_Enable, HIGH);

	//Fibre transferal unit
	digitalWrite(SM5_FTU_Step, LOW);
	digitalWrite(SM5_FTU_Direction, LOW);
	digitalWrite(SM5_FTU_Enable, HIGH);

	//Fibre collection unit
	digitalWrite(SM6_FCU_Step, LOW);
	digitalWrite(SM6_FCU_Direction, LOW);
	digitalWrite(SM6_FCU_Enable, HIGH);

	//Rotating Fibre collection unit
	digitalWrite(SM7_RFCU_Step, LOW);
	digitalWrite(SM7_RFCU_Direction, LOW);
	digitalWrite(SM7_RFCU_Enable, HIGH);

	//Vapourisor Peristaltic Pump
	digitalWrite(SM8_VP_Step, LOW);
	digitalWrite(SM8_VP_Direction, LOW);
	digitalWrite(SM8_VP_Enable, HIGH);

	digitalWrite(VP_MS, HIGH);

	//Relay Set up
	digitalWrite(R1_PS, LOW);
	digitalWrite(R2_AP, LOW);
	digitalWrite(R3_Vap, LOW);
	digitalWrite(R4_LED, LOW);
	digitalWrite(R5_CPG, LOW);

}

void homing() { //here the program will set all the actuators to their respective 0 positions

	resetPins();
	//Value Check
	//Serial.println("Limit Switch Values:");
	Serial.println(digitalRead(LS1_LimSP));
	Serial.println(digitalRead(LS2_LimCEU1));
	Serial.println(digitalRead(LS3_LimCEU2));
	Serial.println(digitalRead(LS4_LimRM));
	Serial.println(digitalRead(LS5_LimFTU));
	Serial.println(digitalRead(LS6_LimFCU));
	Serial.println(digitalRead(LS7_LimRFCU));
	Serial.println(digitalRead(LS8_LimD));

	//Buttons
	//Serial.print("Button Values:");
	//Serial.println(digitalRead(FwdSyringe));
	//Serial.println(digitalRead(BwdSyringe));

	//Control Variable
	//Serial.print("Control Variable Value:");
	Serial.println(homingval);

	//Homes all stepper motors
	if (homingval == 0) {
		Serial.println("HOMING STAGE 1");
		Serial.println(" ");
		Serial.println("CAUTION!: PLEASE REMOVE ALL SYRINGES, EXTRUDERS, COLLECTORS AND ADDITIONAL DEVICES BEFORE STARTING HOMING OPERATIONS");
		Serial.println("NOTE: You must complete the homing functions before you can continue");
		//Serial.println("");
		Serial.println("Close the door and enter 'A' to home all machine motors");
		while (x == 0) {
			if (Serial.available() > 0) {
				UserIn = Serial.readString();
				if (UserIn != "A" && UserIn != "a") {
					Serial.println("That is not an option");
				}
				if (UserIn == "A" || UserIn == "a") {
					if (digitalRead(LS8_LimD) != 1) {
						Serial.println("Close the door to continue");
						homing();
					}
					if (homingval == 0 && digitalRead(LS8_LimD) == 1) {
						homeallmotors();
						Serial.println("Done Homing Motors");
						homingval = 1;
						homing();
					}
				}
			}
		}
	}

	//User promted to prime the syringe Pump
	if (homingval == 1) {
		syringepumpsetup();
	}

	//Homes and primes the vapour mechanism
	if (homingval == 2) {
		Serial.println("HOMING STAGE 3");
		Serial.println("");
		Serial.println("Vapour mechanism setup/homing");
		/*Serial.println("");
		Serial.println("You must now purge any residual solution in this mechanism");
		Serial.println("Follow the following steps:");
		Serial.println("1- Open the Transducer latch");
		Serial.println("2- Open/move the transducer away from the solution-vapour channel");
```

```
                        Serial.println("3- Place an empty container underneath the solution-vapour channel");
                        Serial.println("4- Remove the Input Solution container and replace this with a container filled with water");
                        */Serial.println("5- Enter 'A' to begin the flushing the solution piping");
                        Serial.println("");

                        while (x == 0) {
                                if (Serial.available() > 0) {
                                        UserIn = Serial.readString();
                                        if (UserIn != "A" && UserIn != "a") {
                                                Serial.println("That is not an option");
                                        }
                                        if (UserIn == "A" || UserIn == "a") {
                                                primevapourmechanism();
                                        }
                                }
                        }
                }

                //Finishes the homing function
                if (homingval == 3) {
                        Serial.println("System Homing finished");

                        SPPos = 0;
                        CUE1Pos = 0;
                        CUE2Pos = 0;
                        FTUPos = 0;
                        FCUPos = 0;
                        RFCUPos = 0;
                        RMPos = 0;

                        resetPins();
                        enterX();
                }

}

void homeallmotors() {
                int all_atLimits = 0;

                homeservomotors();
                activateshomingservomotors();

                CV_SP = 0;
                CV_CEU = 0;
                CV_CEU2 = 0;
                CV_RM = 0;
                CV_FTU = 0;
                CV_FCU = 0;
                CV_RFCU = 0;

                digitalWrite(SP_MS, LOW);

                delayTimeSM1_SP = 1;
                delayTimeSM2andSM3_ZS = 1;
                delayTimeSM4_RM = 10;
                delayTimeSM5_FTU = 1;
                delayTimeSM6_FCU = 1;
                delayTimeSM7_RFCU = 1;
                delayTimeSM8_VP = 1;

                float priorTime_home = millis();

                //All motors run at the same time until limits are activated
                while (all_atLimits != 7) {

                        if (CV_SP == 0) {
                                runmotorstolimit(SM1_SP_Direction, SM1_SP_Enable, SM1_SP_Step, priorTime_home, ResetTimeSM1_SP, delayTimeSM1_SP, LS1_LimSP, 1, CV_SP);
                        }

                        if (CV_CEU == 0) {
                                runmotorstolimit(SM2_CEU_Direction, SM2_CEU_Enable, SM2_CEU_Step, priorTime_home, ResetTimeSM2_ZS1, delayTimeSM2andSM3_ZS, LS2_LimCEU1, 1, CV_CEU);
                        }

                        if (CV_CEU2 == 0) {
                                runmotorstolimit(SM3_CEU_Direction, SM3_CEU_Enable, SM3_CEU_Step, priorTime_home, ResetTimeSM3_ZS2, delayTimeSM2andSM3_ZS, LS3_LimCEU2, 1,
CV_CEU2);
                        }

                        /*if (CV_RM == 0) {
                                runmotorstolimit(SM4_RM_Direction, SM4_RM_Enable, SM4_RM_Step, priorTime_home, ResetTimeSM4_RM, delayTimeSM4_RM, LS4_LimRM, 1, CV_RM);
                        }

                        /*if (CV_FTU == 0) {
                                runmotorstolimit(SM5_FTU_Direction, SM5_FTU_Enable, SM5_FTU_Step, priorTime_home, ResetTimeSM5_FTU, delayTimeSM5_FTU, LS5_LimFTU, 1, CV_FTU);
                        }

                        /*if (CV_RFCU == 0) {
                        runmotorstolimit(SM7_RFCU_Direction, SM7_RFCU_Enable, SM7_RFCU_Step, priorTime_home, ResetTimeSM7_RFCU, delayTimeSM7_RFCU, LS7_LimRFCU, 1, CV_RFCU);
                        }*/
                        if (CV_FCU == 0) {
                                runmotorstolimit(SM6_FCU_Direction, SM6_FCU_Enable, SM6_FCU_Step, priorTime_home, ResetTimeSM6_FCU, delayTimeSM6_FCU, LS6_LimFCU, 1, CV_FCU);
                        }

                        if (CV_SP == 1 && CV_CEU == 1 && CV_CEU2 == 1 && /*CV_RM == 1 && /*CV_FTU == 1 && */CV_FCU == 1 /*&& CV_RFCU == 1*/) {
                                CV_SP = 0;
                                CV_CEU = 0;
                                CV_CEU2 = 0;
                                CV_RM = 0;
                                CV_FTU = 0;
                                CV_FCU = 0;
                                CV_RFCU = 0;
                                homeservomotors();
                                all_atLimits = 7;
                        }
                }
}


//Timer Based Homing
void runmotorstolimit(const int motordirect, const int motorenable, const int motorpin, float PriorTime, float &resetcondition, float delay_speed, const int limitpin, int variable, int &controlvar) {
                float overwritetime = millis();         //this finds the current time for the loop and is used to overwrite all previous time in the below line of code
                float Time = overwritetime - PriorTime;  // here any previous time for the code is removed e.e. if prior to this loop the time was 456 ms, then the overwrite time will be 457 ms for the second run of the
loop meaning that the Time control variable will act to count up (e.g. 456-457 = 1) for each loop.
```

```
		if (digitalRead(limitpin) != variable) {
			digitalWrite(motorenable, LOW);
			digitalWrite(motordirect, LOW);
		}
		if (digitalRead(limitpin) != variable && (Time - resetcondition) >= delay_speed) {
			if (digitalRead(motorpin) == HIGH) {
				digitalWrite(motorpin, LOW);
			}
			else {
				digitalWrite(motorpin, HIGH);
			}
			resetcondition = resetcondition + delay_speed;
		}
		if (digitalRead(limitpin) == variable) {
			digitalWrite(motorpin, LOW);
			digitalWrite(motorenable, HIGH);
			controlvar = 1;
			resetcondition = 0;
		}
}

void runmotorstodistance(const int motordirect, const int motorenable, const int motorpin, float PriorTime, float &resetcondition, float delay_speed, float &currentdistance, float variable) {
		float overwritetime = millis();		//this finds the current time for the loop and is used to overwrite all previous time in the below line of code
		float Time = overwritetime - PriorTime;  // here any previous time for the code is removed e.e. if prior to this loop the time was 456 ms, then the overwrite time will be 457 ms for the second run of the loop meaning that the Time control variable will act to count up (e.g. 456-457 = 1) for each loop.
		//Serial.println("this works");
		float stepvalue = 0;
		if (currentdistance != variable) {
			digitalWrite(motorenable, LOW);
			if (variable - currentdistance > 0) {
				digitalWrite(motordirect, HIGH);
				stepvalue = 0.5;
			}
			else {
				digitalWrite(motordirect, LOW);
				stepvalue = -0.5;
			}
		}
		if (currentdistance != variable && (Time - resetcondition) >= delay_speed) {
			if (digitalRead(motorpin) == HIGH) {
				digitalWrite(motorpin, LOW);
				currentdistance = currentdistance + stepvalue;
			}
			else {
				digitalWrite(motorpin, HIGH);
				currentdistance = currentdistance + stepvalue;
			}
			resetcondition = resetcondition + delay_speed;
		}
		if (currentdistance == variable) {
			digitalWrite(motordirect, LOW);
			digitalWrite(motorpin, LOW);
			digitalWrite(motorenable, HIGH);
			resetcondition = 0;
		}
}

void runmotorsawayfromlimit(const int motordirect, const int motorenable, const int motorpin, float PriorTime, float &resetcondition, float delay_speed, const int limitpin, int variable, int &controlvar) {
		float overwritetime = millis();		//this finds the current time for the loop and is used to overwrite all previous time in the below line of code
		float Time = overwritetime - PriorTime;  // here any previous time for the code is removed e.e. if prior to this loop the time was 456 ms, then the overwrite time will be 457 ms for the second run of the loop meaning that the Time control variable will act to count up (e.g. 456-457 = 1) for each loop.
		//Serial.println("this works");
		if (digitalRead(limitpin) != variable) {
			digitalWrite(motorenable, LOW);
			digitalWrite(motordirect, HIGH);
		}
		if (digitalRead(limitpin) != variable && (Time - resetcondition) >= delay_speed) {
			if (digitalRead(motorpin) == HIGH) {
				digitalWrite(motorpin, LOW);
			}
			else {
				digitalWrite(motorpin, HIGH);
			}
			resetcondition = resetcondition + delay_speed;
		}
		if (digitalRead(limitpin) == variable) {
			digitalWrite(motordirect, LOW);
			digitalWrite(motorpin, LOW);
			digitalWrite(motorenable, HIGH);
			controlvar = 2;
			resetcondition = 0;
		}
}

void changemotorDirection(const int motorDirectionPin) {
		if (digitalRead(motorDirectionPin) == LOW) {
			digitalWrite(motorDirectionPin, HIGH);
		}
		else {
			digitalWrite(motorDirectionPin, LOW);
		}
}


void homeservomotors() {
		//Ensures all servos are out of the way
		ServM1_RM_pos = 120;
		ServM2_RFCU_pos = 10;
		ServM3_HVC_pos = 70;

		ServM1_RM.write(ServM1_RM_pos);
		ServM2_RFCU.write(ServM2_RFCU_pos);
		ServM3_HVC.write(ServM3_HVC_pos);

}

//UPDATE THE REQUIRED SERVOMOTOR ANGLES
void activateshomingservomotors() {
		//Activates the servos with limit switches to the desired position
		ServM1_RM_pos = 60;
		ServM2_RFCU_pos = 90;
```

```
		//ServM3_HVC_pos = 45; //ONLY ENABLE THIS WHEN TESTING COMPONENTS

		ServM1_RM.write(ServM1_RM_pos);
		ServM2_RFCU.write(ServM2_RFCU_pos);
		ServM3_HVC.write(ServM3_HVC_pos); //ONLY ENABLE THIS WHEN TESTING COMPONENTS
}

void syringepumpsetup() {
		Serial.println("HOMING STAGE 2");
		Serial.println("All Motors are homed");
		Serial.println("");
		Serial.println("Syringe Pump Setup");
		Serial.println("");
		//Serial.println("Enter which value you would like to modify: (e.g. enter: 'A' to modify the 'Syringe ml/mm capacity' value");
		Serial.print("A) Syringe ml/mm capacity: ");
		Serial.print(SyrMlitrePerMmitre);
		Serial.println(" ml/mm");
		Serial.println("B) Begin pump adjustment to load syringe and prime extruder");

		while (x == 0) {
			if (Serial.available() > 0) {
				UserIn = Serial.readString();

				if (UserIn != "A" && UserIn != "a" && UserIn != "B" || UserIn != "b") {
					Serial.println("That is not an option");
				}

				if (UserIn == "A" || UserIn == "a") {
					Serial.println(" ");
					//Serial.println("NOTE: For flowrates less than or equal to 1ml per hour, utilise syringes having less than 10ml total capacity ");
					Serial.println(" ");
					Serial.println("Enter the value for the millilitre (ml) output per millimetre(mm) actuation of the utilised syringe");
					while (x == 0) {
						if (Serial.available() > 0) {
							UserIn = Serial.readString();
							Serial.println(UserIn);
							SyrMlitrePerMmitre = UserIn.toFloat();
							Serial.print("You have set the Syringe ml/mm as:");
							Serial.print(SyrMlitrePerMmitre);
							Serial.println("ml/mm");

							Serial.println(" ");
							syringepumpsetup();
						}
					}
				}

				if (UserIn == "B" || UserIn == "b") {
					primesyringepump();
				}

			}
		}
}

//The SM1_SPstepperlimit is set here from manual component evaluation
void primesyringepump() {
		digitalWrite(SP_MS, LOW);
		delayTimeSM1_SP = 1;

		Serial.println("You may now open the door to load the desired syringe");
		SM1_SPstepperlimit = 10050;			//value derived from manual measure measurement!!!!
		limitSyr = 0;
		Serial.println(" ");
		Serial.println("Use the FWD and BWD Buttons to move load the syringe or enter '/' when done");

		while (x == 0) {
			if (Serial.available() > 0) {
				UserIn = Serial.readString();

				if (UserIn != "/") {
					Serial.println("You have entered an invalid character");
					Serial.println(" ");
					Serial.println("Use the FWD and BWD Buttons to move load the syringe or enter '/' when done");
				}

				if (UserIn == "/") {
					Serial.println("done");
					Serial.println(" ");

					digitalWrite(SM1_SP_Enable, HIGH);
					digitalWrite(SM1_SP_Direction, HIGH);
					digitalWrite(SM1_SP_Step, LOW);

					SM1_SPstepperlimit = SM1_SPstepperlimit * 16;

					digitalWrite(SP_MS, HIGH);

					if (homingval == 1) {
						homingval = 2;
						homing();
					}

					if (homingval == 3) {
						TotalMenuCheck();
					}
				}

			}

			if (digitalRead(FwdSyringe) == 0 && limitSyr < SM1_SPstepperlimit && digitalRead(BwdSyringe) != 0) {
				digitalWrite(SM1_SP_Enable, LOW);
				digitalWrite(SM1_SP_Direction, HIGH);
				digitalWrite(SM1_SP_Step, HIGH);
				delay(1);
				digitalWrite(SM1_SP_Step, LOW);
				delay(1);
				limitSyr = limitSyr + 1;
			}

			if (digitalRead(FwdSyringe) == 0 && limitSyr == SM1_SPstepperlimit) {
				Serial.println("Motor cannot move further forwards");
				Serial.println(" ");
			}
```

```
                        if (digitalRead(BwdSyringe) == 0 && limitSyr > 0 && digitalRead(FwdSyringe) != 0) {
                                digitalWrite(SM1_SP_Enable, LOW);
                                digitalWrite(SM1_SP_Direction, LOW);
                                digitalWrite(SM1_SP_Step, HIGH);
                                delay(1);
                                digitalWrite(SM1_SP_Step, LOW);
                                delay(1);
                                limitSyr = limitSyr - 1;
                        }

                        if (digitalRead(BwdSyringe) == 0 && limitSyr == 0) {
                                Serial.println("Motor cannot move further backwards");
                                Serial.println(" ");
                        }
                }
}

void primevapourmechanism() {
                digitalWrite(VP_MS, LOW);
                //digitalWrite(SM8_VP_Direction, HIGH); // ONLY HAVE THIS ACTIVATED WHEN YOU WISH TO RUN THE PUMP IN REVERSE aka AFTER THE FAB CYCLE AND YOU WANT TO REMOVE/RECLAIM MATERIAL
FROM PIPES
                Serial.println(" ");
                Serial.println("Use the FWD button to pump the water through the vapour generator");
                /*Serial.println("Water should flow through the device into the collecting container");
                Serial.println("Once clean water flows through the device, remove the Input water container");
                Serial.println("Continue to press the button to remove any residual water");
                Serial.println("Place the Input Solution container loaded with desired material back into the mechanism");
                Serial.println("Now press the FWD button to prime the mechanism with the desired solution");
                Serial.println("The mechanism is considered primed when the desired solution flows from the solution-vapour channel");*/
                Serial.println("When primed, you may now enter '/' to end this homing stage");

                while (x == 0) {
                        if (Serial.available() > 0) {
                                UserIn = Serial.readString();
                                if (UserIn != "/") {
                                        Serial.println("You have entered an invalid character");
                                        Serial.println(" ");
                                        Serial.println("Use the Pump button to pump the water through else enter '/' when done");
                                        Serial.println(digitalRead(PeriP));
                                }
                        }
                        if (digitalRead(PeriP) == 0) {
                                digitalWrite(SM8_VP_Enable, LOW);
                                digitalWrite(SM8_VP_Step, HIGH);
                                delay(1);
                                digitalWrite(SM8_VP_Step, LOW);
                                delay(1);
                        }

                        if (UserIn == "/") {
                                Serial.println("done");
                                Serial.println(" ");

                                digitalWrite(SM8_VP_Enable, HIGH);
                                digitalWrite(SM8_VP_Step, LOW);

                                digitalWrite(VP_MS, HIGH);

                                if (homingval == 3) {
                                        TotalMenuCheck();
                                }

                                if (homingval == 2) {
                                        homingval = 3;
                                        homing();
                                }
                        }
                }
}

//=======================================
//------ USER INTERFACE INTERVAL --------
//=======================================

void enterX() {
                resetTimmers();
                userinputval = 0;

                if (FirstInputRun == 0) {
                        //Printing Parameter Variables
                        FirstInputRun = 1;
                        UserInputHeights();     //Extruder Height and Collector Height
                }

                if (FirstInputRun == 1) {
                        FirstInputRun = 2;
                        UserInputPumps();     //Values for Syringe Pump and Peristaltic Pump Actuation
                }

                if (FirstInputRun == 2) {
                        FirstInputRun = 3;
                        UserInputTime();      //Values relating to time based operations
                }

                if (FirstInputRun == 3) {
                        FirstInputRun = 4;
                        UserInputProcesses();    //Relating to Desired Printing Processes
                }

                if (FirstInputRun == 4) {
                        FirstInputRun = 5;
                        UserInputMethod();      //Relating to Desired printing Method
                }

                if (FirstInputRun == 5) {
                        userinputval = 1;
                        TotalMenuCheck();
                }
}

void resetTimmers()
{
                TimeOn = 0;   // stores the value of millis() in each iteration of loop()
```

```
		ResetTimeSM1_SP = 0;
		ResetTimeSM2_ZS1 = 0;
		ResetTimeSM3_ZS2 = 0;
		ResetTimeSM4_RM = 0;
		ResetTimeSM5_FTU = 0;
		ResetTimeSM6_FCU = 0;
		ResetTimeSM7_RFCU = 0;
		ResetTimeSM8_VP = 0;
}

//UPDATE VARIABLES FOR DISTANCES IF CEU ACTUATORS OR POE RECESS IS INCREACED
void UserInputHeights() {
		int extruderrecess = 200; //200mm is the standard distance of the recess (gap between bottom of lead screws and bottom of POEattacment) in the machine
		int collectorleadscrew = 420; //The step limit for the CEU actuators is coded as 10625steps which at 250stps/mm equals 425mm (given 5mm tolerance


		Serial.println("USER INPUT STAGE 1");
		Serial.println("");
		Serial.println("Enter which value you would like to modify: (e.g. enter: 'A' to modify the 'Extruder Height' value");
		Serial.print("A) Extruder Height: ");
		Serial.print(EH);
		Serial.println(" mm");
		Serial.print("B) Collector Height: ");
		Serial.print(CH);
		Serial.println(" mm");
		Serial.println("");
		Serial.println("Enter '/' to confirm these values");

		while (x == 0) {
			if (Serial.available() > 0) {
				UserIn = Serial.readString();
				if (UserIn != "A" && UserIn != "a" && UserIn != "B" && UserIn != "b" && UserIn != "/") {
					Serial.println("That is not an option");
				}
				if (UserIn == "A" || UserIn == "a") {
					Serial.println(" ");
					Serial.println("Enter Height of Extruder in mm");
					while (x == 0) {
						if (Serial.available() > 0) {
							UserIn = Serial.readString();
							EH = UserIn.toFloat();
							Serial.print("You have set the Extruder Height as:");
							Serial.print(EH);
							Serial.println("mm");
							Serial.println(" ");
							userinputval = 1;
							totalworkabledistance = collectorleadscrew + (extruderrecess - EH);


							UserInputHeights();
						}
					}
				}
				if (UserIn == "B" || UserIn == "b") {
					if (userinputval == 0) {
						Serial.println("Set the value for Extruder height first as future values are dependant on this.");
						UserInputHeights();
					}
					if (userinputval == 1) {
						Serial.println(" ");
						Serial.println("Enter the distance between the extruder and collector in mm");
						while (x == 0) {
							if (Serial.available() > 0) {
								UserIn = Serial.readString();
								CH = UserIn.toFloat();

								if (CH < (extruderrecess - EH)) {
									Serial.println("Due to the utilised extruder height, the machine cannot actuate
to this distance.");

									Serial.print("the current minimum distance is:");
									Serial.print((extruderrecess - EH));
									Serial.println(" mm");
									Serial.println("Please enter a viable distance");
									CH = 0;
									UserInputHeights();
								}

								if (CH > totalworkabledistance) {
									Serial.println("This value is greater than the maximum distance capable by the
machine");

									Serial.print("the current maximum distance capable is:");
									Serial.print(totalworkabledistance);
									Serial.println(" mm");
									Serial.print("Please enter a viable distance");
									CH = 0;
									UserInputHeights();
								}

								Serial.print("You have set the distance as as:");
								Serial.print(CH);
								Serial.println("mm");
								Serial.println(" ");
								UserInputHeights();
							}
						}
					}
				}
				if (UserIn == "/") {
					Serial.print("Values Confirmed");
					enterX();
				}
			}
		}
}

//REMEMBER TO HARD CODE THE VAPOURISOR STEPPER FLOWRATE PER REVOLUTION!!!!
void UserInputPumps() {
		//Stepper Motor Process Variables
		NoRevE = DF / (SyrMlitrePerMmitre * 2); //THE DENOMINATOR RELATES TO THE Syringe ml/mm which then compared to the motor mm/rev (2mm/rev in standard) equals a ml/rev value. e.g.
		NoRevV = VF / 0.38; //denominator value indicative of motor ml per revolution output
		delayTimeSM1_SP = ((3600000 / (3200 * NoRevE)) / 2); // will provide the delay in microseconds for a flowrate in rev/hour for motor having 16th microstepping e.g. h/(stps*rev/h) = h^2/revsteps namely
How much time (h) is required between the steps necessary
		delayTimeSM8_VP = ((3600000 / (200 * NoRevV)) / 2);
```

```
		Serial.println("USER INPUT STAGE 2");
		Serial.println("");
		Serial.println("Enter which value you would like to modify:");
		Serial.println("");
		Serial.print("A) Desired Electrospinning Syringe Pump Flowrate: ");
		Serial.print(DF);
		Serial.println(" mL/h");
		Serial.print("B) Desired Vapour Flowrate: ");
		Serial.print(VF);
		Serial.println(" mL/h");
		Serial.println("");
		Serial.print("Resultant Time Syringe Pump delay : ");
		Serial.print(delayTimeSM1_SP);
		Serial.println(" um");
		Serial.print("Resultant Time Peristaltic Pump delay : ");
		Serial.print(delayTimeSM8_VP);
		Serial.println(" um");
		Serial.println("");
		Serial.println("Enter '/' when done");
		while (x == 0) {
			if (Serial.available() > 0) {
				UserIn = Serial.readString();
				if (UserIn != "A" && UserIn != "a" && UserIn != "B" && UserIn != "b" && UserIn != "/") {
					Serial.println("That is not an option");
				}
				if (UserIn == "A" || UserIn == "a") {
					Serial.println(" ");
					Serial.println("Enter the Desired Electrospinning Syringe Pump Flowrate:");
					while (x == 0) {
						if (Serial.available() > 0) {
							UserIn = Serial.readString();
							DF = UserIn.toFloat();
							Serial.print("You have set the Desired Electrospinning Syringe Pump Flowrate as:");
							Serial.print(DF);
							Serial.println("ml");
							Serial.println(" ");
							UserInputPumps();
						}
					}
				}
				if (UserIn == "B" || UserIn == "b") {
					Serial.println(" ");
					Serial.println("Enter the Desired Vapour Flowrate:");
					while (x == 0) {
						if (Serial.available() > 0) {
							UserIn = Serial.readString();
							VF = UserIn.toFloat();
							Serial.print("You have set the Desired Vapour Flowrate as:");
							Serial.print(VF);
							Serial.println("ml");
							Serial.println(" ");
							UserInputPumps();
						}
					}
				}
				if (UserIn == "/") {
					Serial.println(" ");
					Serial.println("Done");
					Serial.println(" ");
					enterX();
				}
			}

		}
}

void UserInputTime() {

		Serial.println("USER INPUT STAGE 3");
		Serial.println("");
		Serial.println("Set the values below, if correct enter '/' to confirm");
		Serial.print("A) Electrospinning Time: ");
		Serial.print(((MachineTimeOn) / 1000));
		Serial.println(" seconds");
		Serial.println("NOTE some of these are derived values(they will effect one another)");
		Serial.print("B) Collection Angle Factor: ");
		Serial.print(DR);
		Serial.println(" degrees");
		/*Serial.print("C) Number of collection instances ");
		Serial.print(NC);
		Serial.println(" collections");
		Serial.print("D) Time between collection ");
		Serial.print(TC);
		Serial.println(" seconds");
		Serial.println("");*/
		Serial.println("Enter '/' to confirm these values");

		while (x == 0) {
			if (Serial.available() > 0) {
				UserIn = Serial.readString();
				if (UserIn != "A" && UserIn != "a" && UserIn != "/") {
					Serial.println("That is not an option");
				}
				if (UserIn == "A" || UserIn == "a") {
					Serial.println("Enter the desired electrospinning time in seconds:");
					Serial.println(" ");
					while (x == 0) {
						if (Serial.available() > 0) {
							UserIn = Serial.readString();
							MachineTimeOn = UserIn.toFloat();
							Serial.print("You have set the desired time as:");
							Serial.print(MachineTimeOn);
							MachineTimeOn = MachineTimeOn * 1000;
							Serial.println("This equals");
							Serial.print(MachineTimeOn);
							Serial.print(" in milliseconds");
							Serial.println(" ");
							userinputval = 1;
							UserInputTime();
						}
					}
				}
				if (UserIn == "B" || UserIn == "b") {
					if (userinputval == 0) {
```

```
                                                Serial.println("Set the value for Electrospinning Time first as future values are dependant on this.");
                                                UserInputTime();
                                        }
                                        if (userinputval == 1) {
                                                Serial.print("Enter the desired change in rotational degree per collection/cut:");
                                                while (x == 0) {
                                                        if (Serial.available() > 0) {
                                                                UserIn = Serial.readString();
                                                                DR = UserIn.toFloat();
                                                                Serial.print("You have set the desired collections degree as:");
                                                                Serial.print(DF);
                                                                Serial.println(" degrees");
                                                                UserInputTime();
                                                        }
                                                }
                                        }
                                }
                                if (UserIn == "C" || UserIn == "c") {
                                        if (userinputval == 0) {
                                                Serial.println("Set the value for Electrospinning Time first as future values are dependant on this.");
                                                UserInputTime();
                                        }
                                        if (userinputval == 1) {
                                                Serial.print("Enter the desired Number of collection instances:");
                                                while (x == 0) {
                                                        if (Serial.available() > 0) {
                                                                UserIn = Serial.readString();
                                                                NC = UserIn.toFloat();
                                                                TC = MachineTimeOn / NC;
                                                                Serial.print("You have set the desired number of collections as:");
                                                                Serial.print(NC);
                                                                Serial.println(" collections");
                                                                UserInputTime();
                                                        }
                                                }
                                        }
                                }
                                if (UserIn == "D" || UserIn == "d") {
                                        if (userinputval == 0) {
                                                Serial.println("Set the desired Electrospinning Time first");
                                                UserInputTime();
                                        }
                                        if (userinputval == 1) {
                                                Serial.print("Enter the desired time between cuts:");
                                                while (x == 0) {
                                                        if (Serial.available() > 0) {
                                                                UserIn = Serial.readString();
                                                                TC = UserIn.toFloat();
                                                                if (TC > MachineTimeOn) {
                                                                        Serial.print("Invalid value: Entered values cannot exceed desired
electrospinning time");
                                                                        TC = 0;
                                                                        UserInputTime();
                                                                }
                                                                NC = MachineTimeOn / TC;
                                                                Serial.print("You have set the desired number of collections as:");
                                                                Serial.print(NC);
                                                                Serial.println(" collections");
                                                                UserInputTime();
                                                        }
                                                }
                                        }
                                }
                                if (UserIn == "/") {
                                        Serial.print("Values Confirmed");
                                        enterX();
                                }
                        }
                }

}

void UserInputProcesses() {

                NoRevM = rpmIn * 60; //rev/hour
                delayTimeSM4_RM = ((3600000 / (200 * NoRevM)) / 2);

                Serial.println("USER INPUT STAGE 4");
                Serial.println("");
                //Serial.println("This printer has many processes please confirm which processes you wish to utilise");
                Serial.println("Enter the values of the processes you which to include and '/' to confirm once done");
                Serial.println("");
                Serial.println("A) Process 1: Rotating Mandrel");
                if (P1 == 0) {
                                Serial.println("Confirmed: OFF");
                }
                if (P1 == 1) {
                                Serial.println("Confirmed: ON");
                                Serial.print("Rpm = ");
                                Serial.print(rpmIn);
                                Serial.print(" revolutions per minute = Resultant Mandrel Motor Time delay : ");
                                Serial.println(delayTimeSM4_RM);
                }

                Serial.println("");
                Serial.println("B) Process 2: Vapour Exposure");
                if (P2 == 0) {
                                Serial.println("Confirmed: OFF");
                }
                if (P2 == 1) {
                                Serial.println("Confirmed: ON");
                                Serial.print("Time Set = ");
                                Serial.print(P2timeset);
                                Serial.println(" milliseconds ");
                }

                Serial.println("");
                Serial.println("C) Process 3: UV lithographic Exposure");
                if (P3 == 0) {
                                Serial.println("Confirmed: OFF");
                }
                if (P3 == 1) {
                                Serial.println("Confirmed: ON");
                                Serial.print("Time Set = ");
```

```
                Serial.print(P3timeset);
                Serial.println(" milliseconds ");
}

Serial.println("");
Serial.println("D) Process 4: Corona Plasma Discharge Exposure");
if (P4 == 0) {
                Serial.println("Confirmed: OFF");
}
if (P4 == 1) {
                Serial.println("Confirmed: ON");
                Serial.print("Time Set = ");
                Serial.print(P4timeset);
                Serial.println(" milliseconds ");
}
Serial.println("");
Serial.println("Enter '/' to confim values and continue");

while (x == 0) {
                if (Serial.available() > 0) {
                                UserIn = Serial.readString();
                                if (UserIn != "A" && UserIn != "a" && UserIn != "B" && UserIn != "b" && UserIn != "C" && UserIn != "c" && UserIn != "D" && UserIn != "d" && UserIn != "/") {
                                                Serial.println("That is not an option");
                                }
                                if (UserIn == "A" || UserIn == "a") {
                                                Serial.println("Enter 'Y' to turn on this process or 'N' to leave this off");
                                                while (x == 0) {
                                                                if (Serial.available() > 0) {
                                                                                UserIn = Serial.readString();
                                                                                if (UserIn != "Y" && UserIn != "y" && UserIn != "N" && UserIn != "n") {
                                                                                                Serial.println("That is not an option");
                                                                                }
                                                                                if (UserIn == "Y" || UserIn == "y") {
                                                                                                Serial.println("You have set this process 'On'");
                                                                                                rotatingmandrelUserInput();
                                                                                }
                                                                                if (UserIn == "N" || UserIn == "n") {
                                                                                                Serial.println("You have set this process 'OFF'");
                                                                                                P1 = 0;
                                                                                                UserInputProcesses();
                                                                                }
                                                                }
                                                }
                                }
                                if (UserIn == "B" || UserIn == "b") {
                                                Serial.println("Enter 'Y' to turn on this process or 'N' to leave this off");
                                                while (x == 0) {
                                                                if (Serial.available() > 0) {
                                                                                UserIn = Serial.readString();
                                                                                if (UserIn != "Y" && UserIn != "y" && UserIn != "N" && UserIn != "n") {
                                                                                                Serial.println("That is not an option");
                                                                                }
                                                                                if (UserIn == "Y" || UserIn == "y") {
                                                                                                Serial.println("You have set this process 'On'");
                                                                                                Serial.println("Enter The value in seconds you wish this process to run:");
                                                                                                while (x == 0) {
                                                                                                                if (Serial.available() > 0) {
                                                                                                                                UserIn = Serial.readString();
                                                                                                                                Serial.print(UserIn);
                                                                                                                                P2timeset = UserIn.toFloat();
                                                                                                                                Serial.print("You have set the desired time as:");
                                                                                                                                Serial.print(P2timeset);
                                                                                                                                P2timeset = P2timeset * 1000;
                                                                                                                                Serial.println("This equals");
                                                                                                                                Serial.print(P2timeset);
                                                                                                                                Serial.print(" in milliseconds");
                                                                                                                                Serial.println(" ");
                                                                                                                                P2 = 1;
                                                                                                                                UserInputProcesses();
                                                                                                                }
                                                                                                }
                                                                                }
                                                                                if (UserIn == "N" || UserIn == "n") {
                                                                                                Serial.println("You have set this process 'OFF'");
                                                                                                P2 = 0;
                                                                                                UserInputProcesses();
                                                                                }
                                                                }
                                                }
                                }
                                if (UserIn == "C" || UserIn == "c") {
                                                Serial.println("Enter 'Y' to turn on this process or 'N' to leave this off");
                                                while (x == 0) {
                                                                if (Serial.available() > 0) {
                                                                                UserIn = Serial.readString();
                                                                                if (UserIn != "Y" && UserIn != "y" && UserIn != "N" && UserIn != "n") {
                                                                                                Serial.println("That is not an option");
                                                                                }
                                                                                if (UserIn == "Y" || UserIn == "y") {
                                                                                                Serial.println("You have set this process 'On'");
                                                                                                Serial.println("Enter The value in seconds you wish this process to run:");
                                                                                                while (x == 0) {
                                                                                                                if (Serial.available() > 0) {
                                                                                                                                UserIn = Serial.readString();
                                                                                                                                P3timeset = UserIn.toFloat();
                                                                                                                                Serial.print("You have set the desired time as:");
                                                                                                                                Serial.print(P2timeset);
                                                                                                                                P3timeset = P3timeset * 1000;
                                                                                                                                Serial.println("This equals");
                                                                                                                                Serial.print(P2timeset);
                                                                                                                                Serial.print(" in milliseconds");
                                                                                                                                Serial.println(" ");
                                                                                                                                P3 = 1;
                                                                                                                                UserInputProcesses();
                                                                                                                }
                                                                                                }
                                                                                }
                                                                                if (UserIn == "N" || UserIn == "n") {
                                                                                                Serial.println("You have set this process 'OFF'");
                                                                                                P3 = 0;
                                                                                                UserInputProcesses();
                                                                                }
                                                                }
                                                }
                                }
```

```
                                        }
                                        if (UserIn == "D" || UserIn == "d") {
                                                Serial.println("Enter 'Y' to turn on this process or 'N' to leave this off");
                                                while (x == 0) {
                                                        if (Serial.available() > 0) {
                                                                UserIn = Serial.readString();
                                                                if (UserIn != "Y" && UserIn != "y" && UserIn != "N" && UserIn != "n") {
                                                                        Serial.println("That is not an option");
                                                                }
                                                                if (UserIn == "Y" || UserIn == "y") {
                                                                        Serial.println("You have set this process 'On'");
                                                                        Serial.println("Enter The value in seconds you wish this process to run:");
                                                                        while (x == 0) {
                                                                                if (Serial.available() > 0) {
                                                                                        UserIn = Serial.readString();
                                                                                        P4timeset = UserIn.toFloat();
                                                                                        Serial.print("The time is set as:");
                                                                                        Serial.print(P4timeset);
                                                                                        P4timeset = P4timeset * 1000;
                                                                                        Serial.println("This equals");
                                                                                        Serial.print(P2timeset);
                                                                                        Serial.print(" in millinseconds");
                                                                                        Serial.println(" ");
                                                                                        P4 = 1;
                                                                                        UserInputProcesses();
                                                                                }
                                                                        }
                                                                }
                                                                if (UserIn == "N" || UserIn == "n") {
                                                                        Serial.println("You have set this process 'OFF'");
                                                                        P4 = 0;
                                                                        UserInputProcesses();
                                                                }
                                                        }
                                                }
                                        }
                                        if (UserIn == "/") {
                                                Serial.println(" ");
                                                Serial.println("Done");
                                                Serial.println(" ");
                                                enterX();
                                        }
                                }
                        }
                }

//REMEMBER TO HARDCODE THE MAXIMUM RPM FOR THE MOTOR!!!!! currently this is 200 :(
void rotatingmandrelUserInput() {
                        int maxmotorRPM = 200; //YOU NEED TO WORK THIS OUT EXPERIMENTALLY!!!!! A limit variable to contain the maximum rpm capable for the motor
                        Serial.println("Please enter the desired RPM for the rotating mandrel");
                        while (x == 0) {
                                if (Serial.available() > 0) {
                                        UserIn = Serial.readString();
                                        rpmIn = UserIn.toFloat();
                                        if (rpmIn > maxmotorRPM) {
                                                Serial.println("The mechanism cannot provide this rpm");
                                                rpmIn = 0;
                                                rotatingmandrelUserInput();
                                        }
                                        if (rpmIn <= maxmotorRPM) {
                                                P1 = 1;
                                                Serial.print("The rotating speed set is: ");
                                                Serial.print(rpmIn);
                                                Serial.println("revolutions per minute");
                                                UserInputProcesses();
                                        }
                                }
                        }
}

void UserInputMethod() {
                        Serial.println("USER INPUT STAGE 5");
                        Serial.println("");
                        Serial.println("This printer is capable of performing two printing methods");
                        Serial.println(" ");
                        Serial.println("Method A");
                        Serial.println(" ");
                        Serial.println("This method will collect fibre a desired number of times.");
                        Serial.println("AFTER this the collection will be expossed to the desired processes.");
                        Serial.println(" ");
                        if (MA == 0) {
                                Serial.println("Method Confirmed: OFF");
                        }
                        if (MA == 1) {
                                Serial.println("Method Confirmed: ON");
                                Serial.print("Number of times fibre is collected Prior to additional processing:");
                                Serial.println(NPX);
                        }
                        Serial.println(" ");
                        Serial.println("Method B");
                        Serial.println(" ");
                        Serial.println("This method will collect spun fibre, afterwhich it will expose this to the previously assigned processes.");
                        Serial.println("This method repeats this collection-exposure sequence for a desired number of times.");
                        Serial.println(" ");
                        if (MB == 0) {
                                Serial.println("Method Confirmed: OFF");
                        }
                        if (MB == 1) {
                                Serial.println("Method Confirmed: ON");
                                Serial.print("Number of times fibre collection-exposure process occurs:");
                                Serial.println(NX);
                        }
                        Serial.println(" ");
                        Serial.println("Please enter either 'A' or 'B' to select the desired Method");
                        Serial.println(" ");
                        Serial.println("Enter '/' when done");

                        while (x == 0) {
                                if (Serial.available() > 0) {
                                        UserIn = Serial.readString();
                                        if (UserIn != "A" && UserIn != "a" && UserIn != "B" && UserIn != "b" && UserIn != "/") {
                                                Serial.println("That is not an option");
                                        }
                                        if (UserIn == "A" || UserIn == "a") {
```

```
                                                Serial.println("Please enter 'Y' to turn on Method A or 'N' to leave this off");
                                                while (x == 0) {
                                                        if (Serial.available() > 0) {
                                                                UserIn = Serial.readString();
                                                                if (UserIn != "Y" && UserIn != "y" && UserIn != "N" && UserIn != "n") {
                                                                        Serial.println("That is not an option");
                                                                }
                                                                if (UserIn == "Y" || UserIn == "y") {
                                                                        Serial.println("You have set this process 'On'");
                                                                        Serial.println("Please enter the number of times you wish to repeat the collection PRIOR to
further process exposure.");
                                                                        while (x == 0) {
                                                                                if (Serial.available() > 0) {
                                                                                        UserIn = Serial.readString();
                                                                                        NPX = UserIn.toFloat();
                                                                                        Serial.println("here");
                                                                                        MA = 1;
                                                                                        UserInputMethod();
                                                                                }
                                                                        }
                                                                }
                                                                if (UserIn == "N" || UserIn == "n") {
                                                                        Serial.println("You have set this process 'OFF'");
                                                                        MA = 0;
                                                                        UserInputMethod();
                                                                }
                                                        }
                                                }
                                        }
                                        if (UserIn == "B" || UserIn == "b") {
                                                Serial.println("Please enter 'Y' to turn on Method B or 'N' to leave this off");
                                                while (x == 0) {
                                                        if (Serial.available() > 0) {
                                                                UserIn = Serial.readString();
                                                                if (UserIn != "Y" && UserIn != "y" && UserIn != "N" && UserIn != "n") {
                                                                        Serial.println("That is not an option");
                                                                }
                                                                if (UserIn == "Y" || UserIn == "y") {
                                                                        Serial.println("You have set this process 'On'");
                                                                        Serial.println("Please enter the number of times you wish to repeat the collection-exposure
process.");
                                                                        while (x == 0) {
                                                                                if (Serial.available() > 0) {
                                                                                        UserIn = Serial.readString();
                                                                                        NX = UserIn.toFloat();
                                                                                        MB = 1;
                                                                                        UserInputMethod();
                                                                                }
                                                                        }
                                                                }
                                                                if (UserIn == "N" || UserIn == "n") {
                                                                        Serial.println("You have set this process 'OFF'");
                                                                        MB = 0;
                                                                        UserInputMethod();
                                                                }
                                                        }
                                                }
                                        }
                                        if (UserIn == "/") {
                                                Serial.println(" ");
                                                Serial.println("Done");
                                                Serial.println(" ");
                                                enterX();
                                        }
                                }
                        }
                }
}

void TotalMenuCheck() {
                        //temporary testing values
                        CV_SP = 0;
                        CV_CEU = 0;
                        CV_CEU2 = 0;
                        CV_RM = 0;
                        CV_FTU = 0;
                        CV_FCU = 0;
                        CV_RFCU = 0;

                        digitalWrite(SP_MS, LOW);

                        delayTimeSM2andSM3_ZS = 1;
                        delayTimeSM4_RM = 10;
                        delayTimeSM5_FTU = 1;
                        delayTimeSM6_FCU = 1;
                        delayTimeSM7_RFCU = 10;

                        SM1_SPstepperlimit = 10050;                     //value derived from manual measure measurement!!!!

                        limitSyr = 0;

                        DR = 45;
                        EH = 160;
                        CH = 300;
                        totalworkabledistance = 420 + (200 - EH);
                        DF = 1;
                        VF = 50;
                        DR = 45;
                        P1 = 1;
                        rpmIn = 100;
                        P2 = 1;
                        P3 = 1;
                        P4 = 1;
                        SyrMlitrePerMmitre = 0.01;
                        P2timeset = (10000);
                        P3timeset = (10000);
                        P4timeset = (10000);
                        MachineTimeOn = (60000);
                        NoRevM = rpmIn * 60; //rev/hour
                        delayTimeSM4_RM = ((3600000 / (200 * NoRevM)) / 2);
                        //Stepper Motor Process Variables
                        NoRevE = DF / (SyrMlitrePerMmitre * 2); //THE DENOMINATOR RELATES TO THE Syringe ml/mm which then compared to the motor mm/rev (2mm/rev in standard) equals a ml/rev value. e.g.
                        NoRevV = VF / 0.38; //denominator value indicative of motor ml per revolution output
                        delayTimeSM1_SP = ((3600000 / (3200 * NoRevE)) / 2); // will provide the delay in microseconds for a flowrate in rev/hour for motor having 16th microstepping e.g. h/(stps*rev/h) = h^2/revsteps namely
How much time (h) is required between the steps necessary
```

```
delayTimeSM8_VP = ((3600000 / (200 * NoRevV)) / 2);
MB = 1;
NX = 3;
SPPos = 0;
CUE1Pos = 0;
CUE2Pos = 0;
FTUPos = 0;
FCUPos = 0;
RFCUPos = 0;
RMPos = 0;

Serial.println(digitalRead(LS1_LimSP));
Serial.println(digitalRead(LS2_LimCEU1));
Serial.println(digitalRead(LS3_LimCEU2));
Serial.println(digitalRead(LS4_LimRM));
Serial.println(digitalRead(LS5_LimFTU));
Serial.println(digitalRead(LS6_LimFCU));
Serial.println(digitalRead(LS7_LimRFCU));
Serial.println(digitalRead(LS8_LimD));

Serial.println("USER FINAL CHECK");
Serial.println("Please enter the value you would like to modify or enter 'P' to finalise the setup : ");
Serial.println("H) Rehome the motors(required for additional/re-printing)");
Serial.println("A) User Inputted Mechanism Heights: ");
Serial.print("Extruder Height = ");
Serial.print(EH);
Serial.print(" mm");
Serial.print(" and ");
Serial.print("Collector Height = ");
Serial.print(CH);
Serial.println(" mm");
Serial.println(" ");
Serial.println("B) User Inputted Extruder/Pump Values: ");
Serial.print("Desired Electrospinning Syringe Pump Flowrate = ");
Serial.print(DF);
Serial.print(" mL/h");
Serial.print(" and ");
Serial.print("Desired Vapour Flowrate: ");
Serial.print(VF);
Serial.println(" mL/h");
Serial.println("");
Serial.print("Resultant Time Syringe Pump delay = ");
Serial.print(delayTimeSM1_SP);
Serial.print(" um");
Serial.print(" and ");
Serial.print("Resultant Time Peristaltic Pump delay : ");
Serial.print(delayTimeSM8_VP);
Serial.println(" um");
Serial.println("");
Serial.println("C) User Input Time Related Values: ");
Serial.print("Electrospinning Time = ");
Serial.print(((MachineTimeOn / 1000)));
Serial.print(" seconds");
Serial.print(" and ");
Serial.print("Collection Angle Factor = ");
Serial.print(DR);
Serial.print(" degrees");
/*Serial.print(" and ");
Serial.print("Number of collection instances = ");
Serial.print(NC);
Serial.print(" collections");
Serial.print(" and ");
Serial.print("Time between collection = ");
Serial.print(TC);
Serial.println(" seconds");
Serial.println(" ");*/
Serial.println("D) User Confirmed Processes: ");
Serial.println("Process 1: Rotating Mandrel = ");
if (P1 == 0) {
                Serial.print("OFF");
}
if (P1 == 1) {
                Serial.print("ON");
                Serial.print(" and ");
                Serial.print("Rpm = ");
                Serial.print(rpmIn);
                Serial.print(" revolutions per minute = Resultant Mandrel Motor Time delay : ");
                Serial.print(delayTimeSM4_RM);
}
Serial.print(" and ");
Serial.println("Process 2: Vapour Exposure = ");
if (P2 == 0) {
                Serial.print("OFF");
}
if (P2 == 1) {
                Serial.print("ON t = ");
                Serial.print(((P2timeset / 1000)));
                Serial.print(" seconds");
}
Serial.print(" and ");
Serial.println("Process 3: UV lithographic Exposure = ");
if (P3 == 0) {
                Serial.print("OFF");
}
if (P3 == 1) {
                Serial.print("ON t = ");
                Serial.print(((P3timeset / 1000)));
                Serial.print(" seconds");
}
Serial.print(" and ");
Serial.println("Process 4: Corona Plasma Discharge Exposure = ");
if (P4 == 0) {
                Serial.print("OFF");
}
if (P4 == 1) {
                Serial.print("ON t = ");
                Serial.print(((P4timeset / 1000)));
                Serial.print(" seconds");
}
Serial.println(" ");
Serial.println("E) User Confirmed Method: ");
if (MA == 1) {
                Serial.println("Method A = ");
                Serial.print("ON");
```

```
                Serial.print(" and ");
                Serial.print("Number of times fibre is collected Prior to additional processing:");
                Serial.print(NPX);
        }
        if (MB == 1) {
                Serial.println("Method B = ");
                Serial.print("ON");
                Serial.print(" and ");
                Serial.print("Number of times fibre collection-exposure process occurs:");
                Serial.println(NX);
        }
        Serial.println(" ");
        Serial.println("enter 'P' to end the setup");
        //
        while (x == 0) {
                if (Serial.available() > 0) {
                        UserIn = Serial.readString();
                        if (UserIn != "H" && UserIn != "h" &&UserIn != "A" && UserIn != "a" &&  UserIn != "B" && UserIn != "b" && UserIn != "C" && UserIn != "c" && UserIn != "D" && UserIn !=
"d" && UserIn != "E" && UserIn != "e" && UserIn != "P" && UserIn != "p") {
                                Serial.println("That is not an option");
                        }
                        if (UserIn == "H" || UserIn == "h") {
                                Serial.println(" ");
                                Serial.println("CAUTION: REMOVE Any loaded material/syringe before homing");
                                Serial.println("Enter Y to rehome the motors or 'M' to return to the menu");
                                while (x == 0) {
                                        if (Serial.available() > 0) {
                                                UserIn = Serial.readString();
                                                if (UserIn != "Y" && UserIn != "y" && UserIn != "M" && UserIn != "m") {
                                                        Serial.println("That is not an option");
                                                }
                                                if (UserIn == "Y" || UserIn == "y") {
                                                        homeallmotors();
                                                        TotalMenuCheck();
                                                }
                                                if (UserIn == "M" || UserIn == "m") {
                                                        TotalMenuCheck();
                                                }
                                        }
                                }
                        }
                        if (UserIn == "A" || UserIn == "a") {
                                UserInputHeights();
                        }
                        if (UserIn == "B" || UserIn == "b") {
                                Serial.println(" ");
                                Serial.println("CAUTION: REMOVE Any loaded material/syringe before homing");
                                Serial.println("Enter S to reprime the syringe motor, V to reprime the vapour motor, U to set the user values or 'M' to return to the menu");
                                while (x == 0) {
                                        if (Serial.available() > 0) {
                                                UserIn = Serial.readString();
                                                if (UserIn != "S" && UserIn != "s" &&  UserIn != "V" && UserIn != "v" && UserIn != "U" && UserIn != "u" && UserIn
!= "M" && UserIn != "m") {
                                                        Serial.println("That is not an option");
                                                }
                                                if (UserIn == "S" || UserIn == "s") {
                                                        syringepumpsetup();
                                                }
                                                if (UserIn == "V" || UserIn == "v") {
                                                        primevapourmechanism();
                                                }
                                                if (UserIn == "U" || UserIn == "u") {
                                                        UserInputPumps();
                                                }
                                                if (UserIn == "M" || UserIn == "m") {
                                                        TotalMenuCheck();
                                                }
                                        }
                                }
                        }
                        if (UserIn == "C" || UserIn == "c") {
                                UserInputTime();
                        }
                        if (UserIn == "D" || UserIn == "d") {
                                UserInputProcesses();
                        }
                        if (UserIn == "E" || UserIn == "e") {
                                UserInputMethod();
                        }
                        if (UserIn == "P" || UserIn == "p") {
                                PrintingDeviceSetup();
                        }
                }
        }
}

void PrintingDeviceSetup() {
        Serial.println(" ");
        Serial.println("Enter Y to begin device setup or M to return to the menu");
        while (x == 0) {
                if (Serial.available() > 0) {
                        UserIn = Serial.readString();
                        if (UserIn != "Y" && UserIn != "y" && UserIn != "M" && UserIn != "m") {
                                Serial.println("That is not an option");
                        }
                        if (UserIn == "M" || UserIn == "m") {
                                Serial.println(" ");
                                TotalMenuCheck();
                        }
                        if (UserIn == "Y" || UserIn == "y") {
                                if (digitalRead(LS8_LimD) == 0) {
                                        Serial.println("Close the door to continue ");
                                        Serial.println(" ");
                                        PrintingDeviceSetup();
                                }
                                if (digitalRead(LS8_LimD) == 1) {
                                        digitalWrite(R1_PS, HIGH);
                                        Serial.println("The High Voltage Power Supply may now be turned on and set ");
                                        Serial.println("Once set enter P to continue, else enter M to return to the menu");
                                        while (x == 0) {
                                                if (digitalRead(LS8_LimD) == 0) {
                                                        Serial.println(" ");
                                                        Serial.println("ERROR: Door unexpectidly opened, returning to menu");
                                                        Serial.println(" ");
```

```
                                                                                digitalWrite(R1_PS, LOW);
                                                                                TotalMenuCheck();
                                                                        }
                                                                        if (Serial.available() > 0) {
                                                                                UserIn = Serial.readString();
                                                                                while (x == 0) {
                                                                                        if (UserIn != "P" && UserIn != "p" && UserIn != "M" && UserIn != "m") {
                                                                                                Serial.println("That is not an option");
                                                                                                Serial.println(" ");
                                                                                        }
                                                                                        if (UserIn == "M" || UserIn == "m") {
                                                                                                digitalWrite(R1_PS, LOW);
                                                                                                TotalMenuCheck();

                                                                                        }
                                                                                        if (UserIn == "P" || UserIn == "p") {
                                                                                                digitalWrite(R1_PS, LOW);
                                                                                                Serial.println(" ");
                                                                                                Serial.println("Set Up Complete");
                                                                                                //x = 1;
                                                                                                SM1_SPstepperlimit = SM1_SPstepperlimit * 16;
                                                                                                limitSyr = limitSyr * 16;

                                                                                                if (MA == 1) {
                                                                                                        PrintingMethodA();

                                                                                                }

                                                                                                if (MB == 1) {
                                                                                                        PrintingMethodB();
                                                                                                }
                                                                                        }
                                                                                }
                                                                        }
                                                                }
                                                        }
                                                }
                                        }
                                }
                        }
                }
}

//=========================================
//---------- PRINTING INTERVAL ----------
//=========================================

void PrintingMethodA() {

                Serial.println("Printing method A");

                for (int a = 0; a < NPX; a++) {

                                int ftuready = 0;

                                float prior_time = millis();
                                while (ftuready == 0) {
                                        runmotorstodistance(SM5_FTU_Direction, SM5_FTU_Enable, SM5_FTU_Step, prior_time, ResetTimeSM5_FTU, delayTimeSM5_FTU, FTUPos, 37500);

                                        if (FTUPos == 37500) {
                                                ftuready = 1;
                                        }
                                }

                                setcollectiondistance();
                                Serial.println("Collection Distance set");
                                //Serial.println(oldTime);

                                oldTime = millis();
                                FibreDevelopmentProcess();
                                Serial.println("Electrospinning Phase Over");
                                TimeOn = 0;

                                homeservomotors();
                                FibreTransferalMotors();
                                collected = 0;

                }

                AdditionalProcesses();
                x = 0;

                StopElectrospinning(); //this must end everything and rehome the various actuators

                if (digitalRead(LS8_LimD) == 0) {
                                homeservomotors();
                                Serial.println(" ");
                                Serial.println("ERROR: Door unexpectidly opened - you must rehome the machine");
                                Serial.println(" ");
                                //homing();
                                TotalMenuCheck();
                }
}

void PrintingMethodB() {

                Serial.println("Printing method B");

                for (int b = 0; b < NX; b++) {
                                int ftuready = 0;

                                float prior_time = millis();
                                while (ftuready == 0) {
                                        runmotorstodistance(SM5_FTU_Direction, SM5_FTU_Enable, SM5_FTU_Step, prior_time, ResetTimeSM5_FTU, delayTimeSM5_FTU, FTUPos, 37500);

                                        if (FTUPos == 37500) {
                                                ftuready = 1;
                                        }
                                }

                                setcollectiondistance();
                                Serial.println("Collection Distance set");
                                //Serial.println(oldTime);

                                oldTime = millis();
                                FibreDevelopmentProcess();
```

```
                Serial.println("Electrospinning Phase Over");

                homeservomotors();
                FibreTransferalMotors();
                collected = 0;

                int fculoop = 0;

                CV_FCU = 0;
                CV_RFCU = 0;

                prior_time = millis();

                while (fculoop == 0) {
                        if (CV_FCU == 0) {
                                runmotorstolimit(SM6_FCU_Direction, SM6_FCU_Enable, SM6_FCU_Step, prior_time, ResetTimeSM6_FCU, delayTimeSM6_FCU, LS6_LimFCU, 1,
CV_FCU);
                        }

                        if (CV_FCU == 1) {
                                CV_FCU = 0;
                                CV_RFCU = 0;
                                FCUPos = 0;
                                fculoop = 1;
                        }

                }

                AdditionalProcesses();
        }

        x = 0;
        StopElectrospinning();

        if (digitalRead(LS8_LimD) == 0) {
                homeservomotors();
                Serial.println(" ");
                Serial.println("ERROR: Door unexpectidly opened - you must rehome the machine");
                Serial.println(" ");
                //homing();
                TotalMenuCheck();
        }

}

void setcollectiondistance() {
        CV_RM = 0;
        //in order to know this you need to know the mm/revolution of the linear actuator
        //1mm = 25 steps
        //after homing we are at the maximum distance (collectorleadscrew)

        //CH = mm desired distance, ASSUMPTION as above 1mm per 25steps)
        int desiredzCEUheight = ((totalworkabledistance - CH) * 25); //this equals the number of steps to reach the desired distance

        int Time_setCED = 0;
        int coldistLoop = 0;

        //Gets CEUs where they needs to be
        float priorTime_setCED = millis();
        while (coldistLoop == 0) {
                //Rotating fibre control unit
                runmotorstodistance(SM2_CEU_Direction, SM2_CEU_Enable, SM2_CEU_Step, priorTime_setCED, ResetTimeSM2_ZS1, delayTimeSM2andSM3_ZS, CUE1Pos, desiredzCEUheight);
                runmotorstodistance(SM3_CEU_Direction, SM3_CEU_Enable, SM3_CEU_Step, priorTime_setCED, ResetTimeSM3_ZS2, delayTimeSM2andSM3_ZS, CUE2Pos, desiredzCEUheight);
                runmotorstolimit(SM4_RM_Direction, SM4_RM_Enable, (SM4_RM_Step), priorTime_setCED, ResetTimeSM4_RM, delayTimeSM4_RM, P1, 0, CV_RM);


                /*Serial.println("Fibre collection distance");
                Serial.println(zCEUheight1);
                Serial.println(zCEUheight2);
                Serial.println(desiredzCEUheight);
                Serial.println(digitalRead(SM2_CEU_Enable));
                Serial.println(SM3_CEU_Enable);
                Serial.println(SM2_CEU_Step);
                Serial.println(SM3_CEU_Step);*/

                if (CUE1Pos == desiredzCEUheight && CUE2Pos == desiredzCEUheight) {
                        coldistLoop = 1;
                }

                if (digitalRead(LS8_LimD) == 0) {
                        homeservomotors();
                        Serial.println(" ");
                        Serial.println("ERROR: Door unexpectidly opened - you must rehome the machine");
                        Serial.println(" ");
                        //homing();
                        TotalMenuCheck();
                }
        }
}

void FibreDevelopmentProcess() {
        CV_RM = 0;
        ServM3_HVC_pos = 35; //25
        ServM3_HVC.write(ServM3_HVC_pos);
        TimeOn = 0;
        int limdelay = 0;

        digitalWrite(SP_MS, HIGH);
        digitalWrite(R1_PS, HIGH);

        if (digitalRead(LS8_LimD) == 0) {
                digitalWrite(R1_PS, LOW);
                homeservomotors();
                Serial.println(" ");
                Serial.println("ERROR: Door unexpectidly opened - you must rehome the machine");
                Serial.println(" ");
                //homing();
                TotalMenuCheck();
        }

        if (limitSyr == SM1_SPstepperlimit) {
                homeservomotors();
                Serial.println(" ");
                Serial.println("ERROR: The process has run out of available material - you will need to rehome the machine");
```

```
                        Serial.println(" ");
                        homing();
                }

                if (HasCollected == 1 && MB == 1) {
                        AdditionalProcesses();
                        if (P2 == 0 && P3 == 0 && P4 == 0) {
                                Serial.println("Proccesing Phase Over");
                        }
                }

                float oldTime = millis();
                while (TimeOn <= MachineTimeOn) {
                        currentTime = millis();
                        TimeOn = currentTime - oldTime;   // capture the latest value of how long the machine has been on
                                                                                                                        //Serial.println("ON");
                        runmotorstolimit(SM4_RM_Direction, SM4_RM_Enable, (SM4_RM_Step), oldTime, ResetTimeSM4_RM, delayTimeSM4_RM, P1, 0, CV_RM);


                        runmotorstodistance(SM1_SP_Direction, (SM1_SP_Enable), (SM1_SP_Step), oldTime, ResetTimeSM1_SP, delayTimeSM1_SP, limitSyr, SM1_SPstepperlimit);

                        if (TimeOn == MachineTimeOn) {
                                digitalWrite(SM4_RM_Enable, HIGH);
                                digitalWrite(SM4_RM_Step, LOW);
                                digitalWrite(SM1_SP_Enable, HIGH);
                                digitalWrite(SM1_SP_Step, LOW);
                                digitalWrite(R1_PS, LOW);

                                ServM3_HVC_pos = 60;
                                ServM3_HVC.write(ServM3_HVC_pos);

                        }

                        if (digitalRead(LS8_LimD) == 0) {
                                limdelay = limdelay + 1;
                        }

                        if (digitalRead(LS8_LimD) == 1) {
                                limdelay = limdelay * 0;
                        }


                        if (digitalRead(LS8_LimD) == 0 && limdelay == 5) {
                                digitalWrite(R1_PS, LOW);
                                homeservomotors();
                                Serial.println(" ");
                                Serial.println(limdelay);
                                Serial.println("ERROR: Door unexpectidly opened - you must rehome the machine");
                                Serial.println(digitalRead(LS8_LimD));
                                Serial.println(" ");
                                //homing();
                                TotalMenuCheck();
                        }
                }

}

///YOU MUST SET THE SIZE FOR THE COLLECTOR HERE OR ADD THIS MENU LATER
void FibreTransferalMotors() {
                Serial.println("Fibre transferal motors");

                int CEUtocollectdist = 0;
                CV_CEU = 0;
                CV_CEU2 = 0;
                CV_RFCU = 0;
                CV_FCU = 0;
                CV_RM = 0;
                RMPos = 0;

                float ceutodisttime = millis();
                while (CEUtocollectdist == 0) {
                        runmotorstolimit(SM2_CEU_Direction, SM2_CEU_Enable, SM2_CEU_Step, ceutodisttime, ResetTimeSM2_ZS1, delayTimeSM2andSM3_ZS, LS2_LimCEU1, 1, CV_CEU);
                        runmotorstolimit(SM3_CEU_Direction, SM3_CEU_Enable, SM3_CEU_Step, ceutodisttime, ResetTimeSM3_ZS2, delayTimeSM2andSM3_ZS, LS3_LimCEU2, 1, CV_CEU2);

                        if (CV_CEU == 1 && CV_CEU2 == 1) {
                                CUE1Pos = 0;
                                CUE2Pos = 0;
                                CEUtocollectdist = 1;
                        }
                }

                int FTUloop = 0;

                activateshomingservomotors();
                int fibretransferaldelayTimeSM4_RM = 10;

                float priorTime_home = millis();
                while (FTUloop == 0) {
                        if (FTUPos != 80500) {
                                runmotorstodistance(SM5_FTU_Direction, SM5_FTU_Enable, SM5_FTU_Step, priorTime_home, ResetTimeSM5_FTU, delayTimeSM5_FTU, FTUPos, 80500);
                        }
                        if (CV_RM == 0) {
                                runmotorstolimit(SM4_RM_Direction, SM4_RM_Enable, SM4_RM_Step, priorTime_home, ResetTimeSM4_RM, fibretransferaldelayTimeSM4_RM, LS4_LimRM, 1,
CV_RM);
                        }
                        if (CV_FCU == 0) {
                                runmotorstolimit(SM6_FCU_Direction, SM6_FCU_Enable, SM6_FCU_Step, priorTime_home, ResetTimeSM6_FCU, delayTimeSM6_FCU, LS6_LimFCU, 1, CV_FCU);
                        }

                        if (FTUPos == 80500 && CV_RM == 1 && CV_FCU == 1) {
                                priorTime_home = millis();
                                while (RMPos != 10) {
                                        runmotorstodistance(SM4_RM_Direction, SM4_RM_Enable, SM4_RM_Step, priorTime_home, ResetTimeSM4_RM, fibretransferaldelayTimeSM4_RM,
RMPos, 10);
                                }

                                if (RMPos == 10) {
                                        CV_CEU = 0;
                                        CV_CEU2 = 0;
                                        CV_RFCU = 0;
                                        CV_FCU = 0;
                                        CV_RM = 0;
                                        CUE1Pos = 0;
                                        CUE2Pos = 0;
```

```
                                                FCUPos = 0;
                                                RFCUPos = 0;
                                                RMPos = 0;
                                                homeservomotors();
                                                FTUloop = 1;
                                        }
                                }
                        }

                        if (FTUloop == 1) {
                                for (int rm = 0; rm <= 3; rm++) {
                                        rotatemandrel();
                                        for (int c = 0; c <= 4; c++) {
                                                collectfibre((79000 - (c * 3000))); //collector = 25mm therefore 25000 steps is enough but we will add a tolerance of 500 thus 3000
                                        }
                                        rotatemandrel();
                                        for (int cf = 0; cf <= 4; cf++) {
                                                collectfibre((67000 + (cf * 3000))); //collector = 25mm therefore 25000 steps is enough but we will add a tolerance of 500 thus 3000
                                        }
                                }
                        }
}

// The desiredFTUpos variable will vary according to the size of the collecctng surface
void collectfibre(float desiredFTUpos) {

                        Serial.println("In the collected Fibre function");

                        rotatecollector();

                        int FCULoop = 0;

                        float priorTime_home = millis();
                        while (FCULoop == 0) {
                                runmotorstodistance(SM5_FTU_Direction, SM5_FTU_Enable, SM5_FTU_Step, priorTime_home, ResetTimeSM5_FTU, delayTimeSM5_FTU, FTUPos, desiredFTUpos);

                                if (FTUPos == desiredFTUpos) {

                                        float priorTime_home = millis();
                                        while (FCULoop == 0) {
                                                runmotorstodistance(SM6_FCU_Direction, SM6_FCU_Enable, SM6_FCU_Step, priorTime_home, ResetTimeSM6_FCU, delayTimeSM6_FCU, FCUPos,
10800);

                                                if (FCUPos == 10800) {

                                                        float priorTime_home = millis();
                                                        while (FCULoop == 0) {
                                                                runmotorstodistance(SM6_FCU_Direction, SM6_FCU_Enable, SM6_FCU_Step, priorTime_home,
ResetTimeSM6_FCU, delayTimeSM6_FCU, FCUPos, 8000);

                                                                if (FCUPos == 8000) {
                                                                        FCULoop = 1;
                                                                }
                                                        }
                                                }
                                        }
                                }
                        }
}

void rotatecollector() {
                        Serial.println("In the rotatcollector function");

                        delayTimeSM7_RFCU = 10;

                        float RFCUangle = 0;
                        int stepsToRotate = ((DR * 200) / 360);

                        int RCLoop = 0;

                        //Gets RFCU where it needs to be
                        float priorTime_rotate = millis();
                        while (RCLoop == 0) {
                                //Rotating fibre control unit
                                runmotorstodistance(SM7_RFCU_Direction, (SM7_RFCU_Enable), (SM7_RFCU_Step), priorTime_rotate, ResetTimeSM7_RFCU, delayTimeSM7_RFCU, RFCUangle, stepsToRotate);
                                if (RFCUangle == stepsToRotate) {
                                        RCLoop = 1;
                                }
                        }
}

//HardCode Here the Angle between the struts of the rotating mandrel if required
void rotatemandrel() {
                        //Need to home the motor here
                        //Activate servos for the RM homing
                        int collectiondelayTimeSM4_RM = 10;
                        Serial.println("In the rotatemandrelfunction");
                        float MandrelCollectAngle = 0;
                        float desiredMandrelCollectAngle = ((45 * 200) / 360); //This will find the steps required in rotating the mandrel by 90 degrees

                        int RMLoop = 0;

                        //Gets RFCU where it needs to be
                        float priorTime_mandrel = millis();
                        while (RMLoop == 0) {
                                //Rotating mandrel control
                                runmotorstodistance(SM4_RM_Direction, (SM4_RM_Enable), (SM4_RM_Step), priorTime_mandrel, ResetTimeSM4_RM, collectiondelayTimeSM4_RM, MandrelCollectAngle,
desiredMandrelCollectAngle);
                                if (MandrelCollectAngle == desiredMandrelCollectAngle) {
                                        RMLoop = 1;
                                }
                        }
}

//PLEASE UPDATE THE PLACEHOLDER VALUES
void AdditionalProcesses() {
                        Serial.println("Additional Processes");
                        Serial.println(" ");

                        Serial.println(P2);
                        Serial.println(P3);
                        Serial.println(P4);

                        AP2 = 1;
```

```
	AP3 = 1;
	AP4 = 1;

	Aproc = 0;

	while (Aproc != 1) {
		if (P2 == 1) {
			Process2();
		}
		else {
			AP2 = 0;
		}
		if (P3 == 1) {
			Process3();
		}
		else {
			AP3 = 0;
		}
		if (P4 == 1) {
			Process4();
		}
		else {
			AP4 = 0;
		}
		if (AP2 == 0 && AP3 == 0 && AP4 == 0) {
			Aproc = 1;
			Serial.println("done?");
			//				return;
		}
	}
}

void Process2() {
	Serial.println("Process 2 - Vapour");
	Serial.println(P2timeset);
	Serial.println(AP2);
	Serial.println(AP3);
	Serial.println(AP4);

	P2_FTUpos = 27000;

	//tests

	//VF = 1000; Water test for ml/h

	//NoRevV = VF / 0.38; //
	//delayTimeSM8_VP = ((3600000 / (3200 * NoRevV)) / 2);

	float overwritetime_process = 0;
	float Time_process = 0;
	float priorTime_process = millis();

	while (AP2 == 1) {
		//runmotorstodistance(SM5_FTU_Direction, (SM5_FTU_Enable), (SM5_FTU_Step), priorTime_process, ResetTimeSM5_FTU, delayTimeSM5_FTU, FTUPos, P2_FTUpos);
		FTUPos = P2_FTUpos; //TEST

		if (FTUPos == P2_FTUpos) {
			priorTime_process = millis();
			while (AP2 == 1) {
				runmotorstodistance(SM6_FCU_Direction, (SM6_FCU_Enable), (SM6_FCU_Step), priorTime_process, ResetTimeSM6_FCU, delayTimeSM6_FCU,
FCUPos, 1500);
				//FCUPos = 5000; //TEST

				if (FCUPos == 1500) {

					priorTime_process = millis();
					while (Time_process <= P2timeset) {
						overwritetime_process = millis();
						Time_process = overwritetime_process - priorTime_process;

						runmotorstolimit(SM7_RFCU_Direction, SM7_RFCU_Enable, SM7_RFCU_Step, priorTime_process,
ResetTimeSM7_RFCU, delayTimeSM7_RFCU, P2, 0, CV_RFCU);
						runmotorstolimit(SM8_VP_Direction, SM8_VP_Enable, SM8_VP_Step, priorTime_process, ResetTimeSM8_VP,
delayTimeSM8_VP, P2, 0, CV_RM);

						digitalWrite(R3_Vap, HIGH);
						digitalWrite(R2_AP, HIGH);

						if (Time_process == P2timeset) {
							CV_FTU = 0;
							digitalWrite(R3_Vap, LOW);
							digitalWrite(R2_AP, LOW);

							priorTime_process = millis();
							while (AP2 == 1) {
								runmotorstodistance(SM6_FCU_Direction, (SM6_FCU_Enable),
(SM6_FCU_Step), priorTime_process, ResetTimeSM6_FCU, delayTimeSM6_FCU, FCUPos, 500);
								//FCUPos = 500; //TEST

								if (FCUPos == 500) {
									digitalWrite(SM8_VP_Enable, HIGH);
									digitalWrite(SM8_VP_Step, LOW);
									digitalWrite(SM7_RFCU_Enable, HIGH);
									digitalWrite(SM7_RFCU_Step, LOW);
									Serial.println("Process 1 done");
									AP2 = 0;
									return;
								}
							}
						}
					}
				}
			}
		}
	}
}

void Process3() {
	Serial.println("Process 3 - Lithography");
	Serial.println(P3timeset);
	Serial.println(AP2);
	Serial.println(AP3);
	Serial.println(AP4);
```

```
		P3_FTUpos = 14500;


		float overwritetime_process = 0;
		float Time_process = 0;
		float priorTime_process = millis();

		priorTime_process = millis();
		while (AP3 == 1) {
			//runmotorstodistance(SM5_FTU_Direction, (SM5_FTU_Enable), (SM5_FTU_Step), priorTime_process, ResetTimeSM5_FTU, delayTimeSM5_FTU, FTUPos, P3_FTUpos);
			FTUPos = P3_FTUpos; //TEST

			if (FTUPos == P3_FTUpos) {

				priorTime_process = millis();
				while (AP3 == 1) {
					//runmotorstodistance(SM6_FCU_Direction, (SM6_FCU_Enable), (SM6_FCU_Step), priorTime_process, ResetTimeSM6_FCU, delayTimeSM6_FCU,
FCUPos, 2500);
					FCUPos = 2500; //TEST

					if (FCUPos == 2500) {
						priorTime_process = millis();
						while (Time_process <= P3timeset) {
							overwritetime_process = millis();
							Time_process = overwritetime_process - priorTime_process;
							ServLED.write(90);
							digitalWrite(R4_LED, HIGH);

							if (Time_process == P3timeset) {
								digitalWrite(R4_LED, LOW);
								priorTime_process = millis();
								while (AP3 == 1) {
									//runmotorstodistance(SM6_FCU_Direction, (SM6_FCU_Enable),
(SM6_FCU_Step), priorTime_process, ResetTimeSM6_FCU, delayTimeSM6_FCU, FCUPos, 500);
									FCUPos = 500; //TEST

									if (FCUPos == 500) {
										Serial.println("Process 2 done");
										ServLED.write(10);
										AP3 = 0;
										return;
										//AdditionalProcesses();
									}
								}
							}
						}
					}
				}
			}
		}
}

void Process4() {
		Serial.println("Process 4 - Corona Plasma Discharge");
		Serial.println(P4timeset);
		Serial.println(AP2);
		Serial.println(AP3);
		Serial.println(AP4);

		P4_FTUpos = 3000;

		float overwritetime_process = 0;
		float Time_process = 0;
		float priorTime_process = millis();

		priorTime_process = millis();
		while (AP4 == 1) {
			runmotorstodistance(SM5_FTU_Direction, (SM5_FTU_Enable), (SM5_FTU_Step), priorTime_process, ResetTimeSM5_FTU, delayTimeSM5_FTU, FTUPos, P4_FTUpos);
			//FCUPos = P4_FTUpos; //TEST

			if (FTUPos == P4_FTUpos) {
				priorTime_process = millis();
				while (AP4 == 1) {
					runmotorstodistance(SM6_FCU_Direction, (SM6_FCU_Enable), (SM6_FCU_Step), priorTime_process, ResetTimeSM6_FCU, delayTimeSM6_FCU,
FCUPos, 1000);
					//FCUPos = 1000;

					if (FCUPos == 1000) {
						priorTime_process = millis();
						while (Time_process <= P4timeset) {
							overwritetime_process = millis();
							Time_process = overwritetime_process - priorTime_process;
							digitalWrite(R5_CPG, HIGH);

							if (Time_process == P4timeset) {
								digitalWrite(R5_CPG, LOW);
								priorTime_process = millis();

								while (AP4 == 1) {
									runmotorstodistance(SM6_FCU_Direction, (SM6_FCU_Enable),
(SM6_FCU_Step), priorTime_process, ResetTimeSM6_FCU, delayTimeSM6_FCU, FCUPos, 500);
									//FCUPos = 500;

									if (FCUPos == 500) {
										Serial.println("Process 4 done");
										AP4 = 0;
										Serial.println(P4);
										return;
										//AdditionalProcesses();
									}
								}
							}
						}
					}
				}
			}
		}
}

void StopElectrospinning() {
		//this must end everything and rehome the various actuators

		Serial.println("Printing finished: rehoming motors and returning to the menu");
```

```
		homeservomotors();
		activateshomingservomotors();

		int control = 0;

		float priorTime_home = millis();
		int rehomedelayTimeSM4_RM = 10;
		while (control == 0) {
			//activateshomingservomotors();
			priorTime_home = millis();
			while (control == 0) {
				//runmotorstodistance(SM5_FTU_Direction, SM5_FTU_Enable, SM5_FTU_Step, priorTime_home, ResetTimeSM6_FCU, delayTimeSM6_FCU, FTUPos, 5000);

				if (CV_RM == 0) {
					runmotorstolimit(SM4_RM_Direction, SM4_RM_Enable, SM4_RM_Step, priorTime_home, ResetTimeSM4_RM, rehomedelayTimeSM4_RM,
LS4_LimRM, 1, CV_RM);
				}
				if (CV_FTU == 0) {
					runmotorstolimit(SM5_FTU_Direction, SM5_FTU_Enable, SM5_FTU_Step, priorTime_home, ResetTimeSM5_FTU, delayTimeSM5_FTU, LS5_LimFTU, 1,
CV_FTU);
				}
				if (CV_CEU == 0) {
					runmotorstolimit(SM2_CEU_Direction, SM2_CEU_Enable, SM2_CEU_Step, priorTime_home, ResetTimeSM2_ZS1, delayTimeSM2andSM3_ZS,
LS2_LimCEU1, 1, CV_CEU);
				}
				if (CV_CEU2 == 0) {
					runmotorstolimit(SM3_CEU_Direction, SM3_CEU_Enable, SM3_CEU_Step, priorTime_home, ResetTimeSM3_ZS2, delayTimeSM2andSM3_ZS,
LS3_LimCEU2, 1, CV_CEU2);
				}
				if (CV_FCU == 0) {
					runmotorstolimit(SM6_FCU_Direction, SM6_FCU_Enable, SM6_FCU_Step, priorTime_home, ResetTimeSM6_FCU, delayTimeSM6_FCU, LS6_LimFCU, 1,
CV_FCU);
				}

				if (CV_RM == 1 && CV_FTU == 1 && CV_FCU == 1 && CV_CEU == 1 && CV_CEU2 == 1) {
					homeservomotors();
					setup();
				}
			}
		}
}


void loop() {
		//Serial.println(TimeOn);

		/*} 132352.941176470588235294117647O6/2 This is to print 1ml/h utilise 11029.411764705882352941764705882/2 to test at mm at 5minutes*/
}
```